

Lymphocyte and Epithelial Contributions to Crohn's Disease Studied in the  
SAMP1/YitFc Murine Ileitis Model

Timothy Steven Olson  
Houston, Texas

B.A., Rice University, 1998

A Dissertation presented to the Graduate Faculty  
Of the University of Virginia in Candidacy for the Degree of  
Doctor of Philosophy

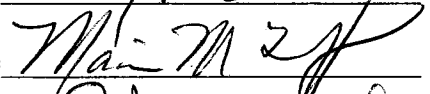
Department of Molecular Physiology

University of Virginia  
January, 2005

Tim Bender



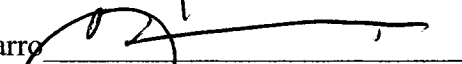
Marcia McDuffie



Kodi Ravichandran



Theresa Pizarro



Klaus Ley



## Abstract

Immunologic mechanisms and etiologic agents that contribute to the development of human Crohn's disease remain poorly understood. SAMP1/YitFc mice spontaneously develop discontinuous, transmural ileitis with histopathologic features strikingly similar to those observed in human Crohn's disease. I first investigated differences in the composition of mesenteric lymph node (MLN) CD4<sup>+</sup> T cell populations in SAMP1/YitFc versus wildtype AKR mice in an attempt to differentiate ileitis-producing and non-pathogenic mucosal CD4<sup>+</sup> T lymphocyte populations. I identified increases in several SAMP1/YitFc MLN lymphocyte subsets including overlapping populations of  $\alpha_E$  integrin<sup>+</sup> and CD25<sup>+</sup> CD4<sup>+</sup> T cells that express cytokines characteristic of regulatory T cells. These cells block colitis *in vivo* and effector cell proliferation *in vitro*, but are incapable of preventing ileitis both in SAMP1/YitFc mice and when adoptively transferred along with effector cells into SCID mice. Based on the observations that the size of the  $\alpha_E$ <sup>+</sup> CD4<sup>+</sup> cell population correlates with MLN B cell expansion, and that MLN B cell population size is greatly increased in SAMP1/YitFc versus AKR mice, I next determined the phenotype and pathogenicity of SAMP1/YitFc MLN B cells. These B cells produce increased IgA levels, worsen the severity of adoptively transferred ileitis, and promote effector T cell proliferation by inhibiting regulatory T cell function. Finally I determined if SAMP1/YitFc ileitis originates from a primary defect in immune cells or in non-hematopoietic tissues such as the epithelium by generating chimeric mice using bone marrow transplantation. SAMP1/YitFc mice reconstituted with AKR bone marrow developed substantial ileitis, whereas SAMP1/YitFc bone marrow did not confer ileitis to AKR mice. Increased permeability and decreased expression of the peroxisome-

proliferator-activated receptor (Ppar) $\gamma$  by SAMP1/YitFc epithelium suggest that this primary non-hematopoietic susceptibility leading to SAMP1/YitFc ileitis is derived from epithelial cells. Taken together, the results presented herein indicate that SAMP1/YitFc ileitis is likely caused by epithelial dysfunction leading to the initiation of ileal inflammatory responses involving Th1-polarized T cells and pro-inflammatory B cells that cannot be effectively controlled by regulatory T cells.

# Table of Contents

<b><i>Abstract.....</i></b>	<b><i>2</i></b>
<b><i>I. Introduction .....</i></b>	<b><i>6</i></b>
Research Objectives .....	6
Acknowledgements .....	9
List of Figures and Tables.....	13
Glossary of Abbreviations.....	15
<b><i>II. Background and Significance.....</i></b>	<b><i>16</i></b>
Introduction to Crohn's Disease: prevalence, pathology, and treatment.....	16
Environmental versus Genetic Factors.....	18
Mouse Models of IBD .....	23
Maintenance of Mucosal Homeostasis.....	31
Epithelial barrier function and contributions to innate immunity .....	31
Leukocyte compartments and trafficking requirements .....	33
Tolerance, regulatory T cells, and control of mucosal immune responses .....	40
How Homeostasis Is Broken....Potential Etiologies of Crohn's Disease .....	44
Infection and bacterial flora abnormalities .....	44
Aberrant Th1 polarization and overactivation of the immune system .....	45
Breakdown in immunological tolerance and regulatory T cell function .....	46
B lymphocyte function and Immunoglobulin Reactivity .....	48
Defects in Innate Immunity and Epithelial Dysfunction.....	49
The SAMP1/YitFc Model: Previous Work and Study Rationale.....	50
<b><i>III. Functional Differentiation of SAMP1/YitFc MLN CD4<sup>+</sup> T cell Subsets and Analysis of Regulatory T cell Function .....</i></b>	<b><i>55</i></b>
Rationale.....	55
Materials and Methods .....	58
Mice .....	58
Flow cytometry and antibodies .....	59
Cell isolations and adoptive transfer.....	59
Measurement of in vivo cell proliferation using bromodeoxyuridine.....	63
Chemotaxis assays .....	64
Real time RT-PCR for Chemokine receptor and TGF- $\beta$ expression .....	64
Cell Culture, Cytokine Analysis, and T cell proliferation assays .....	66
Histology .....	67
Two color in vivo homing assay.....	67
Statistics.....	69
Results and Discussion .....	69
Expansion and proliferation of CD4 <sup>+</sup> T cells and B Cells in SAMP1/YitFc MLN.....	69
Chemokine receptor expression and function in SAMP1/YitFc MLN and ileum .....	80
Function of SAMP1/YitFc MLN Regulatory CD4 <sup>+</sup> T cells in vitro and in vivo .....	89

#### ***IV. B cell and Immunoglobulin Contributions to SAMP1/YitFc Ileitis ..... 109***

##### **Rationale..... 109**

##### **Materials and Methods ..... 111**

Mice .....	111
Flow cytometry and confocal microscopy .....	112
Cell isolations and adoptive transfer .....	113
Cell culture and T cell proliferation assays .....	114
Measurement of immunoglobulin levels .....	115
Histology and immunohistochemistry .....	116
Real time PCR for GITR ligand expression .....	117
Statistics .....	117

##### **Results and Discussion ..... 118**

Immunoglobulin production and subset analysis of SAMP1/YitFc B cells .....	118
MLN $\alpha_E\beta_7^+$ CD4 <sup>+</sup> T cell involvement in B cell expansion and function .....	125
Contribution of B cells to SAMP1/YitFc and adoptively transferred ileitis .....	133

#### ***V. Epithelial Barrier Function and the Origins of Ileitis Susceptibility in SAMP1/YitFc Mice ..... 146***

##### **Rationale..... 146**

##### **Materials and Methods ..... 148**

Mice .....	148
Bone marrow transplantation .....	149
Histology .....	149
Quantification of hematopoietic cell reconstitution .....	150
Transepithelial electrical resistance assays .....	151
In Vivo disaccharide permeability assays .....	152
Epithelial cell isolation and real time rt-PCR for Pparg expression .....	153
Flow cytometry .....	154
Cell culture .....	155
Statistics .....	155

##### **Results and Discussion ..... 156**

BM transplant between SAMP1/YitFc and AKR mice results in full leukocyte reconstitution .....	156
Ileitis phenotype tracks with SAMP1/YitFc host/epithelium, not SAMP1/YitFc bone marrow .....	158
SAMP1/YitFc and AKR BM → SAMP mice exhibit epithelial barrier dysfunction .....	162
Epithelial cell expression of Pparg is decreased in SAMP1/YitFc versus AKR mice .....	168
Size and pathogenicity of MLN lymphocyte subsets determined by inflammatory status of host .....	171

#### ***VI. Conclusions and Future Directions..... 177***

##### **Conclusions ..... 177**

##### **Model Explaining Disease Development in SAMP1/YitFc Mice ..... 180**

##### **Suggestions for Future Work ..... 183**

# I. Introduction

## Research Objectives

The overarching goal of this dissertation is to further the understanding of the pathogenic mechanisms and etiologic agents that lead to the development of ileitis in human Crohn's disease. As will be discussed, few experimental systems exist that recapitulate the pathophysiologic changes in the small intestine seen in people afflicted with this condition. Most studies to date in these systems have focused on the pathogenic roles played by pro-inflammatory Th1-polarized T lymphocytes. In the studies presented herein, we have utilized the SAMP1/YitFc mouse strain to examine the contributions made by regulatory T cells, B lymphocytes, and the epithelium to the spontaneous ileitis that develops in this mouse strain. The specific objectives of this project are:

**Objective 1:** To differentiate ileitis-producing and non-pathogenic mucosal CD4<sup>+</sup> T lymphocyte populations in SAMP1YitFc mice on the basis of distinct cell surface marker, adhesion molecule, and chemokine receptor expression patterns, and to test the functionality of SAMP1/YitFc regulatory T cell populations.

**Objective 2:** To test whether SAMP1/YitFc mucosal B cell populations exacerbate or regulate ileitis and to identify subsets of T cells responsible for driving mucosal B cell proliferation and antibody production.

**Objective 3:** To determine if the primary etiologic agent leading to ileitis in SAMP1/YitFc mice is derived from leukocyte populations or non-hematopoietic cells, and to test whether SAMP1/YitFc mice exhibit defective epithelial cell function.

The thesis is divided into 6 chapters. Chapter II provides background information, including a general introduction to Crohn's disease, environmental and genetic influences linked to disease development, an overview of relevant animal models, a review of pathways governing mucosal homeostasis, potential mechanisms as to how this homeostasis is broken, and finally an introduction to the SAMP1/YitFc model. Chapter III focuses on objective 1, beginning with the characterization of proliferating CD4<sup>+</sup> T cell subset expansion in SAMP1/YitFc mesenteric lymph nodes (MLN). Chemokine receptor expression and function is then examined on SAMP1/YitFc MLN cells and whole ileal tissue. Finally, the identification of regulatory T cell subsets in SAMP1/YitFc MLN precedes an investigation of the functionality of these cells both *in vitro* and *in vivo*. Chapter IV focuses on objective 2, beginning with the characterization of B cell subsets and immunoglobulin production in SAMP1/YitFc MLN. These experiments are followed by the identification of helper CD4<sup>+</sup> T cell subsets required for B cell expansion and the promotion of isotype-specific immunoglobulin expression patterns. Finally, contributions made by B cells to the ileitis phenotype are studied in both the SAMP1/YitFc host and the SCID adoptive transfer model. Chapter V focuses on objective 3 and the disease phenotype of chimeric mice generated by transplanting SAMP1/YitFc bone marrow into wildtype mice and wildtype bone marrow into SAMP1/YitFc mice. These results are followed by a further examination of epithelial

permeability as well as the examination of anti-inflammatory transcription factor expression in SAMP1/YitFc epithelial cells. Finally, properties of lymphocyte populations in these chimeric mice are examined for their differential abilities to produce inflammation. The structure of Chapters 3-5 consist of a brief rationale section, a detailed methodology section, and a results and discussion section in each chapter. Chapter 6 contains a conclusions section summarizing the major findings of this dissertation, the proposal of a model explaining disease development in the SAMP1/YitFc strain, and suggestions for future experimentation.



## Acknowledgements

I would first like to acknowledge my mentor, Dr. Klaus Ley, for his invaluable support in accepting me into his laboratory, enabling my participation in this project, brainstorming ideas and experiments, and in general teaching me how to think as a scientist. I also thank Dr. Theresa Pizarro for her valued advice and support. I would also like to thank the remaining members of my thesis committee, Dr. Tim Bender, Dr. Kodi Ravichandran, and Dr. Marcia McDuffie for taking the time to serve on this committee and for providing valuable critiques. Thanks to Dr. Fabio Cominelli and the SAMP1/Yit NIH Program Project for providing the funding for these experiments. I would also like to thank the Cardiovascular Research Center, the Molecular Physiology Department, and the Medical Scientist Training Program for providing me with funding and many other resources. A special thanks to Dr. Gary Owens for originally convincing me to come to the University of Virginia and giving me this opportunity.

Many thanks to Tracy Burcin. Without your expertise and many hours of hands-on assistance highlighted by your unique commentary, many of these experiments would simply not have been possible. Thanks to Dr. Margaret Morris for assistance with bone marrow transplants and tail vein injections enabling the work pursued in Chapter 5. Thanks to Dr. Jesús Rivera-Nieves, for all of the valuable advice and for experimental assistance. Thanks to Dr. Peter Ernst and Dr. Makoto Naganuma for their collaborative efforts with the GITR/GITRL and T cell proliferation assays. Thanks also to Dr. Giorgos Bamias for providing raw data for Figure 4.10, and to William Ross for providing countless hours of assistance in acquiring flow cytometry data. Thanks to Kevin Scott and Brian Reuter for their knowledge and assistance with the epithelial permeability

assays and to Leslie Hancock for her help with the TEER assays. Thanks also to Dr.

McDuffie and Dr. Kazu Sugawara for initiating the collaboration leading to the Ppar $\gamma$  rt-PCR studies. I also greatly appreciate the contributions to these projects made by Sharon Huang, Greg Harp, Anthony Bruce, Robert Knight, Jennifer Mounts, Matthew Staples, Dr. Chris Moskalak, Dr. Rusty Mize, and Dr. R. Cartland Burns.

My time in the Ley Lab has given me many valuable friendships that I will always remember. Thanks to Dr. Kai Singbartl and Dr. Markus Sperandio for having the patience to train me and for our collaborations on studies not discussed in this dissertation. Thanks to Dr. Michael Smith and David Smith for their friendship and collaborative scientific efforts, as well as for not letting me drown in West Virginia and watching out for me on the rugby pitch. Thanks to Matt Stark for the countless discussions of the frustrations and fascinations of science and the NFL. I would further like to thank everyone else in the lab that has made my time here such a rich experience.

I would like to thank my family for giving me so much support and encouragement, even through the tough times. To my parents, thank you for persevering through my “colorful” years and encouraging me to continue my education. To my sisters, thank you for making sure I never take setbacks at work too seriously. To my beloved daughter, Dori, thanks for giving me the inspiration to finish this dissertation so that I can finish my schooling before you start yours. Most of all, thank you, Mira, for taking this journey to Virginia with me. Your companionship and love have given me the strength to achieve my goals professionally and to become the person I am today. I’ll always treasure our time here together and the many wonderful memories and experiences we have shared.

## List of Conference Proceedings and Publications by Degree Candidate

### **Publications:**

- Olson TS, Bamias G, Naganuma M, Rivera-Nieves J, Burcin TL, Ross W, Morris MA, Pizarro TT, Ernst PB, Cominelli F, Ley K. Expanded B cell population blocks regulatory T cells and exacerbates ileitis in a murine model of Crohn's disease. *J Clin Invest*. 2004 Aug;114(3):389-98.
- Olson TS, Morris MA, Scott KGE, Reuter BK, Burcin TL, Hancock LN, Meddings JB, Cominelli F, Ley K, and Pizarro TT. The Primary Susceptibility Conferring Crohn's-like Ileitis Derives from a Non-hematopoietic Source. (In preparation).
- Olson TS, Singbartl K, and Ley K. L-selectin is Required for fMLP- but not C5a Induced Margination of Neutrophils in the Pulmonary Circulation. *Am J Physiol Regul Integr Comp Physiol*. 2002 Apr;282(4):R1245-52.
- Olson TS and Ley K. Chemokines and chemokine receptors in leukocyte trafficking. *Am J Physiol Regul Integr Comp Physiol*. 2002 Jul;283(1):R7-28.
- Smith ML\*, Olson TS\*, Ley K. E-selectin- and chemokine-induced neutrophil arrest are redundant during inflammation in vivo. *J. Exp. Med.* (in press) \*Co-first authors.
- Martinez-Gakidis MA, Cullere X, Olson TS, Wilsbacher JL, Moores SL, Ley K, Swat W, Mayadas T, and Brugge JS. Vav GEFs are required for beta2 integrin-dependent functions of neutrophils. *J Cell Biol*. 2004 Jul 19;166(2):273-82.
- Sperandio M, Smith ML, Forlow SB, Olson TS, Xia L, McEver RP, Ley K. P-selectin glycoprotein ligand-1 mediates L-selectin-dependent leukocyte rolling in venules. *J Exp Med*. 2003 May 19;197(10):1355-63.
- Sugawara K, Olson TS, Moskaluk CA, Stevens B, Hoang S, Kozaiwa K, Cominelli F, Ley KF, and McDuffie M. Susceptibility to Crohn's disease is linked to PPAR $\gamma$  in mouse and man. *Gastroenterology* (In Press)
- Rivera-Nieves J, Olson TS, Bamias G, Bruce A, Solga M, Knight RF, Hoang S, Cominelli F, and Ley K. L-selectin,  $\alpha_4\beta_1$ , and  $\alpha_4\beta_7$  integrins participate in CD4<sup>+</sup> T cell recruitment to chronically inflamed intestine. *J. Immunol.* (In Revision)
- Bachmann C, Klibanov A, Olson TS, Cominelli F, Ley K, Lindner JR, Pizarro TT. MAdCAM-1 targeted microbubbles: a novel approach to non-invasively detect and evaluate intestinal inflammation. (Submitted)

### **Conference Proceedings:**

- April, 2001. Orlando, FL: Federation of American Societies for Experimental Biology: Absence or Blockade of L-selectin Prevents fMLP- but not C5a-Induced Sequestration of Neutrophils in the Pulmonary Circulation. T.S. Olson, K. Singbartl, K. Ley
- April 2002. New Orleans, LA: Federation of American Societies for Experimental Biology: Expanded B-cells and Activated CD4<sup>+</sup>  $\alpha_E\beta_7$  T-cells in Mesenteric Lymph Nodes of SAMP1/Yit/FC mice with Spontaneous Ileitis. T.S. Olson, R.C. Burns, J. Rivera-Nieves, W.G. Ross, F. Cominelli, K. Ley

- April 2003. Keystone, CO: Keystone Symposia- The Regulation of Mucosal Inflammation: Increased IgA-Secreting B cells in the SAMP1/Yit/Fc Spontaneous Murine Model of Crohn's Disease. T.S. Olson, T. Pizarro, F. Cominelli, K. Ley
- May, 2004. New Orleans, LA: Digestive Disease Week- American Gastroenterology Association: Evidence that the Primary Defect Conferring Susceptibility to Crohn's-like Ileitis is Derived from a Non-hematopoietic Source T.S. Olson, M. Morris, L. Hancock, F. Cominelli, K. Ley, and Theresa Pizarro. Oral presentation.

## List of Figures and Tables

### Tables

<b><u>Description</u></b>	<b><u>Page</u></b>
<b>Table 2.1.</b> Candidate genes linked to Crohn's disease genetic susceptibility	<b>21</b>
<b>Table 2.2.</b> Mouse Models of IBD	<b>24</b>
<b>Table 2.3.</b> Expression of adhesion molecules and chemokines in mucosal sites	<b>35</b>
<b>Table 2.4.</b> Pathogens implicated as potential infectious agents in Crohn's disease	<b>44</b>
<b>Table 2.5.</b> Reactivity of elevated antibody titers in Crohn's disease	<b>48</b>
<b>Table 3.1.</b> Chemokine receptor mRNA expression in MLN cells and ileum	<b>82</b>
<b>Table 3.2.</b> Chemokine receptors increased in SAMP1/YitFc versus AKR ileum	<b>86</b>
<b>Table 3.3.</b> Chemokine receptor expression in $\alpha_E\beta_7^+$ versus $\alpha_E\beta_7^-$ CD4 <sup>+</sup> T cells	<b>93</b>
<b>Table 3.4.</b> % of CD4 <sup>+</sup> T cells expressing CD25, CD45RB, CD25, and L-selectin	<b>105</b>
<b>Table 5.1.</b> Percentage of hematopoietic cell reconstitution in transplant recipients	<b>158</b>

### Figures

<b><u>Description</u></b>	<b><u>Page</u></b>
<b>Figure 3.1.</b> Purity of isolated CD4 <sup>+</sup> T cells subsets	<b>61</b>
<b>Figure 3.2.</b> Expansion of B cells and CD4 <sup>+</sup> T cells in SAMP1/YitFc MLN.	<b>71</b>
<b>Figure 3.3.</b> Increased proliferation of SAMP1/YitFc MLN T cells and B cells	<b>72</b>
<b>Figure 3.4.</b> Expansion of specific CD4 <sup>+</sup> T cell subsets in SAMP1/YitFc MLN	<b>74</b>
<b>Figure 3.5.</b> Adhesion molecule expression on SAMP1/YitFc CD4 <sup>+</sup> T cell subsets	<b>75</b>
<b>Figure 3.6.</b> Expression of $\alpha_E$ , $\alpha_4$ , $\beta_7$ , and $\beta_1$ integrin chains on MLN CD4 <sup>+</sup> T cells	<b>77</b>
<b>Figure 3.7.</b> Chemokine receptor mRNA expression on MLN CD4 <sup>+</sup> T cells	<b>81</b>
<b>Figure 3.8.</b> Chemotaxis of MLN CD4 <sup>+</sup> T cells	<b>83</b>
<b>Figure 3.9.</b> Chemokine receptor mRNA expression in whole ileum	<b>85</b>
<b>Figure 3.10.</b> Unique surface phenotype of $\alpha_E\beta_7^+$ CD4 <sup>+</sup> T cells	<b>90</b>
<b>Figure 3.11.</b> Chemokine receptor expression in $\alpha_E\beta_7^+$ versus $\alpha_E\beta_7^-$ CD4 <sup>+</sup> T cells	<b>92</b>
<b>Figure 3.12.</b> Cytokine production by $\alpha_E\beta_7^+$ versus $\alpha_E\beta_7^-$ CD4 <sup>+</sup> T cells	<b>94</b>
<b>Figure 3.13.</b> TGF- $\beta$ mRNA expression by $\alpha_E\beta_7^+$ versus $\alpha_E\beta_7^-$ CD4 <sup>+</sup> T cells	<b>96</b>
<b>Figure 3.14.</b> Regulatory function of $\alpha_E\beta_7^+$ CD4 <sup>+</sup> T cells <i>in vitro</i>	<b>97</b>

<b>Figure 3.15.</b> Pathogenicity of $\alpha_E\beta_7^+$ and $\alpha_E\beta_7^-$ T cells in adoptive transfer model	<b>99</b>
<b>Figure 3.16:</b> Histology of SCID ileum transferred with $\alpha_E\beta_7^+$ and $\alpha_E\beta_7^-$ T cells	<b>100</b>
<b>Figure 3.17:</b> Two-color <i>in vivo</i> homing assay with $\alpha_E\beta_7^+$ and $\alpha_E\beta_7^-$ T cells	<b>102</b>
<b>Figure 3.18:</b> Adoptive transfer of SAMP1/YitFc CD4 <sup>+</sup> T cells subsets	<b>104</b>
<b>Figure 4.1:</b> Purity of isolated CD4 <sup>+</sup> T cell and B cell fractions	<b>113</b>
<b>Figure 4.2:</b> Soluble immunoglobulin levels in SAMP1/YitFc and AKR MLN	<b>119</b>
<b>Figure 4.3:</b> IgA production by SAMP1/YitFc and AKR MLN B cells.	<b>121</b>
<b>Figure 4.4:</b> IgA expression on SAMP1/YitFc MLN B1 versus B2 cells	<b>122</b>
<b>Figure 4.5:</b> Spleen B cell, IgA <sup>+</sup> cell, and B2 versus B1 cell distributions	<b>124</b>
<b>Figure 4.6:</b> Increased IgA production requires SAMP1/YitFc T cell help	<b>126</b>
<b>Figure 4.7:</b> Interactions between MLN B cells and $\alpha_E\beta_7^+$ CD4 <sup>+</sup> T cells	<b>129</b>
<b>Figure 4.8:</b> Correlation between percentage of B cells and $\alpha_E\beta_7^+$ CD4 <sup>+</sup> T cells	<b>130</b>
<b>Figure 4.9:</b> Ig production driven by $\alpha_E\beta_7^+$ versus $\alpha_E\beta_7^-$ CD4 <sup>+</sup> T cells	<b>131</b>
<b>Figure 4.10:</b> SAMP1/YitFc B cell expansion correlates with ileitis severity	<b>134</b>
<b>Figure 4.11:</b> B cells increase severity of adoptively transferred ileitis	<b>136</b>
<b>Figure 4.12:</b> Immunostaining for CD20 and IgA in adoptively transferred ileum	<b>138</b>
<b>Figure 4.13:</b> Serum and MLN IgA in adoptively transferred SCID mice	<b>140</b>
<b>Figure 4.14:</b> Immunostaining for CD3 and GR1 in adoptively transferred ileum	<b>141</b>
<b>Figure 4.15:</b> Expression of GITR and GITRL in SAMP1/YitFc MLN	<b>142</b>
<b>Figure 4.16:</b> B cells block regulatory cell function <i>in vitro</i>	<b>143</b>
<b>Figure 5.1:</b> Real-time PCR detecting % reconstitution of transplant recipients	<b>157</b>
<b>Figure 5.2:</b> Ileitis severity in bone marrow transplant recipients	<b>159</b>
<b>Figure 5.3:</b> Histology of ilea from transplant recipients	<b>161</b>
<b>Figure 5.4:</b> Transepithelial electrical resistance assays	<b>163</b>
<b>Figure 5.5:</b> <i>In vivo</i> epithelial permeability assays	<b>164</b>
<b>Figure 5.6:</b> Expression of Ppar $\gamma$ 1 in SAMP1/YitFc versus AKR mice	<b>169</b>
<b>Figure 5.7:</b> MLN lymphocyte populations in transplant recipients	<b>172</b>
<b>Figure 5.8:</b> Cytokine production by transplant recipient MLN CD4 <sup>+</sup> T cells	<b>174</b>
<b>Figure 6.1:</b> Model of SAMP1/YitFc ileitis development	<b>181</b>

## Glossary of Abbreviations

APC – antigen presenting cells, allophycocyanin  
 CD – cluster of differentiation marker  
 CFSE - 5,6-carboxyfluorescein diacetate succinimidyl ester  
 CTLA– cytotoxic T lymphocyte-associated antigen  
 CY3 – cyanin fluorochrome 3  
 FITC – fluorescein isothiocyanate  
 GPCR- glucocorticoid induced TNF receptor  
 IBD – inflammatory bowel disease  
 ICAM – intercellular adhesion molecule  
 ICOS - inducible costimulator of T cells  
 IEL – intraepithelial lymphocyte  
 IFN - interferon  
 Ig – immunoglobulin  
 IL – interleukin  
 LFA-1 - lymphocyte function-associated antigen 1  
 LPL – lamina propria lymphocyte  
 MAdCAM - mucosal addressin cellular adhesion molecule  
 MAP - *Mycobacterium avium* paratuberculosis  
 MFI – mean fluorescent intensity  
 MLN - mesenteric lymph node  
 MALT - mucosa-associated lymphatic tissue  
 NF- $\kappa$ B – nuclear factor kappa B  
 PE – phycoerythrin  
 PERCP – peridinin chlorophyll protein  
 PP – Peyer’s patch  
 Ppar - peroxisome-proliferator-activated receptor  
 PSGL-1 – P-selectin glycoprotein ligand-1  
 SAMP1/YitFc – senescence accelerated mouse strain P1/YitFc  
 SCID – severe combined immunodeficient  
 STAT - signal transducer and activator of transcription  
 TCR – T cell receptor  
 TEER – transepithelial electrical resistance assays  
 TGF – Transforming Growth Factor- $\beta$   
 T<sub>FH</sub> – follicular helper T cell  
 Th1 – T helper cell type I  
 Th2 – T helper cell type II  
 TLR- Toll-like receptor  
 TNF – tumor necrosis factor  
 Treg – regulatory T cells  
 VCAM – vascular cell adhesion molecule

## **II. Background and Significance**

### **Introduction to Crohn's Disease: prevalence, pathology, and treatment**

Crohn's disease is one of two disorders, along with ulcerative colitis, that comprise the classification of inflammatory bowel disease (IBD). A recent review of epidemiologic data states that Crohn's disease may have a prevalence of up to 160 cases per 100,000 people in the United States, suggesting that close to 500,000 Americans may be afflicted with this disease (1). The disorder is even more prevalent in certain areas of Canada, while many regions in northern Europe, including the United Kingdom, Scandinavia, Northern France, and The Netherlands, have similar prevalence rates to those seen in the United States (1). While incidence rates in several of these high prevalence regions have stabilized over the past two decades (2;3), previously low prevalence areas are beginning to experience rising incidences (4-6), suggesting that the global prevalence will continue to increase for the foreseeable future.

Crohn's disease affects women at slightly higher rates than men, and the typical age of onset for both genders is in the second and third decades of life, with a second peak in incidence rates occurring in the sixth to seventh decades (7). The clinical presentation of Crohn's disease depends on the regions involved, but typically include colicky right lower quadrant pain, diarrhea or constipation depending on the degree of fibrostenosis present, a palpable mass in the lower right quadrant of the abdomen, low grade fevers, emaciation, and delayed growth in children (8). Left untreated, Crohn's disease can result in fatal complications such as full obstruction, hemorrhage, peritonitis from perforated bowel segments, and colorectal cancer (8).



In the original description of Crohn's disease by B.B. Crohn in 1932 (9), the disease was defined as regional ileitis in the absence of any inflammatory sequelae beyond the terminal ileum. Many of the hallmark pathological features of the disease were first identified in this report, including villus blunting and mucosal aphthoid ulceration leading to "cobblestoning" of the mucosal surface, appearance of normal segments of bowel separating diseased areas, hypertrophy of the submucosae and muscularis layers, mixed infiltration of neutrophils, mononuclear cells, and plasma cells, and profound fibrotic changes in more advanced lesions leading to stenosis, obstruction, fistula formation with the colon and abdominal wall, and free perforation into the abdominal cavity (9). It was later discovered that lesions with similar histopathological features were found throughout the gastrointestinal tract from the oropharynx to the perianal area in certain patients, and thus the scope of the disease definition was extended to include these patients as well. In addition to ileal and colonic lesions, Crohn's patient's may also suffer from many extraintestinal manifestations, including ankylosing spondylitis, osteopenia, peripheral arthritis, skin lesions such as erythema nodosum, episcleritis, hepatic steatosis, cholelithiasis, and renal calculi (10). Nonetheless, estimates suggest that between 70 and 95% of Crohn's patients have ileal involvement alone or in combination with lesions present at other sites, with the remaining population exhibiting colitis alone (8). Soon after the discovery that the Th1-class of T lymphocytes was responsible for delayed type hypersensitivity (11-13) and produced a distinct pattern of inflammation in both infectious and autoimmune conditions (14), the ileal inflammatory response seen in Crohn's disease was shown to be associated with a similar type of Th1 inflammation involving Th1 T cells, macrophages, and aberrantly high

production of Th1 cytokines, including interferon (IFN)- $\gamma$ , interleukin (IL)-12, and tumor necrosis factor (TNF)- $\alpha$  (15-18).

Prior to the late 1990's, treatment of Crohn's disease consisted of corticosteroid therapy for treatment of active disease and the use of anti-metabolites such as azathioprine and 6-mercaptopurine for maintenance therapy (19). Patients who were not responsive to medical therapy or could not tolerate the expansive side effects of these therapies underwent surgical resection. The advent of therapy using infliximab, a humanized monoclonal antibody recognizing TNF- $\alpha$ , that decreases inflammation not only by neutralizing the soluble protein but also by inducing apoptosis of lamina propria inflammatory cells (20;21), has revolutionized Crohn's therapy. While surgical resection is still required in advanced cases, infliximab is used both in active Crohn's therapy and in remission maintenance, with low side effects compared to previous therapies (22;23).

Several other novel therapies for Crohn's disease have been proposed in the last few years. Antibiotic and/or probiotic therapies designed to alter the intestinal microflora have been tested in several clinical trials to varying degrees of success (24;25).

Nataluzimab, a humanized monoclonal antibody directed against  $\alpha_4$  integrins on the surface of infiltrating leukocytes, induced significant improvement in patients with active Crohn's disease, but was not as effective as infliximab (26).

## **Environmental versus Genetic Factors**

Several studies have reported that Crohn's disease concordance rates in monozygotic twins are approximately 50%, whereas concordance rates in dizygotic twins are only around 4% (27). These findings indicate that both genetic and environmental factors are

required for disease development since concordance is high, but not 100%, in genetically identical individuals. Thus, a model in which environmental agents trigger disease in genetically susceptible individuals may best explain the etiology of Crohn's disease. One potential environmental factor that may be involved is climate, as prevalence rates seem to follow a north-south gradient, with northern regions exhibiting much higher prevalence (28;29). Strengthening this argument is the observation that while African countries exhibit low incidences of Crohn's disease, African-Americans develop IBD at rates comparable to other demographic groups within the United States (30). However, the fact that northern countries have in most cases undergone more extensive modernization and industrial development may confound the climate hypothesis. Alternatively, the "cold chain" hypothesis suggests that the increasing incidence of Crohn's disease in developed countries over the last century may be caused by increasing use of refrigeration (31). In this hypothesis, strains of gut-tropic bacteria capable of growing in food products at 4<sup>0</sup> C are postulated as the primary etiologic agents precipitating disease. Other studies have suggested that changes in dietary habits such as increased consumption of refined sugars and increases in formula- versus breast-feeding of infants may increase the risk of disease through alteration of intestinal flora composition, however the magnitude of these effects appears to be small and the results are controversial (1). Cigarette smoke and the use of non-steroidal anti-inflammatory drugs (NSAIDs) have also been proposed as factors that influence the course of Crohn's disease, although it is unclear whether these agents are etiologic causes or if they simply exacerbate preexisting disease due to their effects on epithelial function (32-34).

The twin studies mentioned above and the findings that certain ethnic groups such as Ashkenazi Jewish or Asian-American populations are particularly susceptible or resistant, respectively, to developing Crohn's disease regardless of geographic residence area, argue strongly in favor of polymorphic genetic loci playing critical roles in disease pathogenesis (35;36). Human genome-wide screens using genetic linkage analysis have identified a number of candidate susceptibility loci as outlined in Table 2.1 (37;38). Many individual genes within these loci known to play roles in inflammation, intestinal epithelial function, or adaptive immune responses have been or are currently being assessed for specific allelic polymorphisms selectively present in Crohn's patients.

The discovery of the first gene to be strongly linked to the etiology of Crohn's disease began with a genome-wide screen in 1996 identifying polymorphisms within the q12 locus on Chromosome 16 that were more prevalent in Crohn's patients than in the general population (39). Two independent groups identified frameshift or missense mutations in the *NOD2* gene that were strongly associated with the development of Crohn's disease (40;41). An analysis of *NOD2* variants present in an ethnically diverse cross-section of Crohn's patients determined that 3 specific mutations accounted for 81% of all *NOD2* variants and that 23% of Crohn's patients versus only 7% of healthy controls possessed one of these variants (42). Including the more rare variants, these estimates suggest that *NOD2* mutations account for up to 20% of the genetic susceptibility to Crohn's disease. *NOD2* is an intracellular pattern recognition receptor that binds to a muramyl dipeptide motif contained in the bacterial cell wall component peptidoglycan (43), the same ligand recognized by the cell surface toll-like receptor (TLR)-2 (44). Upon ligand binding, *NOD2* undergoes oligomerization allowing recruitment of an adaptor protein, RICK,

Locus Desig.	Approx . Site	Relevant Studies	Candidate Genes within Locus	Genes Tested but Excluded within Locus
IBD1	16q12	39, 40, 64	NOD2, CD11 integrins	CD19, IL-4R, CD11B
IBD2	12q13	49, 50, 65	Vitamin D Receptor	STAT6, interferon- $\gamma$
IBD3	6p13	51, 52, 54	MHC, TNF- $\alpha$	-
IBD4	14q11	63, 66	No specific evidence	IL-25
IBD5	5q31	55, 56	IL-4, 5, and 13; OCTN	-
IBD6	19p13	57, 58, 59	ICAM-1 Complement C3	-
IBD7	1p36	51, 61, 67	No specific evidence	IL-10
-	4q	51, 61, 67	No specific evidence	IL-2
-	7q	50, 60	Mucin 3	-
-	3(p21-p26)	50, 61, 62	Ppar- $\gamma$ , G $\alpha$ i2	CCR2 CCR5

**Table 2.1.** Candidate genes linked to Crohn's disease genetic susceptibility. MHC, major histocompatibility complex. TNF, tumor necrosis factor. OCTN, organic cation transporter. ICAM-1, intercellular adhesion molecule. Ppar, peroxisome proliferator-activated receptor. No specific evidence denotes that no gene polymorphisms that correlate with Crohn's disease susceptibility have been identified.

which in turn activates I $\kappa$ B kinase releasing this complex from its inhibitory bond that blocks the nuclear localization signal of the transcription factor NF- $\kappa$ B (45). Thus, NOD2 signaling leads to the translocation of NF- $\kappa$ B into the nucleus and the activation of the many pro-inflammatory genes controlled by NF- $\kappa$ B (46). The NOD2 variants found in Crohn's patients are paradoxically less proficient at activating NF- $\kappa$ B than the prototype NOD2 protein (47), despite the well-established finding that activated NF- $\kappa$ B is dramatically increased in Crohn's lesions (48). Thus the mechanism by which these

variants promote susceptibility remains unclear. Interestingly, a NOD2 mutation appears to be the sole defect that leads to development of skin lesions, arthritis and other maladies in a disease known as Blau syndrome (43), though in this disease the mutation leads to an aberrant gain of function, such that NOD2 constitutively activates NF- $\kappa$ B without the requirement of peptidoglycan binding (47).

A polymorphism in the gene encoding the vitamin D receptor, a steroid receptor expressed by many leukocytes that activates macrophage function but inhibits NF- $\kappa$ B, was found with increased frequency in Crohn's patients (22% homozygous) versus controls (49). Though the mechanism by which polymorphisms in this gene, located in the IBD2 locus (50), confers susceptibility has not been investigated, it may involve a loss of function which prevents the vitamin D receptor from inhibiting pro-inflammatory gene transcription. Specific haplotypes in the major histocompatibility gene region, located within the IBD3 locus (51), have been linked with Crohn's disease development (52). Thus, as in autoimmune diseases including the Crohn's-associated disorder ankylosing spondylitis (53), MHC alleles may contribute a significant portion of the genetic risk in Crohn's disease. While polymorphisms in the promoter region of TNF- $\alpha$  don't segregate Crohn's patients from healthy controls, specific alleles are present with higher frequency in patients with more severe fistulizing disease, indicating that TNF- $\alpha$  genotype influences the severity, but not the initial development, of Crohn's disease (54). Polymorphisms in many other genes located within identified susceptibility loci have also been associated with Crohn's disease, including an organic cation transporter gene (55) in the chromosome 5 locus (56), the intercellular adhesion molecule (ICAM)-1 (57) and complement C3 (58) genes in the chromosome 19 locus (59), the Muc3 gene encoding a

mucin protein (60), in the chromosome 7 locus (50), and the peroxisome-proliferator-activated receptor- (Ppar)- $\gamma$  gene (Sugawara, et.al., *Gastroenterology*, In Press) near the chromosome 3 locus (50;61;62). Polymorphisms linked to Crohn's disease have yet to be found in specific genes from several other identified susceptibility loci, including loci on chromosomes 14, 1, and 7 (51;61;63). In addition, polymorphisms in several initially intriguing gene candidates within the above susceptibility loci have now been shown to not be significantly associated with Crohn's, including genes encoding CD19, Sialophorin, CD11B, IL-4 receptor, STAT6, IFN- $\gamma$ , IL-2, IL-10, and IL-25 (40;64-67). Based on all of the implicated loci and candidate genes, it is likely that combinations of these individual traits may be required for disease development, and epistasis, or synergistic interaction, between susceptibility loci is beginning to be identified (61).

### **Mouse Models of IBD**

A variety of intestinal inflammation models have been employed to further the understanding of pathogenic mechanisms involved in Crohn's disease (68-71). Development of disease in most of these models requires specific genetic, chemical, or immunologic manipulation (Table 2.2). Because the genetic predisposition to Crohn's disease is clearly multifactorial, the specific manipulations used to induce disease in these models likely belie the true complexity of Crohn's disease pathogenesis. Further, while the combined acute and chronic Th1 inflammation seen in many of these models resembles Crohn's colitis, inflammation in most models is delimited to the colon and does not involve the ileum, the hallmark site of Crohn's lesions.

Mouse Model	Description	Tissue	Type
<b>Induced by chemical agents</b>			
Dextran Sodium Sulfate (DSS) Colitis	3-10% dextran sodium sulfate in drinking water for 6-10 days <sup>114</sup>	Colon	Ac, Muc
Trinitrobenzene Sulfonic Acid (TNBS) colitis	Enema of TNBS in 50% ethanol produces strain-dependent Th1 colitis <sup>125</sup>	Colon	Ac, Chr, Trans
Oxazolone Colitis	Oxazolone enema/50% ETOH-Th2 Colitis <sup>126</sup>	Colon	Ac, Muc
<b>Induced by adoptive transfer of CD4<sup>+</sup> T cells</b>			
CD4 <sup>+</sup> CD45RB <sup>hi</sup> L-selectin <sup>hi</sup> Transfer	Transfer of CD4 <sup>+</sup> CD45RB <sup>hi</sup> or L-selectin <sup>hi</sup> splenocytes into SCID recipients <sup>79,80</sup>	Colon	Chr, Trans
OX40L-Tg T cell transfer	Transfer of T cells from mice overexpressing OX40L specifically in T cells into Rag2 -/- <sup>83</sup>	Lungs, Colon	Chr, Trans
<b>Induced by deletion or overexpression of leukocyte signaling or cytokine genes</b>			
IL-2 -/-, IL-2R $\alpha$ -/-	Colitis & autoimmunity <sup>96, 97</sup>	Colon	Ac, Chr, Muc
IL-10 -/-	Strain- and bacterial flora-dependent colitis <sup>90</sup>	Colon	Ac, Chr, Trans
TCR $\alpha$ -/-	Th2 colitis in mice lacking $\alpha\beta$ T cells <sup>109</sup>	Colon	Chr, Muc
Stat4 transgenic	Overexpression of IL-12 pathway signaling molecule leads to Th1 colitis <sup>102</sup>	Colon	Ac, Chr, Trans
TNF $\Delta$ ARE	Deletion of AU-rich elements in TNF $\alpha$ RNA, resulting in systemic overexpression <sup>103</sup>	Ileum, joints	Ac, Chr, Trans
STAT3 -/-	Deletion of transcription factor specifically in myeloid cells leads to IBD <sup>105</sup>	Ileum Colon	Ac, Chr, Trans
<b>Inflammation dependent upon B cell abnormalities or function</b>			
Gai2 -/-	Colitis due to lack of inhibitory G protein <sup>108</sup>	Colon	Ac, Chr, Muc
TCR $\alpha$ -/- X Ig $\mu$ -/-	IgM <sup>+</sup> B cells protective in TCR $\alpha$ -/- colitis <sup>110</sup>	Colon	Chr, Trans
IFN- $\gamma$ -/- T cell + WT B cell cotransfer	Transfer of IFN- $\gamma$ -/- CD45RB <sup>hi</sup> CD4 <sup>+</sup> T cells + WT B cells produces ileitis, not colitis <sup>111</sup>	Ileum	Chr, Muc
<b>Induced by epithelial dysfunction</b>			
mdr1a -/-	Develops Crohn's-like colitis, even when mdr1a -/- is reconstituted with WT marrow <sup>128</sup>	colon	Ac, Chr, Trans
<b>Spontaneous Models</b>			
C3H/HeJBir	Substrain of susceptible C3H/HeJ mice <sup>73</sup>	Colon	Ac, Trans
SAMP1/YitFc	Derived from wildtype mice, strain develops ileitis with 100% penetrance <sup>242</sup>	Ileum	Ac, Chr, Trans

**Table 2.2.** Mouse Models of IBD. Ac, acute. Chr, Chronic. Muc, mucosal only. Trans, transmural.



Along with the SAMP1/YitFc mouse strain, the C3H/HeJBir mouse strain, developed from breeding of colitis-susceptible mice in the parental C3H/HeJ strain, is the only other strain in which IBD develops spontaneously without exogenous manipulation (72).

While inflammation in these mice involves Th1 responses producing transmural lesions consisting of both acute and inflammatory cells, lesions are delimited to the cecum and colon and peak at 3 to 6 weeks of age with disease resolution occurring thereafter (73). Compared to cells from uninflamed C3H/HeJ mice, CD4<sup>+</sup> T cells and B cell-derived immunoglobulin from C3H/HeJBir are highly reactive toward enteric bacterial antigens from non-pathogenic strains present in the colon such as *E. coli*, *Bacteroides* species, and *Eubacteria* species, but not towards epithelial or food-derived antigens (74;75). Cell lines derived from these bacterial antigen-specific CD4<sup>+</sup> T cells are sufficient for transferring the colitis phenotype to severe combined immunodeficient mice (SCID) (76). Regulatory cell lines generated by culturing cells with the same antigenic specificities in the presence of IL-10 can prevent this transferred colitis (77). The C3H/HeJBir phenotype may thus be explained by an overexuberant immune response directed toward commensal flora that is not sufficiently counterbalanced by adequate production of regulatory T cells.

One of the most widely studied models of mucosal inflammation involves the transfer of sorted wildtype splenic CD45RB<sup>hi</sup> CD4<sup>+</sup> T cells into SCID or recombinant activated gene (RAG)-2 mice (78). The resulting transmural colitis with heavy infiltration of mononuclear cells was initially shown to be prevented by cotransfer of the CD45RB<sup>lo</sup> subset (79). Independent studies have shown that cell sorting followed by adoptive transfer of pathogenic L-selectin<sup>hi</sup> cells and regulatory L-selectin<sup>lo</sup> cells results in similar

production and prevention of disease (80). CD45RB<sup>hi</sup> cells, previously thought to represent naïve cells (81), produce a polarized pattern of Th1 cytokines and the induction of colitis by these cells is abrogated by blockade of IFN $\gamma$  and/or TNF $\alpha$ , implicating a Th1 response as the pathogenic mechanism by which disease develops in this model (82). Unfractionated CD4<sup>+</sup> T cells from mice in which the costimulatory molecule OX40 ligand (OX40L) is overexpressed on T cells transfer a similar disease to immunodeficient mice, suggesting that OX40L costimulation may play a role in Th1-mediated colitis (83). The cell subsets responsible for the most potent anti-inflammatory activities of CD45RB<sup>lo</sup> T cells have more recently been defined as CD4<sup>+</sup> cells expressing CD25 (84), the  $\alpha_E\beta_7$  integrin (85), and the glucocorticoid-induced TNF receptor (GITR) (86). The regulatory functions exhibited by these cells are mediated through production of the cytokines IL-10 and TGF- $\beta$  (87;88) and through increased expression of the proliferation inhibitor cytotoxic T lymphocyte-associated antigen-4 (CTLA-4) (89).

Several models of IBD have been created through deletion or overexpression of genes encoding T cell cytokines or related proteins. IL-10 <sup>-/-</sup> mice develop chronic enterocolitis, presumably due to the absence of regulatory T cells (90). The disease is characterized by Th1 inflammatory infiltrate of neutrophils, activated macrophages, T cells, and IgA-producing plasma cells and can be treated using anti-IL-12 antibodies (91). The extent of disease is largely determined by bacteria flora composition, as mice housed in “dirty” conditions develop lesions throughout the colon, ileum, and jejunum, mice housed in specific pathogen-free (SPF) conditions develop only colonic inflammation, and mice house in germ-free conditions develop no inflammation at all (92). This importance of flora constituents is emphasized by the finding that IL-10 <sup>-/-</sup> mice housed

in SPF conditions and infected with *Helicobacter hepaticus* develop much more severe colitis than uninfected IL-10  $-/-$  mice, whereas infected wildtype mice do not develop overt inflammation due to the generation of antigen-specific T cells that secrete IL-10 (93). Colitis in IL-10  $-/-$  mice is also strain-dependent (94), and quantitative trait locus analysis of a cross between disease-susceptible C3H/HeJ mice and resistant C57BL/6 mice has identified a locus on mouse chromosome 3, which includes the gene encoding NF- $\kappa$ B, as the major determinant of colitis susceptibility in IL-10  $-/-$  mice (95).

IL-2  $-/-$  and IL-2 R $\alpha$  chain (CD25)  $-/-$ , but not IL-2R $\beta$  chain  $-/-$ , mice develop colitis in addition to systemic autoimmunity and hemolytic anemia (96-98). While disease is confined to the mucosa as in ulcerative colitis, the inflammation involves a Th1 response with high levels of IFN- $\gamma$  and IL-12 production (99). Unlike in IL-10  $-/-$  mice, inflammation still develops in IL-2  $-/-$  mice housed in germ-free conditions (100). Taken together with the finding that anergy and Fas-mediated cell death responses are impaired in IL-2  $-/-$  T cells (101), these results suggest that impairments in anergic deletion and activation-induced cell death in IL-2  $-/-$  mice lead to expanded lymphocyte populations, which in turn cause colitis development.

In addition to deletions of regulatory cytokines, increased Th1 cytokine signaling also promotes IBD development. Signal transducer and activator of transcription-4 (STAT4) is a transcription factor that mediates the pro-inflammatory transcriptional effects of IL-12, and overexpression of STAT-4 in a transgenic mouse model leads to a chronic transmural colitis phenotype (102). One of the few mouse models displaying small intestinal inflammation, TNF $^{\Delta ARE}$  mice, in which the regulatory AU-rich elements (ARE) found in the 3' untranslated region of TNF- $\alpha$  mRNA have been deleted, exhibit

substantial overproduction of TNF- $\alpha$ , chronic inflammatory arthritis, and severe transmural ileitis with both acute and chronic inflammatory infiltrates (103). Ileitis is dependent on TNF- $\alpha$  signaling through TNF receptor I, as TNF <sup>$\Delta$ ARE</sup> X TNFRI -/- mice do not develop disease, while TNF <sup>$\Delta$ ARE</sup> X TNFRII -/- mice exhibit more severe ileitis. Mice in which the TNF <sup>$\Delta$ ARE</sup> mutation is induced specifically in myeloid or T cells, via Cre/Lox recombination under a lysozyme or lck promoter, respectively, both develop the full ileitis phenotype (104). Further, both wildtype mice reconstituted with TNF <sup>$\Delta$ ARE</sup> leukocytes and TNF <sup>$\Delta$ ARE</sup> mice reconstituted with wildtype leukocytes via bone marrow transplantation also develop severe ileitis (104). These results not only show that total levels and not the specific cellular source of TNF- $\alpha$  are responsible for the TNF <sup>$\Delta$ ARE</sup> phenotype, but also more broadly demonstrate that defects in either hematopoietic or non-hematopoietic cells can lead to the same ileitis phenotype.

Other leukocyte subsets can influence disease development in IBD models. Deletion of STAT3, a transcription factor activated by many cytokine signaling pathways, in myeloid cells (LysMcre/Stat3<sup>flox/-</sup>) or in all hematopoietic cells, but not in T cells, results in an ileitis and colitis phenotype that closely resembles that seen in Crohn's disease (105;106). Defects in TNF- $\alpha$ , IL-6, and nitric oxide downregulation in response to IL-10 in LysMcre/Stat3<sup>flox/-</sup> peritoneal macrophages suggest that primary dysregulation of macrophage function may precipitate the Th1-mediated immune response seen in these mice (105). In a model of ulcerative colitis and carcinoma induced by deletion of the G protein G $\alpha$ i2 (107), the most prominent leukocyte abnormality is the decreased number and function of B1a B cells recognizing T cell-independent antigens and the increased

number of T cell-dependent B2 B cells (108). These alterations lead to decreased B cell responsiveness to lipopolysaccharide (LPS) stimulation in *Gαi2*<sup>-/-</sup> mice, which is speculated to impact the ability of B cells to control normal flora elements at the mucosal interface (108). T cell receptor (TCR)- $\alpha$ <sup>-/-</sup> mice develop a mild superficial chronic colitis that is substantially exacerbated when TCR- $\alpha$ <sup>-/-</sup> mice are crossed with mice lacking B cells (*Igμ*<sup>-/-</sup>) (109;110). The protective effect of B cells in TCR- $\alpha$ <sup>-/-</sup> mice was later attributed to a subset of B1-like cells expressing high levels of CD1D and IL-10 (111). In contrast, CD45RB<sup>hi</sup> CD4<sup>+</sup> T cells from IFN- $\gamma$ <sup>-/-</sup> mice induced chronic ileitis in SCID mice only when cotransferred with B cells (112). The lesions were characterized by villus atrophy, increased goblet cells, and IgA plasma cells infiltration.

Several models have also been developed in which the precipitating event leading to inflammation is an acute disruption of epithelial barrier function. Administration of dextran sodium sulfate (DSS) in the drinking water results in acute colitis in wildtype mice starting at 6 days after ingestion that is associated with a predominately neutrophilic infiltrate, crypt abscesses, weight loss, and rectal bleeding (113). Repeated cycles of DSS can produce chronic colitis with lymphocytes representing the main inflammatory cell-type present. The severity of DSS colitis is strain-dependent (114), and DSS-driven increases in epithelial permeability precede and most likely cause disease onset (115). DSS colitis occurs with similar kinetics and severity in wildtype versus SCID mice (116), emphasizing the primacy of epithelial cell function and innate immunity in the pathogenesis of disease in this model. Because of the ease of inducing DSS colitis in wildtype mice, this model has been used to study many aspects of intestinal inflammatory responses. In particular, trafficking requirements, in terms of

adhesion molecule and chemokine/chemokine receptor usage, have been studied extensively in DSS colitis (117-121), although the contributions of many molecules to disease development including the requirement for mucosal addressin cellular adhesion molecule (MAdCAM)-1-mediated adhesion remain controversial (122;123).

Haptenizing agents such as trinitrobenzene sulfonic acid (TNBS) and oxazolone induce MHC class II-specific immune responses to autologous proteins. These haptenizing agents can produce colitis in susceptible strains of mice, but only when instilled into the colon directly via enema in a solution of ethanol that serves to disrupt the epithelial barrier (124;125). This disruption may be necessary to allow penetration of the hapten to sites where immune cells perceive it as a product of an invading pathogen, as mice given TNBS-haptenized proteins orally prior to the enema develop tolerance to these antigens (126). Interestingly, TNBS and oxazolone induce opposing immune responses, as TNBS elicits a Th1 response blocked by anti-IL-12 antibodies, while oxazolone produces a Th2 response ameliorated by anti-IL-4 antibodies (124;125). Mice in which the gene encoding a multi-drug resistance protein has been deleted (*mdr1a* <sup>-/-</sup>) provide an additional model in which epithelial dysfunction appears to produce colitis (127), though the penetrance of disease in this model is lower than 50%. Wildtype mice reconstituted with *mdr1a* <sup>-/-</sup> bone marrow do not develop disease, whereas colons from many *mdr1a* <sup>-/-</sup> mice reconstituted with wildtype bone marrow remain inflamed. The mechanism by which *mdr1a* function prevents disease is not understood, although given that antibiotic treatment eliminates colitis in most *mdr1a* <sup>-/-</sup> mice and that *mdr1a* proteins serve as molecular transporters at barrier interfaces, it has been speculated that *mdr1a* <sup>-/-</sup>

epithelial cells may have defects in permeability regulation or in the ability to expunge bacterial toxins (127).

## **Maintenance of Mucosal Homeostasis**

### *Epithelial barrier function and contributions to innate immunity*

Up to  $10^{12}$  bacteria per gram of tissue line the luminal surface of the distal ileum and colon in humans (128). Therefore, the maintenance of an active epithelial permeability barrier preventing the transepithelial migration of luminal bacteria serves as the first step toward achieving mucosal homeostasis. Epithelial permeability is primarily controlled at the level of tight junctions. In particular, the density of tight junctional strands plays a critical role in determining tissue-specific restrictions on the size of particles that can pass through tight junctional pores (129), with estimates suggesting that particles bigger than 2000 Da are typically excluded by intestinal epithelial tight junctions (130). While many types of proteins comprise tight junctions, the two major structural constituents are claudin heterohexamers and the adjacent occludin molecules, both of which bind their counterparts on neighboring cells in a homotypic fashion (131). Five isoforms of claudins are known and interactions between these isoforms possess different affinities such that the isoform-specific expression patterns of claudins may provide one method of permeability regulation (132;133). Only one isoform of occludin is known, and its regulation occurs primarily through dephosphorylation, resulting in relocalization of the protein into the cytoplasm and increased epithelial permeability (134). The large protein zonula occludens (ZO)-1 serves as an adaptor protein linking claudins and occludins with

the actinomyosin ring of the epithelial cell, and many cellular signals aimed at altering permeability affect the expression or junctional localization of ZO-1 (135).

Increases in epithelial permeability during infection and inflammation can be elicited through a variety of pathways. Toxins from *Clostridium difficile* disrupt the Rho family of GTPases and produce tight junction disruption through disorganization of the actin cytoskeleton and redistribution of ZO-1 (136). *Giardia* sp. lead to increased permeability through a myosin light chain kinase-dependent mechanism that may involve contraction of the actinomyosin ring that physically pulls ZO-1 out of junctional complexes (137). Enteropathogenic *E. coli* induces dephosphorylation and tight junctional dissociation of occludin thereby increasing permeability (134). The *Vibrio cholerae* zonula occludens toxin and zonulin, an analogue of this toxin produced by intestinal epithelial cells in response to luminal bacterial colonization, produce increased epithelial permeability through disengagement of ZO-1 from tight junctions (138). TNF- $\alpha$  and IFN- $\gamma$  induce large increases in permeability of intestinal epithelial cell monolayers. This barrier disruption requires NF- $\kappa$ B transcriptional activation, still develops when cytokine-induced apoptotic pathways are inhibited, and is characterized by the redistribution of ZO-1, claudins, and occludin from the junctional interface to the cytoplasm (135;139).

In addition to providing a barrier to bacterial migration, the epithelium also plays a critical role in innate immunity and interacts closely with elements of the hematopoietic-derived immune system (130). The polymeric immunoglobulin receptor (pIgR) is expressed by epithelial cells and is responsible for transporting secretory IgA produced by lamina propria plasma cells to the luminal surface where it serves to neutralize bacteria before they can penetrate the barrier (140). The epithelium also produces the



human neonatal Fc receptor (FcRn) which facilitates the bidirectional transport of IgG, enabling not only the luminal secretion of IgG but also the reuptake of IgG bound to luminal antigen for processing by intestinal antigen-presenting cells (141). Epithelial cells, and particularly specialized Paneth cells, also produce and secrete anti-microbial compounds such as  $\alpha$ -defensins, catenins, and lysozyme (142). These compounds are stored in granules and released upon binding of common bacterial motifs by pattern recognition receptors such as TLR's. Of the eleven TLR's identified to date, at least 4, TLR2-5, are expressed by intestinal epithelial cells (143). TLR engagement elicits downstream effects through activation of transcription factors such as NF- $\kappa$ B (144). This signaling pathway along with others activate the expression of proinflammatory cytokines (145) and chemokines (146) by epithelial cells that lead to the recruitment of leukocytes. Therefore in coordination with immune cells, both barrier functions and the innate immune functions of the intestinal epithelium provide the primary defense in preventing infection and inflammation.

#### *Leukocyte compartments and trafficking requirements*

Leukocytes migrate to discrete compartments within the intestinal mucosa and the mucosa-associated lymphatic tissue (MALT) that serve distinct functions in the initiation and downregulation of mucosal immune responses. The lymphotoxin  $\alpha/\beta$  dimer, expressed on lymphoid cells and the lymphotoxin  $\beta$  receptor expressed on non-lymphoid cells are required for MALT formation, as mice in which the genes encoding these molecules have been deleted do not develop MALT or even the primitive anlage that ultimately forms these tissues (147).  $\beta_7$  integrins are also important in the formation of

mucosal lymphoid compartments, as  $\beta_7^{-/-}$  mice exhibit almost complete absence of Peyer's patch, lamina propria, and intraepithelial lymphocytes, while development of the mesenteric lymph node compartment is only partially impaired and spleen and peripheral lymph node populations are normal (148). Expression of the  $\alpha_4\beta_7$  integrin is found on many intestinal lymphocyte populations (149;150) and plays a critical role in the selective migration of cells to mucosal sites (151). Likewise, the endothelial ligand for  $\alpha_4\beta_7$  (152), mucosal addressin cellular adhesion molecule- (MAdCAM)-1, is expressed in a tissue specific pattern by high endothelial venules in intestinal lymphoid tissues and by venules in the intestinal mucosa (153) (Table 2.3). Thus, the  $\alpha_4\beta_7$ / MAdCAM-1 axis forms the primary basis for selective homing of lymphocyte populations to the intestine and associated sites (154).

The initial site of antigen encounter for many mucosal lymphocytes occurs in Peyer's patches (PP) that are most abundantly found at specific sites along the anti-mesenteric border of the ileum. They are separated from the lumen by the follicle-associated epithelium containing specialized M cells that deliver antigens from the lumen directly into the PP interstitium (155). Two extensive intravital microscopy studies revealed the precise adhesion molecule requirements for lymphocyte entry into PP (156;157). L-selectin is required to mediate initial rolling interactions with the endothelium in high endothelial venules (HEV). The ligand through which L-selectin mediates this function is unknown, though it is likely distinct from L-selectin ligands that mediate rolling in peripheral venules in terms of post-translational carbohydrate modification (158). *In vitro* studies have suggested that L-selectin mediates rolling on properly glycosylated MAdCAM-1 harvested from lymphoid organs, though the relevance of this interaction *in*

Molecules expressed by endothelial, epithelial, or tissue stromal cells	PP	MLN	Ileum	Colon
MAdCAM-1	C	C	C,I	C,I
ICAM-1	C	C	C,I	C
VCAM-1	I	n.d.	C,I	C,I
P-selectin	I	n.d.	I	I
E-selectin	-	n.d.	I	I
Peripheral Node Addressin (PNA <sub>d</sub> )	-	C	I	I
Unknown L-selectin Ligands	C	n.d.	n.d.	n.d.
CCL21 (SLC)	C	C	-	-
CXCL12 (SDF-1)	C	C	C	C
CXCL13 (BLC)	C	C	-	-
CCL20 (LARC)	-	-	C	C
CCL25 (TECK)	-	-	C	-
CCL28 (MEC)	-	-	C	C,I
CXCL1 (MIP-2), CXCL5 (ENA-78), CXCL8 (IL-8)	-	-	I	I
CXCL9 (Mig), CXCL10 (IP-10)	-	-	I	I
CCL2 (MCP-1), CCL3 (MIP-1 $\alpha$ ), CCL5 (RANTES)	-	-	I	I

**Table 2.3.** Expression of adhesion molecules and chemokines in mucosal lymphoid and effector sites. C, constitutively expressed. I, induced during inflammation. n.d., not determined. -, not expressed.

*vivo* is unclear (159).  $\alpha_4\beta_7$  plays a minor role in slow rolling of lymphocytes and a major role in arrest, as  $\alpha_4\beta_7$  blockade or  $\beta_7$  deficiency results in almost complete absence of adherent cells in PP HEV (156;157). Blockade of the  $\alpha_L\beta_2$  integrin, also known as lymphocyte function antigen- (LFA)-1, also results in decreased numbers of adherent cells in PP HEV, suggesting that  $\alpha_4\beta_7$  and LFA-1 may play distinct roles in the same pathway leading to firm arrest (157). Blockade of both L-selectin and  $\alpha_4$  is required to completely eliminate homing to PP (151). Conversion of lymphocyte rolling to arrest on PP HEV requires a chemokine-mediated activation step (157). The chemokine CCL21

(SLC) is displayed on the luminal surface of HEV's, initiates signaling events by binding CCR7 on rolling T cells or dendritic cells, and also promotes the chemotaxis of these cells into T cell zones (160). CXCL13 (BLC) is also displayed by PP HEV's and mediates the activation of CXCR5<sup>+</sup> B cell arrest and the migration of this subset into B cell follicles (161).

Mesenteric lymph nodes serve as the primary draining lymphoid tissues for lymphocytes and APC's leaving both Peyer's patches and intestinal mucosa effector sites, thereby enabling interactions between effector cells and cells in the initial stages of activation and programming (162). The importance of MLN in modulation of immune responses is emphasized by the finding that during infection, intact bacteria can be found in MLN in association with antigen presenting cells (163;164). MLN developmental requirements are distinct from that of peripheral lymph nodes and Peyer's patches in that the formation of the MLN lymphocyte compartment does not fully require lymphotoxins (147) and occurs in the absence of  $\beta_7$  integrins (148). Combinatorial blockade or deficiency of  $\beta_7$  and L-selectin abrogates lymphocyte homing to MLN (165). L-selectin plays the dominant role in this blockade, since L-selectin blockade alone leads to an over 80% reduction in lymphocyte migration in to MLN while  $\beta_7$  blockade alone has minimal effects (151). The L-selectin predominance of homing to mesenteric lymph nodes may be due to the fact that in addition to MAdCAM-1 expression, MLN HEV express functional peripheral node addressin (PNAd), a powerful ligand for L-selectin, whereas PP HEV do not (166). The chemokine requirements for cell migration within MLN have not been investigated in detail.

Under homeostatic conditions leukocytes in the lamina propria are largely derived from cells that have trafficked through MALT, and consist of a large population of  $\alpha\beta$  TCR CD4 cells along with smaller populations of CD8<sup>+</sup> T cells, CD19<sup>+</sup> B cells, and CD38<sup>+</sup> IgA- and to a lesser extent IgG-secreting plasma cells (128;167). MAdCAM-1 is expressed constitutively at intermediate levels on lamina propria venules in both the small and large intestine (153). While ICAM-1 and vascular cell adhesion molecule- (VCAM)-1 may be expressed in the normal intestine, albeit at very low levels (168;169),  $\alpha_4\beta_7$  interactions with MAdCAM-1 appear to be the primary pathway through which cells constitutively enter the lamina propria. The number of lamina propria lymphocytes (LPL) in normal conditions is severely decreased by blockade or absence of  $\alpha_4\beta_7$ , but not by VCAM-1 blockade (148;151). Consistent with this finding, the expression of  $\alpha_4\beta_7$  is considerably upregulated on both T cells and B lineage cells that home to the lamina propria as opposed to those that home to other sites (150;170). P- and E-selectin are not expressed in the uninfamed intestine (171). Therefore L-selectin may be required to mediate rolling interactions of leukocytes with lamina propria venules under normal conditions. Indeed, blockade of L-selectin partially inhibits lymphocyte homing to the intestinal wall (151).

During inflammation, expression of VCAM-1, which binds to the  $\alpha_4\beta_1$  integrin expressed by many leukocytes, and MAdCAM-1 is dramatically increased by both ileal and colonic lamina propria venules (172), while ICAM-1 appears to be upregulated by ileal, but not colonic vessels (169;173). Arrest of leukocytes in inflamed colonic lamina propria venules is blocked by anti-MAdCAM-1 or anti-VCAM-1 antibodies, but not by anti-ICAM-1 antibodies (122). P- and E-selectin are both upregulated in the colon during

TNBS colitis, and all three selectins mediate rolling in colonic venules during TNBS colitis, though P-selectin-mediated rolling dominates in the early phases of the response (171). Experimental colitis can be ameliorated by treatment with antibodies blocking VCAM-1, E-selectin, or the selectin ligand PSGL-1, while the effects of MAdCAM-1, ICAM-1, or P-selectin blockade are either minimal or controversial (120-123;169;171). Blockade of  $\alpha_4$  integrins or combinatorial blockade of ICAM-1 and VCAM-1 or MAdCAM-1 and L-selectin inhibit the development of ileal inflammation (173)(Rivera-Nieves, Olson, et. al., In Revision).

Positioning of chemokines at specific sites in the intestinal wall may also play important roles in the constitutive homing of inflammatory cells (174). CCL25, also known as TECK, is constitutively expressed by crypt epithelial cells in the small intestine (175), and virtually all T cells in the lamina propria of the uninflamed small intestine express its receptor CCR9 (175). Activation of MLN, but not cutaneous lymph node, CD4<sup>+</sup> T cells leads to the acquisition of TECK responsiveness, suggesting that CCR9 expression and TECK-mediated homing to the lamina propria involves the specific recruitment of cells primed in gastrointestinal MALT (176). Other subsets of cells derived from MALT, including CD8<sup>+</sup> T cells (177), and IgA-secreting plasma cells (178), have also been shown to migrate to the small intestine via a TECK/CCR9 dependent mechanism. In contrast, CCR9<sup>+</sup> cells and TECK are not prevalent in colonic lamina propria (175), and the increased level of CCL28 (MEC) expressed in the colon relative to the ileum suggests that constitutive trafficking to the colonic mucosa may be controlled by CCL28 binding to CCR10 (179). A third chemokine, LARC is expressed

constitutively by cells comprising the villous epithelium in both ileum and colon, and may mediate the constitutive trafficking of dendritic cells to intestinal sites (180).

During intestinal inflammation epithelial cells express several chemokines that attract myeloid cells such as CXCL8 (IL-8), CXCL5 (ENA-78), and CXCL1 (MIP-2 in mouse, GRO $\alpha$  in humans) (117;146). The expression of CXCL10 (IP-10) and CXCL9 (Mig) are induced by Th1 inflammation *in vivo* and by IFN- $\gamma$  treatment *in vitro* and these chemokines can mediate chemotaxis of most mucosal lymphocytes through interactions with CXCR3 (181;182). Mice deficient in CCR2 or CCR5 do not develop DSS colitis, suggesting that colonic inflammation may require migration mediated by their chemokine ligands CCL2 (MCP-1), CCL3 (MIP-1 $\alpha$ ), and CCL5 (RANTES) (119).

The intraepithelial lymphocyte (IEL) compartment is comprised of a mixture of T cells, including classic lymphoid organ-derived  $\alpha\beta$  TCR T cells (CD8 $^{+}$  > CD4 $^{+}$ ), the locally derived  $\gamma\delta$  TCR T cell population, and the unique self-reactive CD8 $\alpha\alpha^{+}$  T cell population (183).  $\gamma\delta$  TCR T cells and CD8 $\alpha\alpha^{+}$  T cells appear to play roles in the prevention of IBD in DSS colitis and adoptive transfer models, respectively (184;185). During ileal inflammation, the ratio of  $\alpha\beta$  TCR to  $\gamma\delta$  TCR T cell is considerably increased (186). Entrance into the intraepithelial compartment is thought to be controlled through interactions of the  $\alpha_E\beta_7$  integrin, expressed by greater than 90% of IEL's (167), with its epithelial ligand, E-cadherin (187).  $\alpha_E$   $-/-$  mice have considerably decreased numbers of IEL (188), while LPL numbers are also reduced in these mice, suggesting that  $\alpha_E\beta_7$  binding to an unknown endothelial ligand (189) may mediate lamina propria entry.

Splenocytes also exhibit a profound effect on intestinal homeostasis, as evidenced by the colitis-producing and -preventing capacities of splenocyte subsets in the CD45RB<sup>hi</sup> adoptive transfer model described above. A final population of leukocytes that influence the mucosal environment are peritoneal-derived B1 B cells (190). Precursors of this population migrate to the peritoneum early in the neonatal period and generate a self-replenishing pool of B cells that produce either IgM or IgA antibodies (191). Bone marrow chimeras, in which peritoneal B cells and bone marrow cells producing antibodies of different allotypes were used to reconstitute irradiated mice, have shown that roughly half of the IgA in the intestine is derived from B1 cells (192). This IgA does not undergo somatic hypermutation, is produced even in the absence of MHC class II-restricted T cell help (140) and specifically recognizes T-independent common bacterial antigens present on normal intestinal flora (193). B1 cell immunoglobulin is thought to serve an anti-inflammatory function by containing bacteria at the luminal surface, whereas higher affinity B2-derived immunoglobulin functions to help eliminate invasive pathogens (194). CXCL13 <sup>-/-</sup> mice lack peritoneal B1 cells entirely, suggesting that this chemokine and its receptor, CXCR5, play critical roles in B1 cell homing (195).

#### *Tolerance, regulatory T cells, and control of mucosal immune responses*

The induction of immunological tolerance to orally ingested food antigen as well as to antigens of the normal intestinal flora is necessary to prevent induction of pro-inflammatory immune responses directed against these antigens. High dose oral antigen exposure triggers tolerance through the clonal deletion of cells recognizing this antigen, whereas low dose oral antigen exposure leads to tolerance through the induction of antigen-specific regulatory T cells (Treg) that suppress cell proliferation through



transforming growth factor (TGF)- $\beta$  production (196). TNBS enemas do not induce colitis in mice that have been previously given orally administered colonic proteins haptenized *in vitro* with TNBS (126). Administration of rIL-12 or antibodies blocking TGF- $\beta$  function at the same time as the administration of the oral proteins prevents tolerance development, suggesting that the Treg generation is required for this tolerance response. Mice receiving TNBS enemas alone lose tolerance to their own intestinal bacterial antigens as measured by *in vitro* reactivity of mononuclear cells to these antigens (197). This tolerance is restored when rIL-10 or anti-IL-12 antibodies are administered systemically at the same time as TNBS administration (197). The physiologic basis of tolerance is believed to begin with specialized IL-10-producing dendritic cell (DC) populations located in both the subepithelial dome separating Peyer's patches from the follicular associated epithelium and the intestinal mucosa itself (162). These DC sample antigen provided by specialized M cells and normal enterocytes. Interactions between these dendritic cells and T cells likely occur within the MLN, as mice in which MLN and PP formation was prevented by *in utero* injections of TNFR- and LT $\beta$ R-IgG fusion proteins could not develop oral tolerance responses, whereas mice lacking only PP due to *in utero* injection of the LT $\beta$ R-IgG fusion protein displayed normal oral tolerance (198). Further, oral antigen-induced T cell responses can be found within the MLN within a few hours of antigen administration (162).

Whether regulatory T cells (Treg) arise from specific T cell clones selected as regulatory cells in the thymus or from conventional T cells recruited to assume a regulatory phenotype in the periphery remains unclear (199). Regardless, at least 3 distinct classes of T cells have been identified that display regulatory or anti-

inflammatory properties. CD25<sup>+</sup> CD4<sup>+</sup> T cells, also referred to as Th3 cells, are the most widely studied regulatory cell type and are believed to induce their regulatory effects through secretion and cell-surface expression of TGF- $\beta$ , and not IL-10 (200). The Tr1 class of regulatory cells was defined from cell clones that were CD4<sup>+</sup> CD25<sup>-</sup>, expressed high levels of IL-10, but not TGF- $\beta$ , and yet still abrogated adoptively transferred colitis produced by CD45RB<sup>hi</sup> cells (201). Whether Tr1 cells are truly distinct from Th3 cells or whether these subsets are related regulatory populations is unclear. Many reports suggest CD4<sup>+</sup> CD25<sup>+</sup> regulatory cells from spleen express high levels of IL-10 in addition to TGF- $\beta$  (85;202). Further, TGF- $\beta$ -producing regulatory cells have been shown to induce IL-10-producing cells (203), and IL-10 is required for at least some of the downstream effects of TGF- $\beta$ -mediated suppression (204). CD8<sup>+</sup> T cell subsets comprise the third class of cells with regulatory functions *in vivo*, but roles played by these cells in preventing intestinal inflammation have not been established (200).

CD4<sup>+</sup> CD25<sup>+</sup> regulatory T cells, but not naïve or activated effector CD4<sup>+</sup> CD25<sup>-</sup> T cells, express the transcription factor Foxp3. Foxp3 is a member of the Forkhead/winged helix domain family of DNA binding factors that prevents the expression of proliferative and proinflammatory cytokines like IL-2 through inhibiting DNA-binding of the pro-inflammatory transcription factor NFAT (205). Mice lacking functional Foxp3 develop severe lymphoproliferation and systemic autoimmunity, do not develop normal Treg populations, and can be rescued from this phenotype by infusion of wildtype regulatory cells (206). This study also demonstrated that infection of effector CD4<sup>+</sup> T cells with a retroviral construct encoding Foxp3 led to the acquisition of suppressive functions by these cells. Further studies have shown that culture of naïve CD4<sup>+</sup>CD25<sup>-</sup> T cells with

TGF- $\beta$  leads to Foxp3 expression and subsequent conversion of these cells to a regulatory phenotype (207). Foxp3-converted regulatory cells exert suppressive functions through production of both IL-10 and TGF- $\beta$  (206;207). Unlike CD4<sup>+</sup> CD25<sup>+</sup> T cells, classically-derived IL-10-producing Tr1 cells do not express Foxp3, though these are equally capable of suppressing effector T cell functions (208).

The roles played by several other molecules in regulatory T cell function have also recently been identified. Constitutive expression of CTLA-4 only occurs on Treg, and blockade of costimulatory signals provided by this molecule inhibits the ability of Treg to block CD45RB<sup>hi</sup> CD4<sup>+</sup> T cell-mediated colitis (89). A gene array study examining differences in gene expression between CD4<sup>+</sup>CD25<sup>+</sup> and CD4<sup>+</sup>CD25<sup>-</sup> T cells revealed the selective expression of the  $\alpha_E\beta_7$  integrin and GITR by the CD4<sup>+</sup>CD25<sup>+</sup> subset. Compared to  $\alpha_E\beta_7^-$  CD25<sup>+</sup> cells,  $\alpha_E\beta_7^+$  CD25<sup>+</sup> cells have been shown to exhibit more potent inhibition of colitis (85), increased adhesion molecule expression, greater chemotactic responses toward effector chemokines, and increased migration to inflammatory sites (209). Ligation of GITR by either anti-GITR antibodies or GITR ligand expressed by subsets of antigen presenting cells (210;211), leads to proliferation of Treg, abrogation of Treg-mediated suppression of effector T cell proliferation, and development of autoimmune gastritis in otherwise normal mice when the anti-GITR antibodies are administered *in vivo* (212;213). GITR thus serves as a target for other leukocytes attempting to overcome suppressive signals provided by Treg.

## How Homeostasis Is Broken....Potential Etiologies of Crohn's Disease

### *Infection and bacterial flora abnormalities*

Infection mediated by one of several difficult to detect strains of bacteria, including those listed in Table 2.4, has been suggested as an etiologic cause of Crohn's disease. *Mycobacterium avium* paratuberculosis (MAP) is resistant to filtration, chlorination and pasteurization methods used in food and drinking water purification, and produces Johne's disease, a chronic granulomatous intestinal disease resembling Crohn's disease, in both wild and domesticated animals (214). One study showed that MAP RNA was detectable in ileal biopsies from all patients with Crohn's disease whereas it was not present in ileal samples from control subjects (215). Other studies have suggested that Crohn's disease may be caused by refrigeration-resistant *Yersina* species that have been documented to produce ileocolitis in children and young adults through the usage of Yop virulence proteins that interfere with NF- $\kappa$ B function (31). *Helicobacter hepaticus* can infect humans and produces intestinal inflammation in mouse models (93).

<b>Infectious Agent</b>
<i>Mycobacterium avium paratuberculosis</i> (MAP)
<i>Yersina enterocolitica</i>
<i>Yersina paratuberculosis</i>
<i>Listeria monocytogenes</i>
<i>Salmonella typhimurium</i>
<i>Bacteroides vulgatus</i>
<i>Helicobacter hepaticus</i>
Paramyxovirus (measles)

**Table 2.4.** Potential pathogens linked to the development of Crohn's disease

Even if infections do not cause Crohn's disease, bacterial colonization of the intestinal surface is required for its development (71). Genetic susceptibility defects such as NOD2 mutations produce altered function of proteins directly involved in interactions with bacterial flora (43),

and thus defective bacterial sensing may comprise an important part of Crohn's etiology. Antibiotic therapy of Crohn's disease has met with mixed results, though several studies using multi-drug therapy have shown promise (25). Studies in which combinatorial therapy included macrolides, which unlike other antibiotics is active against MAP, have produced clinical improvement in most and remission in some patients (214). Combination therapy including ciprofloxacin, which is active against *Yersina* species, downregulates experimental ileitis (216). Probiotic therapy, in which oral or rectal administration of innocuous *Lactobacilli* species recolonizes the intestinal bacterial flora, has shown promise in animal models, but results from case reports have been mixed, and no large scale clinical trials have been conducted (24).

#### *Aberrant Th1 polarization and overactivation of the immune system*

Since the findings that pro-inflammatory cytokines such as TNF- $\alpha$ , IFN- $\gamma$ , and IL-12 were overexpressed by lamina propria mononuclear cells from Crohn's patients (17;18;217), the predominant paradigm regarding the etiology of Crohn's disease has postulated that the disease is caused by an inherent T cell predisposition to undergo pro-inflammatory Th1 polarization. Certainly these cytokines are directly responsible for many pathological sequelae, including neutrophil infiltration leading to crypt abscess and granuloma formation (218). Overexpression of TNF- $\alpha$  and IL-12 in the TNF <sup>$\Delta$ ARE</sup> and Stat4 transgenic models discussed above show that intrinsic defects in Th1 polarization pathways can lead to the development of Crohn's-like inflammation. However, no genetic studies have found correlations between polymorphisms in genes controlling IFN- $\gamma$  and IL-12 production and the development of Crohn's Disease in humans (65), and

while polymorphisms in the TNF- $\alpha$  gene correlate with disease severity, these alleles do not segregate people who develop disease from those who do not (54). Therefore whether overactivation of Th1 pathways is a cause or a consequence of the primary disease-producing defect remains unclear.

NOD2 was first thought to be exclusively expressed by monocytes (45). In the initial characterization of NOD2 variants in Crohn's patients (40), it was postulated that these variants may lead to overactivation of NF- $\kappa$ B-induced cytokine production. However, it has since been reported that NOD2 is not expressed by tissue macrophages and that epithelial cells may actually express higher levels of NOD2 than do circulating monocytes (219). Further, the NOD2 mutations associated with Crohn's disease are actually less capable of activating NF- $\kappa$ B (47), suggesting that NOD2 mutations do not directly increase Th1 cytokine production through NF- $\kappa$ B-mediated transcription.

The most convincing evidence in favor of intrinsic immunological defects causing Crohn's disease is provided by case reports showing that allogeneic bone marrow transplantation leads to disease remission in many patients (220). However, these findings do not differentiate whether the native marrow in Crohn's patients produced disease due to increased intrinsic pro-inflammatory properties or due to defective tolerance mechanisms or regulatory T cell function.

### *Breakdown in immunological tolerance and regulatory T cell function*

Many studies indicate that tolerance to innocuous antigens is broken in IBD patients. Patients with IBD developed substantially higher titers of antibodies to proteins found in cow's milk compared to healthy controls (221). Lamina propria mononuclear cells from

IBD patients, but not from healthy controls, proliferated and produced high levels of inflammatory cytokines when cultured with autologous intestinal bacterial sonicates (222). T cells from Crohn's patients receiving oral doses followed by subcutaneous injections of a specific antigen exhibited strong proliferative responses toward this antigen, whereas T cells from healthy controls displayed tolerance (223). The latter study was carried out in patients during remission or with only mild disease, suggesting that lack of tolerance was not caused by leakage of orally administered antigen through ulcerated lesions. However, given that epithelial permeability is increased in Crohn's patients even during remission (224), loss of tolerance could still result from inappropriate entry of innocuous antigens into the intestinal mucosa.

Defective tolerance could also be caused by regulatory T cell dysfunction, though no specific evidence exists showing that this mechanism plays a role in human Crohn's disease. Enterocolitis in IL-10  $-/-$  mice suggests that decreased regulatory T cell function can lead to a Crohn's-like phenotype, though specific disease-conferring alleles of the IL-10 gene in humans have not been identified (67). Blockade of regulatory T cell function *in vivo* by treatment with anti-GITR antibodies leads to autoimmune gastrointestinal inflammation in mice (213). Loss of function mutations in the human homolog of the regulatory cell transcription factor Foxp3 lead to a disease known as X-linked autoimmunity-allergic dysregulation syndrome, which presents early in life as multiple autoimmune disorders, including Type I diabetes, thyroiditis, hemolytic anemia, severe allergy, and intestinal inflammation (225). Alterations of GITR or Foxp3 function in Crohn's patients have not been studied in detail.

### *B lymphocyte function and Immunoglobulin Reactivity*

Despite the massive infiltration of plasma cells seen in Crohn's lesions, little was known regarding the role of B cells and immunoglobulin in the pathogenesis of Crohn's disease until the last decade. Recently, many studies have identified elevated antibody titers in Crohn's patients recognizing specific dietary, bacterial, and auto-antigens (Table 2.5) (226-232). Interestingly, most patients with Crohn's disease only possess antibodies responding to one or two antigens, while 15-20% of patient's serum do not react to these antigens (232). Patients responding to 3 or more of these antigens were found to have much more severe disease and more frequently underwent surgical therapy (233). These

Antigen	Description	Increased Isotype Response in CD
Flagellin	Present on most motile bacteria including <i>Salmonella</i> strains	IgG
HupB pANCA	Anti-neutrophil cytoplasmic antibody and mycobacterial homologue	IgA
Gal ( $\alpha$ 1-3) Gal	Galactosyl epitopes expressed ubiquitously by enteric flora	IgM, IgG, IgA
I2	Member of ubiquitous bacterial transcription factor family found in <i>Pseudomonas</i>	IgA, IgG
ASCA	Anti- <i>Saccharomyces cerevesiae</i> antibody	IgA, IgG
OmpC	<i>E. coli</i> outer membrane porin C	IgA
OmpW	<i>Bacteroides</i> outer membrane porin W	IgA
<i>E. coli</i> <i>B. fragilis</i> <i>C. perfringens</i> <i>Ent. Faecalis</i>	Sonicates of these bacteria reacted strongly with mucosal immunoglobulin from Crohn's patients	IgG
Casein, BSA, lactoglobulin	Components of cow's milk	IgG, IgM, +/- IgA
Gliadin	Component of wheat, also causes celiac disease	IgA

**Table 2.5.** Bacterial, food, and auto-antigens toward which Crohn's patients have elevated antibody titers compared to titers in healthy controls. CD, Crohn's disease.



data are consistent with a paradigm in which increased immunoglobulin responses to enteric antigen exacerbate, but do not cause, disease in susceptible individuals.

The role of B cells themselves in IBD pathogenesis is just beginning to be investigated using animal models. Populations of IL-10-expressing B1 type B cells are protective in the TCR $\alpha$  model of colitis (111). In contrast, B cells increase the severity of SCID ileal inflammation induced by IFN- $\gamma$  -/- T cells (112), and B2 type B cells appear to promote disease in the G $\alpha$ i2 -/- colitis model (108). In these models, B cells again play an accessory rather than an etiologic role in disease pathogenesis.

### *Defects in Innate Immunity and Epithelial Dysfunction*

Many studies using a variety of techniques have demonstrated that Crohn's patients exhibit increased small intestinal epithelial permeability relative to unaffected individuals (32). The most persuasive evidence suggesting that Crohn's disease may be a primary disorder of epithelial dysfunction was provided by studies in which up to 10% of unaffected close relatives of Crohn's patients were shown to have considerably increased epithelial permeability relative to the general population (234;235). Interestingly, a similar percentage of relatives eventually develop disease (224). Unaffected relatives with high intestinal permeability also have increased levels of immune activation relative to the general population, as measured by numbers of circulating CD45RO-expressing B cells (236). Generation of these memory cells in response to permeability-dependent increases in bacterial infiltrates may thus represent an early stage of disease onset (224).

NOD2 is expressed at high levels by specialized Paneth epithelial cells that are responsible for many of the antimicrobial properties of the epithelial layer including

TNF- $\alpha$  and defensin production (219). Mutations in NOD2-mediated bacterial sensing may thus produce Crohn's disease through decreased innate immune function of epithelial cells. Toll-like receptor expression by epithelial cells is altered in Crohn's patients versus the general population, suggesting that extracellular bacterial sensing by epithelial cells may also be abnormal in Crohn's patients. These alterations may also be tied to defects in barrier function, as activation of NF- $\kappa$ B through TLR's and NOD2 pathways can significantly increase epithelial permeability (135). Compared to cells from healthy individuals, colonic villus epithelial cells from IBD patients express lower levels of Ppar $\gamma$  (237), a transcription factor that exerts anti-inflammatory effects through inhibition of NF- $\kappa$ B (238), and overexpression of Ppar $\gamma$  abrogates experimental colitis (239). These data suggest that loss of Ppar $\gamma$  function in the epithelium may result in overactivation of NF- $\kappa$ B-mediated effects on epithelial permeability and responses to bacterial flora.

Innate immunity provided by myeloid lineage cells may also be impaired in Crohn's disease. In a small clinical trial, treatment of Crohn's patients with granulocyte-macrophage colony stimulating factor (GM-CSF), a molecule that enhances production, maturation, and function of neutrophils and monocytes, led to clinical improvement in most and remission in half of treated patients (240). The precise mechanism by which this therapy ameliorates disease remains unclear.

### **The SAMP1/YitFc Model: Previous Work and Study Rationale**

The SAMP1/YitFc murine ileitis model provides an excellent system in which to study the contributions made by specific tissues and cell types to the development of

Crohn's disease, partly because it is one of the few models in which inflammation is largely delimited to the ileum, the hallmark site of Crohn's lesions (9). Additionally, this phenotype arose spontaneously, through continuous brother-sister breeding of wildtype AKR mice in the absence of specific chemical, genetic, or immunologic manipulations (241). Therefore, the ileitis susceptibility in this strain may resemble the complex polygenic and environmental susceptibility that causes human Crohn's disease.

The SAMP1/Yit strain was derived in Japan through 20 generations of breeding littermates from the senescence accelerated mouse (SAM)P1 line, which in turn was originally derived from AKR/J littermate breeding (241). Inflammation in the GI tract exhibited 100% penetrance and was limited to the ileum and cecum. Lesions were characterized by acute and chronic inflammation, crypt abscesses, crypt epithelial cell hyperplasia with villous blunting, and transmural wall thickening. Periocular and dorsal inflammatory skin lesions accompanied the ileitis in 90% of mice, whereas liver inflammation occurred in around 50%. Additionally, this report demonstrated that ileitis did not develop in mice housed under germ-free conditions. A follow-up study demonstrated that mice developed disease by 30 weeks of age and that the ileal pathology shared many features with Crohn's ileitis pathology, including granuloma formation, segmental lesion development in which areas of normal bowel separated inflamed sections, expansion of Paneth and mucus-secreting Goblet cells, an increased ratio of  $\alpha\beta$  TCR:  $\gamma\delta$  TCR T cells in the IEL and LPL compartments, and large infiltrations of plasma cells (186). Distinctions that developed between the disease phenotype in mice housed at the University of Virginia and the originally described phenotype, including an inverse correlation between skin and ileal lesions, earlier onset of disease (10 weeks), and the

development of perianal fistulas in a subset of mice, led to the classification of a new substrain, SAMP1/YitFc, to describe mice maintained at the University of Virginia (242).

Inflammation in SAMP1/YitFc mice is thought to develop through a Th1 pathway, as MLN lymphocytes from SAMP1/YitFc, but not AKR, mice produce high levels of IFN- $\gamma$  and TNF- $\alpha$  (186). Downregulation of disease severity produced by antibiotic therapy with ciprofloxacin and metronidazole is accompanied by decreased Th1 cytokine production (216). Similar to the effects of infliximab therapy in Crohn's patients, anti-TNF- $\alpha$  antibodies ameliorate SAMP1/YitFc ileitis severity through a mechanism involving apoptosis of lamina propria mononuclear cells (243). Two recent reports have shown that Th2-polarizing cytokines may augment already established disease (244) (Bamias, et.al., *Gastroenterology*, In Revision). SAMP1/YitFc mesenteric lymph node (MLN) CD4<sup>+</sup> T cells adoptively transfer the ileitis phenotype to SCID mice, though AKR T cells also induce ileitis with somewhat lower severity (186). The severity of adoptively transferred ileitis is decreased by combinatorial blockade of ICAM-1 and VCAM-1 (173) or L-selectin and MAdCAM-1 (Rivera-Nieves, Olson, et.al., *J. Immunol.*, In Revision).

Genetic outcross studies and linkage analysis have identified loci on several SAMP1/YitFc chromosomes containing polymorphic markers that segregate with the ileitis phenotype. Allele determination studies showed that only around 50% of SAMP1/YitFc alleles in microsatellite loci are derived from AKR mice, suggesting that the breedings from which the SAMP1/YitFc mice were derived, as described above, must have introduced a contaminating strain (245). In this study, disease in the F2 generation of a SAMP1/YitFc x C57BL/6J cross segregated with an AKR-derived SAMP1/YitFc allele on mouse chromosome 9, in a region containing genes encoding the IL-10 receptor

$\alpha$  chain and IL-18. This study also demonstrated that differences in microsatellite alleles near the gene for NOD2 on chromosome 8 and the genes determining MHC haplotype on chromosome 17 did not correlate with disease severity (245). A recent study in which SAMP1/YitFc mice were crossed with AKR mice revealed that disease does not develop in the SAMP1/YitFc x AKR F1 generation, and approximately half of mice resulting from a SAMP1/YitFc cross with the (SAMP1/YitFc X AKR)F1 mice developed disease (Sugawara, Olson, et.al., Gastroenterology, In Press). Disease in this cross correlated with a non-AKR-derived allele on Chromosome 6. Within this locus, multiple polymorphisms between AKR and SAMP1/YitFc mice alleles were found in the promoter region of the peroxisome proliferator-activated receptor- $\gamma$  (Ppar $\gamma$ ) gene. These polymorphisms altered the spacing of binding sites for the CDX1 transcription factor that is specifically expressed by crypt epithelial cells.

Infection is an unlikely candidate to explain the SAMP1/YitFc phenotype, since disease develops under specific pathogen free conditions, and the phenotype is reproducible in different animal facilities. Th1 polarization and overactivation of the immune system has repeatedly been shown to play a role in the development of SAMP1/YitFc ileitis, though whether these responses represent an intrinsic susceptibility to disease or a downstream effect of the true susceptibility remains unclear. Possible contributions to the SAMP1/YitFc phenotype made by the remaining etiologies and pathogenic mechanisms discussed above form the basis of this dissertation. In chapter 3, MLN leukocyte subsets in SAMP1/YitFc versus AKR mice are compared in terms of cell surface marker, adhesion molecule, and chemokine receptor expression, and the functions of putative regulatory T cell populations derived from SAMP1/YitFc MLN are explored

in both the host and SCID adoptive transfer models. In chapter 4, the contributions of B cells and immunoglobulin to ileitis development in the SAMP1/YitFc and SCID adoptive transfer models are examined. Finally, in chapter 5, the requirements for SAMP1/YitFc-derived hematopoietic versus non-hematopoietic cells in the development of ileitis are explored. Taken together these results suggest that SAMP1/YitFc regulatory T cells are functional, SAMP1/YitFc B cells contribute to disease pathogenesis, and the primary susceptibility leading to the development of disease in SAMP1/YitFc mice is likely derived from epithelial dysfunction.

### **III. Functional Differentiation of SAMP1/YitFc MLN CD4<sup>+</sup> T cell Subsets and Analysis of Regulatory T cell Function**

#### **Rationale**

CD4<sup>+</sup> T cell subsets defined on the basis of activation and lineage marker expression play differential roles in the development of IBD in several animal models (68). CD69 is a C-type lectin that is upregulated on the surface of recently activated cells (246). The expression of CD45RB on the surface of CD4<sup>+</sup> T cells serves as a marker of naïve (high) versus memory/effector (low) cells (81). Cells expressing low levels of L-selectin possess a more activated phenotype and promote more severe mixed lymphocyte reactions than L-selectin<sup>hi</sup> cells (247), and loss of L-selectin expression allows for T cell emigration from lymphoid organs to effector sites (154). The IL-2 receptor  $\alpha$  chain, CD25, is also upregulated on newly activated effector T cells (248). However, while all CD45RB<sup>lo</sup>, CD25<sup>+</sup>, and/or L-selectin<sup>lo</sup> cells are no longer naïve or quiescent, many of these cells do not possess a pro-inflammatory phenotype. Splenic CD45RB<sup>hi</sup> CD4<sup>+</sup> T cells transfer colitis to immunodeficient mice, whereas CD45RB<sup>lo</sup> CD4<sup>+</sup> cells are protective (79). Subsequent studies have shown that CD25<sup>-</sup> CD4<sup>+</sup> cells present in the CD45RB<sup>hi</sup> fraction are responsible for the colitis producing effects of these cells, whereas CD25<sup>+</sup> CD4<sup>+</sup> cells present in the CD45RB<sup>lo</sup> fraction contain the disease-preventing Treg populations (84). L-selectin<sup>hi</sup> and L-selectin<sup>lo</sup> CD4<sup>+</sup> T cells have also been shown to produce and prevent ileitis, respectively (80). Therefore, understanding the functions of

SAMP1/YitFc MLN CD4<sup>+</sup> T cell subsets differentiated on the basis of these markers requires examination of their regulatory versus pro-inflammatory properties.

Distinct patterns of adhesion molecule and chemokine receptor expression determine which T cells will selectively traffic to the intestine or the associated lymphatic tissue under homeostatic and inflammatory conditions (154;179). The  $\alpha_4\beta_7$  integrin has been shown to direct constitutive homing of lymphocytes to both MLN and Peyer's patches (157;165) and lymphocyte trafficking to the intestinal wall both constitutively and during inflammation (122;151). These interactions are mediated through  $\alpha_4\beta_7$  binding to its endothelial ligand MAdCAM-1, expressed exclusively at these sites (152). L-selectin plays an accessory role along with  $\alpha_4\beta_7$  in the homing of lymphocytes to MLN and Peyer's patches (156;165). The  $\alpha_E\beta_7$  integrin binds E-cadherin present in epithelial cell adherens junctions and an unknown ligand on endothelial cells (187;189), and is required for lymphocyte entry into the epithelial layer and for constitutive lamina propria lymphocyte accumulation (188). While not important for constitutive trafficking of cells to the intestine (151), interactions between endothelial VCAM-1 and the  $\alpha_4\beta_1$  integrin mediate leukocyte adhesion to inflamed lamina propria venules (122). Overlapping adhesion molecule pathways with built-in redundancy appear to guide lymphocyte trafficking to the ileum during SAMP1/YitFc ileitis, as only combinatorial adhesion molecule blockade strategies, such as ICAM-1 plus VCAM-1 (173) or L-selectin plus MAdCAM-1 (Rivera-Nieves, Olson, J Immunol. In Revision), are effective in preventing SAMP1/YitFc T cells from adoptively transferring ileitis to SCID mice.

Through binding of the chemokine receptor CCR9 expressed on  $\alpha_4\beta_7^+$  T cells, thymus-expressed chemokine (TECK, CCL25) is thought to mediate the recruitment of T



cells specifically to the small intestine (175) under homeostatic conditions. Other chemokines, including the CCR10-binding mucosa-associated epithelial chemokine (MEC, CCL28), induce homeostatic homing of lymphocytes to other mucosal sites including the colon (249). Under Th1-type inflammatory conditions, ligands for the chemokine receptor CXCR3 are expressed by intestinal epithelial cells (182) and have been shown to attract intestinal effector T cells (181), implying that chemokine-mediated trafficking of T cells during inflammation may rely on CXCR3.

CD4<sup>+</sup> CD45RB<sup>lo</sup> CD25<sup>+</sup> regulatory T cells (T<sub>reg</sub>) prevent colitis in adoptively transferred SCID mice through mechanisms involving TGF- $\beta$  and IL-10 production (78). Recently, the expression of the  $\alpha_E\beta_7$  integrin was used to define novel subsets of CD4<sup>+</sup> T<sub>reg</sub> cells also capable of preventing colitis (85). Compared to CD4<sup>+</sup> CD25<sup>-</sup> cells, CD4<sup>+</sup> CD25<sup>+</sup> T<sub>reg</sub> cells preferentially express  $\alpha_E\beta_7$  (212). Whether trafficking mediated by  $\alpha_E$  plays a role in regulatory T cell function is unclear. CD4<sup>+</sup> CD25<sup>+</sup> T<sub>reg</sub> cells also express high levels of the glucocorticoid-induced TNF receptor (GITR), a TNF receptor family member that regulates T cell proliferation and activation-induced apoptosis (250). Stimulation of T<sub>reg</sub> with anti-GITR antibody or through binding of GITR ligand (GITRL), expressed by subsets of antigen presenting cells (APC), reverses the suppression of effector T cell proliferation by regulatory T cells *in vitro*, suggesting a role for GITR in promoting pro-inflammatory responses (210-212). Whether this pathway is important in the context of IBD has not been examined.

In this chapter, differences in the size and proliferation rate of MLN lymphocyte subsets from SAMP1/YitFc versus AKR mice are investigated. Specific increases in the size of CD4<sup>+</sup> T cells subsets in SAMP1/YitFc versus AKR MLN on the basis of

activation marker and adhesion molecule expression are also examined. Further experiments are presented that describe the chemotactic responsiveness and chemokine receptor expression of MLN CD4<sup>+</sup> T cells from both strains of mice along with chemokine receptor expression patterns within the ileum of 4 to 40 week-old mice, indicative of the chemokine requirements by which cells may migrate to the intestine during discrete stages of disease development. Finally, the pro- versus anti-inflammatory properties of SAMP1/YitFc MLN CD4<sup>+</sup> T cell subsets are investigated by analyzing cytokine production and severity of ileitis induced by adoptive transfer of these cells into SCID recipients. Taken together, these results demonstrate that SAMP1/YitFc MLN exhibit expansion of both effector and regulatory T cell subsets relative to AKR MLN, and that while SAMP1/YitFc regulatory cells are functional *in vitro* and block colitis development *in vivo*, these cells are ineffective at preventing the development of either SAMP1/YitFc or adoptively transferred ileitis.

## **Materials and Methods**

### *Mice*

SAMP1/YitFc mice, a substrain of the SAMP1/Yit line (242), were obtained from established colonies at the University of Virginia Health Science Center vivarium. Age-matched wildtype AKR/J mice and 6-8 week-old severe combined immunodeficient mice (SCID) on the C3H/HeJ background were obtained from Jackson Laboratories (Bar Harbor, ME). All animals were housed in a specific pathogen-free facility, and all experiments were approved by the institutional committee for animal use.

### *Flow cytometry and antibodies*

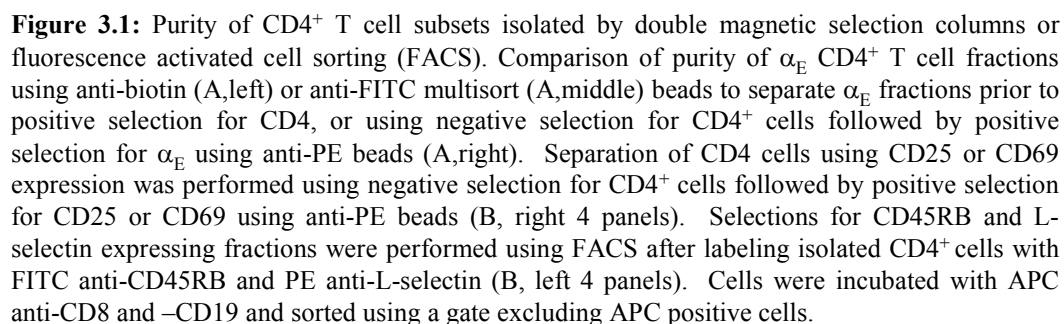
Mesenteric lymph nodes were crushed through 70  $\mu$ M filters into staining buffer containing PBS with 2% fetal calf serum (FCS). Cells were counted using Trypan Blue (Sigma, St. Louis, MO). Cells were stained with combinations of FITC-, PE-, PERCP-, APC-, or biotin-labeled rat anti-mouse CD4 (RM4-5), CD8 (53-6.7), CD19 (1D3),  $\alpha$ E (M290),  $\beta_7$  (M293), CD25 (PC61), L-selectin (MEL-14), CD45RB (16a),  $\alpha_4$  (R1-2),  $\alpha_L$  (2D7), PSGL-1 (2PH1) and hamster anti-mouse CD69 (3E2),  $\beta_1$  (HA2/5),  $\alpha_x$  (HL3) and ICAM-1 (H1.2F3) (BD Pharmingen, San Diego, CA). Cells were stained for 20-30 minutes at 4<sup>0</sup> C, washed 2x in staining buffer and fixed in 1% paraformaldehyde. Flow cytometry data was acquired on a FACS Calibur flow cytometer using Cell Quest software (BD Biosciences, San Diego, CA) and analyzed using WinMIDI 2.8 (Trotter, Scripps Research Institute, La Jolla, CA).

### *Cell isolations and adoptive transfer*

All selections using magnetic bead-based separation techniques were performed according to manufacturer's instructions (Miltenyi Biotec, Auburn, CA). If applicable, antibody labeling of cells before bead incubation was performed according to the cell labeling procedure outlined above or according to manufacturer's instructions. Unbound antibody was removed by washing prior to incubation with beads. Cells were incubated with beads for 15 minutes on ice (10-20  $\mu$ l/ 10<sup>7</sup> cells) in a 1/10 or 1/5 dilution in separation buffer consisting of PBS containing 2mM EDTA and 0.5% bovine serum albumin (BSA). The cells were then diluted 10-fold and pelleted by centrifugation (400 x g) for 5 minutes and resuspended in no less than 500  $\mu$ l/10<sup>8</sup> cells. LS and MS magnetic

columns (Miltenyi Biotec) were used for selections in which the positive (bead-bound) fraction was expected to be greater than or less than  $10^7$  cells, respectively. Columns were first placed in a MIDIMACS (LS) or OCTOMACS (MS) magnet (Miltenyi Biotec) and washed with 500  $\mu$ l (MS) or 3 ml (LS) of separation buffer. Cells were then loaded and washed 3-4x with 500  $\mu$ l (MS) or 3 ml (LS) of buffer. After washing, columns were removed from the magnet and the positive fraction was eluted in 1 ml (MS) or 3 ml (LS) of separation buffer.

SAMP1/YitFc or AKR MLN  $CD4^+$  T cells were isolated by positive selection using anti-mouse  $CD4$  microbeads or negative selection using the mouse  $CD4^+$  negative isolation kit (Miltenyi Biotec), in which anti-biotin beads and biotinylated antibodies recognizing markers on the surface of  $CD8^+$  T cells, B cells, myeloid cells, and erythrocytes are used to bind non- $CD4^+$  subsets. Isolations of  $\alpha_E^+ CD4^+$  and  $\alpha_E^- CD4^+$  subsets were attempted using several different strategies. The first attempts to isolate these cells involved first positively selecting for the  $\alpha_E^+$  fraction using biotinylated anti- $\alpha_E$  (M290, BD Pharmingen) antibodies and streptavidin microbeads (Miltenyi Biotec), followed by a second positive selection for  $CD4^+$  T cells. While this selection resulted in greater than 95% purity in the  $\alpha_E^- CD4^+$  cell fraction, because the anti-biotin beads were not removed from the surface of  $\alpha_E^+$  cells prior to positive selection for  $CD4^+$  cells, the overall purity of the  $\alpha_E^+ CD4^+$  fraction was only 50%, with most of the remaining cells (40%) representing  $\alpha_E^+ CD4^-$  cells (Figure 3.1A, left two panels). Isolations were then attempted using the FITC multi-sort kit (Miltenyi Biotec) in which cells were first positively selected for the  $\alpha_E^+$  fraction using FITC-labeled anti- $\alpha_E$  and anti-FITC beads.



An included cleavage enzyme was then used to remove the FITC fluorophore and the attached bead prior to selecting for CD4<sup>+</sup> cells using anti-CD4 beads. This procedure resulted in high purity of both  $\alpha_E^-$  CD4<sup>+</sup> (95%) and  $\alpha_E^+$  CD4<sup>+</sup> (80%) fractions, with the majority of the impurities in the  $\alpha_E^+$  CD4<sup>+</sup> being  $\alpha_E^+$  CD4<sup>-</sup> cells (11%) (Figure 3.1A, middle two panels). This procedure was used in isolating  $\alpha_E^+$  CD4<sup>+</sup> and  $\alpha_E^-$  CD4<sup>+</sup> cell fractions based for adoptive transfer experiments but was too expensive to continue using in cell culture experiments primarily due to the large volume of FITC anti- $\alpha_E$  that was required (~400  $\mu$ l/experiment). The third method used for cell culture experiments involved first negatively selecting for CD4<sup>+</sup> T cells and then selecting for  $\alpha_E^+$  cells using PE-labeled rat anti-mouse  $\alpha_E$  and anti-PE microbeads (Miltenyi Biotec). By flow cytometry, the  $\alpha_E^-$  and  $\alpha_E^+$  populations in the CD4<sup>+</sup> fraction were greater than 99% and 80% pure, respectively, with the major impurities in the  $\alpha_E^+$  CD4<sup>+</sup> fraction being  $\alpha_E^-$  CD4<sup>+</sup> T cells (Figure 3.1A, right panels). Since only ~7% of cells expressed  $\alpha_E$  after the first selection for CD4, this isolation results in a 11 to 12-fold enrichment of  $\alpha_E^+$  CD4<sup>+</sup> cells. Isolation of a more pure  $\alpha_E^+$  CD4<sup>+</sup> fraction using fluorescence activated cell sorting (FACS) would likely have resulted in too low of a cell yield due to the many hours this sorting would have taken because of the rarity of the  $\alpha_E^+$  CD4<sup>+</sup> population and due to the observed fragility of SAMP1/YitFc MLN cells *in vitro*.

CD69<sup>+</sup>, CD69<sup>-</sup>, CD25<sup>+</sup> and CD25<sup>-</sup> CD4<sup>+</sup> T cells were separated using PE anti-mouse CD25 (PC61) or PE anti-mouse CD69 (3E2) and anti-PE microbeads after selecting for CD4<sup>+</sup> cells by negative selection. Purity in the CD4<sup>+</sup> CD25<sup>+</sup> (83%) and the CD4<sup>+</sup> CD25<sup>-</sup> (94%) fractions was high, whereas the purity in the CD4<sup>+</sup> CD69<sup>+</sup> (70%) and CD4<sup>+</sup> CD69<sup>-</sup>

(88%) fractions was somewhat lower (Figure 3.1B). L-selectin<sup>hi</sup>, L-selectin<sup>lo</sup>, CD45RB<sup>hi</sup>, and CD45RB<sup>lo</sup> CD4<sup>+</sup> T cells were first isolated for CD4 expression with the negative selection method and then separated using labeling with FITC-anti mouse CD45RB (16a) or PE-labeled anti-mouse L-selectin (MEL-14) and FACS sorting with the FACSVantage system (BD Pharmingen).

For adoptive transfers, cells were counted, washed, and resuspended in plain PBS for injection into SCID recipients. T cells were injected intraperitoneally (i.p.) in 500 µl of PBS at a dose of  $5 \times 10^5$  cells. The ilea and/or colons of SCID recipients were harvested 6 weeks after transfer for histologic analysis of disease severity.

#### *Measurement of in vivo cell proliferation using bromodeoxyuridine*

Bromodeoxyuridine incorporation into replicating DNA was measured using the BRDU Flow kit (BD Pharmingen) according to manufacturer's instructions. Briefly, 1 mg of BRDU was injected i.p. into SAMP1/YitFc and AKR mice 4, 12, and 24 hours before MLN cell harvest. Cells were stained with PE anti-CD4 and APC anti-CD19 antibodies, washed and then fixed and permeabilized in Cytotfix/Cytoperm buffer (BD Pharmingen). Cells were then treated with 30 µg DNase for 1 hour at 37<sup>0</sup> C to expose incorporated BRDU, and intracellular staining for BRDU was performed with the provided anti-BRDU antibody at a 1/100 dilution for 20 minutes at room temperature. After washing, cells were resuspended in 20 µl/sample of 7-amino-actinomycin D (7-AAD). After diluting samples in 1 ml of PBS, samples were analyzed by flow cytometry using a log scale for BRDU, CD4, and CD19 levels, and a linear scale for 7-AAD levels.

### *Chemotaxis assays*

The chemokines SLC (CCL21) SDF-1 (CXCL12), MDC (CCL22), and IP-10 (CXCL10) were purchased from Peprotech (Rocky Hill, NJ), whereas TECK (CCL25) was purchased from R&D systems (Minneapolis, MN). 24 well plates containing 5  $\mu$ m-pore size Corning Costar transwell inserts were purchased from Fisher Scientific (Hampton, NH). Chemokines were applied to the bottom well in a total volume of 600  $\mu$ l at concentration ranges specified as optimal for chemotaxis by the manufacturer. Isolated CD4<sup>+</sup> T cells from SAMP1/YitFc and AKR MLN were counted and resuspended in RPMI containing 10% FCS or 0.5% BSA.  $3.3 \times 10^5$  to  $4 \times 10^5$  cells were loaded onto the top well in a volume of 200 or 330  $\mu$ l. In some experiments cells and chemokine were allowed to equilibrate for 30 minutes at 37<sup>0</sup> C prior to loading into the transwell insert. Following preincubation, plates were incubated for 2 hours, at the end of which the inserts containing the top wells were removed and the number of cells in the bottom chamber were counted using a hemocytometer (Reichert, Buffalo, NY). Wells in which the bottom chamber was filled with media only were used to determine baseline levels of non-specific migration.

### *Real time RT-PCR for Chemokine receptor and TGF- $\beta$ expression*

RNA was extracted from isolated cells using Qiashredder columns for homogenization and an RNAeasy isolation kit (Qiagen, Valencia, CA). RNA was extracted from tissues by placing tissue samples in RNA later (Ambion, Austin, TX) for storage, homogenizing using a Tissue Tearor model 398 (Dremel, Racine, WI), and then purifying RNA using the RNAeasy isolation kit. 1  $\mu$ g mRNA from each sample was



converted into cDNA using oligo DT primers and the CDNA Cycle Kit (Invitrogen, Carlsbad, CA) or the Omniscript RT Kit (Qiagen). CDNA was then purified to remove proteins from the reverse transcription reaction using the PCR purification kit (Qiagen).

For chemokine receptor expression 5  $\mu$ l cDNA was run through multiplex PCR reactions using primers and instructions provided in the Mouse CXCR set-1, CCR set-1, and CCR set-2 MPCR kits (Maxim Biotech, San Francisco CA). Cycling parameters were 2 cycles of 1 min 96<sup>0</sup> C and 4 min 60<sup>0</sup> C, 30 cycles of 1 min 94<sup>0</sup> C and 2 min 60<sup>0</sup> C; followed by a 10 min final extension at 70<sup>0</sup> C. PCR products were separated by size using gel electrophoresis on a 1.5% agarose gel containing ethidium bromide. Pictures were taken with a FluorChem 9900 camera and densitometry data was acquired using AlphaEase FC software (AlphaInnotech, San Leandro, CA).

For TGF- $\beta$  expression, primers amplifying a 439 base pair fragment within mouse TGF- $\beta$ 1 cDNA were purchased from R&D Systems (Minneapolis, MN). 2  $\mu$ l of primer and 120 ng of cDNA were used in PCR reactions with the following cycling parameters: 4 min 94<sup>0</sup>C; followed by 30 cycles of 45 sec 94<sup>0</sup> C, 45 sec 55<sup>0</sup> C, and 45 sec 72<sup>0</sup> C; followed by a 10 min final extension at 70<sup>0</sup>C. To normalize for inter-sample differences in total cDNA concentration an additional PCR reaction was performed for each cDNA sample amplifying a fragment of the housekeeping gene, GAPDH with the following primers: GGCTCATGACCACAGTCCAT (forward) and GCCTGCTTCACCACCTTCT (reverse). Following a 4 min incubation at 94<sup>0</sup> C, DNA was amplified for 30 cycles consisting of 30 sec at 94<sup>0</sup> C followed by 1 min at 56.2<sup>0</sup> C. For both TGF- $\beta$  and GAPDH reactions DNA was amplified using Platinum Taq polymerase (Invitrogen, Carlsbad, CA). TGF- $\beta$  and GAPDH PCR products from the same cDNA samples were loaded in

the same well on a 1.5% agarose gel containing ethidium bromide and separated by size via electrophoresis. Pictures were taken and differences in expression levels of TGF- $\beta$  relative to GAPDH were measured using densitometry of band intensity as above.

*Cell Culture, Cytokine Analysis, and T cell proliferation assays*

Culture of  $\alpha_E^+CD4^+$  and  $\alpha_E^-CD4^+$  T cells for cytokine and chemokine receptor analysis was performed in RPMI media containing 10% fetal calf serum, 100 U/ml penicillin, 100  $\mu$ g/ml streptomycin, 2mM glutamine, and 2  $\mu$ g/ml soluble anti-mouse CD28 (37.51) (BD Pharmingen). Cells were cultured at  $10^5$  cells/well in 100  $\mu$ l of media for 48 hours at 37<sup>0</sup> C (5% CO<sub>2</sub>) in 96-well plates that had been incubated overnight at 4<sup>0</sup> C with 10  $\mu$ g/ml anti-mouse CD3 (145-2C11) (BD Pharmingen). For cytokine analysis, undiluted or 1:5 dilutions of supernatant in RPMI/10% FCS were assayed for TNF- $\alpha$ , IFN- $\gamma$ , IL-2, IL-4, IL-5, IL-6, IL-10 and IL-12 levels by cytometric bead array using the mouse inflammation and mouse Th1/Th2 cytokine kits (BD Pharmingen).

For TGF- $\beta$  mRNA analysis, SAMP1/YitFc MLN  $\alpha_E^+$ ,  $\alpha_E^-$ ,  $\alpha_E^-CD25^+$ , and  $\alpha_E^-CD25^-CD4^+$  T cells were activated in culture for 2-3 days with 10  $\mu$ g/ml plate-bound anti-CD3, 2  $\mu$ g/ml soluble anti-CD28, and 20 U/ml soluble recombinant IL-2 (Roche, Indianapolis, IN) in RPMI media containing 10% FCS, 100 U/ml penicillin, 100  $\mu$ g/ml streptomycin, 2mM glutamine, 10 mM HEPES, 1 mM sodium pyruvate, and 50  $\mu$ M  $\beta$ -mercaptoethanol.

For proliferation assays,  $10^5$  irradiated (3000 rad) splenic APC were cultured for 3 days with plate-bound anti-CD3 (10  $\mu$ g/ml) and combinations of  $\alpha_E^+CD4^+$  T cells and  $\alpha_E^-CD4^+$  T cells at  $5 \times 10^4$  cells each/well. Each condition was assayed in 3 separate cultures for each individual experiment. Incorporation of H<sup>3</sup> thymidine (1 $\mu$ Ci/well)

(Biomedicals, Irvine, CA) during the last 24 hrs of culture was measured using a Harvester 96 (Tomtec, Humden, CT) for cell harvest and a 1450 Microbeta Scintillation Counter (Perkin Elmer, Gaithersburg, MD).

### *Histology*

For histology, the ileum and colon were flushed, opened, rolled longitudinally, and fixed in Bouin's fixative (Fisher, Newark, DE). All tissues were embedded in paraffin, and cut into 3-5  $\mu\text{m}$  sections. Hemotoxylin- and eosin-stained slides of ileal or colonic sections were evaluated in a blinded fashion by a trained histopathologist using a standardized histologic scoring system (173) consisting of 3 indices. The active inflammation index measures the progressive infiltration of neutrophils into the lamina propria, the submucosa, and the epithelium, along with neutrophil-driven crypt abscess formation and mucosal ulceration. The chronic inflammation index measures mononuclear cell infiltration in terms of total cell number and the expansion of intercryptal spaces as a consequence of this infiltration. The villus architectural, or villus distortion, component measures the reduction in villus height and the increase in villus width due to architectural remodeling by epithelial cells as a result of inflammation. The severity grade of each index was multiplied by a factor taking into account the cross-sectional area of tissue involved to give a score for each component. Scores from individual indices were then added together to give a total inflammatory score.

### *Two color in vivo homing assay*

$\alpha_E^+$  and  $\alpha_E^-$  CD4<sup>+</sup> T cell subsets were isolated as described above and labeled either with 5,6-carboxyfluorescein diacetate succinimidyl ester (CFSE) (Molecular Probes,

Eugene, OR), a compound that irreversibly couples to cellular proteins and contains a fluorochrome emitting in the FL-1 channel of standard flow cytometers, or with PKH26 (Sigma, St. Louis, MO), a lipid intercalating fluorochrome/linker dye that emits (567 nm) in the FL-2 channel. For CFSE-labeling, cells were resuspended at  $5 \times 10^6$  cells/ml in PBS containing 1  $\mu$ M CFSE and then incubated for 15 min at 37<sup>0</sup> C. For labeling with PKH26, cells were resuspended in  $5 \times 10^6$  cells/ml of the provided assay diluent (Sigma). An equal volume of assay diluent containing 5  $\mu$ l/ml PKH26 was then added and cells were incubated for 3 minutes at room temperature. Incorporation of both labels was stopped by addition of 5 ml FCS. Cells were then diluted further in 8 ml RPMI/10% FCS, centrifuged for 10 min at 400 x g, washed once in plain PBS and resuspended in plain PBS for injection. Approximately 7-8 million total cells were injected in a volume of 500  $\mu$ l of plain PBS into the tail veins of recipient SCID mice. The relative percentage of  $\alpha_E^+$  versus  $\alpha_E^-$  CD4<sup>+</sup> T cells in the injected fraction was determined by flow cytometric analysis of the ratio of PKH26 to CFSE positive events.

After three days, mice were euthanized and cells were harvested for analysis of labeled cell homing by flow cytometry. Cells were collected from the MLN, peripheral blood, spleen, bone marrow (described in Chapter 5), lamina propria, lung liver, and peripheral lymph nodes including the inguinal, axillary, mediastinal, and peribronchial nodes. Isolation of peripheral blood and spleen cells required the addition of a red cell lysis step with 1x lysis buffer (Sigma) followed by resuspension in staining buffer. Lung and liver were digested in PBS containing hyaluronidase, DNase, and collagenase fraction XI (Sigma) for 30 min at 37<sup>0</sup>, filtered through 70  $\mu$ m mesh filters, washed, and resuspended in staining buffer. For lamina propria lymphocyte (LPL) isolation, ilea were

flushed with PBS and cut into 0.5 cm pieces. To remove the epithelial layer, intestines were shaken 4-5x for 10 minutes in HBSS (pH 7.4) containing 15 mM HEPES, 3 mM EDTA, 0.05 mM dithiothreitol (Sigma, St. Louis, MO), and 0.035%  $\text{NaHCO}_3$ , with or without 100 mM N-acetylcysteine (Sigma) and filtered. Intestinal pieces were then incubated for 90 minutes at  $37^\circ\text{C}$  in a fluted flask containing RPMI with 10% FCS, 15 mM HEPES, and 300 U/ml collagenase Fraction VIII. LPL were filtered, washed and resuspended in staining buffer for FACS analysis. For all samples in which total cell number permitted, at least 500,000 lymphocyte-gated events were acquired. The ratio of  $\alpha_E^+$  to  $\alpha_E^-$  cells in the injected fraction was used to normalize ratios of recovered cells.

### *Statistics*

Statistical analysis was performed using the two-tailed unpaired Student's t test, the Mann-Whitney rank sum test, or one-way ANOVA for multiple comparisons using the Student-Newman-Keuls method. Statistical analysis for densitometric analysis of chemokine receptor expression was performed using the one- or two-tailed unpaired Student's t test as indicated. Statistical significance was set at  $P < 0.05$ .

## **Results and Discussion**

### *Expansion and proliferation of $\text{CD4}^+$ T cells and B Cells in SAMP1/YitFc MLN*

One of the characteristic features of the SAMP1/YitFc ileitis phenotype is a macroscopically enlarged mesenteric lymph node (242). SAMP1/YitFc MLN from >30 week-old mice had a 3-fold increase in total lymphocyte number ( $52 \pm 5$  million cells, mean  $\pm$  SEM) compared to MLN from age-matched wildtype AKR mice ( $17 \pm 1$  million cells) (Figure 3.2A). By flow cytometry subset analysis, the largest expansion occurred

in the CD19<sup>+</sup> B cell subset, which was 4.3-fold increased in SAMP1/YitFc versus AKR MLN. CD4<sup>+</sup> T cell number was increased by 2.5-fold in SAMP1/YitFc versus AKR MLN. Due to the greater increase in total B cells, SAMP1/YitFc on average contained a significantly lower percentage of CD4<sup>+</sup> T cells ( $41 \pm 1\%$ , mean  $\pm$  SEM) and a significantly higher percentage of B cells ( $46 \pm 3\%$ ) compared to AKR CD4<sup>+</sup> T cell ( $51 \pm 2\%$ ) and B cell percentage ( $32 \pm 2\%$ ) (Figure 3.2B). This increased average B cell percentage in SAMP1/YitFc MLN does not reflect an increase in B cells in all SAMP1/YitFc mice (Figure 3.2C). Rather, a bimodal distribution of B cell percentage is present wherein approximately half of SAMP1/YitFc MLN contain similar percentages of B cells to those seen in AKR MLN, with the remaining SAMP1/YitFc MLN exhibiting a doubling of B cell percentage.

MLN lymphocyte proliferation rates in SAMP1/YitFc versus AKR mice were then examined by administering intraperitoneal injections of bromodeoxyuridine (BRDU) and analyzing DNA incorporation of BRDU in MLN subsets 4, 12, and 24 hours post-injection. Very few SAMP1/YitFc MLN cells were BRDU<sup>+</sup> 4 hours post-injection ( $<0.05\%$ ), but by 12 hours, increased numbers of SAMP1/YitFc (1.3%) versus AKR (0.5%) MLN cells were BRDU<sup>+</sup> (not depicted). The difference (4.5-fold) in BRDU<sup>+</sup> cells in SAMP1/YitFc versus AKR MLN was even greater at 24 hours post-injection (Figure 3.3A). Most BRDU incorporation at 24 hours was by cells in the early stages of DNA replication (R2 gate), as indicated by the lower staining intensity of 7-AAD, a DNA intercalating dye used for differentiating cells in the G1 phase of the cell cycle from G2 cells that have already duplicated their DNA content. However, there were also increases in the percentage of cells in later stages of DNA synthesis (R3 and R4 gates) that were

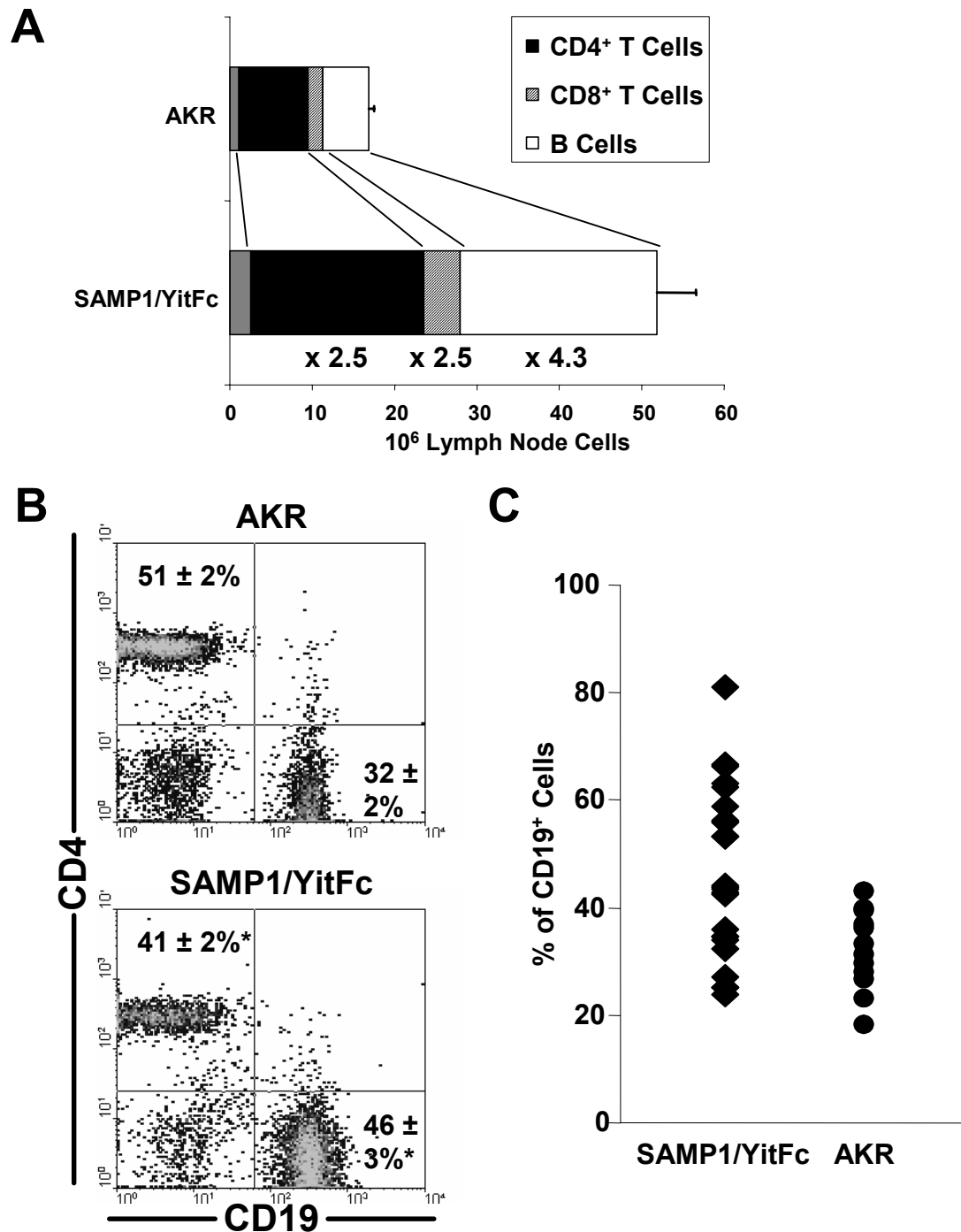


**Figure 3.2:** Expansion of B cells and CD4<sup>+</sup> T cell populations in SAMP1/YitFc versus AKR MLN. Total lymphocyte numbers (mean ± SEM), represented as the percentage of total cells by lymphocyte-gated flow cytometry that are CD4<sup>+</sup> T cells (n= 16;32), CD8<sup>+</sup> T cells (n=10;19), and CD19<sup>+</sup> B cells (n=12;26), in AKR and SAMP1/YitFc MLN, respectively (A). Representative lymphocyte-gated density plots with multiple mouse averages (mean ± SEM), showing the percentage of MLN lymphocytes that are CD4<sup>+</sup> T cells and B cells in SAMP1/YitFc versus AKR mice (B). \*Significantly different from AKR population (P < 0.05). Bimodal distribution of SAMP1/YitFc MLN CD19<sup>+</sup> B cell percentage in individual mice (C).

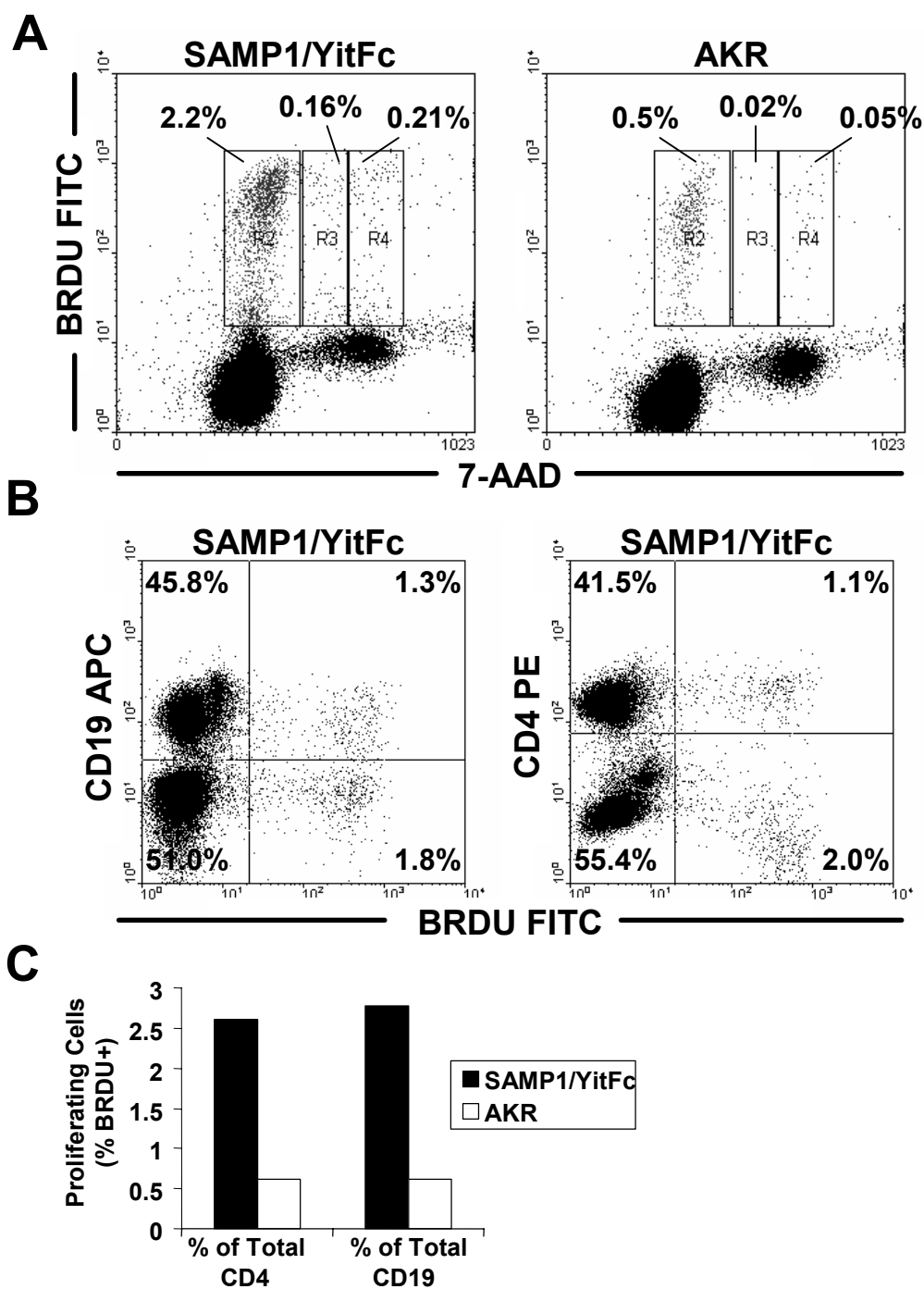


**Figure 3.3:** Increased proliferation of SAMP1/YitFc versus AKR MLN CD4<sup>+</sup> T cells and B cells measured by bromodeoxyuridine (BRDU) incorporation. BRDU was injected 24 hours prior to MLN harvest. Cells were stained with FITC anti-BRDU, subset markers, and the dye 7-amino-actinomycin D (7-AAD), a marker of DNA replication. Compared to AKR cells, SAMP1/YitFc MLN lymphocytes exhibited more BRDU incorporation, particularly in cells in the early stages of DNA replication (gate R2) (A). CD4<sup>+</sup> T cells and B cell subsets in SAMP1/YitFc MLN contribute equally to BRDU incorporating cells (B), and both subsets proliferate more than the respective subsets in AKR MLN (C).



BRDU<sup>+</sup> in SAMP1/YitFc versus AKR MLN. BRDU<sup>+</sup> cells in SAMP1/YitFc MLN were equally divided between the CD4<sup>+</sup> T cell and CD19<sup>+</sup> B cell populations (Figure 3.3B). BRDU<sup>+</sup> cells accounted for approximately 2.5% of either B cells or CD4<sup>+</sup> T cells in SAMP1/YitFc MLN, a 4.5-fold increased in percentage compared to either population in AKR MLN (Figure 3.3C).

Compared to AKR MLN CD4<sup>+</sup> T cells, an increased percentage of SAMP1/YitFc CD4<sup>+</sup> T cells expressed CD25 ( $30 \pm 2\%$  versus  $15 \pm 1\%$ , mean  $\pm$  SEM), and a decreased percentage expressed high levels of L-selectin ( $55 \pm 4\%$  versus  $84 \pm 2\%$ ) and CD45RB ( $55 \pm 4\%$  versus  $75 \pm 1\%$ )(Figure 3.4). The percentage of CD4<sup>+</sup> cells expressing CD69 was not significantly different in SAMP1/YitFc versus AKR MLN. Compared to AKR MLN, SAMP1/YitFc MLN also contained increased percentages of CD4<sup>+</sup> T cells expressing high levels of several adhesion molecules, including the  $\alpha_4$  integrin chain ( $17 \pm 1$  versus  $8 \pm 1\%$ )(Figure 3.5A).  $\alpha_4$  is expressed as either  $\alpha_4\beta_1$  or  $\alpha_4\beta_7$  integrin, and the percentages of CD4<sup>+</sup> T cells expressing high levels of either  $\beta_1$  and/or  $\beta_7$  integrin chains were similarly increased in SAMP1/YitFc ( $19 \pm 1\%$ ,  $17 \pm 1\%$ ) versus AKR MLN ( $7 \pm 1\%$ ,  $8 \pm 1\%$ ). SAMP1/YitFc MLN also contained increased percentages of CD4<sup>+</sup> T cells expressing high levels of the  $\beta_2$  integrin ligand ICAM-1 ( $23 \pm 6\%$  versus  $10 \pm 1\%$ ), and CD11a ( $33 \pm 3\%$  versus  $15 \pm 1\%$ ), the  $\alpha$  chain of the  $\beta_2$  integrin lymphocyte function-associated antigen-1 (LFA-1) (Figure 3.5B). In contrast, CD4<sup>+</sup> T cells expressing low levels of PSGL-1, a ligand that can bind all three known selectins depending on its pattern of glycosylation (251), were increased in SAMP1/YitFc ( $19 \pm 2\%$ ) versus AKR ( $6 \pm 1\%$ ) MLN.

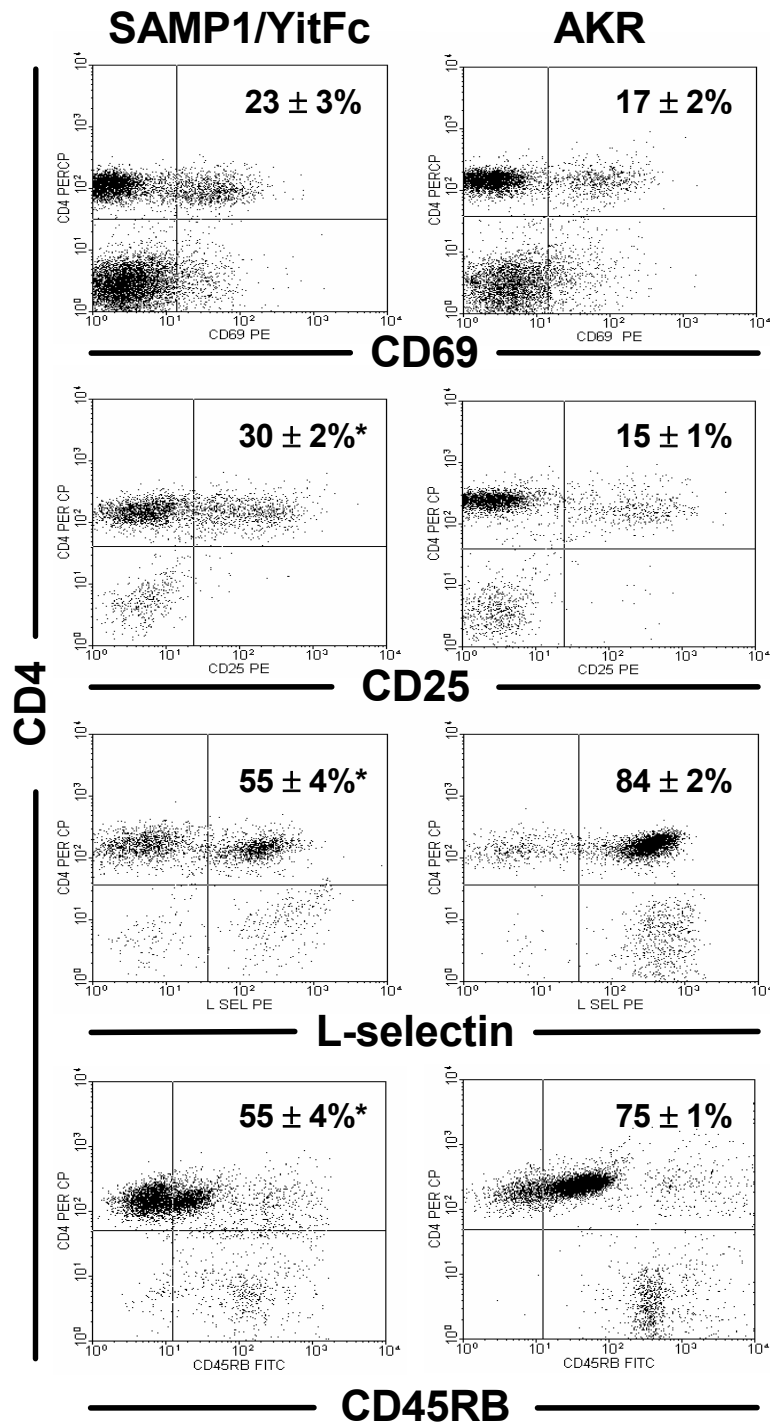


**Figure 3.4:** Expansion of CD4<sup>+</sup> T cell subsets displaying an activated, non-naïve phenotype in SAMP1/YitFc versus AKR MLN. Representative T cell-gated (CD4<sup>+</sup>, CD8<sup>+</sup>) dotplots showing the percentage of CD4<sup>+</sup> T cells expressing the indicated subset marker. Values given indicate the percentage (mean ± SEM) of MLN CD4<sup>+</sup> T cells that are CD69<sup>+</sup> (n=9;3), CD25<sup>+</sup> (n= 10;9), L-selectin<sup>hi</sup> (n= 15;11), and CD45RB<sup>hi</sup> (n= 14;9) for SAMP1/YitFc and AKR mice, respectively. \*Significantly different from AKR percentage (P < 0.05).

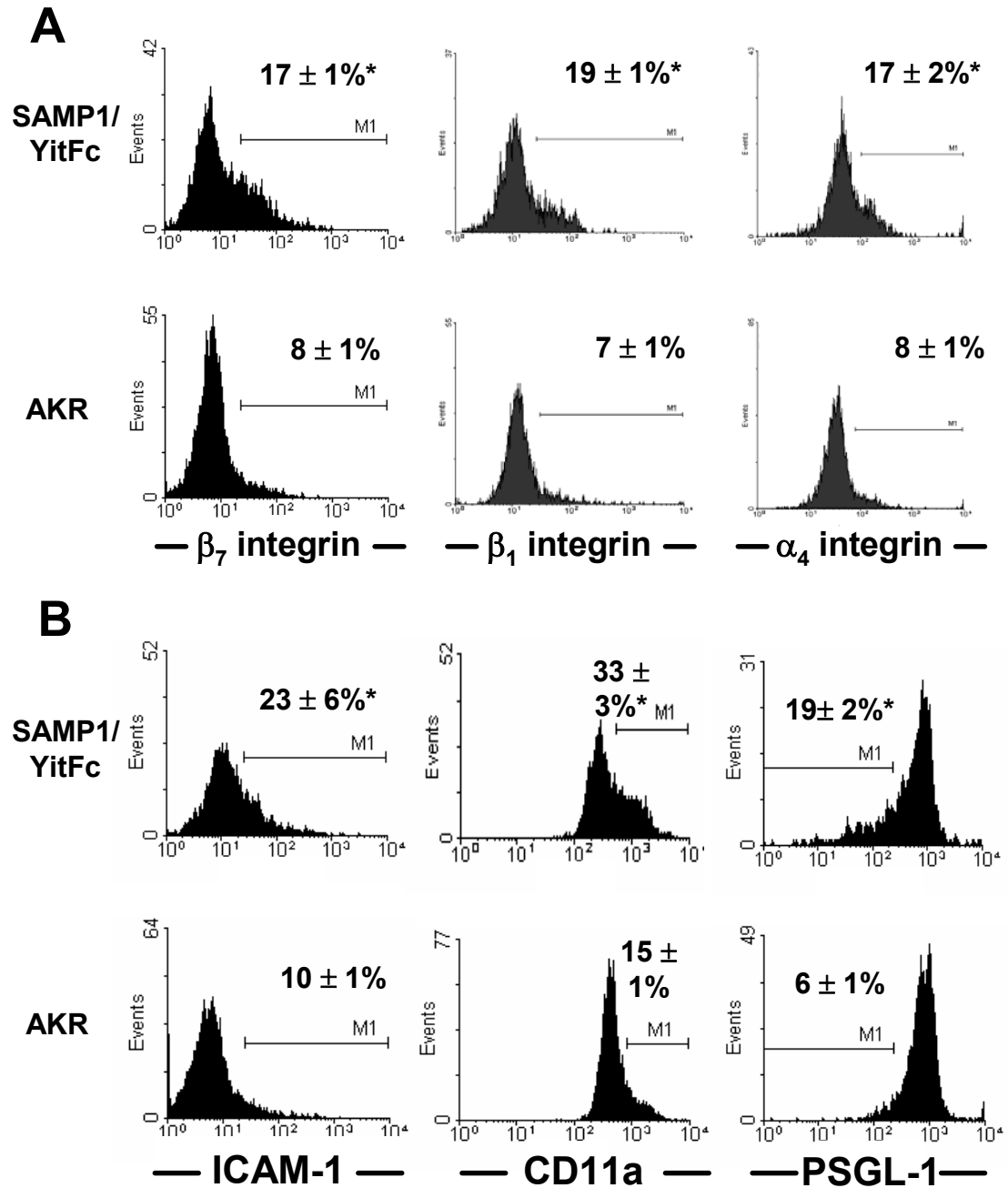


**Figure 3.5:** Expansion of CD4<sup>+</sup> T cell subsets expressing high levels of adhesion molecules in SAMP1/YitFc versus AKR MLN. Representative CD4-gated histograms showing the percentage of CD4<sup>+</sup> T cells expressing the indicated adhesion molecule. Values given indicate the percentage (mean ± SEM) of MLN CD4<sup>+</sup> T cells that are  $\beta_7$  integrin<sup>hi</sup> (n= 24;15),  $\beta_1$  integrin<sup>hi</sup> (n= 4;2),  $\alpha_4$  integrin<sup>hi</sup> (n= 4;2), ICAM-1<sup>hi</sup> (n= 3;6), CD11a<sup>hi</sup> (n= 5;3) and PSGL-1<sup>lo</sup> (n= 3;3) for SAMP1/YitFc and AKR mice, respectively. \*Significantly different from AKR percentage (P < 0.05). Because isotype controls can only be used to set positive versus negative expression gates, high versus low expression gates were set where populations deviated from normal Gaussian distributions using the same gating point in both SAMP1/YitFc and AKR plots for each molecule studied.

We next defined the expression patterns of the  $\alpha_4\beta_1$ ,  $\alpha_4\beta_7$ , and  $\alpha_E\beta_7$  integrin dimers on SAMP1/YitFc MLN T cells. All  $CD4^+$  T cells from SAMP1/YitFc or AKR MLN express low levels of  $\alpha_4\beta_7$  and  $\alpha_4\beta_1$  (Figure 3.6 and not depicted). In contrast, only a subset of SAMP1/YitFc cells expressed  $\alpha_E$  and this expression correlated directly with high levels of  $\beta_7$  expression in a diagonal 1:1 pattern (Figure 3.6A), showing that  $\beta_7^{hi}$  cells specifically express the  $\alpha_E\beta_7$  dimer. Importantly, SAMP1/YitFc  $CD4^+$  T cells stained with isotype control antibodies did not show this pattern, proving that this pattern of expression in cells stained with  $\alpha_E$  and  $\beta_7$  is not due to auto-fluorescence. The percentage of MLN  $CD4^+$  T cells expressing  $\alpha_E\beta_7$  was increased 2.5-fold in SAMP1/YitFc ( $15 \pm 1\%$ , mean  $\pm$  SEM) compared to AKR ( $6.0 \pm 0.5\%$ ) mice (Figure 3.6B).

Comparing  $\alpha_4$  versus  $\beta_7$  expression on a  $CD4^+$ -gated dotplot (Figure 3.6c, left), three discrete populations of cells can be identified, including a population with relative low levels of both  $\alpha_4$  and  $\beta_7$  expression, a population exhibiting high levels of  $\beta_7$  expression but similar levels of  $\alpha_4$  as the first population (R4 gate), and a population with intermediate levels of  $\beta_7$  expression and high levels of  $\alpha_4$  expression (R5 gate). Examination of these populations in cells that have been magnetically sorted on the basis of  $\alpha_E$  expression reveals that the vast majority of  $\alpha_E^+$  cells are located within the R4 gate of  $\beta_7^{hi}$  cells, with virtually no cells appearing in the R5 gate (Figure 3.6C, middle). In contrast  $\alpha_E^-$  cells are found either in the ungated  $\alpha_4^{lo} \beta_7^{lo}$  population or in the R5 gate of  $\alpha_4^{hi} \beta_7^{int}$  cells, but no  $\alpha_E^-$  cells are found in the  $\beta_7^{hi}$  R4 gate (Figure 3.6C, right). Therefore, the  $\beta_7^{hi}$  cells in the R4 gate represent the  $\alpha_E\beta_7^+$  cells discussed above, and the

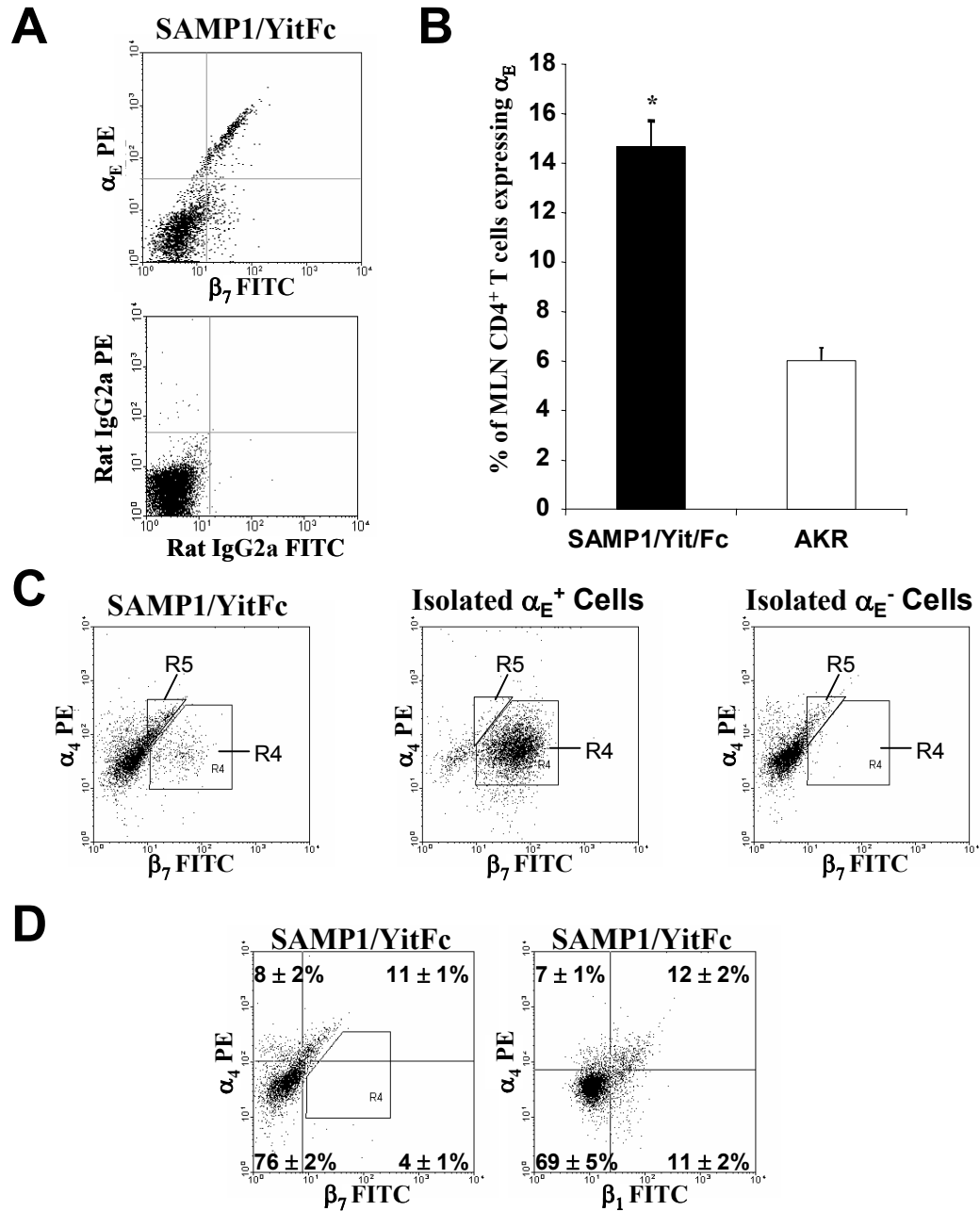


**Figure 3.6:** Expression patterns of  $\alpha_E$ ,  $\alpha_4$ ,  $\beta_7$ , and  $\beta_1$  integrin chains on SAMP1/YitFc MLN CD4<sup>+</sup> T cells. High  $\beta_7$  expression correlates with  $\alpha_E$  expression on a CD4-gated dotplot in a 1:1 ratio (diagonal pattern) not seen in isotype-stained cells, indicating  $\beta_7^{hi}$  cells specifically express the  $\alpha_E\beta_7$ -dimer (A). The percentage of MLN CD4<sup>+</sup> T cells expressing  $\alpha_E$  is increased 2.5-fold in SAMP1/YitFc (n=31) versus AKR (n=21) mice (B). \*Significantly increased (P < 0.05) compared to AKR percentage. A distinct population of  $\beta_7^{int}$  cells (R5 gate) expresses high levels of  $\alpha_4$  integrin on a CD4-gated dotplot (C, left) and is present in isolated  $\alpha_E^-$  cells (C, right), but not isolated  $\alpha_E^+$  cells (C, middle), indicating that  $\beta_7^{int}$  cells are phenotypically distinct from  $\beta_7^{hi}$  cells that express  $\alpha_E$  (R4 gate). Representative CD4-gated dotplots with average quadrant percentages (mean ± SEM, n=4) showing that the majority of  $\alpha_4^{hi}$  cells are also  $\beta_7^{int}$  and  $\beta_1^{hi}$ , suggesting that these cells express increased levels of both  $\alpha_4\beta_7$  and  $\alpha_4\beta_1$  compared to  $\alpha_4^{lo}$  cells (D).  $\beta_7^{hi}$  Cells (R4 gate) were excluded by gating from the left panel of D.

$\beta_7^{\text{int}}$  cells in the R5 gate represent a distinct population. Excluding the  $\alpha_E\beta_7^+$  population in dotplots of unfractionated MLN  $\text{CD4}^+$  T cells by gating out cells in the R4 gate, the  $\alpha_4^{\text{hi}}\beta_7^{\text{int}}$  population represents  $11 \pm 1\%$  (mean  $\pm$  SEM) of the remaining  $\text{CD4}^+$  T cell population in SAMP1/YitFc MLN (Figure 3.6d, left) versus only  $4.8 \pm 0.8\%$  of remaining  $\text{CD4}^+$  T cells in AKR mice (statistically significant,  $P < 0.05$ ). The majority (70%) of  $\beta_7^{\text{int}}$  cells are  $\alpha_4^{\text{hi}}$ , the majority (57%) of  $\alpha_4^{\text{hi}}$  cells are  $\beta_7^{\text{int}}$ , and the pattern of  $\alpha_4$  and  $\beta_7$  expression on  $\alpha_4^{\text{hi}}\beta_7^{\text{int}}$  cells is diagonal suggesting a 1:1 ratio of expression. This data suggests that the increased  $\alpha_4^{\text{hi}}\beta_7^{\text{int}}$  population in SAMP1/YitFc mice specifically expresses higher levels of the  $\alpha_4\beta_7$  dimer than either the  $\beta_7^{\text{lo}}$  or the  $\alpha_E\beta_7^+$   $\text{CD4}^+$  T cell populations. The majority (64%) of  $\alpha_4^{\text{hi}}$  cells also express high levels of the  $\beta_1$  integrin chain (Figure 3.6d, right), and this population of  $\alpha_4^{\text{hi}}\beta_1^{\text{hi}}$  cells, presumably expressing increased levels of  $\alpha_4\beta_1$ , is also significantly increased in SAMP1/YitFc ( $12 \pm 2\%$ ) versus AKR ( $4.6 \pm 0.1\%$ ) MLN. Therefore, the increased SAMP1/YitFc MLN  $\alpha_4^{\text{hi}}\text{CD4}^+$  T cells represents a population with overlapping high levels of  $\alpha_4\beta_1$  and  $\alpha_4\beta_7$  expression.

We have shown that SAMP1/YitFc mice exhibit significant heterogeneity in terms of MLN composition, with MLN from some mice resembling wildtype MLN whereas MLN from other mice exhibiting substantial expansion of the B cell compartment. While 100% of SAMP1/YitFc mice develop at least mild ileitis (186), disease severity varies significantly between individual mice. It is therefore possible that heterogeneity in MLN composition and B cell expansion may be linked to this variability in disease severity. This hypothesis will be investigated in Chapter IV.

We have also shown that expansion of lymphocyte subsets in MLN is not simply due to increased passive accumulation of lymphocytes from draining sites, as both of the major subsets of cells in SAMP1/YitFc versus AKR MLN display increased active proliferation rates. This *in situ* proliferation suggests that important SAMP1/YitFc immune responses are either initiated or perpetuated directly in the MLN, similar to what has been observed in other models (162).

The expanded populations of SAMP1/YitFc MLN CD25<sup>+</sup>, L-selectin<sup>lo</sup>, or CD45RB<sup>lo</sup> CD4<sup>+</sup> T cells could represent activated, effector cells (81;247;248) or T<sub>reg</sub> cells (78;80). The increased number of cells in SAMP1/YitFc versus AKR MLN displaying high levels of adhesion molecule expression indicates that many SAMP1/YitFc CD4<sup>+</sup> T cells have been primed to mediate both leukocyte-endothelial and leukocyte-leukocyte interactions. For instance, the LFA-1<sup>hi</sup> ICAM-1<sup>hi</sup> CD4<sup>+</sup> T cells that are increased in SAMP1/YitFc versus AKR MLN would be able to firmly arrest on endothelial cells expressing ICAM-1 and/or mediate effector functions and cellular activation requiring binding to other leukocytes expressing LFA-1 or ICAM-1 (252).

On the basis of differential  $\alpha_4\beta_1$ ,  $\alpha_4\beta_7$ , and  $\alpha_E\beta_7$  integrin expression, we have defined two distinct populations of T cells that are increased in SAMP1/YitFc versus AKR MLN. SAMP1/YitFc CD4<sup>+</sup> T cells expressing the  $\alpha_E\beta_7$  integrin may be able to preferentially home to the intraepithelial lymphocyte compartment and other sites in the intestinal wall through interactions mediated by this integrin (188). CD4<sup>+</sup> T cells expressing CD25 and  $\alpha_E$  have been shown to possess potent anti-inflammatory function in colitis models (85). The second population of cells that is increased in SAMP1/YitFc MLN expresses overlapping and high levels of  $\alpha_4\beta_1$  and  $\alpha_4\beta_7$ . Blockade of interactions mediated by

these integrins and their ligands VCAM-1 and MAdCAM-1 has been shown to decrease colitis severity through abrogation of leukocyte adhesion to inflamed colonic venules *in vivo* (122). In the SAMP1/YitFc MLN CD4<sup>+</sup> T cell adoptive transfer model, blocking both  $\alpha_4$  integrins, but not either one individually, results in decreased disease severity in SCID recipients (Rivera-Nieves, Olson, et.al., *J. Immunol.*, In Revision). The reason why combinatorial blockade of both  $\alpha_4$  integrins is required could easily be explained if these dual-expressing  $\alpha_4\beta_1^{\text{hi}} \alpha_4\beta_7^{\text{hi}}$  CD4<sup>+</sup> T cells are the critical disease-producing cell subset in this model. The exact function of these  $\alpha_4\beta_1^{\text{hi}} \alpha_4\beta_7^{\text{hi}}$  CD4<sup>+</sup> T cells are not further addressed herein, but should form the basis of future studies.

#### *Chemokine receptor expression and function in SAMP1/YitFc MLN and ileum*

We next examined whether changes in adhesion molecule expression described above were accompanied by alterations in the responsiveness of SAMP1/YitFc versus AKR MLN CD4<sup>+</sup> T cells to chemokines directing homeostatic homing to lymphoid organs or inflammatory trafficking to effector sites. Because of a lack of available flow cytometry reagents detecting receptor expression on the protein level and in order to examine as many candidates as possible, chemokine receptor mRNA expression in SAMP1/YitFc and AKR MLN CD4<sup>+</sup> T cells was identified by multiplex RT-PCR. Using densitometric analysis of electrophoretic band intensity, semiquantitative expression levels of chemokine receptors were determined relative to GAPDH control (Figure 3.7). In contrast to the subset marker and adhesion molecule expression differences described above, no differences in chemokine receptor expression at the transcriptional level were seen in SAMP1/YitFc versus AKR MLN CD4<sup>+</sup> T cells. MLN CD4<sup>+</sup> T cells from both



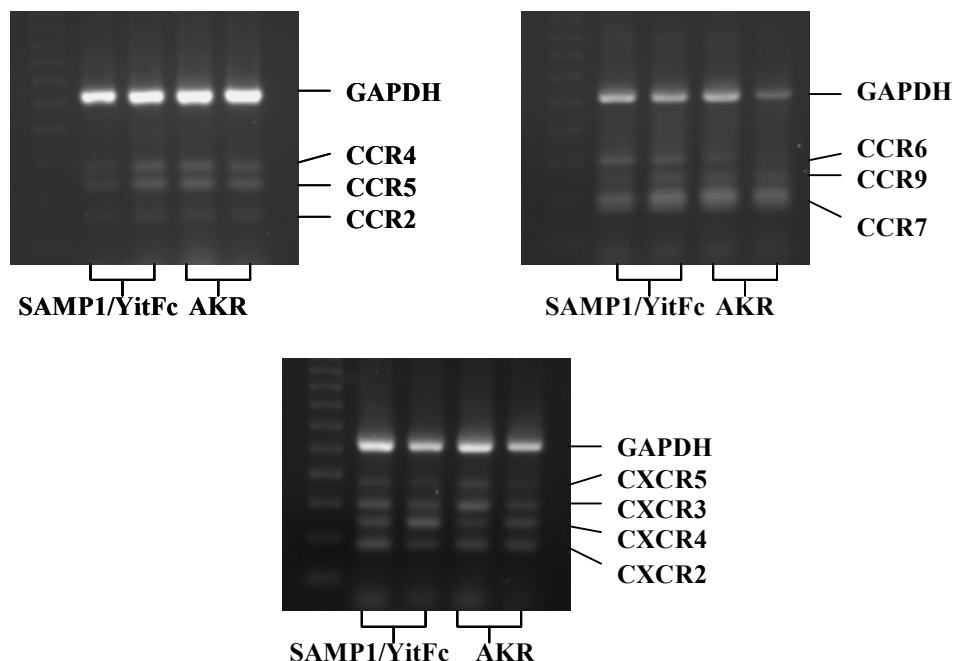


**Figure 3.7:** Representative gel electrophoresis of PCR products generated using CCR set #1 (top, left), CCR set # 2 (top, right), and CXCR (bottom) multiplex PCR kits for mouse chemokine receptor expression (Maxim Biotech, San Francisco, CA) on cDNA generated from SAMP1/YitFc or AKR MLN CD4<sup>+</sup> T cell total mRNA.

strains express CCR2, 4, 5, 6, 7, and 9, as well as CXCR2, 3, 4, and 5 (Table 3.1).

Receptors that do not appear to be expressed on unfractionated MLN CD4<sup>+</sup> T cells include CCR1, CCR3, CCR8, and CX<sub>3</sub>CR1. B cells from both SAMP1/YitFc and AKR MLN displayed similar chemokine receptor expression when compared between strains, but a somewhat distinct pattern when compared with CD4<sup>+</sup> T cells (Table 3.1). MLN B cells expressed CXCR 2, 3, 4, and 5, CX<sub>3</sub>CR1, and CCR1, 2, 5, 6, 7, and 9, while lacking CCR3, 4, and 8 expression.

The functionality of chemokine receptors that play specific roles in mucosal trafficking was assessed using transwell chemotaxis assays to form dose-response curves for chemotaxis toward individual chemokines. Stromal cell-derived factor-1 (SDF-1, CXCL-12) and secondary lymphoid tissue chemokine (SLC, CCL21) bind CXCR4 and

Chemokine Receptor	SAMP & AKR MLN CD4 <sup>+</sup> T cells	SAMP & AKR MLN B cells	SAMP Ileum				AKR Ileum			
			4 week	10 week	20 week	40 week	4 week	10 week	20 week	40 week
CCR1	-	+	++++	+++	+++	-	+++	+++	+++	-
CCR2	+	++	++	++	++	++	++	++	++	+
CCR3	-	-	-	-	-	-	-	-	-	-
CCR4	++	-	-	-	-	-	-	-	-	-
CCR5	++	++	++	++	++	++	++	++	++	+
CCR6	+++	+++	+++	+++	++++	+	+++	++	+++	+
CCR7	++++	+++	+++	+++	+++	+	+++	++	++	+
CCR8	-	-	-	+	++	-	-	-	+	-
CCR9	+++	+	++	+++	+++	++	++	+++	+++	+
CX <sub>3</sub> CR1	-	++	++	+++	++++	++	++	+++	++++	++
CXCR2	++	+++	-	++	+	+	-	++	+	+
CXCR3	++	++	++	++	++	++	++	+	++	+
CXCR4	++	+++	++	+++	++	++	++	++	+++	+
CXCR5	++	++	-	+	++	+	-	+	++	+

**Table 3.1.** Chemokine receptor mRNA expression in isolated MLN CD4<sup>+</sup> T cells and B cells and in whole ileum as measured by multiplex rt-PCR, agarose gel electrophoresis and semi-quantitative densitometric analysis. Expression was defined relative to GAPDH band intensity using the following scale. -, no expression. +, less than 4% of GAPDH band intensity. ++, between 4 and 20% of GAPDH. +++, between 20 and 50% of GAPDH. +++++, over 50% of GAPDH. Data represents average values for n>3 in all groups except CXCR expression in 40 week SAMP1/YitFc where n=2.

CCR7 respectively, and play critical roles in the homing and retention of lymphocyte precursors and naïve lymphocytes within lymphoid organs (253;254). Macrophage-derived chemokine (MDC, CCL22) binding to CCR4, and IFN- $\gamma$  inducible protein (IP-10, CXCL10) binding to CXCR3 promote the trafficking of CD4<sup>+</sup> T cells to sites of Th2- and Th1-type inflammation, respectively (182;255). Interactions between TECK and CCR9 direct the homeostatic homing of T cells to the intestinal wall (175). Significant

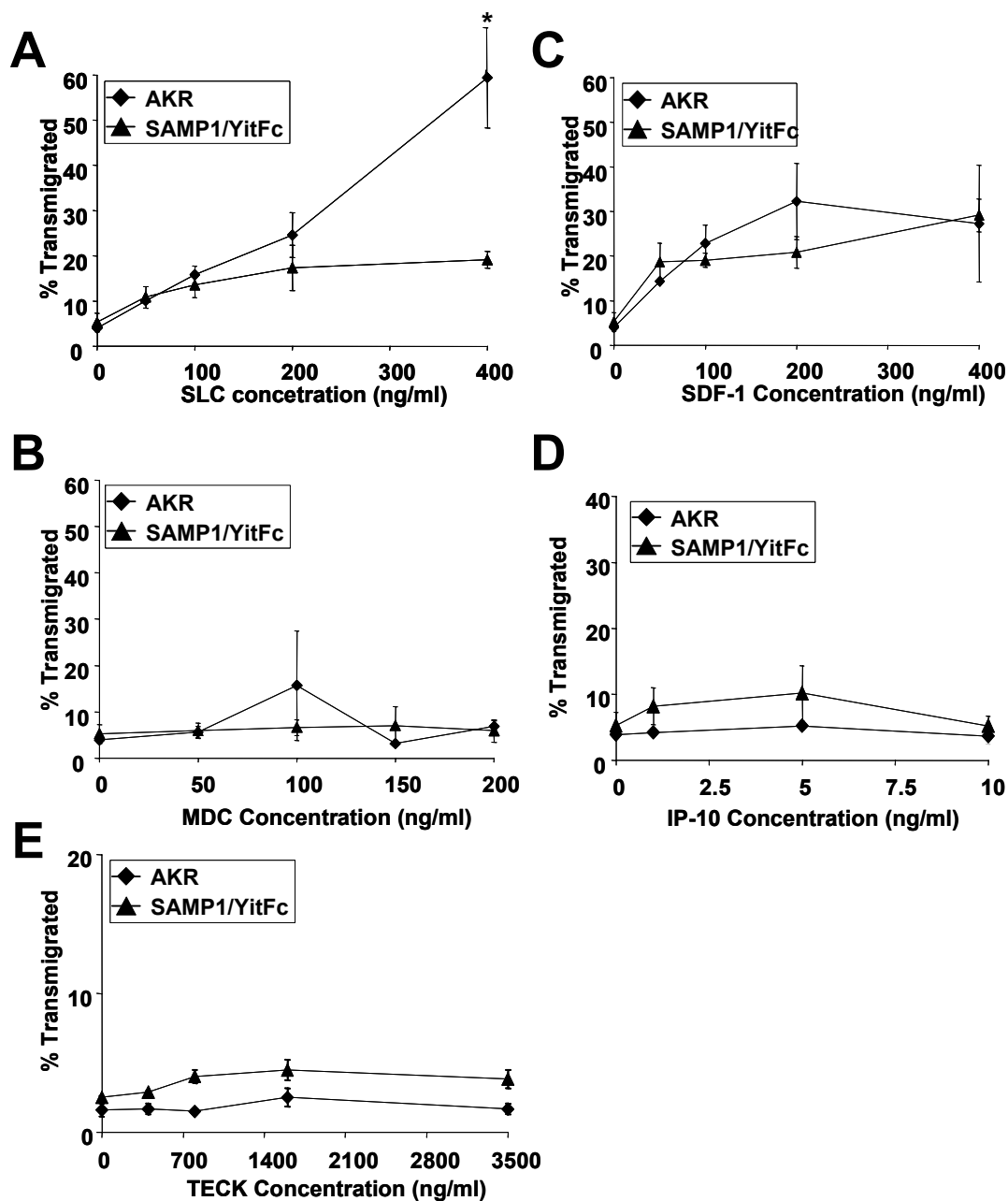


**Figure 3.8:** Dose response curves for the percentage of SAMP1/YitFc or AKR MLN CD4<sup>+</sup> T cells, respectively, that transmigrate to SLC (CCL21) (n=3,4), SDF-1 (CXCL12) (n=3,4), MDC (CCL22) (n=3,4), IP10 (CXCL10) (n=3,3) and TECK (CCL25) (n=2,2) in transwell chemotactic assays.

percentages of both AKR and SAMP1/YitFc MLN CD4<sup>+</sup> T cells exhibited chemotaxis toward SLC and SDF-1, and the magnitude of these responses were mostly similar in cells from both strains (Figure 3.8). At high concentrations (400 ng/ml), an increased percentage of AKR CD4<sup>+</sup> T cells exhibit chemotaxis to SLC compared to SAMP1/YitFc

CD4<sup>+</sup> T cells, though whether this chemokine concentration is physiological remains unclear. Neither AKR nor SAMP1/YitFc CD4<sup>+</sup> T cells exhibited chemotaxis toward MDC above baseline (Figure 3). Slight trends showing higher chemotactic responsiveness toward both IP-10 ( $10 \pm 4\%$  transmigrated versus  $5.2 \pm 0.8\%$ , mean  $\pm$  SEM) and TECK ( $4.5 \pm 0.8\%$  versus  $2.5 \pm 0.7\%$ ) exhibited by SAMP1/YitFc versus AKR cells were not statistically significant.

Because of the similarities in chemokine receptor expression and function in SAMP1/YitFc versus AKR MLN cells, it is possible that strain-based differences in chemokine-mediated trafficking may only become activated once cells have left the MLN and migrated to the intestinal wall. We also hypothesized that chemokine receptors required for the migration of leukocyte subsets to the intestinal wall might vary depending on the stage of disease development. Therefore we measured chemokine receptor expression in whole ileal samples from 4, 10, 20, and 40 week-old SAMP1/YitFc and AKR mice (Figure 3.9). A semiquantitative comparison between strains of the relative expression of various receptors in mice of different ages is shown in Table 3.1. Chemokine receptors for which percent expression relative to GAPDH is significantly higher in SAMP1/YitFc versus AKR ileum from mice of specified ages are listed in Table 3.2. As expected, ileum from 4 week old mice that have yet to develop disease display the smallest range of different chemokine receptor mRNA. CCR1 expression, which has been reported on a number of cell types but most notably on activated or memory T cells (256), is elevated in 4 week SAMP1/YitFc versus AKR ileum, suggesting that interactions between this receptor and its many ligands, including RANTES and MIP-1 $\alpha$  (160), may play critical roles in the initiating phases of the ileal

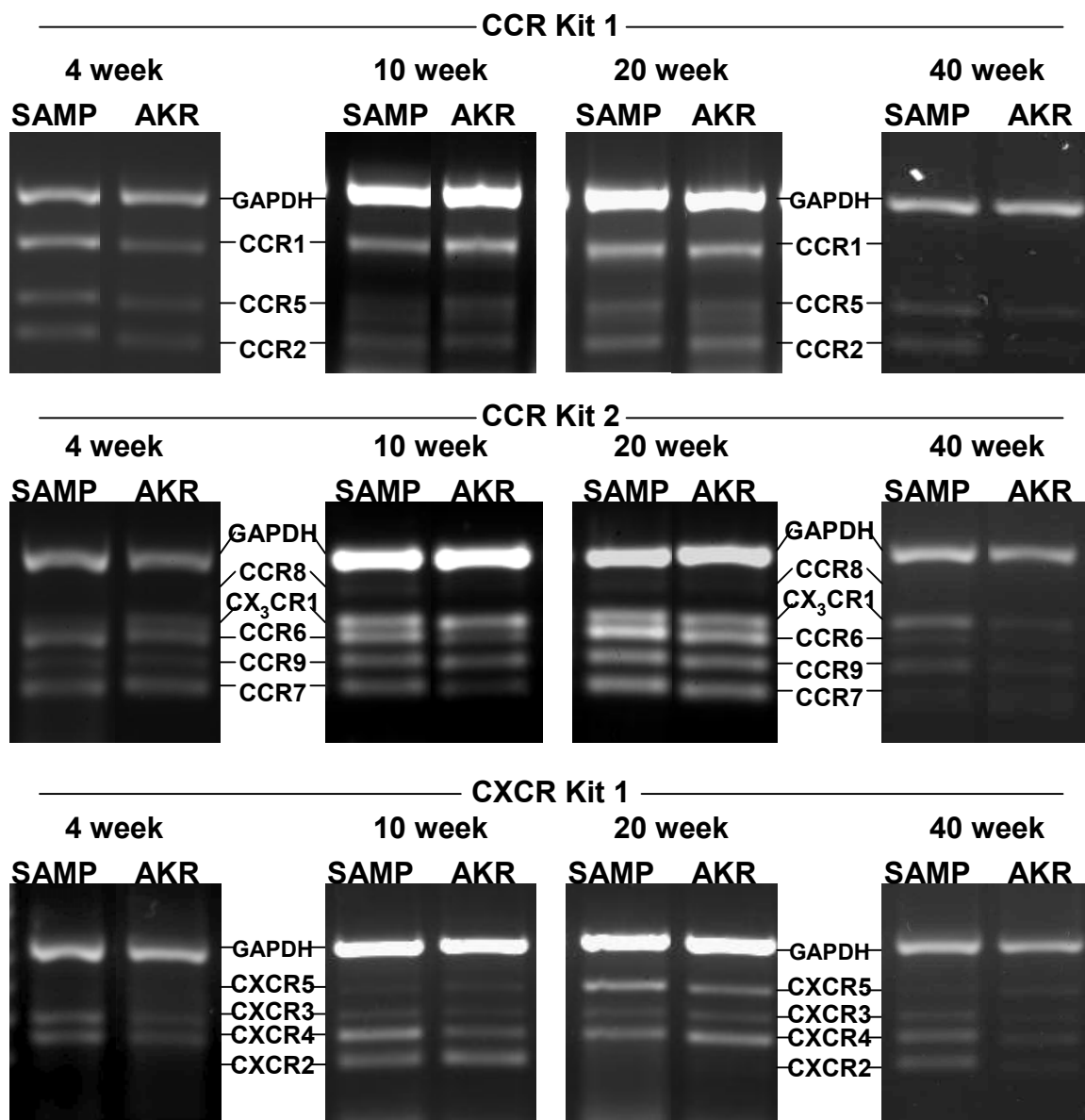


**Figure 3.9:** Representative gel electrophoresis of PCR products generated using CCR set #1 (top), CCR set # 2 (middle), and CXCR (bottom) multiplex PCR kits for mouse chemokine receptor expression (Maxim Biotech, San Francisco, CA) on cDNA generated from 4, 10, 20, and 40 week SAMP1/YitFc and AKR whole ileal mRNA.

immune response. By 10 weeks, the expression of several chemokine receptors is increased in SAMP1/YitFc versus AKR ileum, including CCR6, expressed primarily by B cells and dendritic cells (257), CCR7, expressed by most lymphocytes as described above, and CXCR3, the receptor mediating migration of T cells to Th1 sites of

Chemokine Receptor	Age	Expression as a Percentage of GAPDH Band Intensity	
		SAMP Ileum	AKR Ileum
CCR1	4 weeks	55 ± 1%*	37 ± 7%
CCR6	10 weeks	32 ± 3%*	15 ± 1%
CCR7	10 weeks	25 ± 2%*	3.5 ± 0.5%
CCR8	10 weeks	3 ± 1%#	0.1 ± 0.1%
CX <sub>3</sub> CR1	10 weeks	43 ± 2%*	36 ± 2%
CXCR3	10 weeks	4.9 ± 0.8%#	2.3 ± 0.8%
CXCR4	10 weeks	22 ± 3%#	13 ± 3%
CCR8	20 weeks	7.3 ± 0.8%#	4 ± 1%
CCR2	40 weeks	10 ± 2%*	2.6 ± 0.5%
CCR5	40 weeks	12 ± 2%*	4.0 ± 0.6%
CCR6	40 weeks	2.9 ± 0.7%#	1.1 ± 0.3%
CCR7	40 weeks	1.7% ± 0.2%#	0.8 ± 0.4%
CCR9	40 weeks	8 ± 1%*	3.5 ± 0.5%
CX <sub>3</sub> CR1	40 weeks	18 ± 3%*	9 ± 2%
CXCR3	40 weeks	7 ± 2%*	0.8 ± 0.1%
CXCR4	40 weeks	12 ± 4%*	2 ± 1%

**Table 3.2.** Expression levels of chemokine receptors that are increased in SAMP1/YitFc versus AKR ileum from mice of the indicated ages. Levels are expressed as rt-PCR product band intensity as a % of GAPDH band intensity determined using agarose gel electrophoresis and densitometric analysis.

\*Significantly different compared to AKR ileum ( $P < 0.05$ ) by two-tailed Student's t-test.

#Significantly different compared to AKR ileum ( $P < 0.05$ ) by one-tailed Student's t-test.

inflammation (160). Interestingly, few differences were noted in chemokine receptor expression between strains in 20 week mice. In contrast, 40 week SAMP1/YitFc versus AKR ileum displayed the most differences in expression of any time point studied, with SAMP1/YitFc ileum containing significantly more expression of the intestinal homing receptor CCR9, the monocyte and neutrophil receptors CCR2 and CX<sub>3</sub>CR1, and both Th1 lymphocyte trafficking receptors CXCR3 and CCR5 (160).

AKR and SAMP1/YitFc MLN CD4<sup>+</sup> T cells not only express similar patterns of chemokine receptors, but also display similar patterns of chemotactic responsiveness. While MLN CD4<sup>+</sup> T cells from SAMP1/YitFc and AKR mice express CXCR3, CXCR4, CCR4, CCR7, and CCR9, cells from both strains exhibit significantly greater chemotactic responsiveness to the chemokines that promote homing to lymph nodes (SLC, SDF-1) versus those directing the homeostatic homing (TECK) or inflammatory trafficking of Th1 (IP10) and Th2 (MDC) cells to the intestinal wall. While the trend toward slightly higher TECK- and IP-10-induced chemotaxis in SAMP1/YitFc versus AKR MLN CD4<sup>+</sup> T cells may be an artifact, it may also suggest that small subsets of CD4<sup>+</sup> T cells that are increased in SAMP1/YitFc MLN may be able to migrate to these chemokines in greater numbers than can cells in the remaining population.

Defining differences in mRNA expression levels by conventional rt-PCR and densitometric analysis has several limitations. First, the sensitivity of ethidium bromide labeling is not sufficient to detect small differences in expression. Second, consumption of polymerase and nucleotide reactants can lead to decreasing amplification as PCR reactions progress through high cycle numbers, and thus differences in expression at the end of PCR reactions, as measured by conventional rt-PCR, may be lower than differences measured by real-time rt-PCR during the exponential phase of amplification. Third, slight variability in PCR reaction mixtures and ethidium bromide concentrations of gels limit comparisons between RNA samples to those run in the same reactions and the same gels, though normalization to housekeeping genes such as GAPDH may mitigate some of these effects. In the case of the ileal expression time course study, SAMP1/YitFc and AKR samples from the same ages were run together, whereas samples

from mice of different ages were run separately. An additional issue applicable to the ileal chemokine receptor expression study is that it is unclear whether differences in expression are due to increased overall infiltration of leukocytes or to regulation of specific receptors. Given that GAPDH expression is higher in some cell types than others (258), if infiltrating leukocytes in the ileum express higher levels of GAPDH than surrounding cells, comparison of ileal samples by normalizing to GAPDH will primarily reflect the latter phenomenon. This possibility might explain why differences in SAMP1/YitFc versus AKR ileal chemokine receptor expression are smaller than would be anticipated given the increased leukocyte infiltration in SAMP1/YitFc ileum. A final criticism applicable to any rt-PCR experiment is that mRNA expression does equate to functional protein expression as illustrated by the lack of responsiveness by SAMP1/YitFc CD4<sup>+</sup> T cells to the chemokine MDC despite expressing CCR4 mRNA. Conversely RNA may no longer be present in cells on which some receptors may still be expressed. For instance, despite the large differences in neutrophil numbers in the ilea of SAMP1/YitFc versus AKR mice, we saw no observable differences in SAMP1/YitFc versus AKR ileal mRNA levels of CXCR2, which is present on the surface of most mature neutrophils (160).

In spite of these limitations, several conclusions can be made from the chemokine receptor expression studies. First, because virtually all of the chemokine receptors expressed in SAMP1/YitFc MLN CD4<sup>+</sup> T cells, B cells and ileum are also expressed at some level in the corresponding AKR tissue, increased trafficking to the intestine in the context of SAMP1/YitFc ileitis likely results from increased usage of established chemotactic pathways and not from transcriptional activation of new pathways.



Secondly, cells expressing the chemokine receptors CCR3 and CCR4, receptors that allow migration of cells to Th2 sites of inflammation (255), are not expressed at all in ilea from either strain at any age studied, suggesting that even in wildtype mice, cells migrating to the ileum are biased against trafficking toward Th2 inflammation. Finally, the specific chemokine receptors that are increased in SAMP1/YitFc versus AKR ileum differ with the stage of disease development, suggesting that separate chemotactic pathways may play distinct roles in the development versus maintenance of ileitis.

*Function of SAMP1/YitFc MLN Regulatory CD4<sup>+</sup> T cells in vitro and in vivo*

Because of the expansion of  $\alpha_E\beta_7^+$  CD4<sup>+</sup> T cells in SAMP1/YitFc versus AKR MLN, the characteristics and functions of this subset were further investigated. While the majority of SAMP1/YitFc MLN  $\alpha_E\beta_7^+$  CD4<sup>+</sup> cells were CD69<sup>-</sup> ( $82 \pm 2\%$ ), CD25<sup>-</sup> ( $79 \pm 3\%$ ), L-selectin<sup>hi</sup> ( $58 \pm 5\%$ ), and CD45RB<sup>hi</sup> ( $53 \pm 6\%$ ), most SAMP1/YitFc MLN  $\alpha_E\beta_7^+$  CD4<sup>+</sup> cells were CD69<sup>+</sup> ( $59 \pm 3\%$ ), CD25<sup>+</sup> ( $75 \pm 3\%$ ), L-selectin<sup>lo</sup> ( $66 \pm 4\%$ ), and CD45RB<sup>lo</sup> ( $74 \pm 6\%$ ) (Figure 3.10A), consistent with  $\alpha_E\beta_7^+$  CD4<sup>+</sup> cells possessing an activated (246) and/or a regulatory phenotype (85). Compared to  $\alpha_E^-$  CD4<sup>+</sup> cells, the majority of  $\alpha_E^+$  CD4<sup>+</sup> T cells also expressed high levels of ICAM-1 (64% versus 26%) and LFA-1 (74% versus 24%)(Figure 3.10B). Thus, much of the overall increase in the percentage of SAMP1/YitFc versus AKR CD4<sup>+</sup> T cells that are CD25<sup>+</sup>, L-selectin<sup>lo</sup>, CD45RB<sup>lo</sup>, ICAM-1<sup>hi</sup>, and LFA-1<sup>hi</sup> as shown in Figures 3.4 and 3.5 can be attributed to the expansion of the  $\alpha_E\beta_7^+$  CD4<sup>+</sup> subset. In contrast, the majority of  $\alpha_E\beta_7^+$  CD4<sup>+</sup> cells were PSGL-1<sup>hi</sup>,  $\beta_1^{\text{lo}}$ , and  $\alpha_4^{\text{lo}}$  (Figure 3.10C),. As discussed above,  $\beta_1^{\text{hi}}$  and  $\alpha_4^{\text{hi}}$  cells are virtually identical populations representing cells expressing increased levels of  $\alpha_4\beta_1$ .

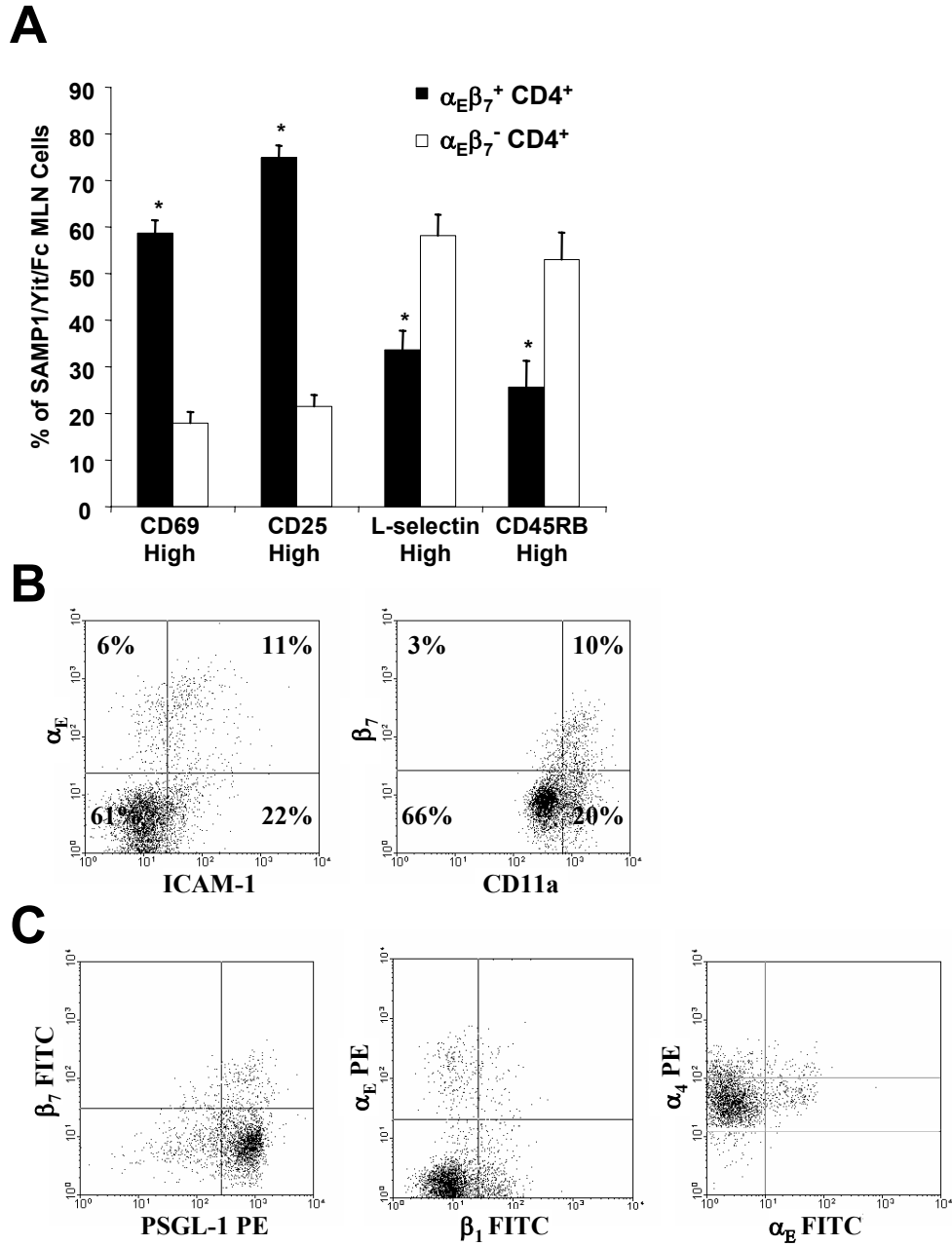


**Figure 3.10:** SAMP1/YitFc MLN  $\alpha_E\beta_7^+ CD4^+$  T cells express high levels of activation markers and adhesion molecules compared to  $\alpha_E\beta_7^- CD4^+$  T cells. Increased percentages (mean  $\pm$  SEM) of  $\alpha_E\beta_7^+ CD4^+$  versus  $\alpha_E\beta_7^- CD4^+$  T cells express high levels of CD69 (n=9), CD25 (n=9), L-selectin (n=14), and CD45RB (n=8) (A). \*Significantly different from  $\alpha_E\beta_7^- CD4^+$  T cell percentage. Representative CD4-gated dotplots, with quadrant percentages, showing that  $\alpha_E\beta_7^+ CD4^+$  T cells express increased levels of ICAM-1 (n=3) and CD11a (n=5) compared to the majority of the remaining  $\alpha_E\beta_7^-$  population (B). In contrast, the  $\alpha_E\beta_7^+ CD4^+$  T cell population is distinct from the increased PSGL-1<sup>lo</sup>,  $\alpha_4^{\text{hi}}$ , and  $\beta_1^{\text{hi}}$  populations found in SAMP1/YitFc MLN (C).

Whether the increased PSGL-1<sup>lo</sup> cells in SAMP1/YitFc mice are related to this second subset has not been investigated.

Compared to  $\alpha_E\beta_7^-$  CD4<sup>+</sup> T cells, freshly isolated SAMP1/YitFc MLN  $\alpha_E\beta_7^+$  CD4<sup>+</sup> T cells expressed higher levels of mRNA for many chemokine receptors, including CCR6 (2-fold increase in band intensity), CCR9 (2-fold), CXCR3 (2-fold), CXCR4 (3-fold), and CXCR5 (3-fold) (Figure 3.11 and Table 3.3). Additionally, freshly isolated  $\alpha_E\beta_7^+$  CD4<sup>+</sup> T cells, but not  $\alpha_E\beta_7^-$  CD4<sup>+</sup> T cells, expressed considerable levels of CCR8 (31% of GAPDH band intensity), which induces cell migration towards two chemokines, I-309 (CCL1) and TARC (CCL22), primarily expressed by activated monocytes, dendritic cells and Th1-polarized T cells (259-261). Once activated in culture for 2 days using anti-CD3 and anti-CD28 stimulation, the overall chemokine receptor expression pattern in these subsets reverses, with  $\alpha_E\beta_7^-$  CD4<sup>+</sup> T cells expressing higher levels of many receptors compared to  $\alpha_E\beta_7^+$  CD4<sup>+</sup> T cells, including CXCR2 (2-fold increase in band intensity), CXCR5 (4-fold), CCR2 (3-fold), CCR4 (6-fold), and CCR5 (5-fold). Activated  $\alpha_E\beta_7^+$  CD4<sup>+</sup> T cells continued to express considerable levels of CCR9, whereas the band for this receptor was only barely detectable in activated  $\alpha_E\beta_7^-$  CD4<sup>+</sup> T cells mRNA. Taken together, these data strongly suggest that, as was the case for adhesion molecule and surface marker expression, SAMP1/YitFc MLN  $\alpha_E\beta_7^+$  and  $\alpha_E\beta_7^-$  CD4<sup>+</sup> T cells may exhibit considerably different chemotactic responsiveness.

To begin assessing differential functions mediated by these subsets, cytokine expression of isolated SAMP1/YitFc MLN  $\alpha_E\beta_7^+$  versus  $\alpha_E\beta_7^-$  CD4<sup>+</sup> T cells was measured by cytometric bead array from 2 day culture supernatants activated with anti-

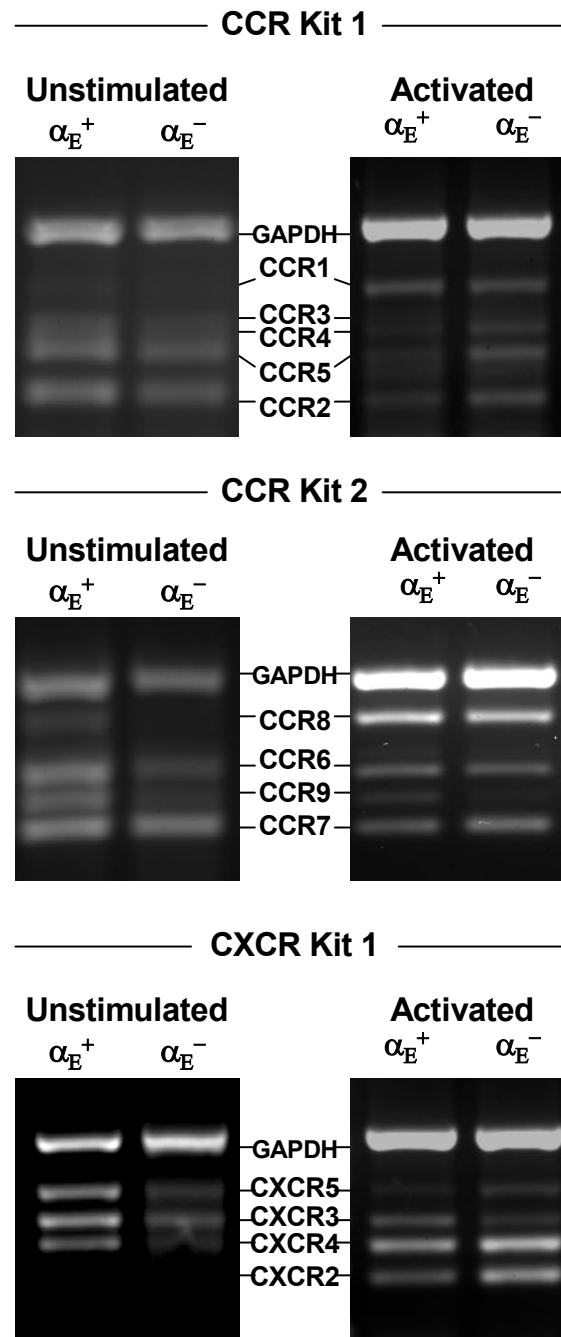


**Figure 3.11:** Distinct chemokine receptor patterns expressed by SAMP1/YitFc MLN  $\alpha_E\beta_7^+$  versus  $\alpha_E\beta_7^-$  CD4<sup>+</sup> T cells. Representative gel electrophoresis of PCR products generated using CCR set #1 (top), CCR set # 2 (middle), and CXCR (bottom) multiplex PCR kits for mouse chemokine receptor expression (Maxim Biotech, San Francisco, CA) on cDNA generated from the RNA of freshly isolated SAMP1/YitFc MLN  $\alpha_E\beta_7^+$  versus  $\alpha_E\beta_7^-$  CD4<sup>+</sup> T cells and in cells activated in culture for two days with immobilized anti-CD3 (10  $\mu$ g/ml) along with soluble rIL-2 (20 U/ml) and anti-CD28 (2  $\mu$ g/ml) stimulation.

Chemokine Receptor	Unstimulated $\alpha_E^+ CD4^+$ T cells	Unstimulated $\alpha_E^- CD4^+$ T cells	Activated $\alpha_E^+ CD4^+$ T cells	Activated $\alpha_E^- CD4^+$ T cells
CCR1	+	+	+++	+++
CCR2	+++	+++	++	++
CCR3	++	++	-	-
CCR4	++	++	+	++
CCR5	+++	+++	+	++
CCR6	++++	+++	++	++
CCR7	++++	++++	++	+++
CCR8	+++	-	++++	++++
CCR9	++++	+++	++	+
CXCR2	++	+	+++	++++
CXCR3	++++	+++	+++	++
CXCR4	+++	++	+++	++++
CXCR5	++++	+++	+	++

**Table 3.3.** Chemokine receptor mRNA expression in freshly isolated SAMP1/YitFc MLN  $\alpha_E\beta_7^+$  versus  $\alpha_E\beta_7^- CD4^+$  T cells and in cells activated in culture for two days with immobilized anti-CD3 (10  $\mu$ g/ml) along with soluble rIL-2 (20 U/ml) and anti-CD28 (2  $\mu$ g/ml) stimulation. Expression was measured by multiplex rt-PCR, agarose gel electrophoresis and semi-quantitative densitometric analysis. Expression was defined relative to GAPDH band intensity using the following scale. -, no expression. +, less than 4% of GAPDH band intensity. ++, between 4 and 20% of GAPDH. +++, between 20 and 50% of GAPDH. +++++, over 50% of GAPDH.

CD3 and anti-CD28 stimulation.  $\alpha_E\beta_7^+ CD4^+$  T cells produced significantly lower levels of TNF- $\alpha$  ( $400 \pm 200$  pg/ml versus  $3000 \pm 600$  pg/ml) and IL-2 ( $600 \pm 400$  pg/ml versus  $5000 \pm 800$  pg/ml) and significantly greater levels of IL-10 ( $900 \pm 100$  pg/ml versus  $310 \pm 80$  pg/ml) than  $\alpha_E\beta_7^- CD4^+$  T cells (Figure 3.12). A trend towards higher production of IFN- $\gamma$  by  $\alpha_E\beta_7^- CD4^+$  T cells versus  $\alpha_E\beta_7^+ CD4^+$  T cells, though this difference did not reach statistical significance due to the large inter-experimental variability in IFN- $\gamma$

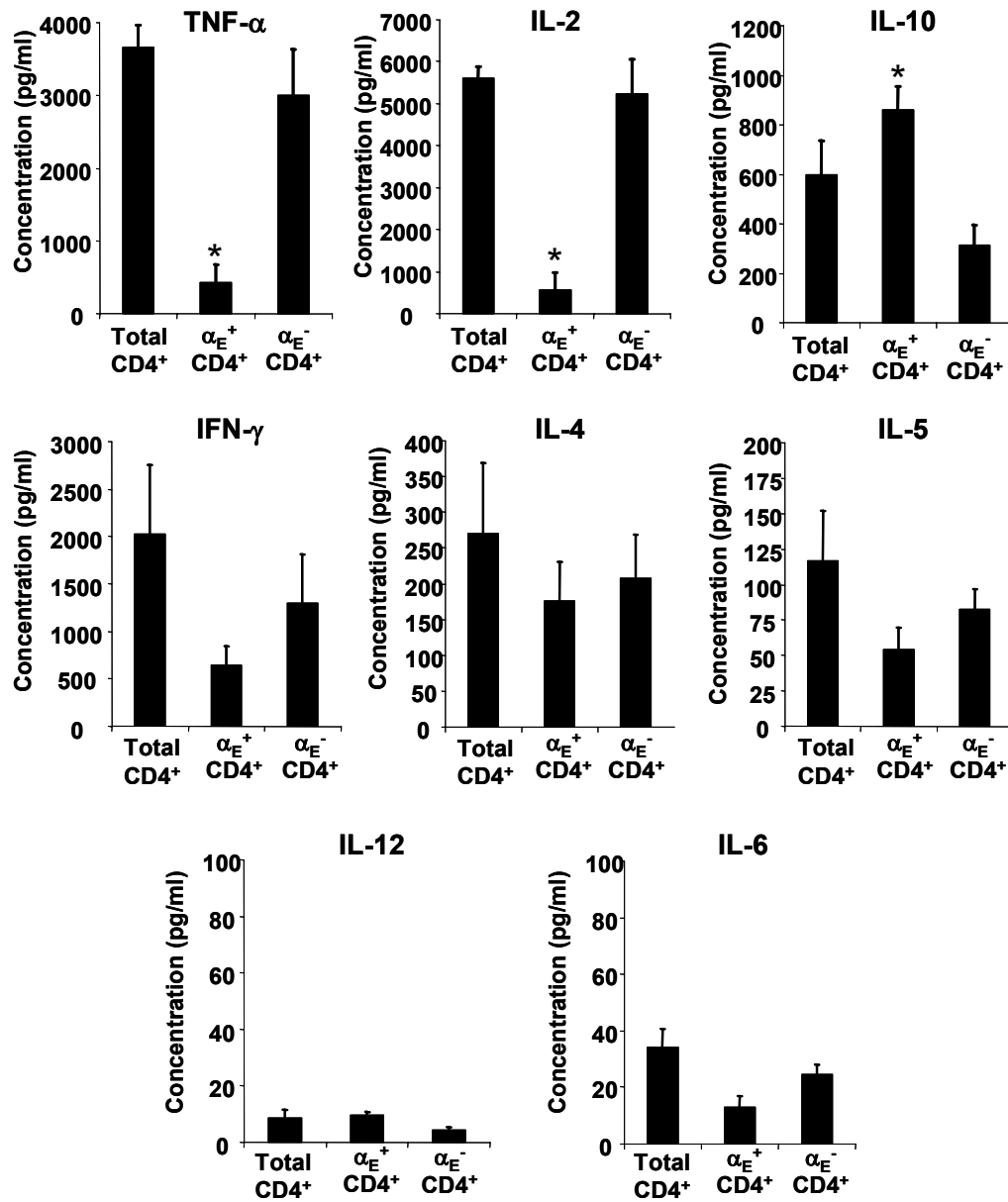


**Figure 3.12:** SAMP1/YitFc MLN  $\alpha_E\beta_7^+$  CD4<sup>+</sup> T cells produce a cytokine profile characteristic of regulatory T cells. Levels of secreted TNF- $\alpha$ , IL-2, IL-10, IFN- $\gamma$ , IL-4, IL-5, IL-12, and IL-6 measured by cytometric bead array in triplicate, from 48 hour cultures of SAMP1/YitFc MLN unfractionated CD4<sup>+</sup> T cells (Total CD4<sup>+</sup>),  $\alpha_E^+$  CD4<sup>+</sup> T cells, or  $\alpha_E^-$  CD4<sup>+</sup> T cells ( $10^5$ /well) stimulated with immobilized anti-CD3 and soluble anti-CD28 antibodies. Data represent the averages of 3 independent experiments for each group. \*Significantly different from levels produced by  $\alpha_E^-$  CD4<sup>+</sup> T cells ( $P < 0.05$ ).

expression by  $\alpha_E\beta_7^-$  cells. No significant differences between subsets were observed in terms of the production of IL-4, IL-5, IL-12 or IL-6.

The increased production of IL-10 and decreased production of IL-2 and TNF- $\alpha$  in  $\alpha_E\beta_7^+$  versus  $\alpha_E\beta_7^-$  CD4 $^+$  T cells suggests that  $\alpha_E\beta_7^+$  CD4 $^+$  T cells may be a regulatory T cell population (208). Since regulatory T cells are also known to exert their effects through IL-10 and TGF- $\beta$  production, I attempted to measure expression of this cytokine in cultured SAMP1/YitFc MLN  $\alpha_E\beta_7^+$  and  $\alpha_E\beta_7^-$  CD4 $^+$  T cells. However, to measure TGF- $\beta$  expression, cells must be cultured in serum-free media because of the high homology between murine TGF- $\beta$  and bovine TGF- $\beta$  present in FCS (202), and SAMP1/YitFc MLN CD4 $^+$  T cells did not survive these culture conditions. To circumvent this issue, we examined TGF- $\beta$  mRNA expression relative to GAPDH standard by rt-PCR and densitometric analysis in freshly isolated SAMP1/YitFc MLN cells and in cells cultured for 3 days in conventional media with anti-CD3, anti-CD28, and rIL-2 stimulation. Compared to freshly isolated  $\alpha_E\beta_7^-$  cells or  $\alpha_E\beta_7^-$  CD25 $^-$  T cells,  $\alpha_E\beta_7^+$  cells exhibited significantly higher TGF- $\beta$  expression, in terms of electrophoretic band intensity (Figure 3.13A). In multiple experiments, cultured  $\alpha_E\beta_7^+$  CD4 $^+$  T cells produced significantly increased TGF- $\beta$  normalized to GAPDH expression ( $37 \pm 4\%$  of GAPDH band intensity versus  $21 \pm 2\%$ , mean  $\pm$  SEM) compared to levels produced by  $\alpha_E\beta_7^-$  CD25 $^-$  CD4 $^+$  T cells (Figure 3.13B and C), although this difference is much lower than the previously published 20-fold difference in TGF- $\beta$  protein production in wildtype splenic regulatory versus effector T cells (202). It is unclear whether this disparity is due to the low sensitivity of the conventional rt-PCR/densitometric analysis method, predominance of translational or post-translational versus transcriptional regulation of TGF- $\beta$  production in T cells (262), or lower levels of

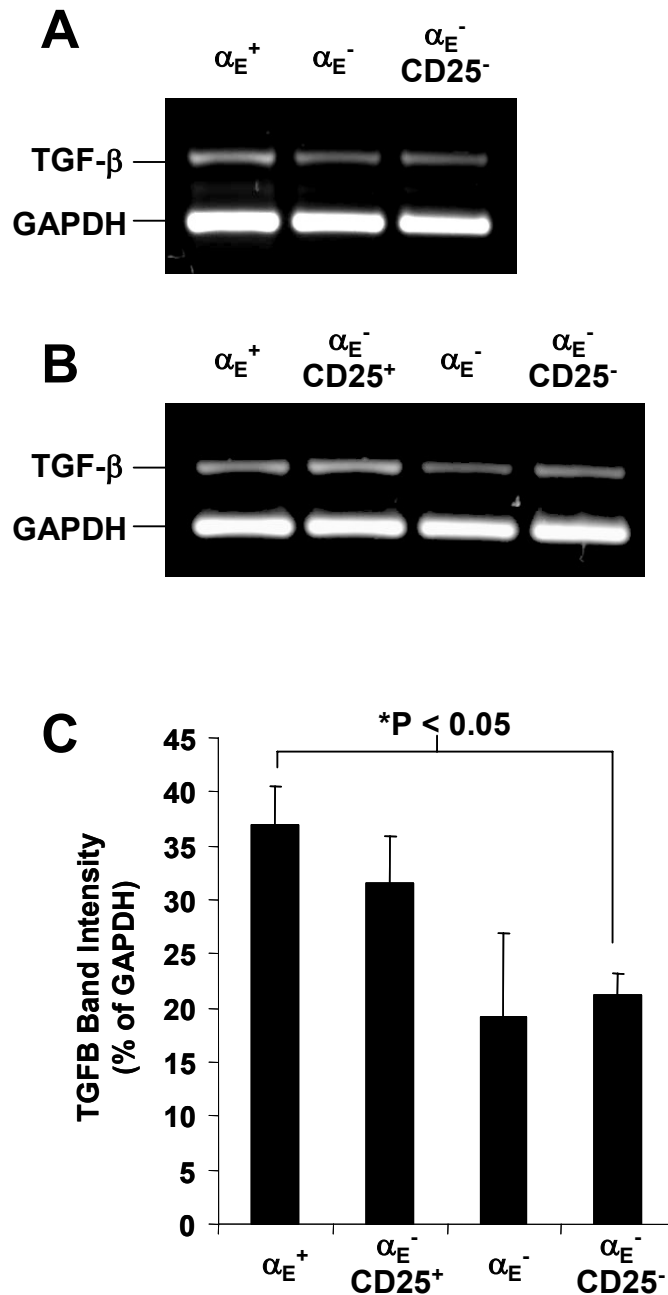


**Figure 3.13:** TGF- $\beta$  mRNA is expressed at slightly higher levels by SAMP1/YitFc MLN  $\alpha_E\beta_7^+$  CD4<sup>+</sup> T cells than by  $\alpha_E\beta_7^-$  CD25<sup>-</sup> effector CD4<sup>+</sup> T cells. Expression analysis was performed by two-step reverse transcriptase PCR. Gel electrophoresis of rt-PCR products showing TGF- $\beta$  expression on freshly isolated  $\alpha_E^+$  CD4<sup>+</sup> T cells,  $\alpha_E^-$  CD4<sup>+</sup> T cells, and  $\alpha_E^-$  CD25<sup>-</sup> CD4<sup>+</sup> T cells (A). In a series of separate experiments (n=3 for each group), isolated  $\alpha_E^+$  CD4<sup>+</sup> T cells,  $\alpha_E^-$  CD25<sup>+</sup> CD4<sup>+</sup> T cells,  $\alpha_E^-$  CD4<sup>+</sup> T cells, and  $\alpha_E^-$  CD25<sup>-</sup> CD4<sup>+</sup> T cells were activated in 60-72 hour cultures using immobilized anti-CD3 (10  $\mu$ g/ml) along with soluble rIL-2 (20 U/ml) and anti-CD28 (2  $\mu$ g/ml) stimulation and then assessed for TGF- $\beta$  expression. Representative gel electrophoresis showing TGF- $\beta$  expression in cultured cells (B). Comparison of TGF- $\beta$  expression in cultured cells by densitometric analysis of band intensity relative to GAPDH expression levels (C).



TGF- $\beta$  expression by SAMP1/YitFc MLN  $\alpha_E\beta_7^+$  CD4 $^+$  T cells relative to expression by wildtype splenocyte Treg cells.

To test whether SAMP1/YitFc MLN  $\alpha_E\beta_7^+$  CD4 $^+$  T cells possess regulatory T cell function, the ability of these cells to block  $\alpha_E^-$  CD4 $^+$  T cell proliferation, measured by  $^3\text{H}$  thymidine incorporation, was examined in cultures with irradiated antigen presenting cells (Figure 3.14).  $\alpha_E\beta_7^-$  CD4 $^+$  T cells showed strong proliferation when cultured with APC alone, while  $\alpha_E\beta_7^+$  CD4 $^+$  T cells underwent minimal proliferation. Addition of  $\alpha_E^+$

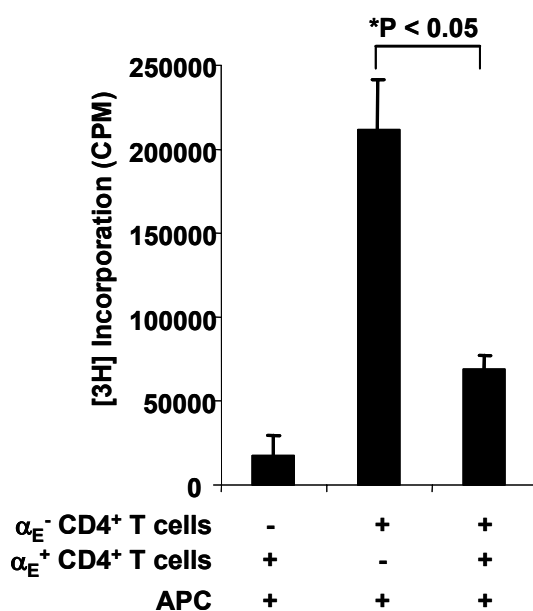


**Figure 3.14:** SAMP1/YitFc MLN  $\alpha_E\beta_7^+$  CD4 $^+$  T cells proliferate poorly in culture and display regulatory T cell function by blocking effector T cell proliferation. SAMP1/YitFc irradiated splenic APC ( $1 \times 10^5$ /well) were cultured with combinations of MLN  $\alpha_E^+$  CD4 $^+$  T cells and  $\alpha_E^-$  CD4 $^+$  T cells ( $5 \times 10^4$  each) stimulated for 3 days with immobilized anti-CD3.  $^3\text{H}$  thymidine was added to the culture 24 hrs before analysis. Data for each condition represents the average of 3 independent cultures each from 2 separate pools of cells isolated from >10 SAMP1/YitFc mice.

CD4 $^+$  T cells to  $\alpha_E\beta_7^-$  CD4 $^+$  T cell cultures markedly suppressed  $\alpha_E\beta_7^-$  CD4 $^+$  T cell proliferation, confirming that SAMP1/YitFc  $\alpha_E^+$  CD4 $^+$  T cells are functional Treg cells.

Next, the ability of SAMP1/YitFc MLN  $\alpha_E\beta_7^+$  CD4 $^+$  Treg to prevent ileitis produced by transfer of SAMP1/YitFc MLN  $\alpha_E\beta_7^-$  CD4 $^+$  effector T cells into

C3H/HeJ SCID mice was investigated. I first determined the utility of the three parameter histologic scoring system developed to measure SAMP1/YitFc ileitis (173) in assessing disease severity in the adoptive transfer model by

injecting SCID mice with PBS sham, AKR MLN CD4<sup>+</sup> T cells, or SAMP1/YitFc CD4<sup>+</sup> T cells and analyzing the resulting inflammation after 6 weeks. Mice receiving PBS sham had no chronic inflammatory score and only a minimal active inflammatory score (Figure 3.15A). However these mice received a sizable villus distortion score ( $2.5 \pm 1.5$ , mean  $\pm$  SEM) that was not significantly different from scores in mice receiving CD4<sup>+</sup> T cells. Further, while SCID mice receiving SAMP1/YitFc CD4<sup>+</sup> T cells exhibit 2-fold higher active + chronic inflammation scores than mice receiving AKR cells, the villus distortion score in these two groups was nearly identical. Thus, while the villus distortion parameter reliably differentiates inflamed SAMP1/YitFc from normal AKR ileum, it appears to have minimal utility in the adoptive transfer model.

SCID mice were then adoptively transferred with  $5 \times 10^5$  unfractionated,  $\alpha_E\beta_7^+$ , or  $\alpha_E\beta_7^-$  CD4<sup>+</sup> T cells i.p., and the resulting ileitis severity was again analyzed after 6 weeks (Figure 3.15B). Compared to mice receiving SAMP1/YitFc  $\alpha_E\beta_7^-$  CD4<sup>+</sup> T cells, SCID mice transferred with SAMP1/YitFc  $\alpha_E\beta_7^+$  CD4<sup>+</sup> T cells had significantly lower active + chronic inflammation ( $4.3 \pm 0.8$  versus  $13.3 \pm 0.9$ , mean  $\pm$  SEM) and total inflammatory scores ( $8 \pm 1$  versus  $21 \pm 1$ ), suggesting that  $\alpha_E\beta_7^-$  CD4<sup>+</sup> T cells contain the major ileitis-producing subset. Ileitis severity produced by SAMP1/YitFc  $\alpha_E\beta_7^+$  CD4<sup>+</sup> T cells was nearly identical to the baseline levels of inflammation produced by AKR CD4<sup>+</sup> T cells in Figure 3.15A. Histologic sections from mice transferred with SAMP1/YitFc  $\alpha_E\beta_7^+$  versus  $\alpha_E\beta_7^-$  CD4<sup>+</sup> T cells reveal increased lesion size (Figure 3.16A) and neutrophil and mononuclear cell infiltrates (Figure 3.16B) in mice receiving  $\alpha_E\beta_7^-$  CD4<sup>+</sup> T cells.

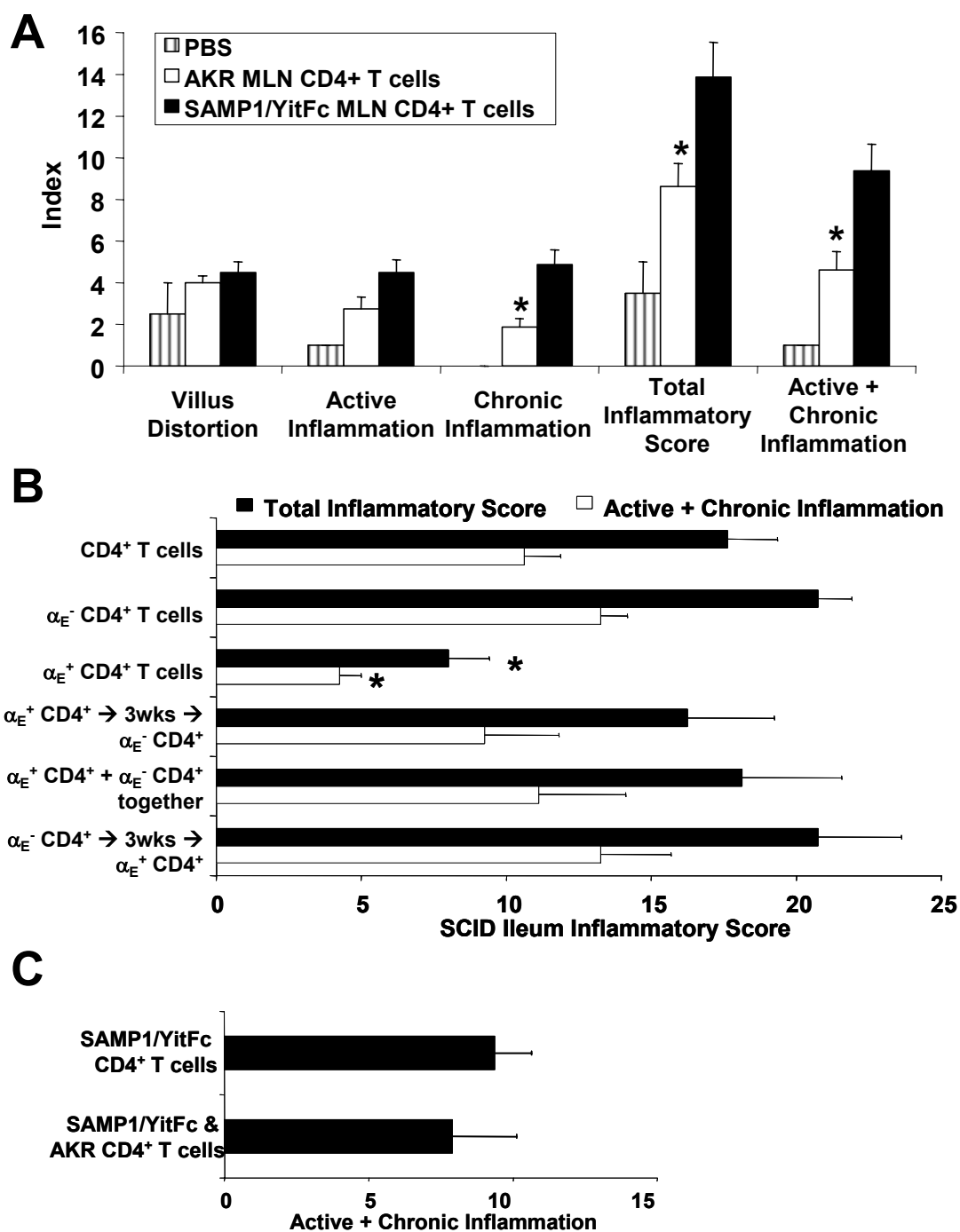


**Figure 3.15:** Comparison of ileitis severity (6 weeks post-transfer, mean  $\pm$  SEM) in SCID mice receiving injections of PBS (n=2) or transfer of SAMP1/YitFc (n=4) or AKR MLN (n=8) CD4<sup>+</sup> T cells (A). Comparison of ileitis severity in SCID recipients (n=4 in each group) induced by  $5 \times 10^5$  SAMP1/YitFc total MLN CD4<sup>+</sup> T cells,  $\alpha_E^-$  CD4<sup>+</sup> T cells,  $\alpha_E^+$  CD4<sup>+</sup> T cells, or combination treatment using  $\alpha_E^+$  CD4<sup>+</sup> T cells injected 3 weeks before, at the same time as, or 3 weeks after  $\alpha_E^-$  CD4<sup>+</sup> T cells (B). In a separate cohort of SCID mice, severity of ileitis induced by  $5 \times 10^5$  CD4<sup>+</sup> T cells (n=4) was not decreased by coinjection of  $5 \times 10^5$  AKR MLN CD4<sup>+</sup> T cells (n=5) (D). \*Significantly different from inflammation severity induced by SAMP1/YitFc total CD4<sup>+</sup> T cells

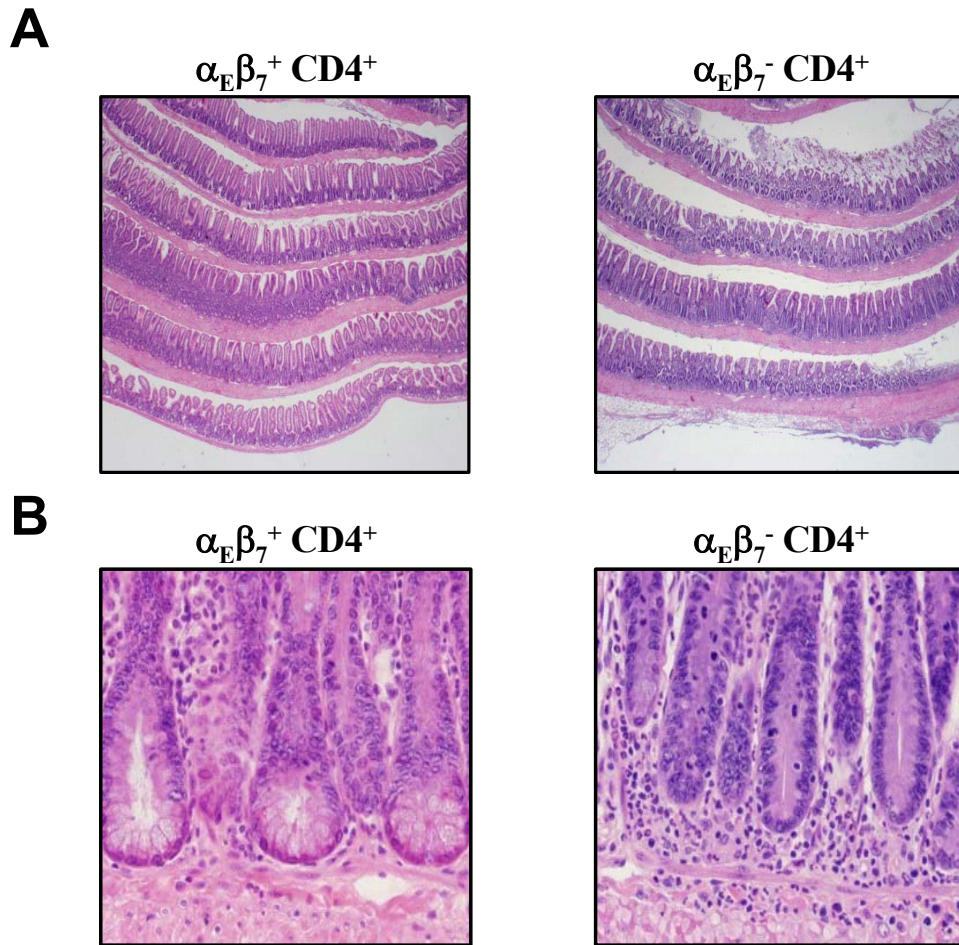


**Figure 3.16:** Histologic sections show increased disease severity in SCID mice receiving SAMP1/YitFc MLN  $\alpha_E\beta_7^-$  versus  $\alpha_E\beta_7^+$  CD4<sup>+</sup> T cells. Low power (20X) view (A) of SCID Ileum in a Swiss roll shows a heavy inflammatory infiltrate and severe villous blunting in  $\alpha_E\beta_7^-$  CD4<sup>+</sup> cell, but not  $\alpha_E\beta_7^+$  CD4<sup>+</sup> cell recipients. High power (200x) view (B) shows increased cellularity at the base of the mucosa and increased neutrophilic infiltrate throughout in mice transferred with  $\alpha_E\beta_7^-$  CD4<sup>+</sup> cells.

A trend towards slightly higher scores is seen in Figure 3.15B in mice receiving  $\alpha_E\beta_7^-$  CD4<sup>+</sup> T cells versus mice receiving unfractionated CD4<sup>+</sup> T cells, particularly when the villus distortion parameter is excluded ( $13.3 \pm 0.9$  versus  $11 \pm 1$ , active + chronic inflammation). Combining this data with scores from another experiment in which only SAMP1/YitFc unfractionated or  $\alpha_E\beta_7^-$  CD4<sup>+</sup> T cells were transferred yields a significant, albeit small, increase in severity in mice transferred with  $\alpha_E\beta_7^-$  versus unfractionated CD4<sup>+</sup> T cells ( $13.6 \pm 0.5$  versus  $10 \pm 1$ ). To test whether  $\alpha_E\beta_7^+$  CD4<sup>+</sup> T cells can

downregulate  $\alpha_E\beta_7^-$  CD4<sup>+</sup> T cell-induced ileitis,  $5 \times 10^5$   $\alpha_E\beta_7^+$  CD4<sup>+</sup> T cells were injected into SCID mice 3 weeks before, at the same time as, or 3 weeks after injection of  $5 \times 10^5$   $\alpha_E\beta_7^-$  CD4<sup>+</sup> T cells (Figure 3.15B). No significant differences were seen in the active + chronic or total inflammatory scores in any of the three groups compared to injection of  $\alpha_E\beta_7^-$  CD4<sup>+</sup> T cells alone, indicating that SAMP1/YitFc  $\alpha_E\beta_7^+$  CD4<sup>+</sup> T cells cannot prevent ileitis produced by  $\alpha_E\beta_7^-$  CD4<sup>+</sup> T cells and may only have anti-inflammatory effects in slightly mitigating the highest severity of disease.

To test whether SAMP1/YitFc  $\alpha_E\beta_7^+$  CD4<sup>+</sup> T cells might have defective regulatory function compared to wildtype Treg, a separate cohort of SCID mice was transferred with  $5 \times 10^5$  SAMP1/YitFc CD4<sup>+</sup> T cells alone or a combination of SAMP1/YitFc plus AKR ( $5 \times 10^5$  cells each) CD4<sup>+</sup> T cells (Figure 3.15C). AKR MLN CD4<sup>+</sup> T cells, presumably containing functional Treg were unable to prevent ileitis produced by SAMP1/YitFc CD4<sup>+</sup> T cells.

To investigate whether differences in pathogenicity of SAMP1/YitFc  $\alpha_E\beta_7^+$  versus  $\alpha_E\beta_7^-$  CD4<sup>+</sup> T cells were linked to differential homing patterns of these subsets, SCID mice were injected with  $\alpha_E\beta_7^+$  or  $\alpha_E\beta_7^-$  cells labeled with CFSE and PKH26, respectively, or vice versa and the tissue-specific accumulation of labeled cells was examined after 3 days (Figure 3.17A and B).  $\alpha_E\beta_7^-$  cells preferentially homed in large numbers to SCID MLN, as labeled SAMP1/YitFc  $\alpha_E\beta_7^-$  cells comprised  $11 \pm 3\%$  (mean  $\pm$  SEM) of total MLN lymphocytes in recipient mice. The ratio of labeled  $\alpha_E\beta_7^-$  to  $\alpha_E\beta_7^+$  cells in the MLN was 7:1, and comparisons of two separate mice in which either  $\alpha_E\beta_7^-$  or  $\alpha_E\beta_7^+$  cells were labeled with CFSE (Figure 3.17A, top, right 2 panels) shows that the

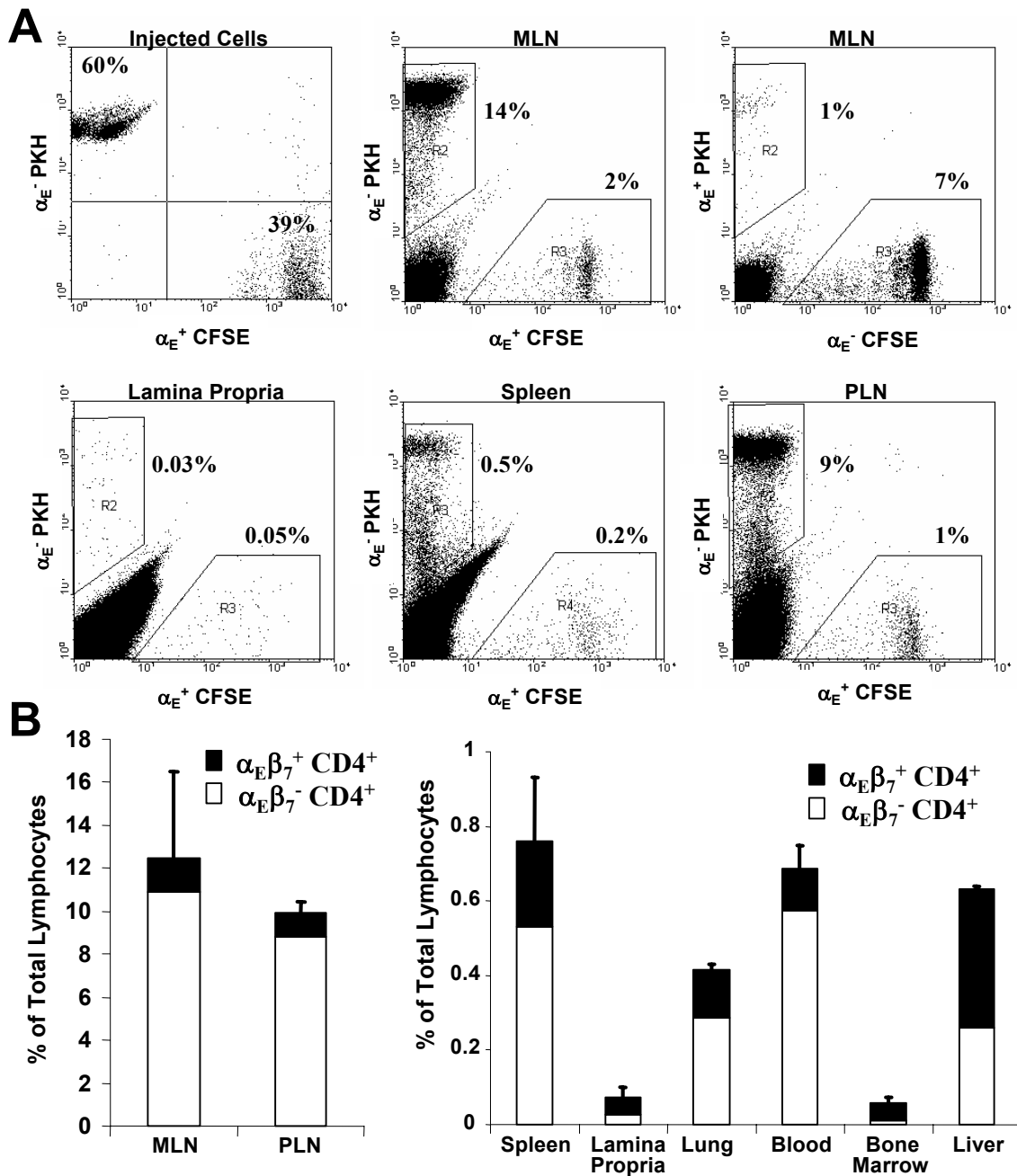


**Figure 3.17:** Two-color short term homing assay performed by injecting one SCID mouse with isolated SAMP1/YitFc MLN  $\alpha_E\beta_7^-$  versus  $\alpha_E\beta_7^+$  CD4<sup>+</sup> T cells labeled with PKH26 (FL-2) and CFSE (FL-1), respectively, and a second mouse with cells labeled in the opposite pattern. The percentage of labeled cells in specified organs was determined 3 days after injection. The ratio of  $\alpha_E\beta_7^-$  versus  $\alpha_E\beta_7^+$  cells in the injected fraction (A, top left) was used to normalize values to starting number of cells in the remaining panels. MLN contain increased ratios of  $\alpha_E\beta_7^-$  to  $\alpha_E\beta_7^+$  cells due to increased number of both divided and undivided cells, as measured by quantal decreases in CFSE intensity (A, top middle and right). Spleen and peripheral lymph nodes (PLN) also have increased  $\alpha_E\beta_7^-$  to  $\alpha_E\beta_7^+$  ratios, whereas the few cells that homed to the lamina propria by 3 days are equally distributed between  $\alpha_E\beta_7^-$  and  $\alpha_E\beta_7^+$  populations (A, bottom 3 panels). Comparison of the contributions of  $\alpha_E\beta_7^-$  and  $\alpha_E\beta_7^+$  fractions to the total number of labeled cells homing to specific SCID tissues (n=2 for each tissue) (B).

increase in  $\alpha_E\beta_7^-$  relative to  $\alpha_E\beta_7^+$  cells corresponds to increases in dividing and non-dividing cells. Peripheral lymph nodes (8:1) and peripheral blood (5:1) displayed  $\alpha_E\beta_7^-$ : $\alpha_E\beta_7^+$  cell ratios similar to MLN, whereas the ratio of labeled cells in spleen was somewhat more equal (2.5:1) (Figure 3.17A and B). While total numbers of labeled cells homing to the lamina propria were low, nearly twice as many  $\alpha_E\beta_7^+$  CD4<sup>+</sup> T cells as  $\alpha_E\beta_7^-$  CD4<sup>+</sup> T cells were present. Due to the low number of total events, these differences in LPL numbers should be interpreted somewhat cautiously.  $\alpha_E\beta_7^+$  CD4<sup>+</sup> T cells also homed at higher rates than  $\alpha_E\beta_7^-$  CD4<sup>+</sup> T cells to the bone marrow and liver (Figure 3.17B). Taken together, the results from these experiments suggest that the early events in ileitis pathogenesis in the adoptive transfer model may require homing and proliferation of effector cells within lymphoid organs, and the lack of migration of  $\alpha_E\beta_7^+$  CD4<sup>+</sup> Treg to these lymphoid organs may be linked to lack of Treg efficacy in preventing ileitis in this model.

Finally, these results showing ineffectiveness of  $\alpha_E\beta_7^+$  CD4<sup>+</sup> Treg in blocking ileitis were confirmed using other well-characterized CD4<sup>+</sup> T cell adoptive transfer models. To this end, a third cohort of SCID mice was transferred with  $5 \times 10^5$  unfractionated SAMPI/YitFc MLN CD4<sup>+</sup> T cells or CD4<sup>+</sup> cells separated on the basis of CD45RB, L-selectin, CD69, or CD25 expression and both ileitis and colitis severity was determined after 6 weeks (Figure 3.18A and B). Mice receiving CD25<sup>+</sup> ( $6 \pm 2$ ), CD69<sup>+</sup> ( $7 \pm 2$ ), or L-selectin<sup>lo</sup> ( $5 \pm 2$ ) CD4<sup>+</sup> T cells developed significantly lower levels of active + chronic ileal inflammation compared to mice receiving unfractionated CD4<sup>+</sup> T cells ( $11.5 \pm 0.3$ ). However, ileitis in mice receiving CD25<sup>-</sup> ( $11 \pm 2$ ), CD69<sup>-</sup> ( $12 \pm 1$ ), or L-selectin<sup>hi</sup>

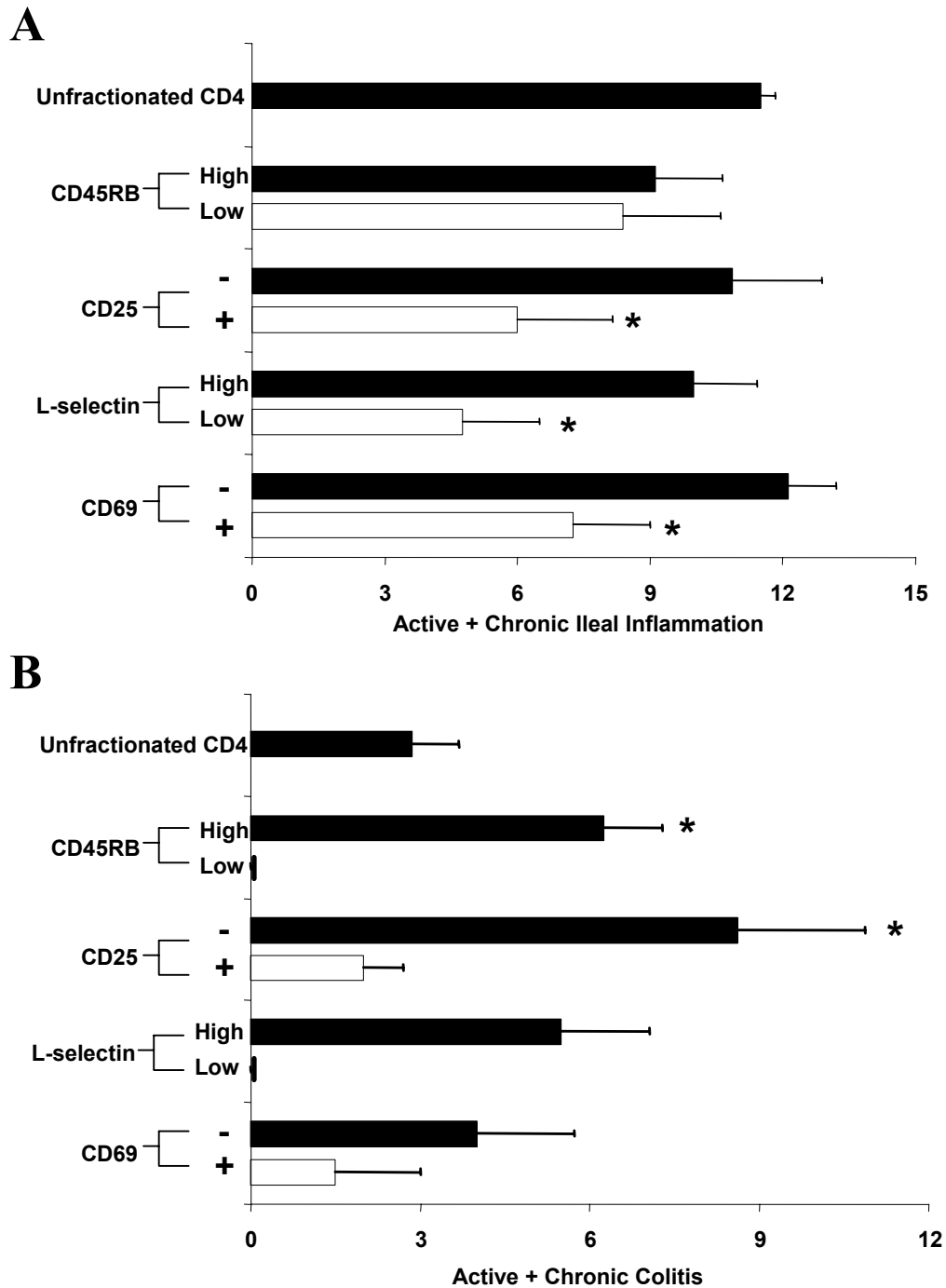


**Figure 3.18:** Regulatory T cell populations prevent colitis, but not ileitis in adoptively transferred SCID mice. Adoptively transferred ileitis (A) and colitis (B) severities were compared among SCID mice six weeks after receiving  $5 \times 10^5$  SAMP1/YitFc MLN unfractionated (n=7), CD45RB<sup>high</sup> (n=4), CD45RB<sup>low</sup> (n=4), CD25<sup>-</sup> (n=4), CD25<sup>+</sup> (n=4), L-selectin<sup>hi</sup> (n=4), L-selectin<sup>lo</sup> (n=4), CD69<sup>+</sup> (n=2), and CD69<sup>-</sup> (n=4) CD4<sup>+</sup> T cells. Since villus distortion is not measured in colitis, the sum of active and chronic inflammatory scores was used for this comparison. Data expressed as mean  $\pm$  SEM. \*Significantly different ( $P < 0.05$ ) compared to ileitis or colitis severity in mice receiving unfractionated CD4<sup>+</sup> T cells.



( $10 \pm 1$ )  $CD4^+$  T cells was not significantly greater than disease in mice receiving unfractionated  $CD4^+$  T cells, implying that potential regulatory functions exhibited by  $CD25^+$ ,  $CD69^+$ , and L-selectin<sup>lo</sup> cells in the unfractionated  $CD4^+$  population are not capable of downregulating ileitis produced by effector cells. Further,  $CD45RB^{lo}$   $CD4^+$  T cells produced nearly identical levels of ileitis compared to  $CD45RB^{hi}$   $CD4^+$  T cells, suggesting that  $CD45RB^{lo}$   $CD4^+$  T cells contain subsets of cells that are pro-inflammatory in the context of ileitis. Combining the results of these experiments with the results of 4-color flow cytometry examining the size of subsets defined on the basis of  $CD45RB$ , L-selectin,  $CD69$ , and  $CD25$  expression demonstrates that the size of the main ileitis producing  $CD69^-$   $CD25^-$  L-selectin<sup>hi</sup> subset represents 41% of the overall SAMP1/YitFc  $CD4^+$  T cell population (Table 3.4).

In contrast, colitis in SCID mice receiving SAMP1/YitFc MLN  $CD45RB^{hi}$  ( $6 \pm 1$ ) or  $CD25^-$  ( $9 \pm 2$ )  $CD4^+$  T cells was significantly more severe than colitis in mice receiving unfractionated  $CD4^+$  T cells ( $2.9 \pm 0.9$ ) containing the  $CD45RB^{lo}$  and  $CD25^+$  T cell

		L-selectin <sup>hi</sup>		L-selectin <sup>lo</sup>	
		CD45RB <sup>hi</sup>	CD45RB <sup>lo</sup>	CD45RB <sup>hi</sup>	CD45RB <sup>lo</sup>
CD25 <sup>+</sup>	CD69 <sup>+</sup>	1.0 $\pm$ 0.1	1.7 $\pm$ 0.2	3.4 $\pm$ 0.8	12 $\pm$ 1
	CD69 <sup>-</sup>	0.9 $\pm$ 0.1	3.1 $\pm$ 0.6	1.3 $\pm$ 0.3	4.3 $\pm$ 0.5
CD25 <sup>-</sup>	CD69 <sup>+</sup>	3.3 $\pm$ 0.2	1.1 $\pm$ 0.1	4.8 $\pm$ 0.7	9.6 $\pm$ 0.7
	CD69 <sup>-</sup>	<b>33 <math>\pm</math> 2</b>	<b>8 <math>\pm</math> 1</b>	4.0 $\pm$ 0.2	7.7 $\pm$ 0.4

**Table 3.4.** Percentage of the 16 subpopulations of  $CD4^+$  T cells in SAMP1/YitFc MLN that can be distinguished by four-color flow cytometry on the basis of L-selectin,  $CD45RB$ ,  $CD25$ , and  $CD69$  expression. Due to the limitation of being able to acquire only four colors on the FACS Calibur flow cytometer and because  $CD4^+$  T cells express distinct levels of  $CD45RB$  from those expressed by other cells in MLN,  $CD45RB^{hi} + CD45RB^{lo}$  was used as a surrogate gate for  $CD4^+$  T cells. The populations shown in bold are the populations shown to be the most proficient in producing ileitis based on the adoptive transfer experiments shown in Figure 3.18.

populations. Trends towards higher colitis scores were also observed in mice receiving L-selectin<sup>hi</sup> ( $6 \pm 2$ ) and CD69<sup>-</sup> ( $4 \pm 2$ ) CD4<sup>+</sup> cells versus those receiving unfractionated CD4<sup>+</sup> T cells, though these differences were not statistically significant. This finding strongly suggests that SAMP1/YitFc CD4<sup>+</sup> Treg cell populations (CD45RB<sup>low</sup>, CD25<sup>+</sup>, or  $\alpha_E\beta_7^+$ ) are not defective since they can suppress the development of colitis in a fashion similar to colitis suppression by T<sub>reg</sub> cells in other adoptive transfer models. Given that virtually all previous data showing the efficacy of Treg in preventing IBD has been generated in models of colitis, it is thus possible that Treg may be incapable of preventing ileitis in a similar fashion.

These studies have demonstrated that SAMP1/YitFc MLN contain an expanded  $\alpha_E\beta_7^+$  CD4<sup>+</sup> subset with a similar phenotype (CD25<sup>+</sup> CD45RB<sup>lo</sup> L-selectin<sup>lo</sup>) to regulatory T cells that prevent inflammation in adoptively transferred colitis models (79;84).  $\alpha_E\beta_7^+$  CD25<sup>+</sup> CD4<sup>+</sup> T cells have recently been shown to have greater anti-inflammatory potency in the context of colitis than  $\alpha_E\beta_7^-$  CD25<sup>+</sup> cells (85). The SAMP1/YitFc  $\alpha_E\beta_7^+$  CD4<sup>+</sup> subset expresses increased levels of many chemokine receptors, and particularly CCR8, relative to expression on  $\alpha_E\beta_7^-$  CD4<sup>+</sup> cells. Other groups have shown that CD25<sup>+</sup> Treg preferentially express high levels of chemokine receptors including CCR8, and Treg, but not effector cells, exhibit chemotaxis towards CCR8 ligands, I-309 and TARC (263). Since these chemokines are expressed specifically by activated monocytes and polarized T cells (260;261) it has been speculated that CCR8-mediated chemotaxis promotes regulatory cell migration towards inflammatory sites and may also promote direct interaction with effector cells at these sites. The high level of ICAM-1 and LFA-1 expression we have observed on SAMP1/YitFc  $\alpha_E\beta_7^+$  CD4<sup>+</sup> cells suggest that this subset

may be particularly suited for direct interactions with effector cells that are required for many regulatory cell functions (202). In accordance with this hypothesis, a study published within the last few months shows that  $\alpha_E\beta^+$  regulatory cells preferentially migrate to sites of inflammation as opposed to homing towards organized lymphoid tissues (209). These data are in accordance with the homing assays we have conducted in this study which show a dramatic increase in homing of SAMP1/YitFc  $\alpha_E\beta_7^-$  versus  $\alpha_E\beta_7^+$  CD4<sup>+</sup> cells to lymphoid organs, whereas SAMP1/YitFc  $\alpha_E\beta_7^+$  CD4<sup>+</sup> cells traffic in equal or slightly higher numbers than  $\alpha_E\beta_7^-$  CD4<sup>+</sup> subset to the lamina propria. Importantly, if the relevant inflammation-initiating events in the ileitis adoptive transfer model occur in the MLN, as suggested by the high number of transferred SAMP1/YitFc  $\alpha_E\beta_7^-$  CD4<sup>+</sup> cells that home to this site, then the lack of homing by  $\alpha_E\beta_7^+$  CD4<sup>+</sup> cells to this site may inhibit their ability to prevent inflammation.

As shown above, SAMP1/YitFc  $\alpha_E\beta_7^+$  CD4<sup>+</sup> cells produce high levels of IL-10 and low levels of TNF- $\alpha$  and IL-2, similar to IL-10-expressing Tr1 regulatory cells in other models (201). While SAMP1/YitFc  $\alpha_E\beta_7^+$  CD4<sup>+</sup> cells produce somewhat higher levels of TGF- $\beta$  mRNA than do  $\alpha_E\beta_7^-$  CD4<sup>+</sup> cells, whether this increase results in the large production of TGF- $\beta$  protein seen in Th3 regulatory cells remains unclear. The effectiveness of SAMP1/YitFc  $\alpha_E\beta_7^+$  CD4<sup>+</sup> cell-mediated blockade of effector cell proliferation in the *in vitro* assay, suggests that whether or not these cells produce high levels of TGF- $\beta$ , they display effective regulatory function. Other studies have shown that Tr1 regulatory cells producing only IL-10 and not TGF- $\beta$  are equally capable of mediating regulatory functions *in vitro* and *in vivo* as are TGF- $\beta$ -producing cells (208).

While SAMP1/YitFc Treg are incapable of preventing adoptively transferred ileitis induced in SCID recipients by SAMP1/YitFc effector cells, these Treg do prevent colitis produced by the same effector cells. The lack of anti-inflammatory capacity of SAMP1/YitFc Treg cells in adoptively transferred ileitis and the increase in Treg populations in SAMP1/YitFc MLN suggest that these Treg, though present and functional in terms of suppressing effector T cell proliferation *in vitro*, may be incapable of preventing host SAMP1/YitFc ileitis as well. Wildtype AKR MLN CD4<sup>+</sup> T cells, presumably containing functional T<sub>reg</sub> populations, cannot prevent ileitis when cotransferred into SCID mice with SAMP1/YitFc CD4<sup>+</sup> T cells. These findings strongly suggest that aberrant proinflammatory signals that override anti-inflammatory pathways, and not inherently defective regulatory cells, are likely the cause of SAMP1/YitFc ileitis. One possible explanation for the ineffectiveness of SAMP1/YitFc Treg in blocking ileitis is that, since T cell homing to the ileum versus the colon requires differential chemokine receptor expression (175), colitis-preventing T<sub>reg</sub> cells may not be effective in curing SAMP1/YitFc ileitis due to an inability to control leukocyte trafficking to or activation within the ileum. An alternative explanation, explored further in Chapter 4, is that other pro-inflammatory cell subsets may directly inhibit regulatory T cell function within the ileum, thereby leading to unchecked expansion and activity of effector T cells.

## IV. B cell and Immunoglobulin Contributions to SAMP1/YitFc Ileitis

### Rationale

While CD4<sup>+</sup> T cell subset functions have been studied in great detail (200), the contributions of other immune cells to the development of IBD are just beginning to be understood. In particular, irregularities in B cell development and antigen-specific immunoglobulin production may also be critical for understanding the pathogenesis of IBD (108;111;226). Abnormal immunoreactivity of serum or mucosal antibodies toward enteric bacterial flora has been reported in both animal models and IBD patients (264). Increases in mucosal IgG immunoglobulin have been demonstrated in several studies of Crohn's patients and in the C3H/HeJBir spontaneous model of colitis (74;226). The IgG2a-specific production in the later model is speculated to occur due to the Th1-type inflammation in these mice. One of the major classes of antigenic proteins that these IgG responses are directed against are flagellins, proteins involved in the locomotion of motile bacteria such as Salmonella species that are present in the intestinal microflora (229). Production of IgA plays a critical anti-inflammatory role in preventing the intestinal invasion of both pathogenic and commensal bacteria (140). However, several studies have reported that Crohn's patients also have increased IgA levels and immunoreactivity to specific motifs found in the intestinal microflora relative to control subjects (230-232), suggesting that IgA may play a role in disease pathogenesis as well.

While classic follicular B-2 lineage cells produce considerable IgA, chimeric mice in which donor bone marrow and peritoneal lymphocytes produce immunoglobulin of

different allotypes have shown that roughly half of intestinal IgA-producing plasma cells are derived from B-1 cells (192). IgD<sup>lo</sup> CD23<sup>lo</sup> B1 cells originate in the peritoneal cavity and share a similar phenotype to CD21<sup>hi</sup> B cells in the splenic marginal zone (MZ). These populations recognize multivalent thymus independent type 2 (TI-2) antigen, such as LPS, present on the surface of non-pathogenic bacteria (190). B1 cells produce IgM or IgA displaying no affinity modulation or somatic mutation, and this secretion can occur in the absence of T cell help, as MHC class II <sup>-/-</sup> mice have normal B1 cell-derived IgA levels (140). B1 cells have recently been shown to block colitis through production of IL-10 (111), demonstrating that B cells can directly influence inflammatory responses through pathways other than immunoglobulin secretion.

In contrast, follicular B cells produce antibodies of all isotypes in a manner that is dependent upon costimulation provided by CD4<sup>+</sup> T cells (265). IgA produced by follicular B2 cells has undergone affinity maturation and binds potentially pathogenic bacteria distinct from those recognized by B1 cell-derived IgA. Bacteria harvested from the intestines are usually coated with IgA derived from either B2 or B1 cells, but not both (193). *In vitro* and *in vivo* studies have shown that TGF- $\beta$  plays an essential role in the IgM to IgA class switching event (266;267), with IL-4 and IL-10 acting in a synergistic fashion and IL-5 acting to enhance IgA secretion once this class switch has occurred (140). Within lymphoid organs, B cell proliferation and isotype class switching are promoted through interactions with follicular helper T cells (T<sub>FH</sub>). T<sub>FH</sub> use the chemokine receptor CXCR5 to gain entry into B cell follicles. Once inside follicles, though they lack T<sub>h</sub>1 or T<sub>h</sub>2 cytokine production, T<sub>FH</sub> greatly enhance B cell IgG and IgA production (268). These T cells express high levels of inducible costimulator of T cells

(ICOS), a costimulatory molecule that through binding of ICOS-L on B cells is required for T cell-mediated B cell help and antibody class switching (265).

Interestingly, the phenotype of  $T_{FH}$  cells that are involved in IgA production appears similar to that of colitis-preventing  $CD4^{+} CD45RB^{lo} CD25^{+}$  regulatory T cells. For instance,  $T_{reg}$  also lack Th1 and Th2 cytokine production, and they exert their anti-inflammatory effects through production of IgA-promoting TGF- $\beta$  and IL-10 (87;89). Though it has been shown that  $T_{reg}$  cells downregulate IgG production, the effects of  $T_{reg}$  cells on IgA production have not been investigated. Equally important, the effects of B cells on regulatory T cell function have also not been studied.

This chapter is focused on investigations of abnormalities in B cell homeostasis and immunoglobulin production in SAMP1/YitFc mice. To link B cell expansion to abnormalities of regulatory T cell function in this model, both T cell activation of B cell expansion and the effects of B cells on T cell function are examined. To address a causal relationship between B cell expansion and disease severity, ileitis severity is assessed in SCID mice adoptively transferred with B cells along with T cells. In contrast to models of colitis where B cells have been shown to decrease disease severity (108;269), these data demonstrate that B cells play an important pro-inflammatory role in SAMP1/YitFc ileitis through mechanisms that may involve inhibition of regulatory T cell function.

## **Materials and Methods**

### *Mice*

SAMP1/YitFc and age matched AKR mice were obtained from the same sources as in Chapter III. 6-8 week-old severe combined immunodeficient mice (SCID) on the

C3H/HeJ background for SAMP1/YitFc B cell and T cell adoptive cotransfer were again obtained from Jackson Laboratories (Bar Harbor, ME). As before, all animals were kept in specific pathogen-free conditions, and experiments were approved by the institutional committee for animal use.

### *Flow cytometry and confocal microscopy*

Mesenteric lymph nodes were harvested, counted, and stained according to procedures outlined in Chapter III. Cells were stained with combinations of biotinylated anti-mouse GITR (BAF524) (R&D Systems, Minneapolis, MN); streptavidin-conjugated Cy-3 (Jackson ImmunoResearch, West Grove, PA), streptavidin APC, FITC-, PE-, PERCP-, APC-, or biotin-labeled rat anti-mouse CD4 (RM4-5), CD19 (1D3),  $\alpha_E$  (M290),  $\beta_7$  (M293), ICOS (7E.17G9), B220 (RA3-6B2), IgM (R6-60.2), IgA (C10-3), IgD (11-26c.2a), CD5 (Ly-1), CD21 (CR2) and CD23 (B3B4) (BD Pharmingen, San Diego, CA). Flow cytometry data was again acquired on a FACS Calibur (BD Biosciences, San Diego, CA) and analyzed using WinMIDI 2.8 (Trotter, Scripps Research Institute, La Jolla, CA).

For confocal microscopy, SAMP1/YitFc MLN cells were stained as above and fixed in 4% paraformaldehyde.  $2 \times 10^5$  cells/ml were loaded into cytofunnels and spun onto slides at 1000 RPM for 10 min in a cytospin 2 centrifuge (Thermo-Shandon Lipshaw, Pittsburgh, PA). Confocal images were taken through a 60x oil objective on a Nikon TE 300 microscope with a BioRad radiance 2000 camera using LaserSharp 2000 software (BioRad, Hercules, CA).



### *Cell purification and adoptive transfer*

SAMP1/YitFc MLN  $CD4^+$  T cells were isolated magnetically positive selection by positive selection using anti- $CD4$  beads or by negative selection using the mouse  $CD4^+$  negative isolation kit (Miltenyi Biotec) as described in Chapter III.  $CD4^+$  T cell fractions were greater than 96% and 98% pure when isolated by positive and negative isolation, respectively, with the impurities mainly being  $CD19^+$  B cells in the positively selected fraction and  $CD4^-CD8^-CD19^-$  cells in the negatively selected fraction. For adoptive transfer experiments, B cells were isolated by positive selection using anti-mouse  $CD19$  microbeads, and this isolation procedure resulted in a population that was 98% pure, with

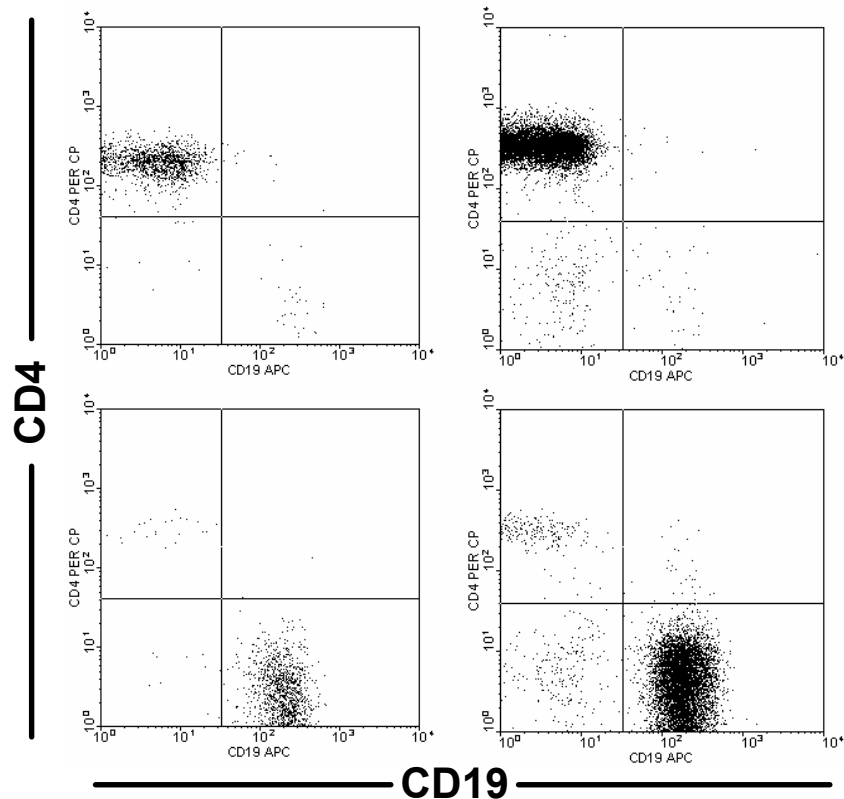


**Figure 4.1:** Purity of  $CD4^+$  T cell and B cell fraction isolated by magnetic selection columns.  $CD4^+$  T cells were isolated by either positive (top left) or negative (top right) selection using either  $CD4^+$  beads or the  $CD4^+$  negative selection kit, respectively. B cells were also selected by either positive (bottom left) or negative (bottom right) selection using  $CD19^+$  beads or beads recognizing  $CD43$ , a cell surface molecule expressed on most leukocytes with the exception of B2 B cells.

most of the remaining cells being CD4<sup>+</sup> T cells (Figure 4.1, bottom left). For cell culture experiments, B cells were isolated by negative selection using anti-mouse CD43 microbeads (Miltenyi Biotec), since CD43 is expressed on most leukocytes with the exception of mature B2 B cells. This procedure resulted in a B cell population that was 94% pure with the remaining cells split between CD4<sup>+</sup>CD19<sup>-</sup> and CD4<sup>-</sup>CD19<sup>-</sup> cells (Figure 4.1, bottom right). For adoptive transfers, cells were washed and resuspended in plain PBS for injection into SCID recipients. T cells and B cells were injected in 500  $\mu$ l of PBS each at doses of  $5 \times 10^5$  cells i.p. and  $2 \times 10^6$  cells i.v. (tail vein), respectively. The ilea and colons of SCID recipients were harvested 6 weeks after transfer.

#### *Cell culture and T cell proliferation assays*

In T cell/B cell coculture experiments,  $10^5$  AKR MLN CD4<sup>+</sup> T cells or SAMP1/YitFc MLN unfractionated,  $\alpha_E^+$ , or  $\alpha_E^-$  CD4<sup>+</sup> T cells and  $10^5$  SAMP1/Yit/Fc or AKR MLN B cells were cultured in 200  $\mu$ l/well for 3, 7, 11, and 13 days. Cells were cultured in 96 well plates at 37<sup>0</sup> C with 5% CO<sub>2</sub> in RPMI media containing 10% fetal calf serum, 100 U/ml penicillin, 100  $\mu$ g/ml streptomycin, and 10  $\mu$ g/ml plate-bound anti-mouse CD3 (145-2C11) (BD Pharmingen) with or without 2  $\mu$ g/ml anti-mouse CD28 (37.51) (BD Pharmingen). For proliferation assays,  $10^5$  irradiated (3000 rad) splenic APC were cultured for 3 days with plate-bound anti-CD3 (10  $\mu$ g/ml) and combinations of  $\alpha_E^+$  CD4<sup>+</sup> T cells,  $\alpha_E^-$  CD4<sup>+</sup> T cells, and B cells at  $5 \times 10^4$  cells each/well. 3 independent cultures for each condition were performed in each individual experiment. As before, incorporation of H<sup>3</sup> thymidine (1 $\mu$ Ci/well) (Biomedicals, Irvine, CA) in the last 24 hours

was measured using a Harvester 96 (Tomtec, Humden, CT) and a 1450 Microbeta Scintillation Counter (Perkin Elmer, Gaithersburg, MD).

### *Measurement of immunoglobulin levels*

The SBA Clonotyping System ELISA (Southern Biotech, Birmingham, AL) was used according to manufacturer's instructions to measure immunoglobulin isotypes in 0.5  $\mu$ l of SAMP1/YitFc and AKR serum samples, 10  $\mu$ l of adoptively transferred SCID serum samples, and 20-40  $\mu$ l of coculture supernatants diluted to a total of 100  $\mu$ l in PBS containing 1% bovine serum albumin. The concentration of Goat anti-mouse Ig capture antibody used was 10  $\mu$ g/ml, while horseradish peroxidase-labeled goat anti-mouse IgA, IgM, IgG, or IgG2a detection antibodies were used at a 1/1000 dilution. Plates were developed for 10-20 minutes using 2,2'-azino-bis 3-ethylbenzthiazoline-6-sulfonic acid (ABTS) substrate, and optical density readings were taken at 405 nm on a microplate reader (Lab systems, Needham Heights, MA). Samples were measured in triplicate.

The mouse immunoglobulin isotyping cytometric bead array (BD Pharmingen) was used to determine relative mesenteric lymph node immunoglobulin concentrations from SAMP1/YitFc and AKR mice. Briefly, MLN were crushed through a 70  $\mu$ M strainer and the cells and supernatant were resuspended in 5 ml of the provided master buffer. The cells were pelleted by a 5 minute centrifugation at 350 x g, and the supernatant was stored at 4<sup>0</sup> C. The bead array was performed according to manufacturer's instructions, using a 1/1 dilution of supernatant for detection of  $\lambda$  light chain immunoglobulin and a 1/100 dilution for detecting  $\kappa$  light chain immunoglobulin. Relative Ig concentrations

were determined from differences in FL-1 ( $\lambda$  light chain) and FL-2 ( $\kappa$  light chain) mean fluorescent intensities of beads with isotype-specific FL-3 intensities.

### *Histology and immunohistochemistry*

For histology, sections of ileum and colon were prepared as described in Chapter III. MLN were fixed directly in Bouin's fixative (Fisher, Newark, DE). All tissues were embedded in paraffin, and cut into 3-5  $\mu$ m sections. Hemotoxylin- and eosin-stained slides of intestinal sections were scored by a pathologist in blinded fashion according to the scoring system described in Chapter III. For immunohistochemistry, sections were stained using an adaptation of previously published methods (270). Deparaffinized slides were blocked for 1 hour (PBS with avidin, 10% normal goat serum and 0.5% gelatin), washed, and incubated overnight at 4<sup>0</sup> C with 1  $\mu$ g/ml of biotinylated goat anti-mouse IgA (Southern Biotech), 0.2  $\mu$ g/ml of purified rat anti-mouse GR-1 (RB6-8C5) (American Type Culture Collection, Manassas, VA), 0.7  $\mu$ g/ml of purified goat polyclonal anti-mouse CD3 (M20), (Santa Cruz Biotechnology, Santa Cruz, CA), 1/200 dilution of purified goat polyclonal anti-mouse CD20 (M-20) (Santa Cruz Biotechnology), and 1  $\mu$ g/ml of purified rat monoclonal anti-mouse neutrophil (7/4) (Serotec, Raleigh, NC). Slides were washed and incubated with 5  $\mu$ g/ml biotinylated rabbit anti-rat or biotinylated rabbit anti-goat antibodies (Vector Laboratories, Burlingame, CA). Slides were then incubated with avidin-biotin peroxidase complexes, developed using DAB substrate (Vector Laboratories) and counterstained with hemotoxylin. Images were acquired using an Olympus BH-2 microscope (Melville, NY) and Imagepro Plus (Carlsbad, CA) software.

### *Real time PCR for GITR ligand expression*

B cell RNA was extracted using RNAeasy (Qiagen, Valencia, CA) reverse transcribed using the Superscript kit (Invitrogen, CA), and assayed for GITRL expression by real-time PCR using a Smart Cycler (Cepheid, CA). Sequences: 5'-CCCAAGGTGTCCAGAATGAAG-3' and 5'-AGTCAGCATGGTTGAGTGAGATG-3' (GITRL primers) and 5'-TET-CTGGAGCAAGAAGATCCAGGATACTG-3' (GITRL probe) (Integrated DNA Technologies, Coralville, IA). PCR cycling conditions: 95°C (300 s) and 40 cycles of 95°C (15 s), 60°C (30 s) and 72°C (30 s). Critical threshold (CT) values and standard curves were used to estimate starting mRNA levels. Values were normalized against 18s rRNA CT values generated using the pre-optimized 18s rRNA primers and probe set (Applied Biosystems).

### *Statistics*

Statistical analysis was performed using the two-tailed unpaired Student's t test, the Mann-Whitney rank sum test, or one-way ANOVA for multiple comparisons using the Student-Newman-Keuls method. Statistical analysis for real-time rt-PCR data was performed using the one-tailed unpaired Student's t test. Statistical significance was set at  $P < 0.05$ . Coefficients of determination,  $R^2$ , were determined using linear regression. Statistical comparisons of the overall differences in the time course of immunoglobulin expression in cultures over 3, 7, 11, and 13 days were performed using two-way analysis of variance on ranks (Friedman's Test), utilizing cell type as one factor with  $\alpha_E^+ CD4^+$  and  $\alpha_E^- CD4^+$  cells as levels for this factor, and days of culture as the other factor with 3, 7, 11, and 13 day values as levels for this second factor. The Holm-Sidak adjustment for multiple comparisons was then used to make pairwise comparisons between the

immunoglobulin production in cocultures with  $\alpha_E^+ CD4^+$  versus  $\alpha_E^- CD4^+$  cells at individual time points, with significance for the adjusted P-value set at  $P < 0.05$ .

## Results and Discussion

### *Immunoglobulin production and subset analysis of SAMP1/YitFc B cells*

As discussed in Chapter III, SAMP1/YitFc MLN contain increased total B cell number, B cells as a percentage of all lymphocytes, and actively proliferating B cells compared to the respective populations in AKR MLN (Figures 3.2 and 3.3). To further characterize the SAMP1/YitFc B cell population, immunoglobulin expression within SAMP1/YitFc and AKR MLN was examined using a cytometric bead array, in which FL-1 and FL-2 mean fluorescent intensities (MFI) of isotype-specific beads correspond to MLN supernatant concentrations of immunoglobulin with  $\lambda$  or  $\kappa$  light chains, respectively (Figure 4.2A). Compared to AKR supernatants, SAMP1/YitFc MLN supernatants contained more IgG $_1$   $\kappa$  (3.4-fold increase in average MFI), IgA  $\kappa$  (4.5-fold), IgM  $\kappa$  (2.3-fold), IgA  $\lambda$  (7.9-fold), and IgM  $\lambda$  (3.7-fold). To test whether increases in the MLN were associated with systemic elevation in immunoglobulin levels, concentrations of immunoglobulin were measured in serum samples from SAMP1/YitFc and AKR mice. Serum IgA was elevated 2.7 fold in SAMP1/YitFc ( $23 \pm 5$   $\mu\text{g/ml}$ , mean  $\pm$  SEM) compared to AKR ( $8.7 \pm 0.8$   $\mu\text{g/ml}$ ) mice (Figure 4.2B), whereas serum concentrations of IgM, IgG2a, and IgG1 were not significantly different between the two strains, demonstrating that elevations in IgA production are not the result of global activation of B cells, but rather increases in cells specifically producing this isotype.

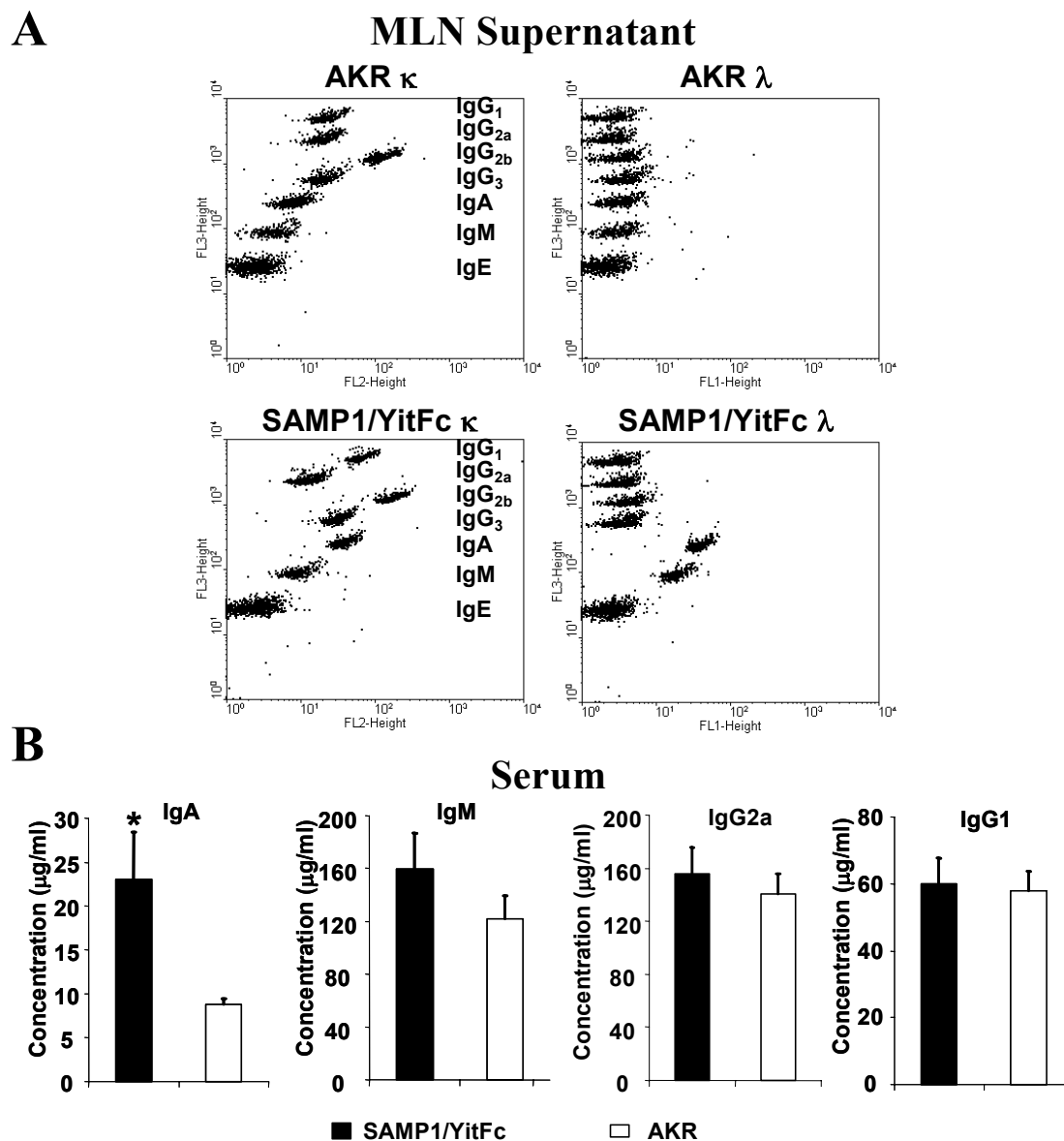


**Figure 4.2:** Representative dotplots of  $\kappa$  (1:100 dilution, FL-2) and  $\lambda$  (1:1, FL-1) light chain antibody isotype levels within MLN supernatants of AKR (n=2) and SAMP1/YitFc (n=2) mice using a cytometric bead array containing isotype-specific beads with preset FL-3 intensities (A). At least a 2-fold increase in IgG1  $\kappa$ , IgA  $\kappa$ , IgM  $\kappa$ , IgA  $\lambda$ , and IgM  $\lambda$  was seen in SAMP1/YitFc versus AKR MLN, with the largest increases occurring in IgA  $\kappa$  and  $\lambda$  isotypes. ELISA detecting IgA (n=12,13), IgM (n=8,8), IgG2a (n=8,8), and IgG1 (n=8,8) antibody concentration (mean  $\pm$  SEM) in serum samples from SAMP1/YitFc and wild-type AKR (n=13) mice, respectively (B). \*Significantly greater than AKR concentrations (P < 0.05).

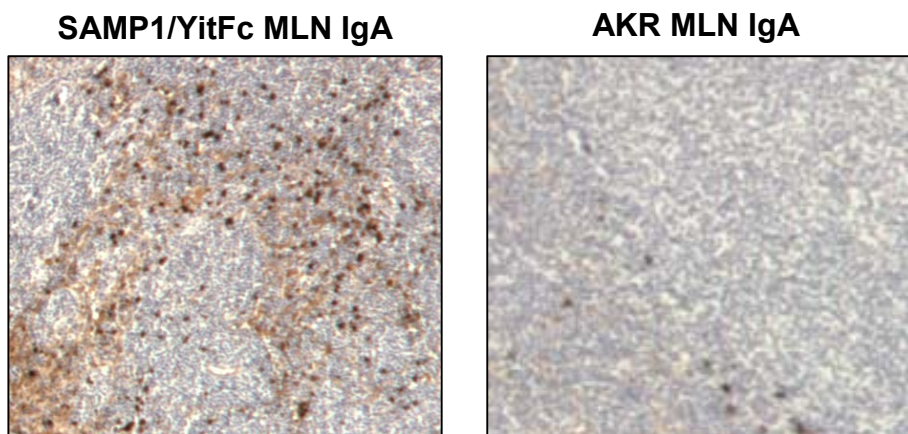
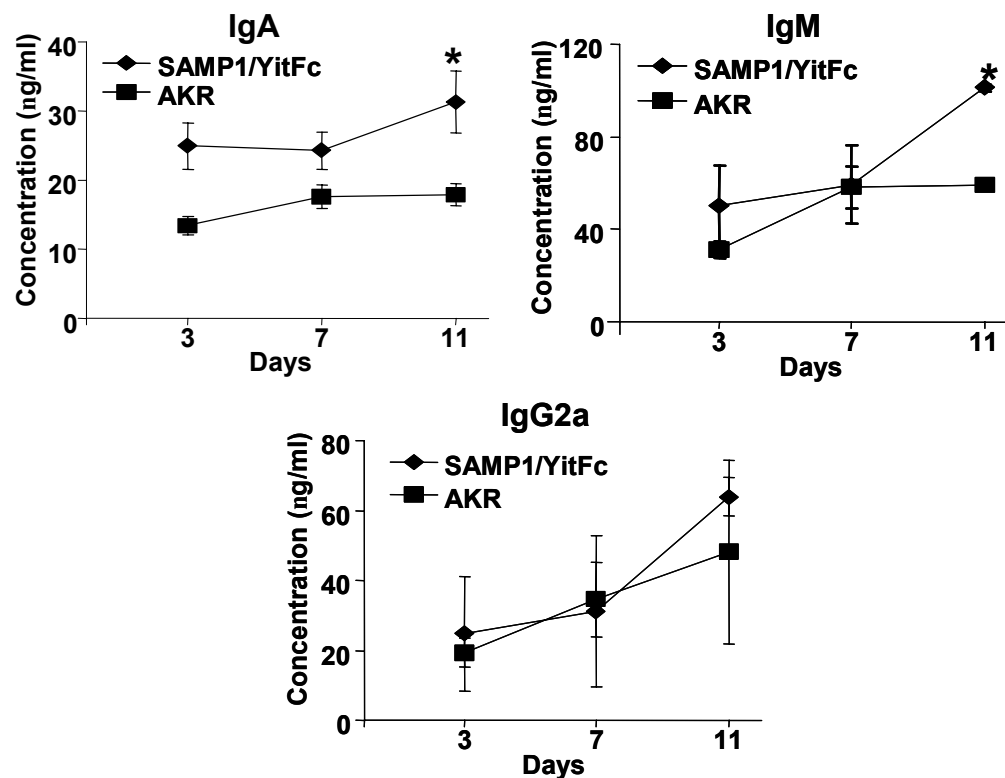
To determine if the increased IgA in SAMP1/YitFc versus AKR MLN was due to local production, immunohistochemical analysis of MLN was performed using anti-IgA antibodies (Figure 4.3A). Immunostained sections revealed increased IgA<sup>+</sup> cells (dark

brown spots) as well as soluble IgA (diffuse lighter brown) in SAMP1/YitFc versus AKR MLN, suggesting that enhanced production of IgA<sup>+</sup> cells might be a key feature of SAMP1/YitFc MLN. To test this hypothesis, immunoglobulin production was measured from SAMP1/YitFc versus AKR MLN mature resting B cells, isolated via negative selection to avoid stimulation through CD19 ligation. B cells were cocultured with CD4<sup>+</sup> T cells from SAMP1/YitFc and AKR MLN respectively in the presence of anti-CD3 stimulation. B cells from the SAMP1/YitFc cocultures produced increased IgA and IgM by 11 days of culture compared to levels produced by AKR cocultures (Figure 4.3B), confirming that SAMP1/YitFc MLN cells are predisposed to producing high levels of IgA. Cocultures of cells from both strains produced similar levels of IgG2a.

The increase in total IgA<sup>+</sup> cells in SAMP1/YitFc ( $10 \pm 1$ ) versus AKR ( $3.8 \pm 0.9$ ) MLN was seen by flow cytometry as well (Figure 4.4A). Most IgA expression was found on mature B cells (B220<sup>hi</sup>), while some was also found on B220<sup>int</sup> cells thought to be differentiating plasmablasts (249). SAMP1/YitFc IgA<sup>+</sup> cells were mostly still IgM<sup>+</sup> and none expressed the plasma cell marker Syndecan-1 (data not shown), suggesting that these cells were in the early stages of plasmablast differentiation.

In addition to immunoglobulin expression, SAMP1/YitFc MLN B cells were also characterized in terms of the relative size of B1 versus B2 cell populations by examining the expression of IgD and CD23 on B cell-gated dotplots of SAMP1/YitFc and AKR MLN cells (Figure 4.4B).  $19 \pm 3\%$  (mean  $\pm$  SEM) of SAMP1/YitFc MLN B cells possessed a B1 cell phenotype (CD23<sup>lo</sup>, IgD<sup>lo</sup>), though this percentage was not significantly greater than the percentage of AKR cells ( $13 \pm 1\%$ ) possessing a B1 phenotype. Most IgA<sup>+</sup> cells (>80%) were CD23<sup>+</sup> follicular B2 cells (Figure 4.4C). Of



**A****B**

**Figure 4.3:** SAMP1/YitFc MLN B cells produce more IgA than AKR MLN B cells. SAMP1/YitFc MLN (A, left) contain considerably more IgA-secreting cells (dark brown spots) and soluble IgA (diffuse light brown) compared to AKR MLN (A, right), as measured by immunostaining of paraffin-embedded MLN sections. Concentrations of IgA (n=4), IgM (n=2), and IgG2a (n=2), measured in triplicate by ELISA, from 3, 7, and 11 day anti-CD3-stimulated cocultures of SAMP1/YitFc CD4<sup>+</sup> T cells and B cells versus AKR CD4<sup>+</sup> T cells and B cells (10<sup>5</sup> T cells and 10<sup>5</sup> B cells/well). \*Significantly greater than AKR concentrations (P < 0.05).

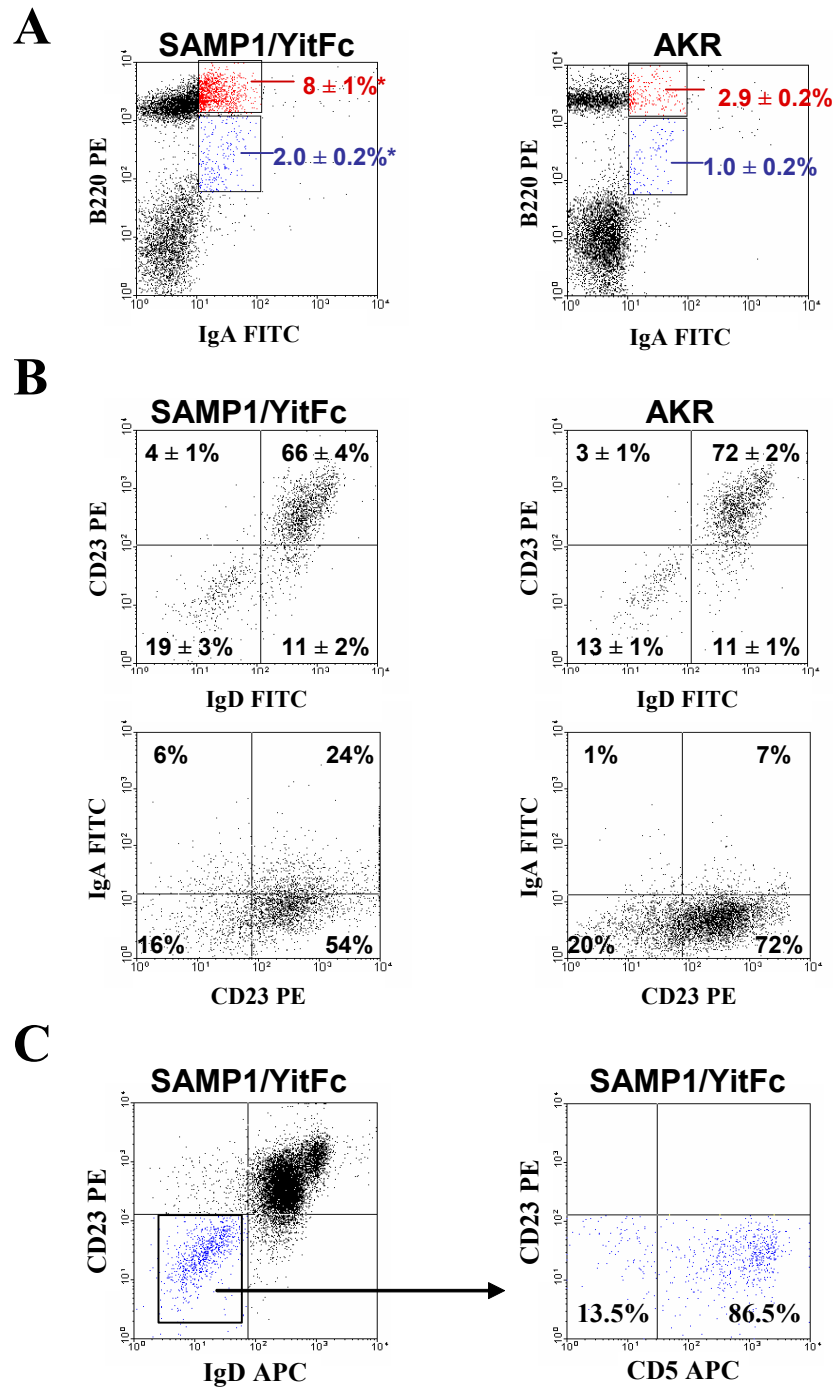


**Figure 4.4:** Representative dotplots of B220 versus IgA expression, with quadrant percentages (mean  $\pm$  SEM), demonstrating an increase in mature B cells (B220<sup>hi</sup>) and plasmablasts (B220<sup>int</sup>) expressing IgA in SAMP1/YitFc (n=13) versus AKR (n=6) MLN (A). \*Significantly greater ( $P < 0.05$ ) than AKR cell percentage. B cell (IgM<sup>+</sup>)-gated dotplots, with quadrant percentages (mean  $\pm$  SEM), showing that less than 20% of SAMP1/YitFc (n=13) or AKR (n=6) MLN B cells have a CD23<sup>-</sup> IgD<sup>-</sup> B1 cell phenotype (B, upper panels). Most IgA is produced by B2 cells (CD23<sup>+</sup>) (B, lower panels). Most of the cells with a B1 phenotype (CD23<sup>-</sup> IgD<sup>-</sup> gate) (c, left) in SAMP1/YitFc MLN express CD5 (C, right), suggesting that these cells belong to the B1a subclass.

the IgD<sup>lo</sup> CD23<sup>lo</sup> B1 cells in SAMP1/YitFc MLN,  $87 \pm 1\%$  belonged to the CD5<sup>+</sup> B1a subclass with the remaining cells belonging to the CD5<sup>-</sup> B1b subclass (Figure 4.4D).

In contrast to the B cell expansion in SAMP1/YitFc versus AKR MLN, spleens and Peyer's patches from SAMP1/YitFc mice contained similar percentages of B cells compared to percentages seen in AKR spleens and Peyer's patches, respectively (Figure 4.5A). Further the number of IgA<sup>+</sup> cells was also similar in SAMP1/YitFc versus AKR spleens (Figure 4.5B). The only difference in B cell-gated plots of SAMP1/YitFc versus AKR splenocytes was a selective 4.7-fold increase in the percentage of IgD<sup>lo</sup> CD23<sup>lo</sup> CD5<sup>+</sup> B1a B cells in SAMP1/YitFc ( $14 \pm 3\%$ ) versus AKR ( $3 \pm 1\%$ ) spleens (Figure 4.5c, middle and right panels). SAMP1/YitFc and AKR spleens contained similar percentages of CD21<sup>hi</sup> CD23<sup>lo</sup> CD5<sup>-</sup> marginal zone B cells ( $17 \pm 3\%$  versus  $13 \pm 1\%$ ). Subtracting the MZ population from the total population of IgD<sup>lo</sup> CD23<sup>lo</sup> CD5<sup>-</sup> cells seen in the right panels of Figure 4.5C reveals no significant differences in the size of the remaining population of B1b cells in SAMP1/YitFc ( $9 \pm 2$ ) versus AKR ( $7 \pm 2$ ) spleens.

The above data suggest that SAMP1/YitFc ileitis is associated with an MLN-restricted expansion in B2 B cells resulting in the overproduction and systemic elevation in IgA antibodies. The spontaneous colitis seen in C3H/HeJBir mice is associated with a primarily IgG2a response to enteric bacteria (74), however the inflammation in these mice is limited to the cecum and the colon (73), and thus immunoglobulin specificity may be different from that in Crohn's-like ileitis. While some studies indicate that mucosal IgG, not IgA, is elevated in Crohn's patients (226), other studies suggest that serum IgA, but not IgG, immunoreactivity is stronger in Crohn's patients than in controls (271). Relative to normal individuals, many Crohn's patients have elevated serum IgA

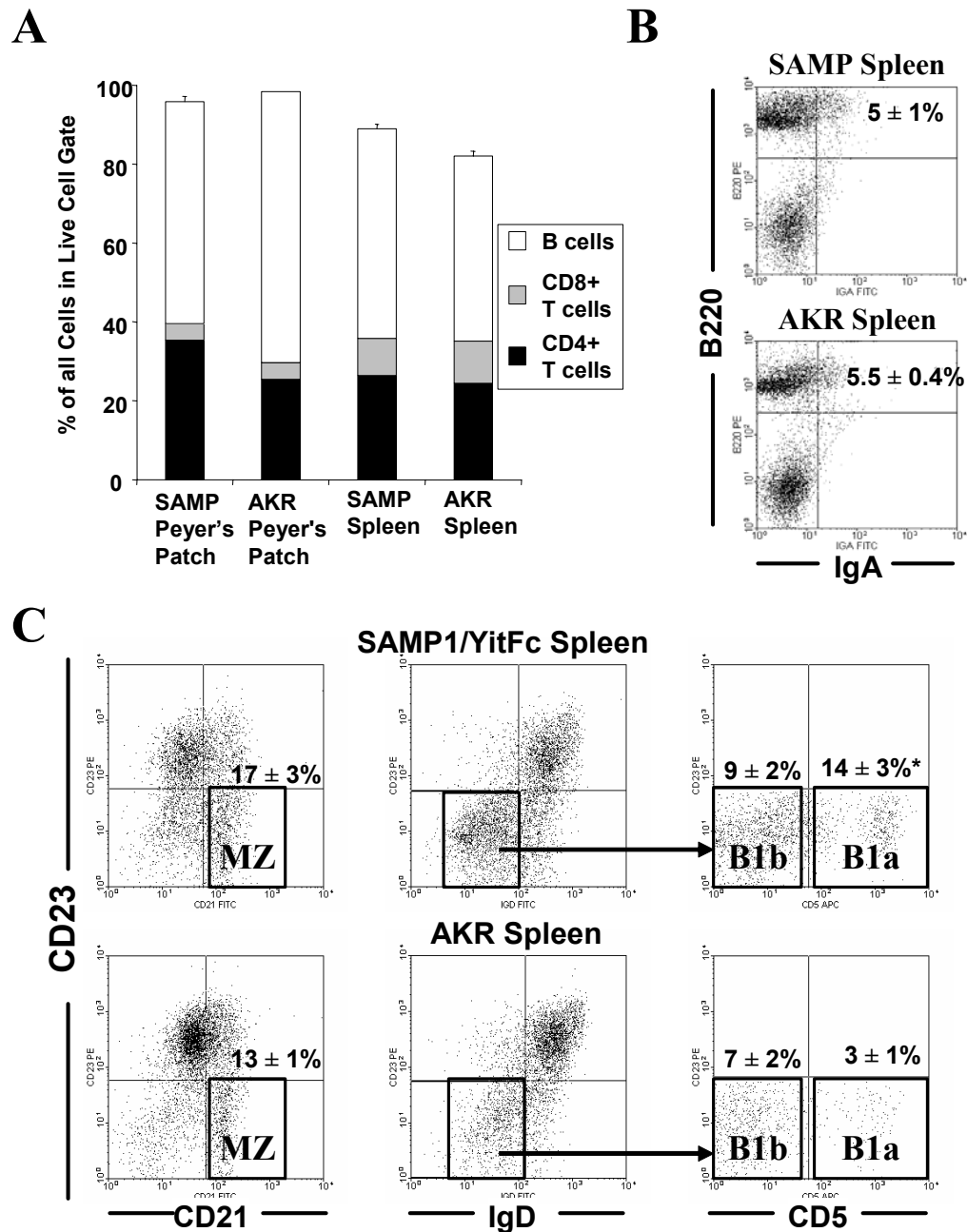


**Figure 4.5:** Comparison of the percentage (mean  $\pm$  SEM) of CD4<sup>+</sup> T cells (black), CD8<sup>+</sup> T cells (gray), and B cells (white) in spleens and Peyer's patches from SAMP1/YitFc and AKR mice, determined by flow cytometry using live cell forward and side scatter gates (A). Dotplots of all lymphocyte-gated events, showing that similar percentages of SAMP1/YitFc versus AKR spleen B cells express IgA (B). B cell (IgM<sup>+</sup>)-gated dotplots with average percentages (mean  $\pm$  SEM) showing that SAMP1/YitFc and AKR spleens contain similar percentages of CD23<sup>lo</sup> IgD<sup>lo</sup> CD21<sup>hi</sup> marginal zone (MZ) B cells (C, left panels). Subtracting MZ cells from the overall CD5<sup>-</sup> CD23<sup>lo</sup> IgD<sup>lo</sup> population in the B1b gate (26% and 20% in SAMP1/YitFc and AKR, respectively) (C, middle and right panels) reveals that SAMP1/YitFc and AKR spleens have similar percentages of B cells that were CD5<sup>-</sup> CD23<sup>lo</sup> IgD<sup>lo</sup> CD21<sup>lo</sup> B1b cells (9% versus 7%). In contrast, the percentage of B cells that were CD5<sup>+</sup> B1a B cells is increased in SAMP1/YitFc versus AKR spleen. \*Significantly increased compared to AKR population ( $P < 0.05$ ).

specifically recognizing HupB, a mycobacterial homologue of anti-neutrophil cytoplasmic antibody (pANCA) antigen (231); I2, a bacterial transcription factor (230); and *Saccharomyces cerevisiae* subspecies (232). While IgA deficiency is common (140), no large clinical trials have tested the link between IgA deficiency and Crohn's disease.

The contribution of the expanded splenic B1a cell population to the development of SAMP1/YitFc ileitis will also require further investigation. Expansion of splenic B1a B cells is associated with autoimmunity in human conditions such as Sjogren's syndrome and rheumatoid arthritis and in mouse models of systemic lupus erythematosus (190). Due to the fact that these cells are not subject to normal mechanisms conferring self-tolerance, B1a cells are hypothesized to contribute to these diseases through production of low affinity IgM or IgA antibodies recognizing autoantigens. While B1a cells may be proinflammatory in the above models, the G $\alpha$ i2 model of colitis is associated with marked decreases in B1a and MZ B cells (108), and B1 cell-derived IgA is generally thought to prevent intestinal inflammation by translocating to the luminal surface of epithelial cells and sequestering commensal bacteria in the luminal compartment (191).

#### *MLN $\alpha_E\beta_7^+$ CD4<sup>+</sup> T cell involvement in B cell expansion and function*

The above findings demonstrate that SAMP1/YitFc versus AKR MLN B cells produce greater levels of IgA and that most of this IgA is derived from T cell-dependent B2 B cells. To test whether SAMP1/YitFc T cells bias B cells towards enhanced IgA production, SAMP1/YitFc CD4<sup>+</sup> T cells were cultured with either SAMP1/YitFc or AKR B cells, and AKR CD4<sup>+</sup> T cells were cultured with either SAMP1/YitFc or AKR B cells. The resulting IgA production was measured after eleven days (Figure 4.6A). As before, SAMP1/YitFc B cells cultured with SAMP1/YitFc CD4<sup>+</sup> T cells produced significantly

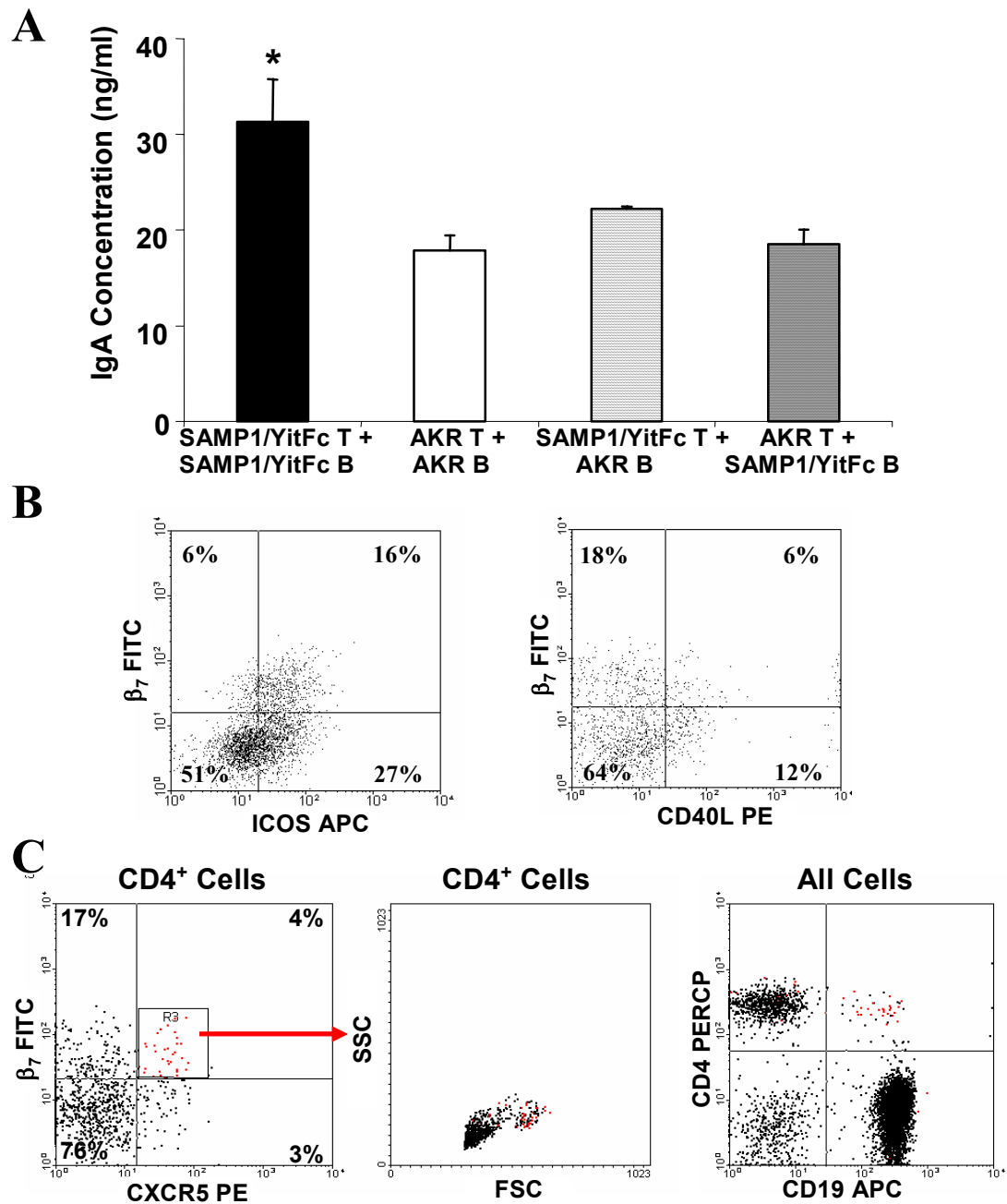


**Figure 4.6:** Comparison of IgA expression (mean  $\pm$  SEM), measured in triplicate by ELISA, in 11 day anti-CD3 stimulated cultures of SAMP1/YitFc CD4<sup>+</sup> T and B cells (n=4), AKR CD4<sup>+</sup> T and B cells (n=4), SAMP1/YitFc CD4<sup>+</sup> T cells and AKR B cells (n=2), and AKR CD4<sup>+</sup> T cells and SAMP1/YitFc B cells (n=2). \*Significantly increased compared to IgA produced in AKR CD4<sup>+</sup> T and B cell cultures. Representative CD4<sup>+</sup>-gated dotplot and average quadrant percentages showing selective expression of the B cell costimulatory molecule ICOS (n=10), but not CD40L (n=2), on  $\beta_7^{\text{hi}}$  ( $\alpha_E\beta_7^+$ ) CD4<sup>+</sup> T cells (B).  $\beta_7^{\text{hi}}$  cells appear to also preferentially express CXCR5, as 18% of  $\beta_7^{\text{hi}}$  cells, but only 3% of  $\beta_7^{\text{lo}}$  cells are CXCR5<sup>+</sup> (C, left) (n=10). However, gating on CXCR5<sup>+</sup>  $\beta_7^{\text{hi}}$  cells (red events) reveals that this population has an increased forward and side scatter profile (C, middle) and is double positive for CD4 and CD19 (C, right), suggesting that this population may represent T cell/B cell doublets and the expression of CXCR5 may be limited to B cells within these doublets.

more IgA ( $31 \pm 4$  ng/ml) compared to AKR B cells cultured with AKR T cells ( $18 \pm 2$  ng/ml). SAMP1/YitFc B cells cultured with AKR T cells ( $19 \pm 2$  ng/ml) and AKR B cells cultured with SAMP1/YitFc T cells ( $22 \pm 1$  ng/ml) produced low IgA levels comparable to AKR B cell + AKR T cell cultures, implying that both B cell and T cell properties specific to SAMP1/YitFc MLN are required for increased IgA production.

To test whether the promotion of IgA production by SAMP1/YitFc  $CD4^+$  T cells was due to specific properties of the increased SAMP1/YitFc  $CD4^+$  T cells subsets described in Chapter III, these subsets were examined for the expression of markers characteristic of follicular helper T cells ( $T_{FH}$ ), specialized T cells that augment B cell immunoglobulin production and class switching (268). Compared to  $\alpha_E\beta_7^-$   $CD4^+$  T cells, most SAMP1/YitFc  $\alpha_E\beta_7^+$   $CD4^+$  T cells ( $73 \pm 2\%$  versus  $35 \pm 3\%$ , mean  $\pm$  SEM) expressed high levels of ICOS, a costimulatory molecule that is required for germinal center formation and immunoglobulin class switching (272) (Figure 4.6B, left). In contrast, there was no difference in the percentage of  $\alpha_E\beta_7^+$  versus  $\alpha_E\beta_7^-$   $CD4^+$  cells expressing CD40 ligand (CD40L) (Figure 4.6B, right), although the function of this molecule and its interactions with CD40 are not specific to B cell/T cell interactions (273).

The percentage of  $CXCR5^+$   $CD4^+$  T cells initially appeared to be greater in the  $\alpha_E\beta_7^+$  ( $19 \pm 4\%$ ) versus the  $\alpha_E\beta_7^-$  ( $3 \pm 1\%$ ) subset (Figure 4.6C, left). Given that  $CXCR5$  is required for the migration of  $T_{FH}$  into B cell follicles (274), this finding seemed to suggest that  $\alpha_E\beta_7^+$   $CD4^+$  T cells may mediate  $T_{FH}$  functions. However, further analysis demonstrated that most  $CXCR5^+$   $\alpha_E\beta_7^+$   $CD4^+$  T cells exhibited increased forward and side scatter characteristic of cell doublets, and this doublet formation seemed to occur

between  $\alpha_E\beta_7^+$  CD4<sup>+</sup> T cells and CD19<sup>+</sup> B cells (Figure 4.6C, middle and right).

Since CXCR5 is expressed on virtually all MLN B cells, it remains unclear whether any of the CXCR5 present on these cell doublets was actually derived from  $\alpha_E\beta_7^+$  T cells, though this subset does appear to express higher levels of CXCR5 mRNA than levels expressed by  $\alpha_E\beta_7^-$  CD4<sup>+</sup> T cells as shown in Figure 3.11.

To test whether  $\alpha_E\beta_7^+$  CD4<sup>+</sup> T cells preferentially interact with B cells in B cell/T cell doublets, we examined  $\alpha_E$  expression on CD4<sup>+</sup> CD19<sup>+</sup> events by flow cytometry. CD4<sup>+</sup> CD19<sup>+</sup> events exhibited increased forward and side scatter characteristic of B cell/ T cell doublets and comprised 1% of all events in SAMPI/YitFc MLN cell suspensions (Figure 4.7A and B). While B cells alone did not express  $\alpha_E$ , the percentage of B cell/ CD4<sup>+</sup> T cell doublets expressing  $\alpha_E$  was 2.5-fold greater than the percentage of cells expressing  $\alpha_E$  in the single positive CD4<sup>+</sup> T cell population, suggesting that  $\alpha_E\beta_7^+$  CD4<sup>+</sup> T cells may preferentially form tight interactions with MLN B cells. In repeated experiments despite changes in overall percentage of CD4<sup>+</sup> T cells that were  $\alpha_E\beta_7^+$  cells, the percentage of  $\alpha_E\beta_7^+$  in the doublet fraction was consistently 2.3-2.5 fold higher than the percentage of  $\alpha_E\beta_7^+$  cells in the CD4<sup>+</sup> single positive fraction (not depicted). Confocal microscopy of MLN cell suspensions showed that many  $\alpha_E^+$  cells appear to be engaged in interactions with B cells (Figure 4.7C). Examining MLN composition in individual mice, we found a positive correlation ( $R = 0.6$ ) between the percentage of MLN CD4<sup>+</sup> T cells that express  $\alpha_E$  and MLN B cell number, as a percentage of total cells, in individual mice (Figure 4.8). To illustrate this correlation more clearly, mice were binned into two groups depending on whether the percentage of CD4<sup>+</sup> T cells expressing  $\alpha_E\beta_7$  was greater than or less than



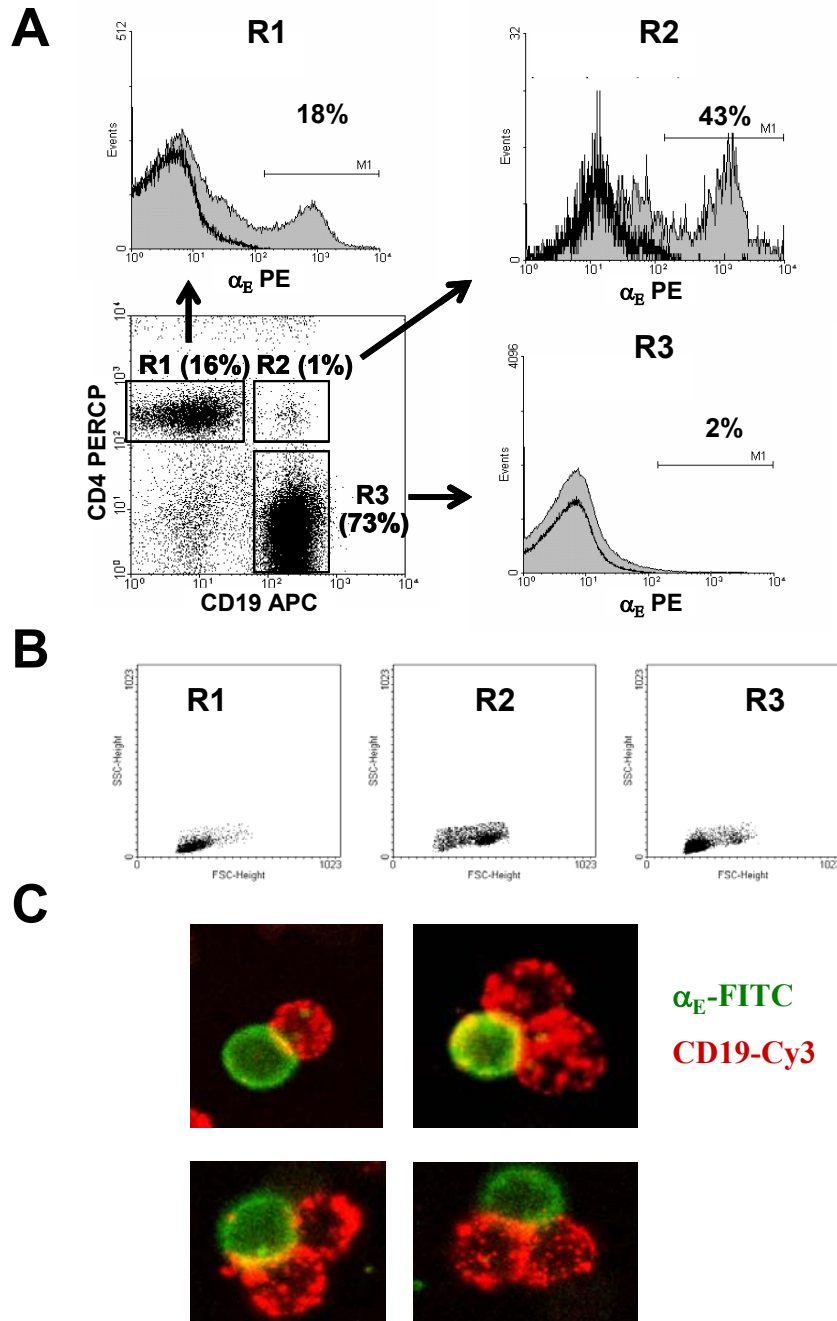


**Figure 4.7:** Compared to  $\alpha_E^-$  CD4<sup>+</sup> T cells,  $\alpha_E^+$  CD4<sup>+</sup> T cells preferentially form doublets with B cells. Dotplot showing that 1% of all MLN lymphocyte-gated events in SAMP1/YitFc MLN are CD4<sup>+</sup> CD19<sup>+</sup> (A, bottom left). Representative comparison (n=2) of the percentage of cells expressing  $\alpha_E$  (filled histograms) relative to isotype control (open histograms) on CD4<sup>+</sup> CD19<sup>-</sup> T cells (A, upper left), CD19<sup>+</sup> CD4<sup>-</sup> B cells (A, lower right), and CD4<sup>+</sup> CD19<sup>+</sup> B cell/T cell doublets (A, upper right). An increased percentage of CD4<sup>+</sup> CD19<sup>+</sup> events (R2) are  $\alpha_E^+$  compared to CD4<sup>+</sup> CD19<sup>-</sup> T cell events (R1), while CD4<sup>-</sup> CD19<sup>+</sup> B cells (R3) do not express  $\alpha_E$ . Forward and side scatter profiles for CD4<sup>+</sup> CD19<sup>-</sup>, CD4<sup>+</sup> CD19<sup>+</sup>, and CD4<sup>-</sup> CD19<sup>+</sup> events, showing that CD4<sup>+</sup> CD19<sup>+</sup> events have an increase in size characteristic of cell doublets (B). Confocal microscopy on MLN cell suspensions demonstrates that many  $\alpha_E^+$  cells (green) are found in close interactions with CD19<sup>+</sup> B cells (red) (C).

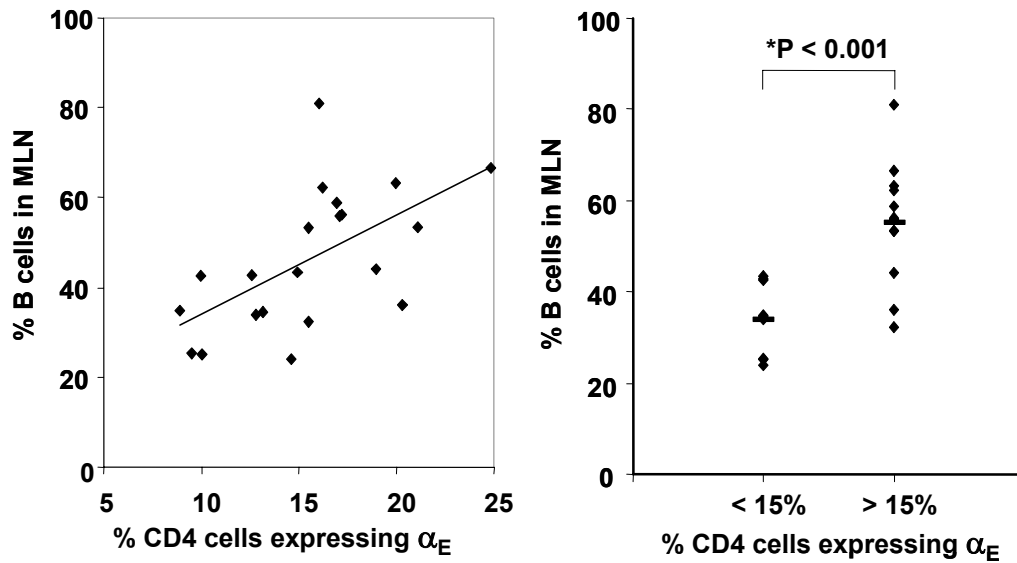


**Figure 4.8:** Correlation ( $R = 0.6$ ) between B cell number as a percentage of all MLN cells and the percentage of MLN  $CD4^+$  cells expressing  $\alpha_E$  in individual SAMP1/YitFc mice ( $n=21$ ) (left). Comparison of the percentage of B cells in MLN of mice with  $\alpha_E^+$   $CD4^+$  cells comprising greater than versus less than 15% of the MLN  $CD4^+$  population (mean is - ) (right).

the mean percentage (15%). In mice where greater than 15% of  $CD4^+$  T cells expressed  $\alpha_E\beta_7$ , B cells comprised  $55 \pm 4\%$  (mean  $\pm$  SEM) of total MLN lymphocytes, whereas in mice where  $\alpha_E^+$  cells constituted less than 15% of the  $CD4^+$  population, only  $34 \pm 3\%$  of total MLN lymphocytes were B cells.

To test whether B cell immunoglobulin production is enhanced by SAMP1/YitFc MLN  $\alpha_E\beta_7^+$   $CD4^+$  T cells, SAMP1/YitFc MLN B cells were cultured with unfractionated,  $\alpha_E\beta_7^+$ , or  $\alpha_E\beta_7^-$   $CD4^+$  T cells and immunoglobulin production was measured at 3, 7, 11, and 13 days of culture. In three independent experiments,  $\alpha_E\beta_7^-$   $CD4^+$  T cells induced significantly more IgG2a and IgM production by B cells at 13 days of culture than was induced by  $\alpha_E\beta_7^+$   $CD4^+$  T cells (Figure 4.9A). Cultures of SAMP1/YitFc B cells with  $\alpha_E\beta_7^+$   $CD4^+$  T cells exhibited significantly increased IgA production over the time course of the culture, with near peak values by day 11 ( $51 \pm 4$  ng/ml) (Figure 4.9B). In contrast,

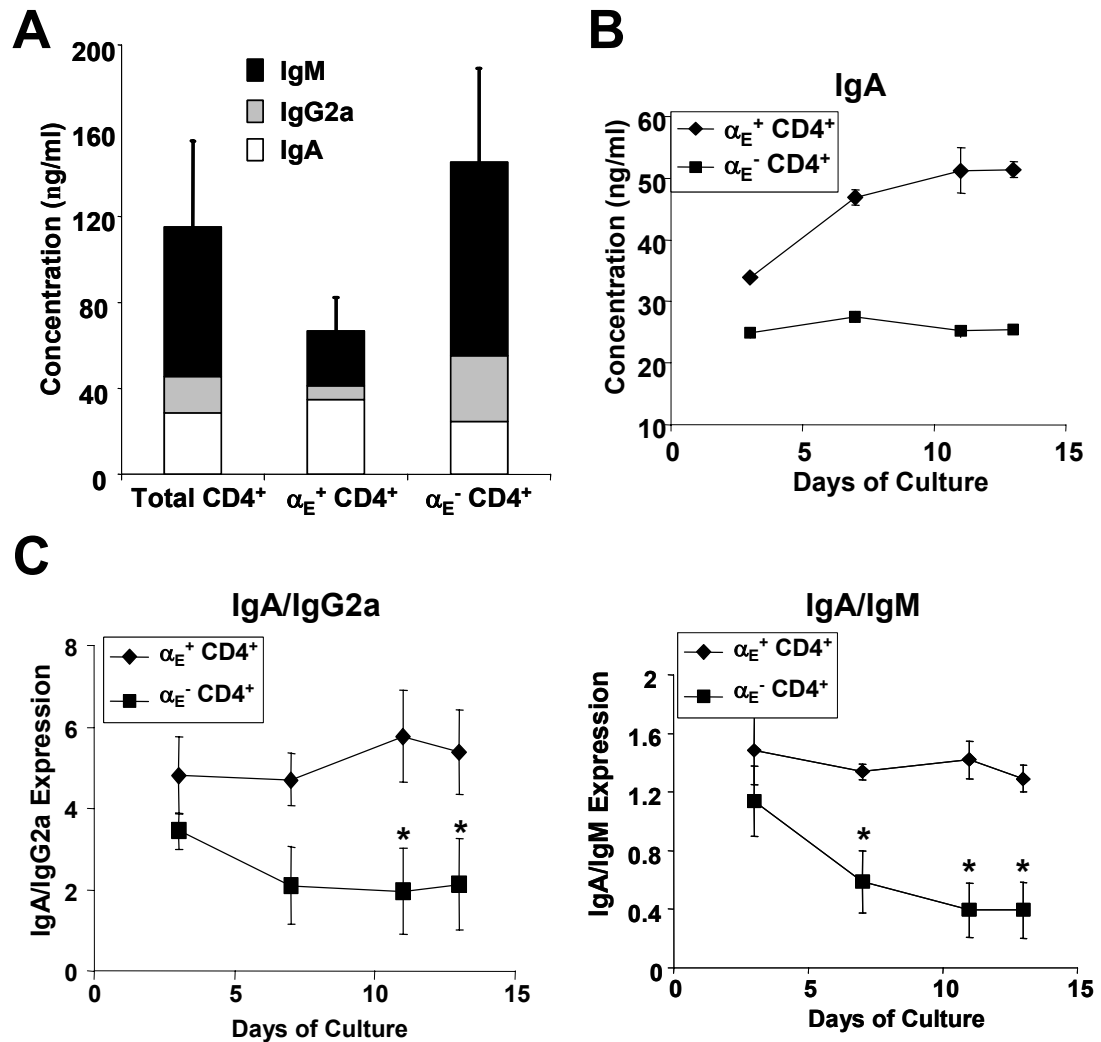


**Figure 4.9:** Comparison of IgA (open), IgG2a (gray), and IgM (black) expression, measured in triplicate by ELISA, by 13 day anti-CD3 stimulated cultures of SAMP1/YitFc MLN B cells with SAMP1/YitFc MLN unfractionated CD4<sup>+</sup> T cells,  $\alpha_E^+$  CD4<sup>+</sup> T cells, or  $\alpha_E^-$  CD4<sup>+</sup> T cells, with values representing mean  $\pm$  SEM of 3 independent experiments for each group. Comparison of IgA expression, measured in triplicate, in which SAMP1/YitFc MLN B cells were cultured for 3, 7, 11, and 13 days with SAMP1/YitFc MLN  $\alpha_E^+$  CD4<sup>+</sup> T cells or  $\alpha_E^-$  CD4<sup>+</sup> T cells (B). Comparisons of the ratios of IgA to IgG2a (C, left) and IgA to IgM expression (C, right) in 3, 7, 11, and 13 day cultures of SAMP1/YitFc B cells with  $\alpha_E^+$  CD4<sup>+</sup> T cells or  $\alpha_E^-$  CD4<sup>+</sup> T cells, demonstrating that cultures with  $\alpha_E^-$  CD4<sup>+</sup> T cells, but not  $\alpha_E^+$  CD4<sup>+</sup> T cells, induce B cell polarization over time to become IgM and IgG2a producing cells. Values represent mean  $\pm$  SEM of 3 independent experiments for each group. \*Significantly decreased ratio compared to cultures with  $\alpha_E^+$  CD4<sup>+</sup> T cells.

no significant increases in IgA levels were seen beyond 3 days of culture. This result was reproduced in a second independent experiment, however in a third experiment, neither  $\alpha_E\beta_7^+$  or  $\alpha_E\beta_7^-$  cells led to increased levels of IgA production beyond 3 day levels (not

depicted). Because of the third experiment, statistical analysis was unable to determine significant differences in IgA production by B cells cultured with  $\alpha_E\beta_7^+$  versus  $\alpha_E\beta_7^-$  cells. However, in this third experiment, SAMP1/YitFc unfractionated  $CD4^+$  T cells also did not increase IgA production above levels seen at the 3 day timepoint (not depicted) contrary to what we have seen in all previous cultures. This evidence suggests that factors required for IgA production may not have been present in the SAMP1/YitFc cells used in this third experiment. Regardless, considering that 2 out of 3 B cell cultures with  $\alpha_E\beta_7^+$  cells and no cultures with  $\alpha_E\beta_7^-$  cells resulted in increasing IgA production over time, these data suggest that  $\alpha_E\beta_7^+$   $CD4^+$  T cells preferentially induce SAMP1/YitFc MLN B cell IgA production. In contrast, B cells cultured with  $\alpha_E\beta_7^-$   $CD4^+$  T cells became increasingly polarized toward IgG2a and IgM production over time, as measured by significantly lower IgA:IgG2a and IgA:IgM ratios in these cultures versus cultures with  $\alpha_E\beta_7^+$   $CD4^+$  T cells at 11 and 13, but not 3 days of culture (Figure 4.9C).

The positive correlation between  $\alpha_E^+$   $CD4^+$  T cell and B cell numbers in SAMP1/YitFc MLN and the preferential involvement of  $\alpha_E^+$   $CD4^+$  T cells in T cell/ B cell doublets suggest that  $\alpha_E^+$   $CD4^+$  T cells may act as  $T_{FH}$  cells *in vivo* to produce B cell expansion. The high level of ICOS expression on  $\alpha_E^+$   $CD4^+$  T cells also supports this hypothesis. As the coculture experiments demonstrate, the  $T_{FH}$  properties of  $\alpha_E\beta_7^+$   $CD4^+$  T cells are limited to increasing the production of IgA, as the production of other immunoglobulin isotypes was supported exclusively by cells within the  $\alpha_E\beta_7^-$   $CD4^+$  population. However, given that the distinctive feature of SAMP1/YitFc MLN B cell expansion is local and systemic overproduction specifically of IgA, it seems plausible to

conclude that the increased numbers of  $\alpha_E\beta_7^+$  CD4<sup>+</sup> T cells in SAMP1/YitFc mice are the driving force behind the observed SAMP1/YitFc MLN B cell expansion *in vivo*.

Under homeostatic conditions, IgA is translocated across intestinal epithelial cells to the luminal surface, where it blocks initiation of immune responses by preventing bacteria from exiting the lumen (140). From this perspective, it makes sense that T<sub>reg</sub>, which produce cytokines proven to induce and enhance IgA production (267), would drive IgA production as part of their anti-inflammatory repertoire (275). However, most IgA that binds to normal flora is derived from B1 cells, whereas B2-derived IgA, such as that seen in SAMP1/YitFc MLN, recognizes potentially pathogenic bacteria and aids in their elimination (191;194). In SAMP1/YitFc ileitis, where epithelial barrier integrity is likely diminished as will be discussed in Chapter V, IgA coating the surface of bacterial antigens that penetrate this leaky barrier may initiate pro-inflammatory responses through opsonization or immune complex formation. However, we have not excluded the possibility that this role, if relevant, may also be played by antibodies of other isotypes, such as IgM which is also increased in SAMP1/YitFc MLN. In this case, the production of pathogenic IgM antibody would be driven by the  $\alpha_E\beta_7^-$  CD4<sup>+</sup> T cell population.

#### *Contribution of B cells to SAMP1/YitFc and adoptively transferred ileitis*

To ascertain the contributions of the expanded MLN B cell population to the development of SAMP1/YitFc ileitis, B cell expansion in the MLN was compared to ileitis severity in the same mouse (Figure 4.10A). In mildly inflamed SAMP1/YitFc mice (total ileal inflammatory scores < 10), there was almost a 2:1 ratio of CD4<sup>+</sup> T cells ( $54 \pm 1\%$ , mean  $\pm$  SEM) to B cells ( $30 \pm 1\%$ ) as a percentage of total MLN lymphocytes.

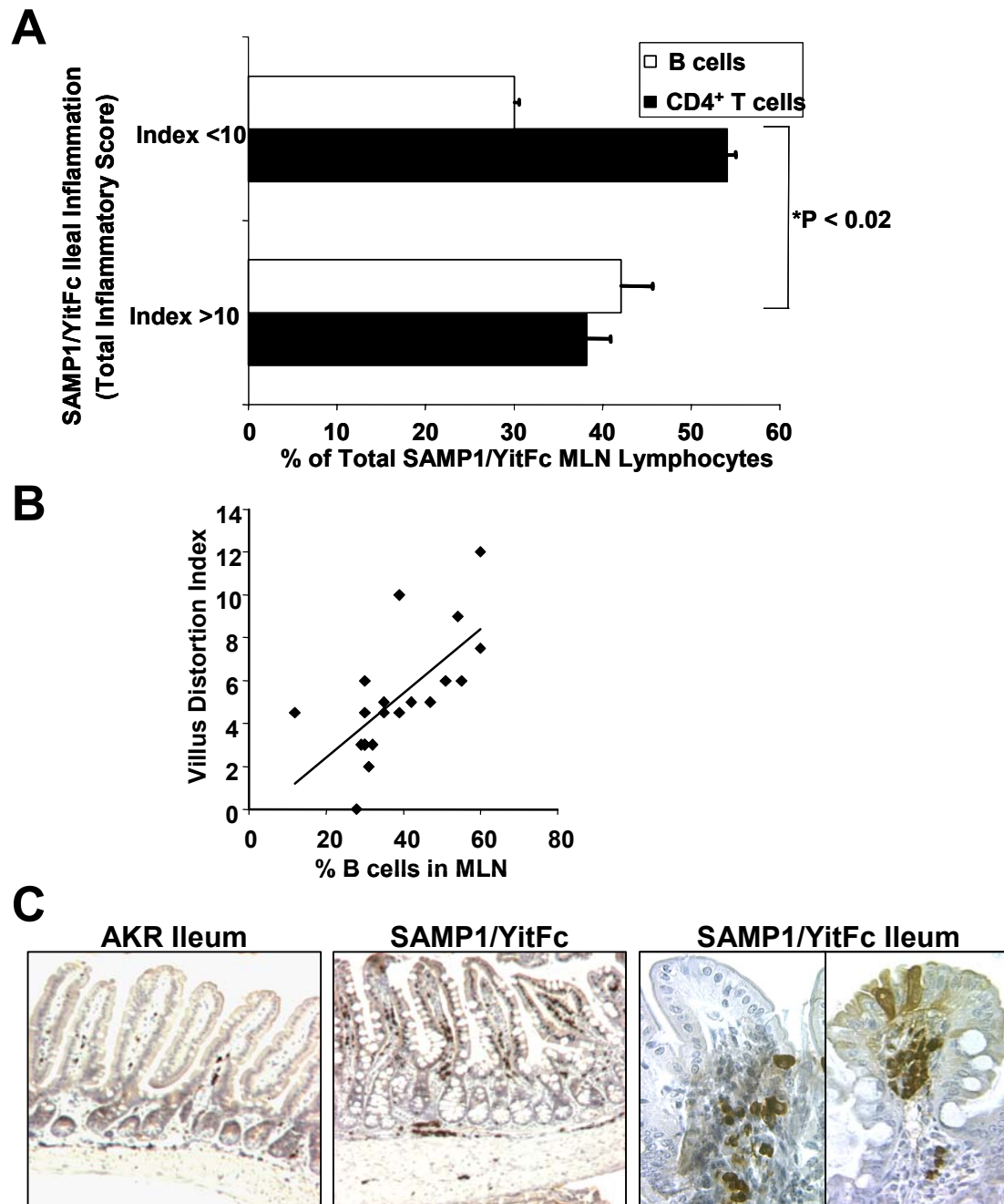


**Figure 4.10:** Percentages of CD4<sup>+</sup> (black) and CD19<sup>+</sup> (open) cells within mesenteric lymph nodes (mean  $\pm$  SEM) of individual SAMP1/YitFc mice ( $n=20$ ) in which the total inflammatory score of the distal ileum was greater than 10 (mean  $\pm$  SEM =  $15 \pm 1$ ,  $n=14$ ) or less than 10 (mean  $\pm$  SEM =  $5 \pm 1$ ,  $n=6$ ) (A). \*CD4<sup>+</sup> T cell and B cell percentages are significantly different ( $P < 0.02$ ) between the two groups. The percentage of B cells in MLN of mice ( $n=20$ ) correlates ( $R = 0.7$ ) with the villus distortion component of the histopathologic scoring index (B). Low power (10x) view of paraffin-embedded ileal sections immunostained for IgA, showing increased concentrations of IgA-secreting cells (dark brown spots) throughout and increased soluble IgA within the villi (diffuse light brown) in SAMP1/YitFc versus AKR ilea (C, left two panels). High power views (40x) show IgA-secreting cells and soluble IgA concentrated in the base (left) and the tip (right) of two villi within SAMP1/YitFc ilea (C, right).

In severely inflamed mice (total scores > 10), the B cell population ( $42 \pm 4\%$ ) exceeded the number of  $CD4^+$  T cells ( $38 \pm 3\%$ ) within the MLN. Multiple regression analysis revealed that B cell expansion within the MLN correlated most closely with the villus distortion index (Figure 4.10B), suggesting that B cells may play a major role in responses that disrupt villus architecture. In AKR ileal sections immunostained for IgA expression,  $IgA^+$  cells were found as single cells or in small clusters, evenly distributed throughout the intestine (Figure 4.10C). Most of the free IgA staining was located within crypts or near the base of villi. In SAMP1/YitFc ilea,  $IgA^+$  cells were found in large clusters and distributed in a focally concentrated pattern. Interestingly, most of these clusters of  $IgA^+$  cells were found in areas where the tissue architecture was only moderately distorted. Soluble IgA was found throughout the villi, with the densest staining intensity near the tips.

Since the above results were correlative in nature, it was unclear whether the increased B cells contribute to ileitis, or whether they expand in severely inflamed mice as part of a compensatory pathway. To test whether SAMP1/YitFc MLN B cells were pro- or anti-inflammatory, we cotransferred  $5 \times 10^5$  SAMP1/YitFc MLN  $CD4^+$  T cells with or without  $2 \times 10^6$  SAMP1/YitFc or AKR MLN B cells into SCID recipients (Figure 4.11A). Mice receiving  $CD4^+$  T cells and SAMP1/YitFc B cells had significantly greater chronic inflammatory indices ( $4.6 \pm 0.5$  versus  $2.8 \pm 0.3$ , mean  $\pm$  SEM) and total inflammatory scores ( $15 \pm 1$  versus  $10 \pm 2$ ) than mice receiving T cells alone. SCID mice receiving AKR B cells along with SAMP1/YitFc  $CD4^+$  T cells displayed an intermediate phenotype with similar levels of chronic inflammation ( $5.5 \pm 0.5$  versus  $4.6 \pm 0.5$ ) but significantly decreased active inflammation ( $2.5 \pm 0.6$  versus  $5 \pm 1$ ) compared to mice

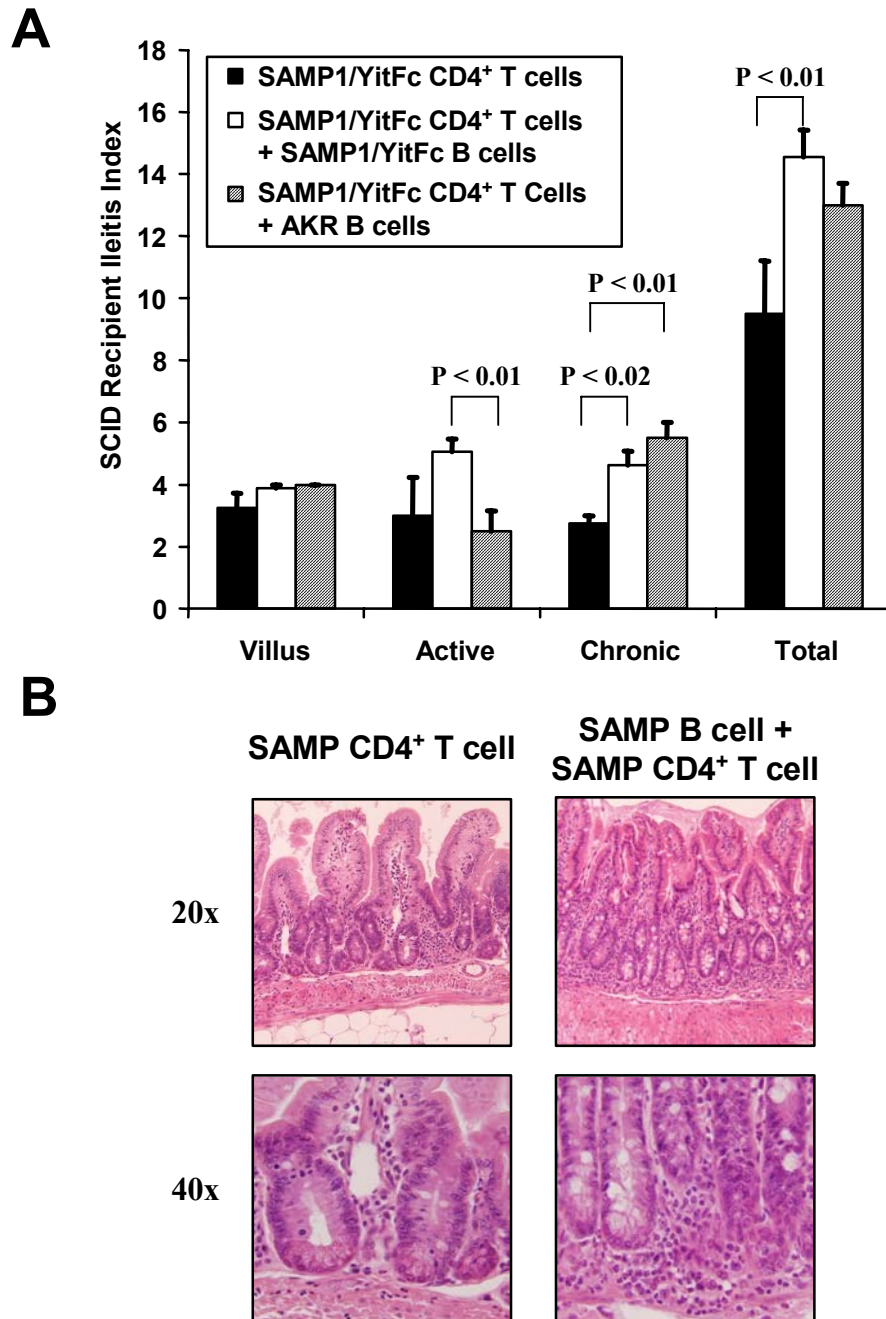


**Figure 4.11:**  $5 \times 10^5$  CD4<sup>+</sup> T cells from pooled SAMP1/YitFc MLN (n=6) were injected intraperitoneally into SCID mice either alone (n=4) or in combination with  $2 \times 10^6$  SAMP1/YitFc (n=8) or AKR (n=4) MLN B cells intravenously. After 6 weeks, SCID mice receiving the SAMP1/YitFc T cells and SAMP1/YitFc B cell combination had greater chronic and total inflammatory scores than mice receiving T cells alone, while mice receiving AKR B cells and SAMP1/YitFc T cells had an intermediate phenotype (A). H + E stained ileal sections from representative SCID mice showing an increase in overall cellular infiltrates, crypt architectural changes, and muscularis thickening in the ileum of a SCID mouse that received the SAMP1/YitFc B and T cell combination compared to a mouse receiving only CD4<sup>+</sup> T cells (B).



receiving SAMP1/YitFc B cells and CD4<sup>+</sup> T cells. H + E stained sections demonstrate increased architectural abnormalities, inflammatory cell infiltrates, and muscularis thickening in mice receiving SAMP1/YitFc CD4<sup>+</sup> T cells and SAMP1/YitFc B cells compared with mice receiving T cells alone (Figure 4.11B). As in the T cell only transfers performed in Chapter 4, the size of the villus distortion parameter did not differ significantly among groups. Colitis scores were also significantly increased in SCID mice receiving SAMP1/YitFc CD4<sup>+</sup> T cells and either SAMP1/YitFc (4.1 ± 0.5, active + chronic inflammation) and AKR (4.9 ± 0.1) B cells compared to mice receiving CD4<sup>+</sup> T cell alone (2 ± 1) (data not shown). Interestingly, transfer of the SAMP1/YitFc B cell fraction alone also resulted in severe ileitis (total score, 13 ± 1) with the largest component of the histologic score being active inflammation (5.3 ± 0.8)(data not shown). However, due to the fact that this population was only 98% pure with many of the remaining cells being CD4<sup>+</sup> T cells, it is possible that around 2 x 10<sup>4</sup> CD4<sup>+</sup> T cells could have been transferred with the B cells in these mice. While this population represents an insignificant increase of 4% of the total T cells transferred in mice receiving both B cells and T cells, it may be large enough to influence disease development in mice receiving only the B cell fraction. Thus, though the phenotype of mice receiving only this B cell fraction is unique in that these mice develop high levels of active and low levels of chronic inflammation, definitive proof that B cells alone produce this phenotype would require future experiments with higher purity in the transferred B cell fraction.

Surprisingly, no CD20<sup>+</sup> B cells were found in the ilea of mice receiving cotransfer of B cells from either strain along with SAMP1/YitFc CD4<sup>+</sup> T cells (Figure 4.12). While slightly more IgA<sup>+</sup> plasma cells were detectable in the ilea of SCID mice receiving

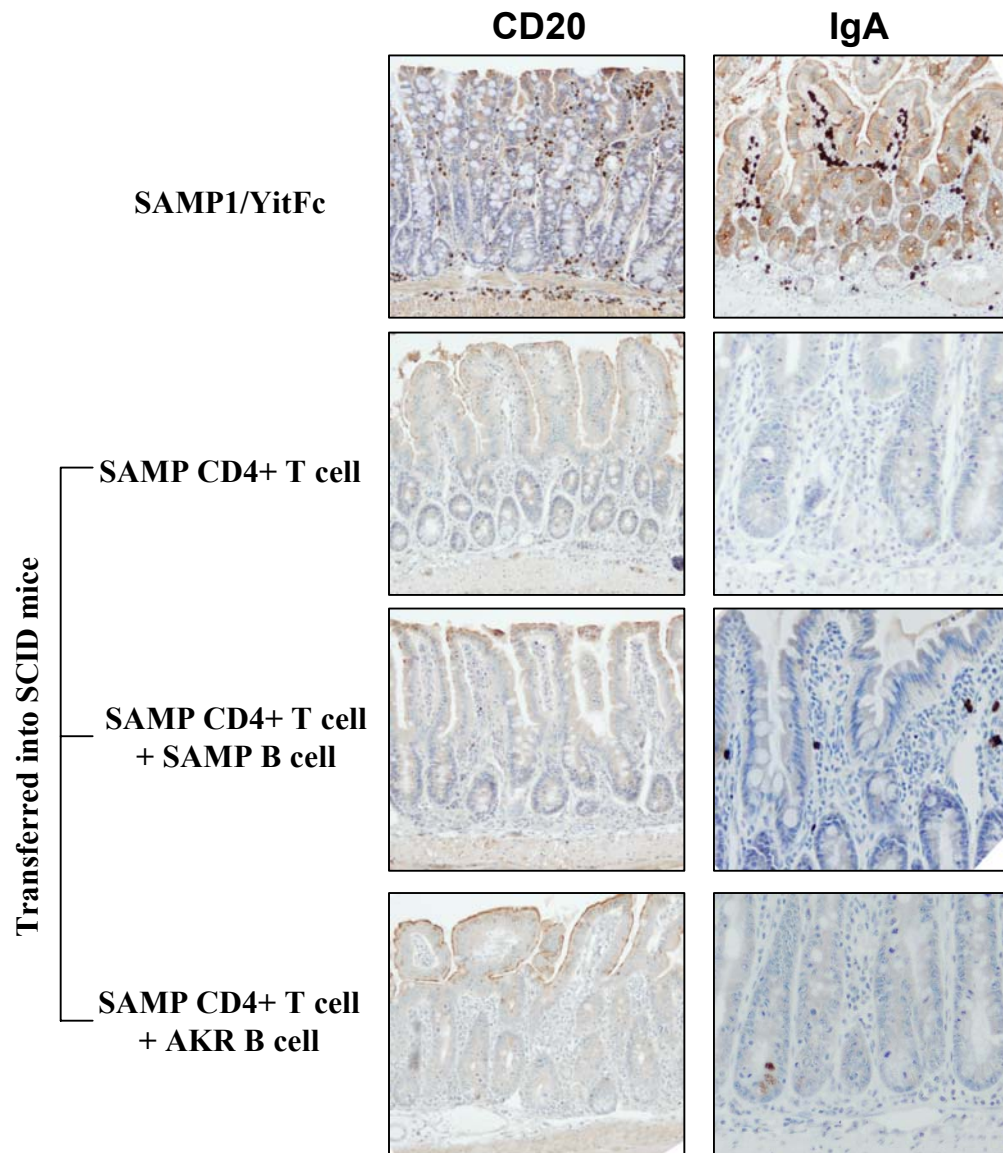


**Figure 4.12:** Immunostaining of paraffin-embedded ileal sections demonstrating that while CD20<sup>+</sup> B cells and IgA-expressing cells are prevalent in ilea from SAMP1/YitFc mice, no CD20<sup>+</sup> and only scattered IgA-expressing cells are seen in SCID ilea from mice adoptively transferred (AT) SAMP1/YitFc B cells along with CD4<sup>+</sup> T cells. Even fewer IgA<sup>+</sup> cells are seen in ilea from SCID mice receiving SAMP1/YitFc T cells and AKR B cells, whereas no IgA<sup>+</sup> cells are seen in ilea from mice receiving T cells alone.

SAMP1/YitFc B cell cotransfer compared to mice receiving AKR B cell cotransfer or SAMP1/YitFc CD4<sup>+</sup> T cells alone, the number of positive cells was considerably smaller than that seen in SAMP1/YitFc ileum. Very few MLN cells in mice receiving CD4<sup>+</sup> T cells alone were IgA<sup>+</sup>, whereas 16% of MLN cells in mice receiving SAMP1/YitFc B

cells alone were IgA-expressing cells (Figure 4.13A). 10% of MLN cells were IgA<sup>+</sup> in mice receiving SAMP1/YitFc CD4<sup>+</sup> T cells and SAMP1/YitFc B cells, whereas 6% were IgA<sup>+</sup> in mice receiving the AKR B cell transfer (Figure 4.13A). Serum IgA was not detectable in most SCID mice receiving CD4<sup>+</sup> T cells alone, whereas IgA could be detected albeit at low levels ( $0.1 \pm 0.04$  µg/ml, mean  $\pm$  SEM) in mice receiving SAMP1/YitFc CD4<sup>+</sup> T cells along with AKR B cells (Figure 4.13B, left). In contrast, the majority of mice receiving both CD4<sup>+</sup> T cells and B cells from SAMP1/YitFc mice displayed high levels of serum IgA ( $2.1 \pm 0.9$  µg/ml). Binning all mice in this study (n=16) according to whether ileal inflammatory scores were greater than or less than the mean value (13), demonstrates that SCID mice with more severe inflammation had significantly higher IgA levels by rank-sum statistical analysis than mice with less severe inflammation (Figure 4.13B, right). Parallel with these findings, immunostaining of ileal sections with anti-GR1 antibody demonstrated that compared to ilea from mice receiving SAMP1/YitFc CD4<sup>+</sup> T cells alone or in combination with AKR B cells, mice receiving SAMP1/YitFc CD4<sup>+</sup> T cells and SAMP1/YitFc B cells displayed heavy submucosal neutrophil infiltrates in the ileum (Figure 4.14).

Further immunostaining of ileal sections revealed a large increase in CD3<sup>+</sup> cellular infiltrate size in mice receiving SAMP1/YitFc CD4<sup>+</sup> T cells along with either SAMP1/YitFc or AKR B cells compared to mice receiving T cells alone (Figure 4.14), suggesting that cotransfer of B cells may somehow promote effector T cell proliferation. Since interactions with GITRL can inhibit GITR<sup>+</sup> Treg suppression of effector cell proliferation (210), we examined the expression of GITR on SAMP1/YitFc  $\alpha_E$ <sup>+</sup> CD4<sup>+</sup> T cells by flow cytometry and GITRL on MLN B cells by real time RT-PCR. The majority

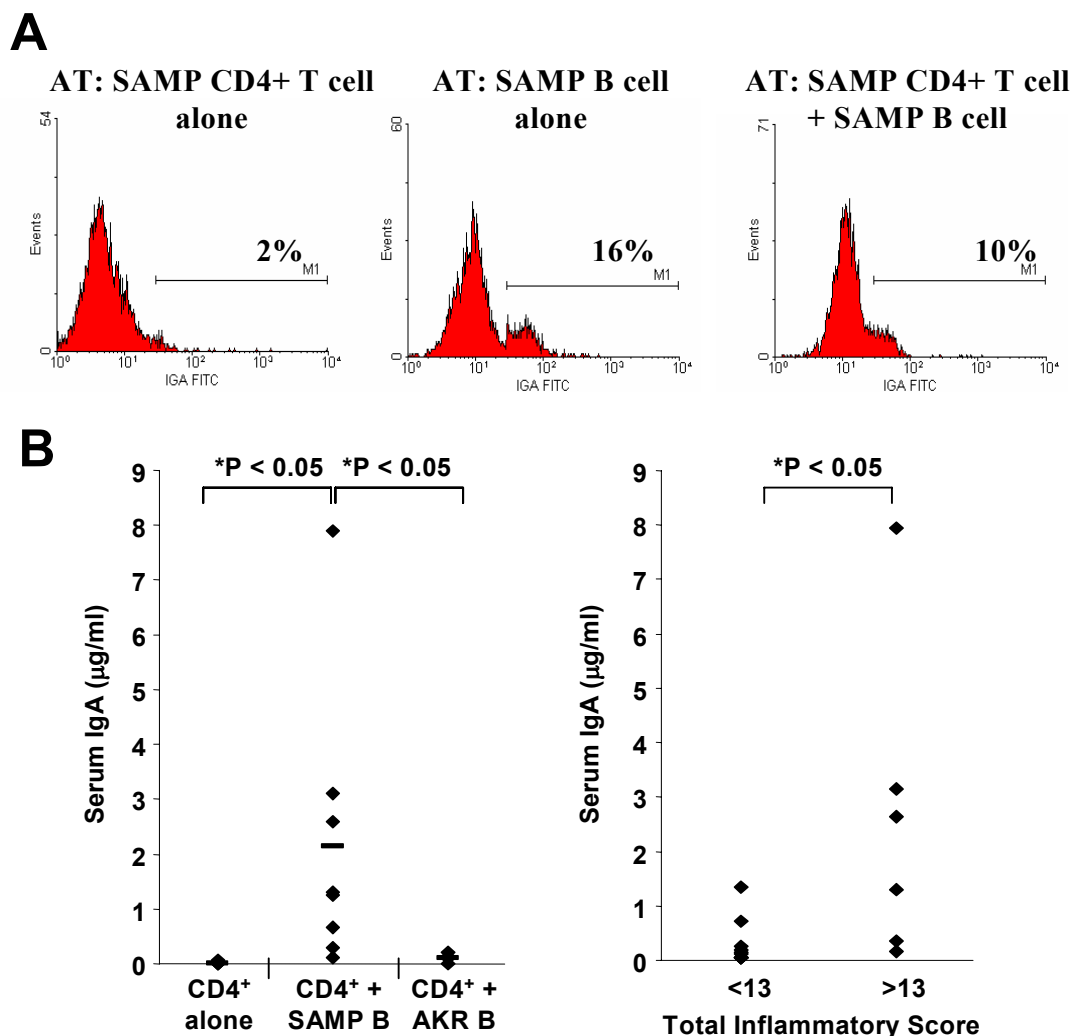


**Figure 4.13:** Total lymphocyte-gated histograms with percentage of positive cells given, showing the percentage of MLN lymphocytes expressing IgA in SCID mice receiving SAMP1/YitFc CD4<sup>+</sup> T cells alone or in combination with  $2 \times 10^6$  SAMP1/YitFc (n=8) or AKR (n=4) MLN B cells (A). Data was collected on cells pooled from 4 mice per treatment group. Serum IgA levels, measured by ELISA, are significantly higher in SCID mice receiving SAMP1/YitFc T cells along with SAMP1/YitFc B cells (n=8) compared to mice receiving SAMP1/YitFc T cells alone (n=4) or in combination with AKR B cells (n=4) (B, left). SCID mice in this study with the highest levels of serum IgA exhibit ileitis severity greater than the mean total inflammatory score (13) in this experiment (B, right).

of freshly isolated  $\alpha_E^+$  CD4<sup>+</sup> T cells expressed GITR, while most  $\alpha_E^-$  CD4<sup>+</sup> T cells did not

(Figure 4.15A). SAMP1/YitFc B cells expressed mRNA encoding GITRL at higher levels than did AKR B cells (Figure 4.15B).

We next tested whether B cells could interfere with  $\alpha_E^+$  CD4<sup>+</sup> T cell regulatory function by measuring cell proliferation in 3 day cultures of irradiated APC and

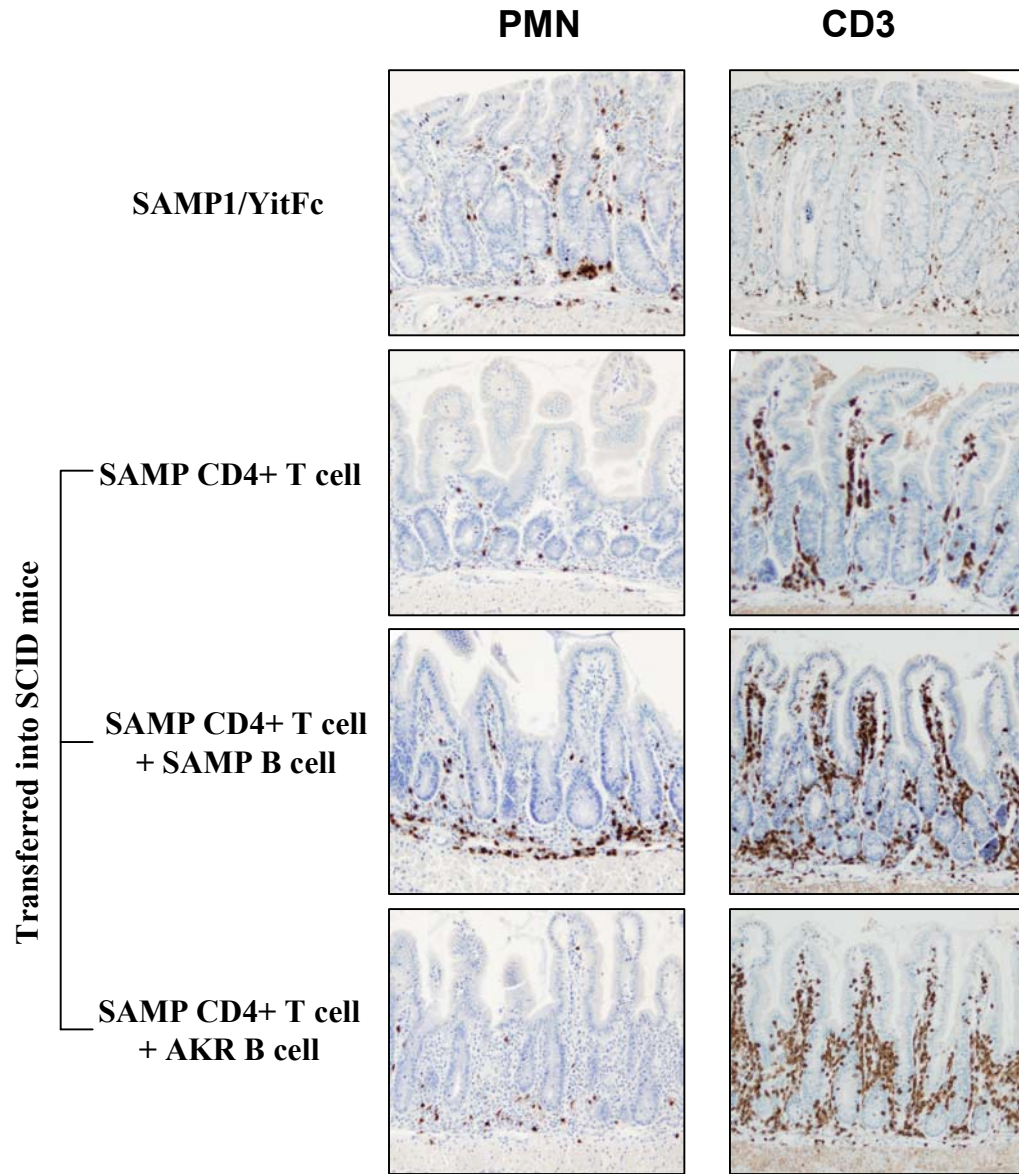


**Figure 4.14:** Immunostaining of paraffin-embedded ileal sections revealing an increase in T cell (CD3<sup>+</sup> cells) infiltrates in SCID mice receiving cotransfer of B cells from either strain compared to mice receiving T cells alone, and an increased neutrophil (GR-1<sup>+</sup> cells) infiltrate in mice cotransferred specifically with SAMP1/YitFc B cells (B). The CD3<sup>+</sup> infiltrate appears to be larger than that seen in native SAMP1/YitFc mice, whereas the neutrophil infiltrate in SAMP1/YitFc appears more localized within the villi and crypts than the submucosal infiltrate seen in SCID mice receiving SAMP1/YitFc B and T cells. Neutrophil staining in SAMP1/YitFc mice was carried out using the 7/4 clone that recognizes a strain-specific cell surface marker on neutrophils that is not present on neutrophils from C3H/HeJ SCID mice. Neutrophil staining in SCID mice was carried out using an antibody recognizing the neutrophil marker GR-1.

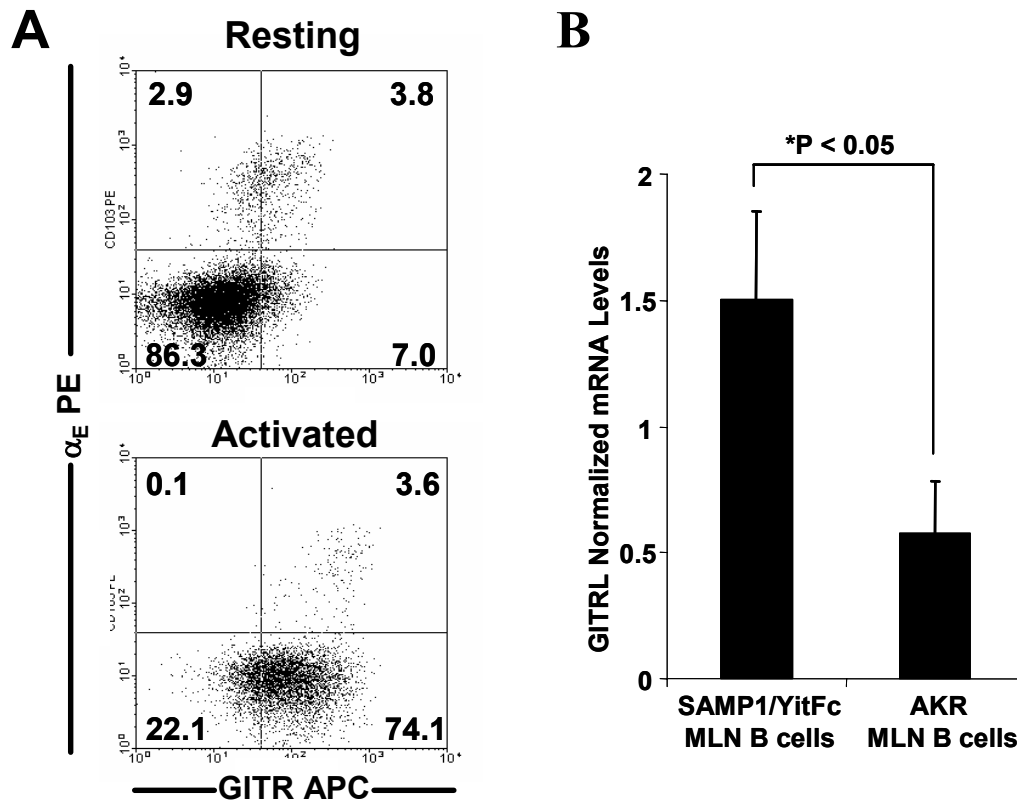


**Figure 4.15:** Increased expression of GITR on freshly isolated or 24 hour-activated (anti-CD3)  $\alpha_E^+$  versus  $\alpha_E^-$  CD4 $^+$  T cells (A). Increased mRNA expression of GITR ligand, measured by real time RT PCR and normalized to total 18s rRNA, on isolated MLN B cells from SAMP1/YitFc (n=8) versus AKR (n=6) mice (B).

SAMP1/YitFc cell subsets (Figure 4.16). Since B cells alone did not proliferate, and addition of B cells to either  $\alpha_E^+$  or  $\alpha_E^-$  CD4 $^+$  T cells alone did not significantly increase the proliferation in these wells, it is unlikely that B cells underwent proliferation in this assay. As discussed in Chapter III,  $\alpha_E^-$  CD4 $^+$  T cells showed strong proliferation when cultured with APC alone, and addition of  $\alpha_E^+$  CD4 $^+$  T cells markedly suppressed this proliferation. Addition of B cells to cultures containing both  $\alpha_E^+$  and  $\alpha_E^-$  CD4 $^+$  T cells almost completely blocked the suppressive effect of  $\alpha_E^+$  CD4 $^+$  T cells, leading to levels of H $^3$  incorporation similar to cultures of effector  $\alpha_E^-$  CD4 $^+$  T cells alone.

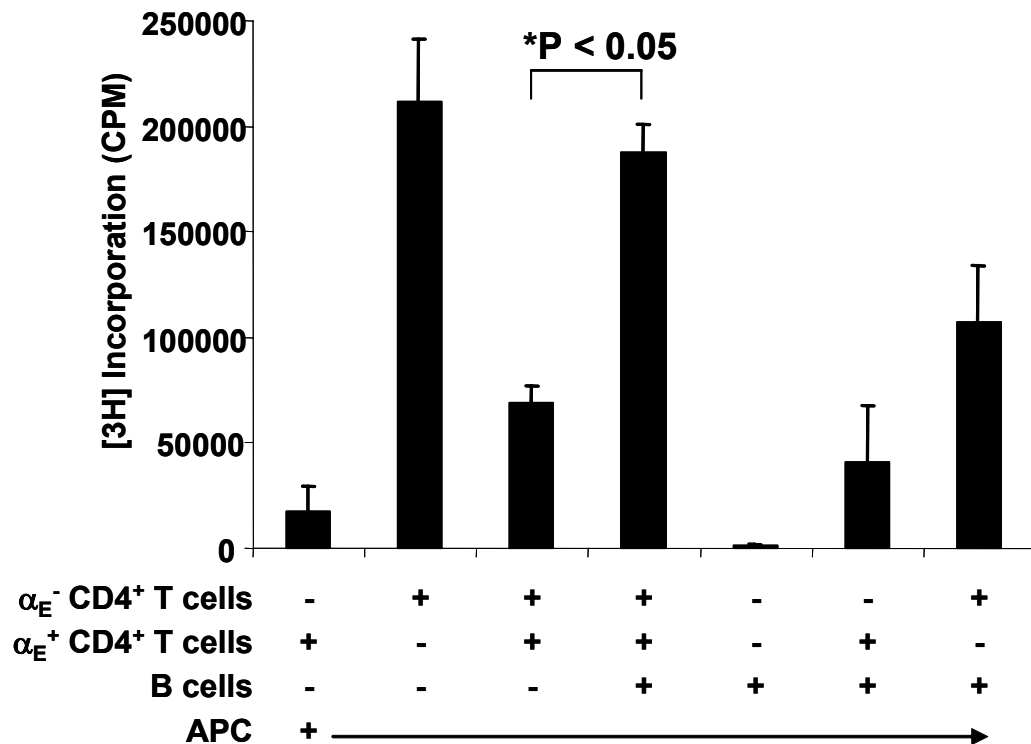


**Figure 4.16:** B cells expressing GITRL block  $\alpha_E^+$  CD4<sup>+</sup> regulatory T cell function. SAMP1/YitFc irradiated splenic APC ( $1 \times 10^5$ /well) were cultured with combinations of MLN  $\alpha_E^+$  CD4<sup>+</sup> T cells,  $\alpha_E^-$  CD4<sup>+</sup> T cells, and B cells ( $5 \times 10^4$  each) stimulated for 3 days with immobilized anti-CD3.  $H^3$  thymidine was added to the culture 24 hrs before analysis.  $\alpha_E^+$  Treg blocked the proliferation of effector T cells, while the addition of B cells to the coculture blocked the Treg-mediated inhibition. Data for each condition represents the average of 3 independent cultures each from 2 separate pools of cells isolated from greater than 10 SAMP1/YitFc mice.

SAMP1/YitFc MLN B cells may contribute to ileal inflammation through the production of immunoglobulin recognizing specific antigenic epitopes. The elevated IgA in severely inflamed mice adoptively transferred with both CD4<sup>+</sup> T cells and B cells provides correlative evidence supporting this hypothesis. This increased IgA produced by SAMP1/YitFc B cells is linked to an increase in neutrophil infiltration within the ileal submucosa of these adoptively transferred SCID mice. It is unclear whether this IgA is produced by B cells that have differentiated into IgA-secreting cells before or after transfer into SCID mice. It is also not known whether the elevated IgA is specific for certain antigens or whether the increase is due to a general expansion of the B cell

compartment in the immunodeficient SCID mouse. However, the finding that IgA is elevated when SAMP1/YitFc, but not AKR, B cells are transferred argues against the latter possibility. This increased neutrophil infiltration could result from the formation of immune complexes, which contribute to adhesion and tissue recruitment of neutrophils through a Mac-1 integrin-dependant pathway (276).

The findings in chapter III strongly suggest that aberrant proinflammatory signals that override anti-inflammatory pathways, and not inherently defective regulatory cells, are likely the cause of SAMP1/YitFc ileitis. The increased B cells present within the MLN of SAMP1/YitFc mice express GITRL, increase the severity of adoptively transferred ileitis, and can abrogate regulatory T cell function *in vitro*. Therefore, B cells may be a critical cell population responsible for overriding anti-inflammatory signals *in vivo*. This mechanism of Treg inhibition by B cells cannot fully explain the lack of effectiveness of SAMP1/YitFc Treg in the adoptive transfer model, because Treg cannot prevent this ileitis even in the absence of B cells. It is possible that other GITRL-expressing cells native to SCID mice, such as dendritic cells (210), may be responsible for blocking Treg function via the same general mechanism. Additionally, given that SAMP1/YitFc  $\alpha_E\beta_7^+$  Treg may have a minor effect on severe ileitis development, as illustrated by the slightly higher inflammatory scores in mice receiving  $\alpha_E\beta_7^-$  versus unfractionated  $CD4^+$  T cells discussed in Chapter III, a portion of the increase in disease severity induced by cotransfer of B cells along with  $CD4^+$  T cells may be due to this novel mechanism.

Findings in the previous section demonstrate a positive correlation between the number of  $\alpha_E\beta_7^+$   $CD4^+$  T cells and the number of B cells within SAMP1/YitFc MLN. I postulated that this correlation is due to  $\alpha_E\beta_7^+$   $CD4^+$  T cells driving B cell expansion and



immunoglobulin production. Alternatively, this correlation and the paradoxical increase in  $\alpha_E^+$  CD4<sup>+</sup> regulatory cells in SAMP1/YitFc versus AKR mice could be explained by a model in which B cell expansion precedes and induces expansion of  $\alpha_E^+$  CD4<sup>+</sup> T cells through GITR/GITRL-mediated interactions. These interactions have been shown previously to induce IL-2 responsiveness and proliferation in T<sub>reg</sub> cells. These two mechanisms explaining the  $\alpha_E\beta_7^+$  CD4<sup>+</sup> T cell/B cell correlation are not mutually exclusive, as interactions between T cells and B cells can elicit downstream proliferative effects in both cell types (277).

B cells have recently been shown to directly modulate intestinal inflammation in several other models. Backcrossing TCR $\alpha$ <sup>-/-</sup> mice with Ig $\mu$ <sup>-/-</sup> mice results in mice with more severe chronic colitis than TCR $\alpha$ <sup>-/-</sup> alone, and reconstitution of double-knockout mice with mature splenic B cells ameliorates this increased inflammation severity (269). The anti-inflammatory B cell subset in this model expresses IL-10 and high levels of CD1D, a marker of marginal zone cells (111;278). CD45RB<sup>high</sup> T cells from IFN- $\gamma$ <sup>-/-</sup> mice can induce ileitis when transferred to SCID mice only when cotransferred with B cells (112), consistent with our data suggesting that the pro-inflammatory activity of intestinal B cells may be particularly relevant in the ileum. Furthermore, in the *Gai2*<sup>-/-</sup> model of IBD, a selective deficit in B1 cells and an increase in B2 cells are linked to the development of intestinal inflammation (108). Since SAMP1/YitFc MLN B cells are predominantly B2 cells, our findings and these previous studies are consistent with a model in which mucosal B2 cells are pro-inflammatory and B1 cells are anti-inflammatory in the context of IBD.

## V. Epithelial Barrier Function and the Origins of Ileitis Susceptibility in SAMP1/YitFc Mice

### Rationale

While striking advances have been made in the field of Crohn's disease research, enabling both the understanding of mucosal inflammatory mechanisms (200) and the advent of effective treatment modalities (19), the primary defect in genetically susceptible individuals that initiates the cascade of events leading to disease development remains largely unknown (32;275). The discovery that mutations in the CARD15/NOD2 gene predispose individuals to develop Crohn's disease (40;41) represents one of the first breakthroughs shedding light on one potential precipitating factor. However, individuals with these mutations only account for ~20% of Crohn's patients (42), and the mechanism through which defective NOD2 function leads to the development of intestinal inflammation has not been established (43). One of the key unresolved issues regarding this susceptibility trait, underscored by the fact that NOD2 is expressed and possesses independent functions in both hematopoietic cells and intestinal epithelial cells (45;279), concerns the cells or tissue in which this precipitating factor originates.

Much evidence suggests that a primary immunologic defect may be responsible for causing Crohn's disease (200). Aberrant lamina propria mononuclear cell overexpression of Th1 polarizing cytokines such as IL-12 and interferon- $\gamma$  (IFN- $\gamma$ ) has long been postulated as a potential causal factor of Crohn's (17;18). In murine adoptive transfer models, CD45RB<sup>hi</sup> or CD25<sup>-</sup> CD4<sup>+</sup> T cell populations expressing these cytokines are sufficient to induce colitis in SCID mice (79;84). Primary defects in the function of

regulatory T cells may give rise to intestinal inflammation by allowing excessive effector responses to non-pathogenic floral or food antigens (222;223). Increased serum autoreactivity in Crohn's patients suggest that B lymphocyte specificity may be involved in initiating the disease (112;271), while the curative effect of enhancing myeloid cell function in a cohort of Crohn's patients (240) suggests that defects in neutrophils and/or other innate immune cells may also play a critical role. Most convincingly, case reports have demonstrated complete remission in several Crohn's patients following irradiation and allogeneic bone marrow transplantation (220), suggesting a primary defect in immune cell function in these individuals.

Conversely, there are several lines of evidence suggesting that intestinal epithelial cells confer the primary susceptibility to Crohn's disease. In the intestine, NOD2 is expressed at higher levels by specialized epithelial Paneth cells than by lamina propria mononuclear cells in both normal and Crohn's disease tissue (219). Epithelial NOD2 from normal patients may play a critical role in the ability of epithelial cells to expel luminal bacteria, whereas Crohn's-variant NOD2 lacks this function (279). Epithelial Toll-like receptor expression is also altered in Crohn's patients (143), suggesting that the ability of the epithelium to respond properly to common bacterial motifs might lead to disease initiation. Epithelial cytokine and chemokine expression is increased in the context of Crohn's (145;146), possibly enabling the initial recruitment of inflammatory cells to lesion sites. Importantly, alterations in epithelial barrier function may be a primary etiologic agent leading to Crohn's disease, as intestinal permeability is dramatically increased in Crohn's patients relative to normal controls or ulcerative colitis patients (32;224). Importantly, first degree relatives of Crohn's patients, who are at

increased risk for developing disease, often have increased intestinal permeability relative to the remaining population (234;235), and increased epithelial permeability often precedes and predicts relapse following remission for Crohn's patients (280).

The studies in this chapter have investigated whether the primary etiologic agent responsible for SAMP1/YitFc ileitis originates from immune cells or a non-hematopoietic source such as the epithelium, using chimeric mice generated via bone marrow transplantation in which AKR and SAMP1/YitFc mice have been reconstituted with SAMP1/YitFc and AKR bone marrow, respectively. After assaying for the severity of ileitis in these mice, we then investigated epithelial barrier function and expression of Ppar $\gamma$  in SAMP1/YitFc and AKR mice. Finally, the effect of exchanging hematopoietic cell compartments on the size of lymphocyte subsets and the pathogenicity of CD4<sup>+</sup> T lymphocytes in terms of cytokine production were examined in recipient mice. Taken together, our data demonstrates that a non-hematopoietic tissue, likely intestinal epithelial cells, contains the primary ileitis susceptibility factor in SAMP1/YitFc mice.

## **Materials and Methods**

### *Mice*

SAMP1/YitFc mice were obtained from colonies at the University of Virginia vivarium. AKR/J were obtained from colonies at the University of Virginia or purchased from Jackson Laboratories (Bar Harbor, ME). All mice were between 6-12 weeks unless otherwise indicated, and all experiments were approved by the institutional committee for animal use.

### *Bone marrow transplantation*

Mice receiving bone marrow transplantation were irradiated with 2 doses of 600 RAD each, one the morning of transplantation and the other 4-6 hours later, immediately prior to injection of donor cells. Bone marrow was obtained by inserting a 25g needle into the bone marrow cavities of donor femurs and tibias and flushing contents with RPMI containing 10% fetal calf serum. After centrifugation ( $300\times g$ ,  $4^{\circ}C$ , 10 min) and resuspension, an aliquot of cells was stained with Trypan blue (Sigma, St. Louis, MO), diluted in a 1:1 ratio with 4% acetic acid to lyse red blood cells, and counted using a hemocytometer (Reichert, Buffalo, NY). Cell suspensions were washed and diluted to a concentration of  $15 \times 10^6$  cells/ml in plain RPMI.  $7.5 \times 10^6$  bone marrow cells in a volume of 500  $\mu$ l were injected intravenously into the lateral tail veins of recipient mice. Transplanted mice were given antibiotic water containing 0.7 mM neomycin sulfate, 80 mg sulfamethoxazole, and 0.37 mM trimethoprim for two weeks following irradiation. After this period, mice received plain autoclaved water in order to reconstitute normal gut flora. SAMP1/YitFc mice receiving AKR bone marrow were designated as AKR BM  $\rightarrow$  SAMP, whereas AKR mice receiving SAMP1/YitFc bone marrow were designated as SAMP BM  $\rightarrow$  AKR. Control SAMP1/YitFc mice reconstituted with SAMP1/YitFc bone marrow were designated as SAMP BM  $\rightarrow$  SAMP and AKR mice reconstituted with AKR bone marrow were designated as AKR BM  $\rightarrow$  AKR.

### *Histology*

Sections of ilea from SAMP1/YitFc, AKR, and transplant recipient mice were prepared as described in chapter III. Briefly, the distal 10 cm of ileum was removed, flushed with plain PBS to remove fecal contents, opened to expose the mucosal surface,

rolled longitudinally, and fixed in Bouin's fixative. Tissues were embedded in paraffin and cut into 5  $\mu$ M sections for staining with hemotoxylin and eosin (H+E).

Ileitis severity was assessed by a trained pathologist in a blinded fashion using the same standardized histologic scoring system outlined in Chapter III.

### *Quantification of hematopoietic cell reconstitution*

To verify reconstitution of hematopoietic cells in bone marrow recipient mice, a cohort of female recipients was transplanted with bone marrow cells from male donors and the percentages of bone marrow cells, splenocytes, and MLN lymphocytes possessing a Y chromosome were determined 6 weeks after transplantation using quantitative real-time PCR amplifying a segment of the Y6 gene. DNA was extracted from cell populations using the DNeasy kit (Qiagen, Valencia, CA). PCR analysis was conducted in a multiplex fashion using a BioRad iCycler (Hercules) and specific probes that bound sequences in the Y6 and GAPDH genes, such that the amount of Y6 DNA was normalized to variations in total DNA concentration, measured by GAPDH, within each well. Primers and probes were obtained from Integrated DNA Technologies (Coralville, IA). The primer sequences for the Y6 gene were ACATCCACATTTTGAGGTCCTC (forward) and TCTCTACACGGTCCAGTTTACT (reverse), and the probe sequence was Fam-CACAGGCAGCAGACACACCCC-Black Hole Quencher 1. The primer sequences for GAPDH were GGCTCATGACCACAGTCCAT (forward) and GCCTGCTTCACCACCTTCT (reverse), and the probe sequence was Rox-CCTGGAGAAACCTGCCAAGTATGATGAC-Black Hole Quencher 1. DNA was amplified using Platinum Taq polymerase (Invitrogen, Carlsbad, CA) for 40 cycles

consisting of 30 sec at 94<sup>0</sup> C followed by 1 min at 56.2<sup>0</sup> C, with fluorescence measurements taken at the end of each cycle. Standard curves were constructed from the critical threshold (CT) values of 0:100, 10:90, 25:75, 50:50, 75:25, 90:10, and 100:0 percent ratios of male:female DNA from normal SAMP1/YitFc and AKR splenocytes, bone marrow cells, or MLN lymphocytes. These standard curves were used to calculate the percentage of DNA derived from the male donor cells in each population.

#### *Transepithelial electrical resistance assays*

Resistance assays were performing using adaptations of previously published methods (138). Briefly, distal ilea from SAMP1/YitFc, AKR, and transplant recipients (6 weeks post-transplant) were removed, flushed with plain 0.9% NaCl saline, cleaned by removing mesentery and adipose tissue, and opened longitudinally to expose the mucosal surface. A 3 mm<sup>2</sup> section was excised from the distal 2.5 cm of ileum and positioned on the membrane of a 0.4 µm Corning Costar transwell insert (Fisher Scientific, Hampton, NH). The membrane was then sandwiched between two custom-designed plexiglass discs with laser-etched openings, allowing exposure of both the serosal and mucosal surfaces. After insertion of the membrane apparatus back into the transwell insert such that the luminal surface of the ileum faced the upper chamber, the insert was placed into a 6 well plate containing DMEM with glutamine, non-essential amino acids, 100 U/ml penicillin, and 100 µg/ml streptomycin. Electrical resistance readings were taken using an EVOM voltmeter with an EndOhm chamber attachment (World Precision Instruments, Sarasota, FL) immediately after assembling the transwell apparatus and after 1 hour incubation at 37<sup>0</sup> C. Baseline resistance readings were determined in wells in which the

transwell insert did not contain intestinal tissue, and this background reading was subtracted from each sample resistance value.

### *In Vivo disaccharide permeability assays*

Transplant recipient mice were assayed for intestinal permeability to disaccharide probes several days prior to initial irradiation and 3 and 6 weeks post-transplantation using an adaptation of previously published methods (137;281). Briefly, mice were fasted for 2 hours prior to receiving an oral gavage of 0.2 ml of H<sub>2</sub>O containing 500 mg/ml of sucrose, 60 mg/ml of lactulose, 40 mg/ml of mannitol, and 30 mg/ml of sucralose. Mice were then transferred to individual metabolic cages for 22 hours, after which the cages were rinsed, the urine collected, and the total volume of urine was recorded. Concentrations of sucrose, lactulose, and mannitol within collected urine specimens were determined by pulsed amperometric detection using a Dionex HPLC with MA-1 columns (Dionex, Mississauga, ON) and NaOH-based elution as previously described (281). Similarly, sucralose concentrations were determined using Dionex Ionpac NS1 columns (Dionex) and a gradient of acetonitrile in water as the eluent for HPLC analysis, as previously described (281).

Sucrose is degraded in the duodenum of mice, and thus the fractional urinary excretion of sucrose, defined as the percentage of the total amount given that is present in the urine, is used as a measure of gastric permeability (281). Lactulose and mannitol are degraded by colonic microflora. Lactulose is not absorbed by the small intestine, while the absorption rate of mannitol serves as a measure of small intestinal surface area. Thus, the ratio of the fractional urinary excretion of lactulose to mannitol is used as a



measure of small intestinal permeability. The fractional excretion of sucralose, which is not degraded in the gastrointestinal tract, is used as a measure of colonic permeability.

*Epithelial cell isolation and real time rt-PCR for Ppar $\gamma$  expression*

For epithelial cell isolation, immediately after animal euthanization, mouse ilea were removed, flushed with PBS to remove contents, and placed in cold PBS for 5 minutes. Peyer's patches were removed and the ilea were opened longitudinally to expose the mucosal surface. After cutting the tissue into 0.5 cm transverse pieces, samples were shaken 4-5x for 10 minutes each in an HBSS solution (pH 7.4) containing 15 mM HEPES, 3 mM EDTA, 0.05 mM dithiothreitol (Sigma, St. Louis, MO), and 0.035% NaHCO<sub>3</sub>, with or without 100 mM N-acetylcysteine (Sigma). After each shake, cells were decanted through a 70  $\mu$ M mesh filter and centrifuged for 8 minutes at 400 x g. Following the last shake, cells were resuspended in RPMI/10%FCS and layered onto a 20x/40x/70x percoll gradient (Amersham Biosciences, Netherlands) to remove intraepithelial lymphocytes. Gradients were spun at 2500 RPM for 20 minutes. Epithelial cells were removed from the 20x/40x interface, counted using Trypan Blue (Sigma), and flash frozen in liquid nitrogen. RNA was extracted using Qias shredder columns for homogenization and an RNeasy isolation kit (Qiagen).

mRNA samples from whole tissue samples of liver, jejunum and terminal ileum along with isolated splenocytes and MLN lymphocytes were also collected. Jejunal sections were taken 2-3 cm distal from the duodenum, whereas ileal samples were taken just proximal to the cecum. Specific expression of the Ppar $\gamma$ 1 isoform was determined by quantitative real-time reverse-transcriptase PCR (qPCR). A forward primer within exon

A1 (5'- GGGCTGAGGAGAAGTCAC -3') and a reverse primer spanning the junction between exons A1 and A2 (5'- TTCTTTCAAATCTTGTCTGTCAC-3') amplified a 129 bp fragment. This strategy was used so as to avoid amplification of Ppary1 genomic DNA, and because exons A1 and A2 are specific to isoform 1. Correct band amplification was tested using conventional two-step RT-PCR and gel electrophoresis. Ppary1 expression from each sample was then quantified by real-time reverse-transcriptase PCR using Quantitect SYBR Green (Qiagen, Valencia, CA) incorporation on a BioRad iCycler (Hercules, CA), using the following cycling parameters: 30 min 50<sup>0</sup> C, 10 min 95<sup>0</sup> C, 4 min 94<sup>0</sup> C, and 40 cycles of 15 sec 94<sup>0</sup> C; 30 sec 50<sup>0</sup> C; 45 sec 72<sup>0</sup> C; and 15 sec 78.5<sup>0</sup> C for SYBR Green fluorescence measurement during each cycle. A melt curve, from 50 to 95<sup>0</sup> C, was obtained at the end of each experiment to ensure proper product formation. A single sample of B6 liver was used to generate the standard curve for all experiments. To verify that starting concentrations of total RNA in each sample were similar, levels of 18s ribosomal RNA were quantified using 18s rRNA-specific primers and probe labeled with the VIC-fluorophore according to manufacturer's instructions (Applied Biosciences, Branchburg, NJ). Average 18srRNA concentrations within tissues did not vary between strains by more than 2-fold.

### *Flow cytometry*

MLN lymphocytes from SAMP1/YitFc, AKR, or transplant recipient mice were harvested and prepared for flow cytometry as described in Chapter III. Cells (1 x10<sup>6</sup>/sample) were stained with combinations of FITC-, PE-, PERCP-, and APC-labeled hamster anti-mouse CD69 (H1.2F3) and rat anti-mouse CD4 (RM4-5), CD19 (1D3),

B220 (RA3-6B2), IgA (C10-3),  $\alpha_E$  integrin (M290),  $\beta_7$  integrin (M293), CD25 (PC61), CD44 (IM7), and L-selectin (MEL-14) (BD Pharmingen, San Diego, CA).

### *Cell culture*

Plates were incubated with 1  $\mu$ g/ml anti-mouse CD3 (145-2C11) (BD Pharmingen) in PBS overnight at 4<sup>0</sup> C, and washed once with plain PBS prior to addition of cell suspensions. CD4<sup>+</sup> T cells from MLN of SAMP1/YitFc, AKR, AKR BM  $\rightarrow$  SAMP, and SAMP BM  $\rightarrow$  AKR mice were cultured in 96 well plates at 37<sup>0</sup> C with 5% CO<sub>2</sub> in RPMI media containing 10% fetal calf serum, 100 U/ml penicillin, 100  $\mu$ g/ml streptomycin, 1mM sodium pyruvate, 1mM non-essential amino acids, and 50  $\mu$ M 2-mercaptoethanol. T cell subsets were stimulated with plate-bound anti-CD3 for 48 hours at 10<sup>5</sup> cells/well in 100  $\mu$ l of media. Undiluted supernatants were assayed for TNF- $\alpha$ , IFN- $\gamma$ , IL-2, IL-4, and IL-5 using the mouse Th1/Th2 cytokine kit (BD Pharmingen).

### *Statistics*

Statistical analysis was performed using the two-tailed Student's t test unless otherwise indicated, with statistical significance set at  $P < 0.05$ . Coefficients of Determination,  $R^2$ , were determined by linear regression. Statistical comparison of the slopes of linear regression correlations was performed using the formula: t statistic =  $(b_1 - b_2) / S(b_1 - b_2)$ , where  $b_1$  and  $b_2$  are the slopes of the lines and  $S(b_1 - b_2)$  is the standard error of the difference of the regression slopes. This t statistic was compared to the critical t stat for the relevant degrees of freedom using  $P < 0.05$  to determine significance. Statistical comparisons of cytokine expression were performed using two-way analysis of variance on ranks (Friedman's Test), utilizing mouse strain as one factor with

SAMP1/YitFc, AKR, AKR BM  $\rightarrow$  SAMP, and SAMP BM  $\rightarrow$  AKR as levels for this factor, and cytokine expression as the other factor with TNF- $\alpha$ , IFN- $\gamma$ , IL-2, and IL-5 with or without IL-4 as levels for this second factor. The Holm-Sidak adjustment for multiple comparisons was then used to make pairwise comparisons between mouse strains in terms of individual cytokine production.

## Results and Discussion

### *BM transplant between SAMP1/YitFc and AKR mice results in full leukocyte reconstitution*

In order to test the relative contributions of the epithelium and leukocytes to the primary ileitis susceptibility in SAMP1/YitFc mice, bone marrow chimeras were generated by reconstituting irradiated 6-12 week old SAMP1/YitFc mice with age-matched wildtype AKR bone marrow (AKR BM  $\rightarrow$  SAMP) and irradiated AKR mice with SAMP1/YitFc bone marrow (SAMP BM  $\rightarrow$  AKR). These chimeras were first tested for hematopoietic cell reconstitution by transplanting a cohort of female recipients with bone marrow from male donors and assaying for the amount of Y chromosome DNA within leukocyte compartments 6 weeks after transplantation using quantitative real-time PCR. Splenocyte DNA from AKR BM  $\rightarrow$  SAMP and SAMP BM  $\rightarrow$  AKR mice generated from male donors and female recipients underwent amplification above critical threshold for a Y chromosome gene at roughly the same cycle as splenocyte DNA from a control male mouse (Figure 5.1), indicating that hematopoietic cell reconstitution in these mice was nearly complete. By generating a standard curve using known ratios of male:female DNA from native AKR mice and by normalizing each sample for

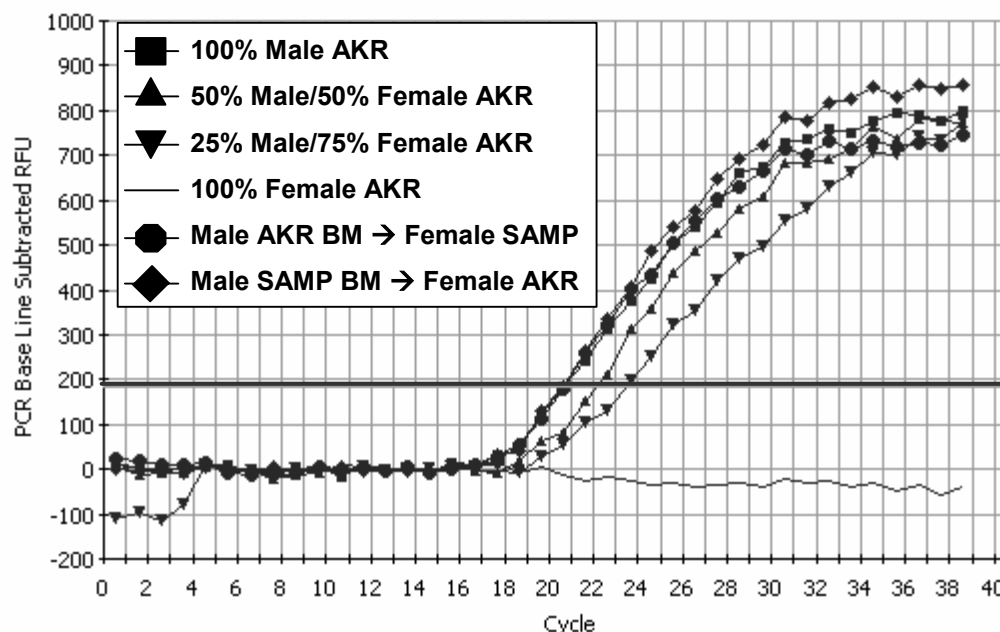


**Figure 5.1:** Tracing of relative fluorescence units (y) versus amplification cycle number (x) from real-time RT-PCR reactions using primers and a fluorescent probe amplifying and detecting, respectively, a sequence within the Y6 gene located on the Y chromosome. Splenocyte DNA from AKR BM  $\rightarrow$  SAMP or SAMP BM  $\rightarrow$  AKR mice, in which the bone marrow donors were male and recipients were female, contained similar levels of male DNA as unmixed male AKR control splenocytes, as measured by the critical threshold cycle number of Y6 amplification. Amplification of pre-mixed splenocyte DNA standards containing 50% male/50% female or 25% male/75% female AKR control DNA occurred at higher cycle numbers, whereas no amplification occurred in samples containing unmixed female AKR control splenocyte DNA.

differences in total DNA in a multiplex fashion using GAPDH amplification, the percentage of splenocytes, MLN cells, and bone marrow cells that were derived from the male bone marrow donors were determined (Table 5.1). The percentage of reconstitution was greater than 80% in all tissues assayed, with a trend toward slightly higher reconstitution in SAMP BM  $\rightarrow$  AKR mice versus AKR BM  $\rightarrow$  SAMP mice.

The values listed in Table 5.1 serve as a conservative estimate for percentage reconstitution, as the raw data before normalization to GAPDH suggests the percentage reconstitution may in fact be somewhat higher. For instance, the percentage reconstitution of MLN cells in AKR BM  $\rightarrow$  SAMP mice using the Y6 gene alone data

Mouse	% Reconstitution by Donor Hematopoietic Cells		
	Splenocytes	MLN	Bone Marrow
<b>AKR BM → SAMP</b>	<b>94 ± 3%</b>	<b>81 ± 5%</b>	<b>90 ± 3%</b>
<b>SAMP BM → AKR</b>	<b>106 ± 2%</b>	<b>97 ± 5%</b>	<b>95 ± 4%</b>

**Table 5.1.** Estimates of the percentage reconstitution in hematopoietic compartments of AKR BM → SAMP and SAMP BM → AKR mice, as determined by real-time multiplex PCR detecting Y6, a y chromosome gene, and GAPDH concentrations in female recipients receiving male bone marrow. Percentages were determined by dividing the ratio of Y6:GAPDH present in each sample by the same ratio in control male AKR splenocytes, MLN, and bone marrow cells, respectively.

alone is 90%. Errors in normalization can occur when the housekeeping gene used as a normalizing factor is regulated slightly, as is the case for GAPDH (258). Systems in which congenic mice, differing only in the expression of certain allotypic markers on the surface of leukocytes, such as CD45.1/CD45.2 and Thy1.1/Thy1.2, are used separately as donors and recipients allow for direct and easy quantification by flow cytometry of not only the number of total cells that are reconstituted but also the reconstitution percentage in any subset (282). Unfortunately, because SAMP1/YitFc and AKR express identical allotypes of these markers (data not shown) and because CD45.2-expressing mice are the only AKR mice commercially available, we were unable to employ this strategy to determine whether certain long-lived recipient-derived populations such as plasma cells and macrophages persisted in either of our transplant recipient groups.

*Ileitis phenotype tracks with SAMP1/YitFc host/epithelium, not SAMP1/YitFc bone marrow*

Inflammation severity was assessed in AKR BM → SAMP and SAMP BM → AKR mice 6 weeks post-transplant using the standardized histologic scoring system discussed in Chapters 3 and 4. AKR BM → SAMP mice exhibited a trend toward slightly higher

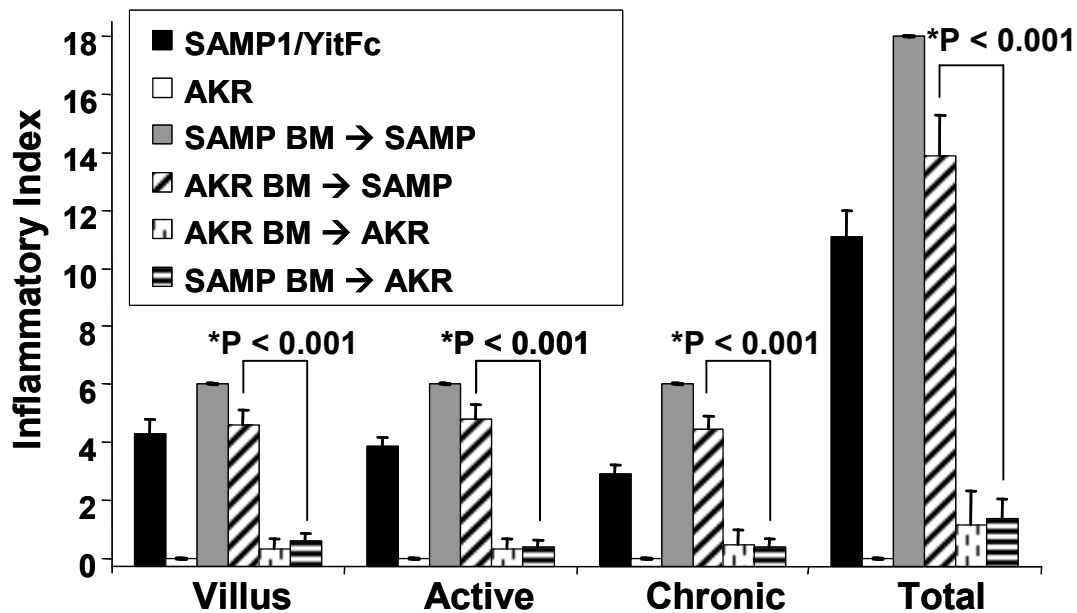


**Figure 5.2:** Comparison of ileitis severity in SAMP1/YitFc (n=7), AKR (n=5), SAMP BM → SAMP (n=5), AKR BM → SAMP (n=10), AKR BM → AKR (n=3) and SAMP BM → AKR (n=10) mice. Ileal from mice receiving bone marrow transplants were assessed for disease severity 6 weeks after irradiation and transplantation. \*Significant difference in inflammatory score between SAMP BM → AKR and AKR BM → SAMP mice.

levels of overall inflammation (total inflammatory score,  $14 \pm 1$ , mean  $\pm$  SEM) compared to native SAMP1/YitFc mice ( $11 \pm 1$ ) (Figure 5.2). The transplantation procedure itself may increase the severity of SAMP1/YitFc ileitis, as irradiated SAMP1/YitFc mice reconstituted with SAMP1/YitFc bone marrow (SAMP BM → SAMP) possessed significantly higher ileal inflammatory scores ( $18 \pm 0$ ) compared to native SAMP1/YitFc mice. SAMP BM → SAMP ileitis was not significantly more severe than AKR BM → SAMP ileitis. Furthermore, the inflammatory scores in AKR BM → SAMP ilea for all 3 individual histologic indices, including architectural destruction, active inflammation, and chronic inflammation, were comparable to scores from native SAMP1/YitFc mice. In contrast, SAMP BM → AKR mice developed only mild, if any, inflammation ( $1.4 \pm 0.7$ ), comparable to levels seen in irradiated AKR mice reconstituted with AKR bone

marrow ( $1.2 \pm 1.2$ ) suggesting the primary susceptibility leading to ileitis in SAMP1/YitFc mice originates from a non-hematopoietic source. Ileal inflammatory scores from either AKR BM  $\rightarrow$  SAMP or SAMP BM  $\rightarrow$  AKR mice at 12 weeks post transplant followed a similar pattern, with AKR BM  $\rightarrow$  SAMP mice exhibiting severe ileitis ( $16 \pm 1$ ) and 4 out of 5 SAMP BM  $\rightarrow$  AKR mice developing mild if any inflammation ( $1.5 \pm 0.9$ ). Interestingly, the fifth mouse in this 12 week SAMP BM  $\rightarrow$  AKR cohort developed severe inflammation (total inflammatory score, 18). Even with this mouse, the scores in the SAMP BM  $\rightarrow$  AKR at 12 weeks post transplant were not significantly different from SAMP BM  $\rightarrow$  AKR scores at 6 weeks post-transplant and were significantly lower than 12 week post-transplant AKR BM  $\rightarrow$  SAMP scores.

The ileitis in AKR BM  $\rightarrow$  SAMP mice 6 weeks post-transplant was histopathologically similar to that seen in native SAMP1/YitFc mice (Figure 5.3). Both AKR BM  $\rightarrow$  SAMP and native SAMP1/YitFc ileum had thickening of the muscularis layer and dense inflammatory infiltrates composed of both acute and chronic inflammatory cells throughout the villi and within the submucosae. Additionally, several epithelial abnormalities seen in SAMP1/YitFc mice were also seen in AKR BM  $\rightarrow$  SAMP mice, including villus blunting, crypt hypertrophy and elongation, and abnormal hypertrophy and hyperplasia of Paneth cells.

The presence of severe ileitis in SAMP1/YitFc mice reconstituted with AKR bone marrow, but not in AKR mice reconstituted with SAMP1/YitFc bone marrow, demonstrates that the primary factor responsible for the induction of ileitis in SAMP1/YitFc mice originates within a non-hematopoietic tissue. The finding that AKR BM  $\rightarrow$  SAMP mice exhibit disease as late as 12 weeks after transplant, a time at which



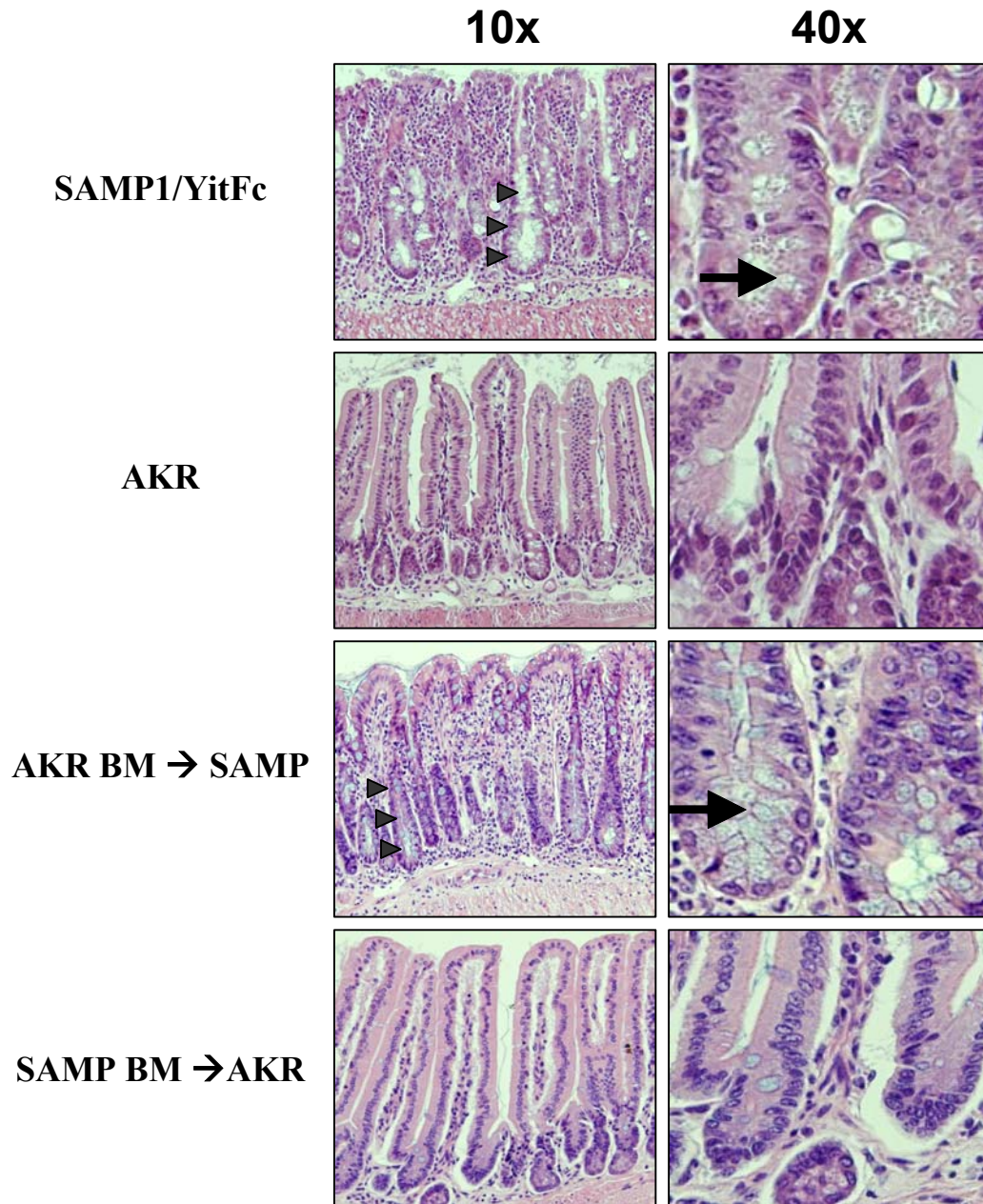


**Figure 5.3:** Low and high power views of H+E stained ileal sections from SAMP1/YitFc and AKR BM → SAMP mice display large inflammatory infiltrates and epithelial abnormalities including villus blunting, crypt hypertrophy and elongation (arrow heads), and paneth cell hyperplasia (arrows). In contrast, sections from AKR and SAMP BM → AKR mice display normal ileal architecture.

even many of the longest-lived radiation-resistant leukocytes are likely to have been cleared, strongly suggests that all of the inflammatory responses in these mice are orchestrated by the transplanted AKR-derived cells. Since bone marrow transplantation

was not attempted in SAMP1/YitFc mice less than 4 weeks of age prior to the onset of ileitis, whether AKR hematopoietic cells are as capable as SAMP1/YitFc cells in terms of initiating the very early stages of disease was not directly tested.

Based on this finding, the overactive immune responses seen in SAMP1/YitFc mice, including the previously described increased production of Th1 cytokines by SAMP1/YitFc T cells (186) and the expansion of pro-inflammatory B cells described in Chapter IV, are likely a downstream consequence of this as yet unknown precipitating factor and not the primary cause themselves. As a corollary, this finding also establishes that AKR hematopoietic cells transplanted into SAMP1/YitFc do not prevent ileitis, confirming the results discussed in Chapter III suggesting that SAMP1/YitFc ileitis is not caused by defects in SAMP1/YitFc regulatory T cell function.

*SAMP1/YitFc and AKR BM → SAMP mice exhibit epithelial barrier dysfunction*

To investigate whether epithelial dysfunction may be responsible for the non-hematopoietic ileitis susceptibility trait in SAMP1/YitFc mice, ileal epithelial permeability to charged ions was measured in ilea from SAMP1/YitFc, AKR, AKR BM → SAMP, and SAMP BM → AKR mice using a transepithelial electrical resistance (TEER) assay (138) (Figure 5.4). While ilea from AKR mice maintained their baseline electrical resistance after 1 hour of culture ( $\Delta\text{TEER}$  at 1 hour,  $60 \pm 100 \Omega/\text{mm}^2$ , mean  $\pm$  SEM), SAMP1/YitFc ilea exhibited a substantial drop in TEER during the same time period ( $-250 \pm 50 \Omega/\text{mm}^2$ ), suggesting that SAMP1/YitFc epithelium may not be able to maintain an effective permeability barrier. Ileal from AKR BM → SAMP mice also exhibited a decrease in electrical resistance at 1 hour ( $-170 \pm 30 \Omega/\text{mm}^2$ ), whereas SAMP

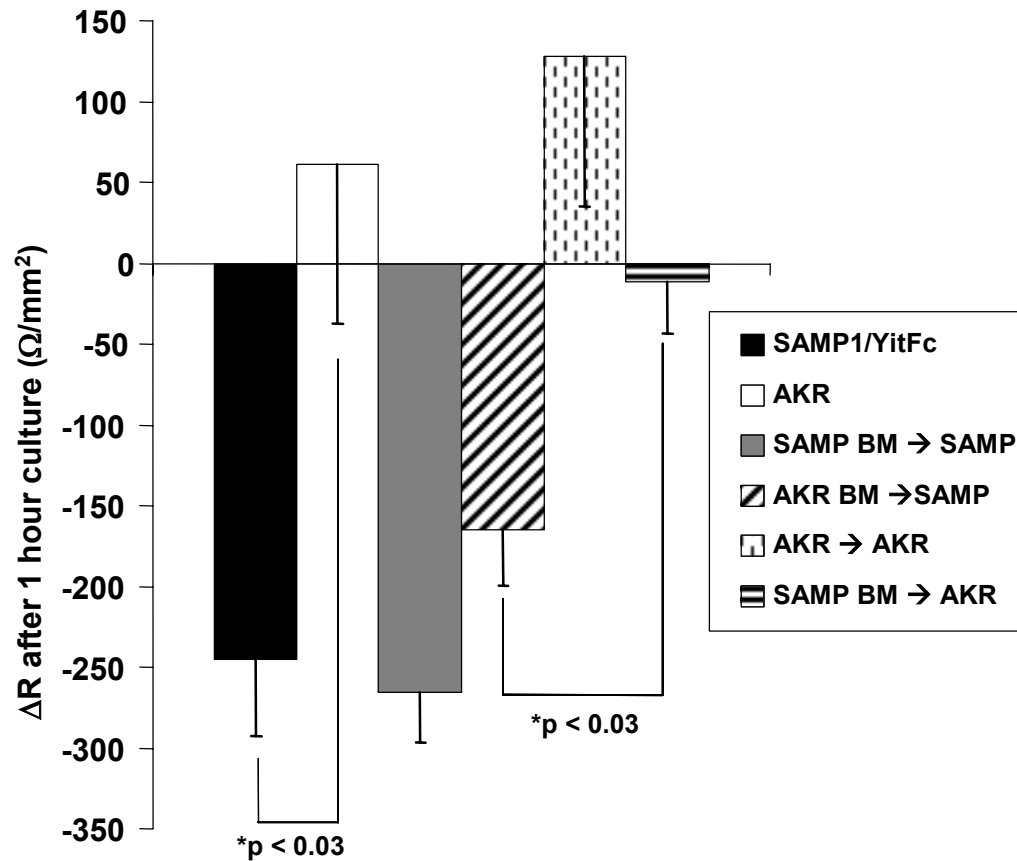


**Figure 5.4:** Transepithelial electrical resistance assays on ilea from SAMP1/YitFc (n=8), AKR (n=8), SAMP BM → SAMP (n=5), AKR BM → SAMP (n=4), AKR BM → AKR (n=3) and SAMP BM → AKR (n=4) mice. A section of ileum from each mouse was placed in a modified transwell insert with the mucosal surface facing the upper chamber, and an ohmmeter was used to measure the electrical resistance across the ileal section both immediately after harvesting and following 1 hour of culture at 37° C. Ileal from SAMP1/YitFc, SAMP BM → SAMP, and AKR BM → SAMP mice exhibited considerable decreases in electrical resistance indicative of increased epithelial permeability after 1 hour of culture, whereas ilea from AKR, AKR BM → AKR, and SAMP BM → AKR mice maintained an effective epithelial resistance barrier.

BM → AKR ilea maintained their baseline electrical resistance levels ( $-10 \pm 30 \Omega/\text{mm}^2$ ), suggesting that the epithelial permeability defect in SAMP1/YitFc mice is not dependent upon the specific factors produced preferentially by SAMP1/YitFc hematopoietic cells.

To examine epithelial permeability *in vivo* and to determine the specific sites along the gastrointestinal (GI) tract that may display an epithelial permeability defect in SAMP1/YitFc and AKR BM → SAMP mice, we gave AKR BM → SAMP and SAMP

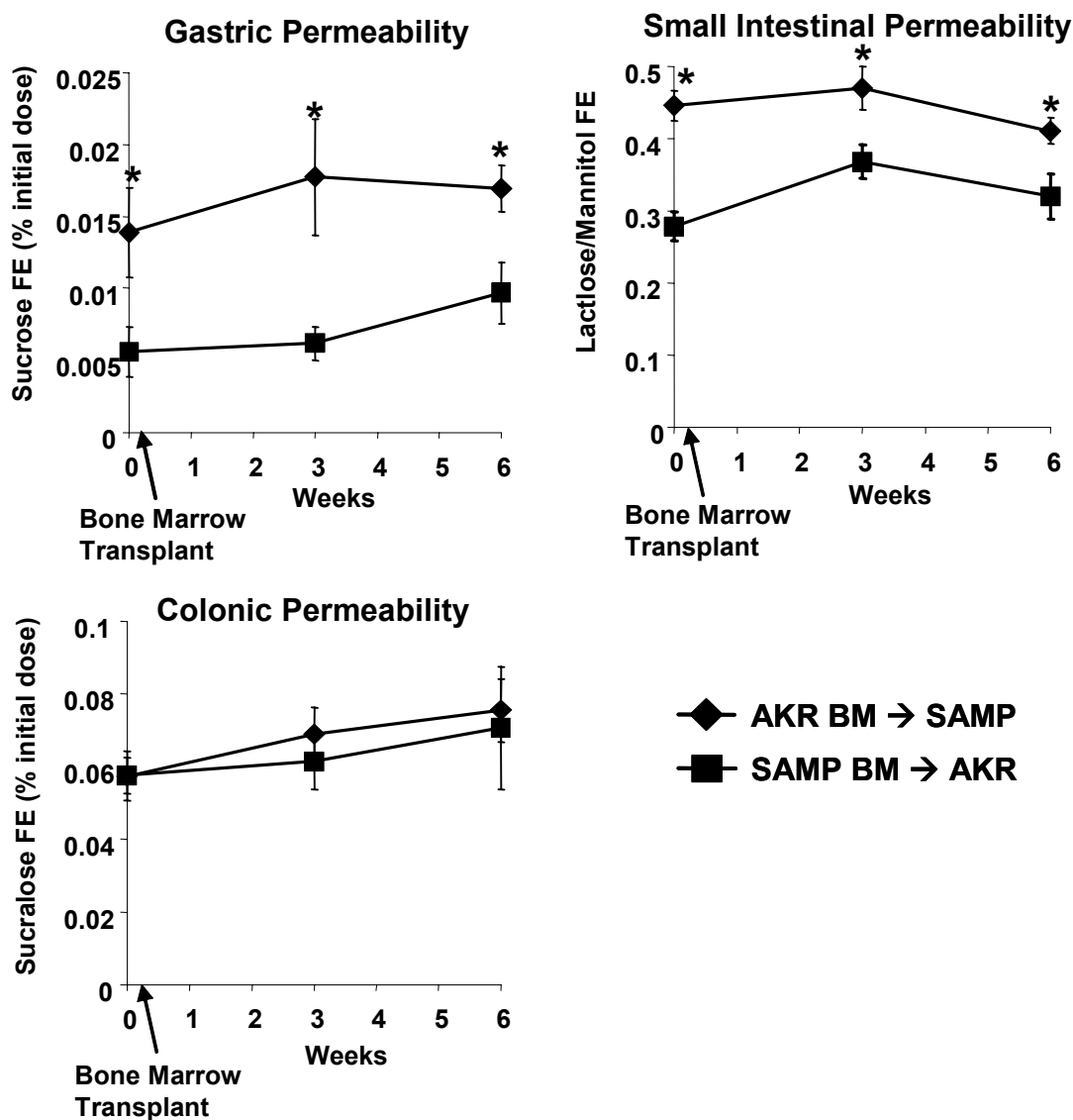


**Figure 5.5:** *In vivo* permeability assays measuring permeability to solutes in spatially distinct regions of the gastrointestinal tract of AKR BM → SAMP (◆) (n=6) and SAMP BM → AKR (■) (n=6) mice. Mice were fasted and orally gavaged with specific disaccharides that are absorbed by epithelial cells or broken down at specific sites within the lumen of the gastrointestinal tract. The fractional urinary excretion of sucrose (left) and sucralose (right) were used as measures of gastric and colonic epithelial permeability, respectively, whereas the ratio of the fractional urinary excretion of lactulose to mannitol (middle) was used as a measure of small intestinal permeability. The fractional urinary excretions displayed at time 0 were collected prior to irradiation and bone marrow transplantation and thus represent the permeability of native SAMP1/YitFc (◆) and AKR (■) mice in each of these tissues. The remaining data represents permeability at 3 and 6 weeks following bone marrow transplantation. \*Significantly increased ( $P < 0.05$ ) compared to SAMP BM → AKR mice.

BM → AKR mice an orogastric gavage of a disaccharide probe containing sucrose, lactulose, mannitol, and sucralose before and for several weeks following bone marrow

transplantation. We then analyzed the fractional urinary excretion (FUE) of these sugars in the 24 hour period following probe administration to determine epithelial permeability in specific regions in the GI tract as previously described (281). Prior to receiving irradiation and bone marrow transplant, SAMP1/YitFc mice (AKR BM → SAMP, time 0) had elevated lactulose to mannitol FUE ratios relative to AKR mice (SAMP BM → AKR, time 0) (Lactulose FUE/Mannitol FUE,  $0.44 \pm 0.02$  versus  $0.28 \pm 0.02$ , mean  $\pm$  SEM), indicative of increased small intestinal epithelial permeability in SAMP1/YitFc mice (Figure 5.5, top right panel). AKR BM → SAMP mice also displayed increased epithelial permeability in the small intestine relative to SAMP BM → AKR mice both 3 weeks ( $0.47 \pm 0.03$  versus  $0.37 \pm 0.02$ , mean  $\pm$  SEM) and 6 weeks ( $0.41 \pm 0.02$  versus  $0.32 \pm 0.03$ ) post-transplant. Additionally, SAMP1/YitFc mice displayed increased gastric epithelial permeability relative to AKR mice, as measured by sucrose FUE (sucrose FUE,  $0.014 \pm 0.003\%$  versus  $0.005 \pm 0.002\%$ ) (Figure 5.5, left panel). AKR BM → SAMP mice also exhibited increased gastric epithelial permeability relative to SAMP BM → AKR mice both 3 weeks ( $0.018 \pm 0.004\%$  versus  $0.006 \pm 0.001\%$ ) and 6 weeks ( $0.017 \pm 0.002\%$  versus  $0.010 \pm 0.002\%$ ) after transplantation. In contrast, no differences were seen in FUE of sucralose, an indicator of colonic permeability, among SAMP1/YitFc, AKR, AKR BM → SAMP, and SAMP → AKR mice (Figure 4, right panel).

The lactulose:mannitol ratios found in normal AKR mice are similar to those reported in other wild-type mouse strains and in normal rat intestine (137;281). The percentage increase in SAMP1/YitFc and AKR BM→ SAMP lactulose:mannitol ratios relative to AKR and SAMP BM → AKR ratios ranged from 27 to 57%. This range of permeability

increase is nearly identical to what is seen when rats are treated with non-steroidal inflammatory agents such as aspirin and indomethacin, drugs that produce significant intestinal damage through mechanisms involving increased epithelial permeability (281). Therefore the magnitude of the barrier defect in SAMP1/YitFc and AKR BM → SAMP mice is likely sufficient to allow inflammation development.

The epithelial barrier defect seen in SAMP1/YitFc and AKR BM → SAMP mice suggests that epithelial cell dysfunction may be primarily responsible for the development of ileitis in this model. SAMP1/YitFc ileal possess many abnormalities in epithelial appearance and composition that have been previously reported, including the observations that crypt elongation and hypertrophy and increased epithelial mitotic figures and proliferation are prominent features of the ileitis phenotype (241). Further studies have demonstrated markedly expanded populations of Paneth cells and goblet cells in SAMP1/YitFc ileum (186), similar to epithelial phenotype changes observed in human Crohn's (283). Recent studies by Vidrich A and Cohn S.M., et. al. (submitted) have identified more phenotypic abnormalities of SAMP1/YitFc epithelium, including expansion of the replicative zone; aberrant rearrangement of Paneth, Goblet, and intermediate cells along the crypt-villus junction in inflamed areas; and global enhancement of crypt stem cell survival and crypt regeneration throughout the small intestine due to increased circulating growth factor expression.

Since epithelial barrier dysfunction can be induced by pro-inflammatory cytokines (139), it remains to be definitively proven whether the epithelial permeability defect observed in SAMP1/YitFc mice is a cause or a consequence of ileitis in this model. However, this permeability defect is not dependent upon strain-specific pro-inflammatory

properties of SAMP1/YitFc leukocytes, as AKR BM → SAMP mice also exhibit this epithelial permeability defect. Additionally, decreased barrier function was also observed in gastric epithelium even though the stomach is not inflamed in SAMP1/YitFc mice, suggesting that barrier dysfunction may be a primary characteristic of much of the epithelium lining the GI tract in SAMP1/YitFc mice. Interestingly, colonic epithelium exhibited normal barrier function when compared with wildtype mice, a finding that may explain the lack of colonic inflammation in this model. In a parallel study conducted by Scott K.G-E. and Reuter B.K., et. al. (submitted), significant epithelial barrier dysfunction was found even in 4 week-old SAMP1/YitFc mice, an age by which significant ileal inflammation has not yet developed, providing the most conclusive evidence in favor of the primacy of barrier dysfunction as an etiologic agent in SAMP1/YitFc ileitis. Scott and Reuter also observed that changes in epithelial cell composition, including goblet and Paneth cell expansion, were present in mice by 4 weeks of age prior to disease onset, suggesting that changes in epithelial composition are also not a consequence of inflammation but rather a primary feature of SAMP1/YitFc mice. In the same report, studies using transmission and scanning electron microscopy revealed no ultrastructural differences between SAMP1/YitFc versus AKR ileum, suggesting that decreased density of tight junctional strands, which can lead to “loosening” of paracellular permeability pathways (32), is not responsible for the high permeability of SAMP1/YitFc ileum. Further, there were no differences between SAMP1/YitFc versus AKR ileum in the localization of zonula occludens-1 the scaffolding protein that connects tight junctional complexes with the actin cytoskeleton, suggesting that unlike barrier dysfunction produced by infection in vivo (137) or

inflammatory mediators in vitro (135), the high epithelial permeability in SAMP1/YitFc mice may not be caused by reorganization of cytoskeletal connections with tight junctions, but rather by claudin isoform-specific alterations in the composition of the tight junctions themselves (Scott K.G-E., Reuter B.K., et. al., submitted).

*Epithelial cell expression of Ppar $\gamma$  is decreased in SAMP1/YitFc versus AKR mice*

Genetic linkage studies in which SAMP1/YitFc mice were outcrossed to AKR mice have revealed that the SAMP1/YitFc ileitis phenotype segregates with the presence of specific allelic polymorphisms on chromosome 6 that differ in SAMP1/YitFc versus AKR alleles (Sugawara, Gastroenterology, 2004). These polymorphisms occur in the promoter region of the gene encoding Ppar $\gamma$ , a transcription factor that can inhibit pro-inflammatory gene transcription pathways (238). Two isoforms of Ppar $\gamma$  have been identified, and while Ppar $\gamma$ 2 is primarily expressed by adipose tissue, Ppar $\gamma$ 1 is widely expressed by many cells including leukocytes (284) and intestinal epithelial cells (285). In order to ascertain whether aberrant expression of Ppar $\gamma$ 1 in either leukocytes or non-hematopoietic tissues is linked to the SAMP1/YitFc ileitis phenotype, the expression of Ppar $\gamma$ 1 was ascertained in whole ileum, jejunum, and liver and in isolated ileal epithelial cells, splenocytes, and MLN lymphocytes. Comparison of Ppar $\gamma$ 1 expression in whole tissues from 2 separate cohorts of SAMP1/YitFc, AKR, and C57BL/6 mice (Figure 5.6A and data not shown) revealed that AKR mice exhibited substantially higher Ppar $\gamma$ 1 expression in the ileum (4 -to 6-fold) and jejunum (10- to 20-fold) than that seen in SAMP1/YitFc tissues. C57BL/6 mice possess a Ppar $\gamma$  allele that appears to be identical to the SAMP1/YitFc allele, and likewise displays decreased Ppar $\gamma$  expression in the ileum



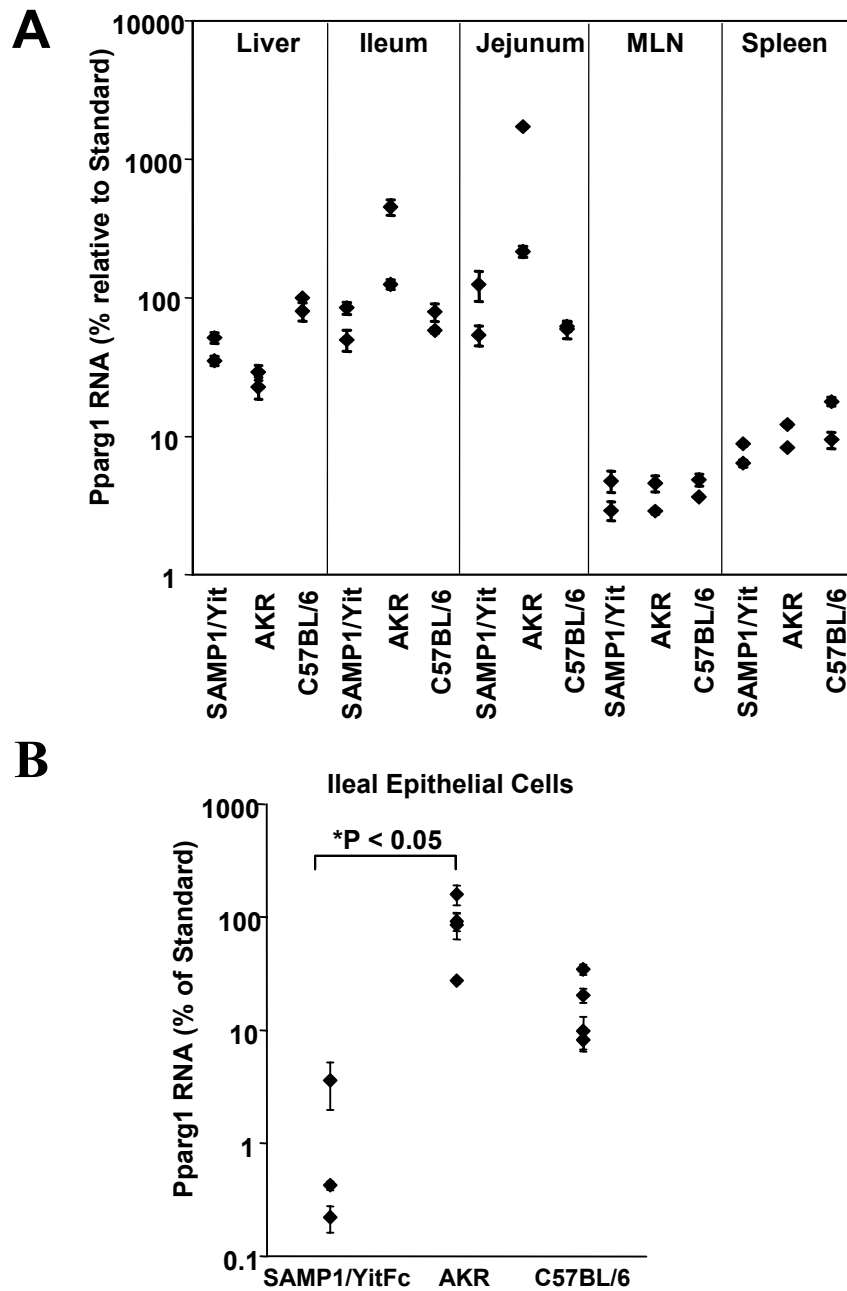


**Figure 5.6:** Expression of Pparg 1 is decreased in an epithelial specific fashion in SAMP1/YitFc versus wildtype AKR or C57BL/6 mice. Expression in whole liver, ileum, and jejunum (n=2, each) in one of two representative experiments and in isolated MLN lymphocytes (n=2), splenocytes (n=2), and ileal epithelial cells (n=3 to 4) was determined by real-time reverse-transcriptase PCR utilizing a forward primer within exon A1 and a reverse primer spanning exons A1 and A2, creating a PCR product specific to RNA of Pparg isoform 1. Amplification was quantified using SYBR Green incorporation. Values are expressed as % of expression (mean  $\pm$  SEM of 3 replicates) relative to the C57BL/6 liver sample used to generate the standard curve for all experiments. Average differences for samples within each tissue in 18s rRNA, a marker of total RNA concentration in each sample, were less than 2 fold, and normalization to 18s rRNA values did not significantly alter the results shown.

and jejunum relative to expression in AKR tissues. In contrast, MLN lymphocyte and splenocyte expression of Ppar $\gamma$ 1 was similar in all strains studied, indicating that the differences in Ppar $\gamma$ 1 expression in the ileum and jejunum may be due to differences in expression by non-leukocyte sources. Therefore, we examined Ppar $\gamma$ 1 expression by isolated ileal epithelial cells from each of these strains. SAMP1/YitFc epithelial cells expressed significantly lower levels of Ppar $\gamma$ 1 compared to AKR epithelial cells, with the average expression in AKR being 64-fold higher (Figure 5.6B). C57BL/6 epithelial cells express intermediate levels of Ppar $\gamma$ 1 compared to expression in the other two strains, suggesting that factors in addition to the specific Ppar $\gamma$  allele present may lead to decreased Ppar $\gamma$ 1 expression in SAMP1/YitFc epithelial cells. This finding implicates decreased epithelial expression of Ppar $\gamma$ 1 as one of the potential non-hematopoietic factors leading to the development of SAMP1/YitFc ileitis.

Ppar $\gamma$  is a ligand-activated member of the nuclear hormone receptor family of transcription factors that activates transcription of genes involved in lipid metabolism and also mediates anti-inflammatory functions through the inhibition of pro-inflammatory NF- $\kappa$ B pathways. The mechanism by which Ppar $\gamma$  mediates repression of NF- $\kappa$ B has not been firmly established, but may involve competitive binding of coactivating molecules, direct physical interactions with NF- $\kappa$ B, or interference with MAP kinase function upstream of NF- $\kappa$ B activation (238). Ppar $\gamma$  expression is decreased in intestinal tissue from some IBD patients (237), and DSS-induced experimental colitis is markedly reduced in animals receiving an adenovirus construct encoding the Ppar $\gamma$  gene (239). Given that increases in epithelial permeability have been shown to require NF- $\kappa$ B

activation (135), the epithelial barrier dysfunction in SAMP1/YitFc mice might be explained by a model in which decreased Ppar $\gamma$  expression leads to lack of inhibition and excessive activation of NF- $\kappa$ B pathways in SAMP1/YitFc ileal epithelial cells, which in turn leads to dysregulation of tight junction formation and composition. Since the functions of NOD2 involve alterations of NF- $\kappa$ B activation and signaling pathways and NF- $\kappa$ B overexpression is part of the pathophysiology of human Crohn's disease (43), a similar mechanism leading to primary epithelial barrier dysfunction may apply to Crohn's patients with mutations in NOD2.

*Size and pathogenicity of MLN lymphocyte subsets determined by inflammatory status of host*

As demonstrated in Chapters III and IV, SAMP1/YitFc MLN contain increased percentages of many lymphocyte subpopulations relative to AKR MLN. In 6-12 week old mice used as bone marrow donors, SAMP1/YitFc MLN had increased percentages of IgA<sup>+</sup> B cells ( $8.2 \pm 0.8\%$  versus  $2.6\% \pm 0.3\%$ , mean  $\pm$  SEM) and CD4<sup>+</sup> T cells expressing the activation marker CD69 ( $29 \pm 2\%$  versus  $13 \pm 1\%$ , mean  $\pm$  SEM) relative to AKR MLN (Figure 5.7A and B). Interestingly, MLN from AKR BM  $\rightarrow$  SAMP mice contained elevated percentages of CD4<sup>+</sup> T cells expressing CD69 ( $31 \pm 2\%$ ) and IgA<sup>+</sup> B cells ( $12 \pm 1\%$ ) similar to the percentages seen in native SAMP1/YitFc MLN, even though the vast majority of MLN lymphocytes in AKR BM  $\rightarrow$  SAMP mice are derived from AKR bone marrow. Likewise, MLN from SAMP BM  $\rightarrow$  AKR contained low percentages of CD4<sup>+</sup> T cells expressing CD69 and IgA<sup>+</sup> B cells, similar to the size of these populations in native AKR mice, even though MLN lymphocytes in SAMP BM  $\rightarrow$

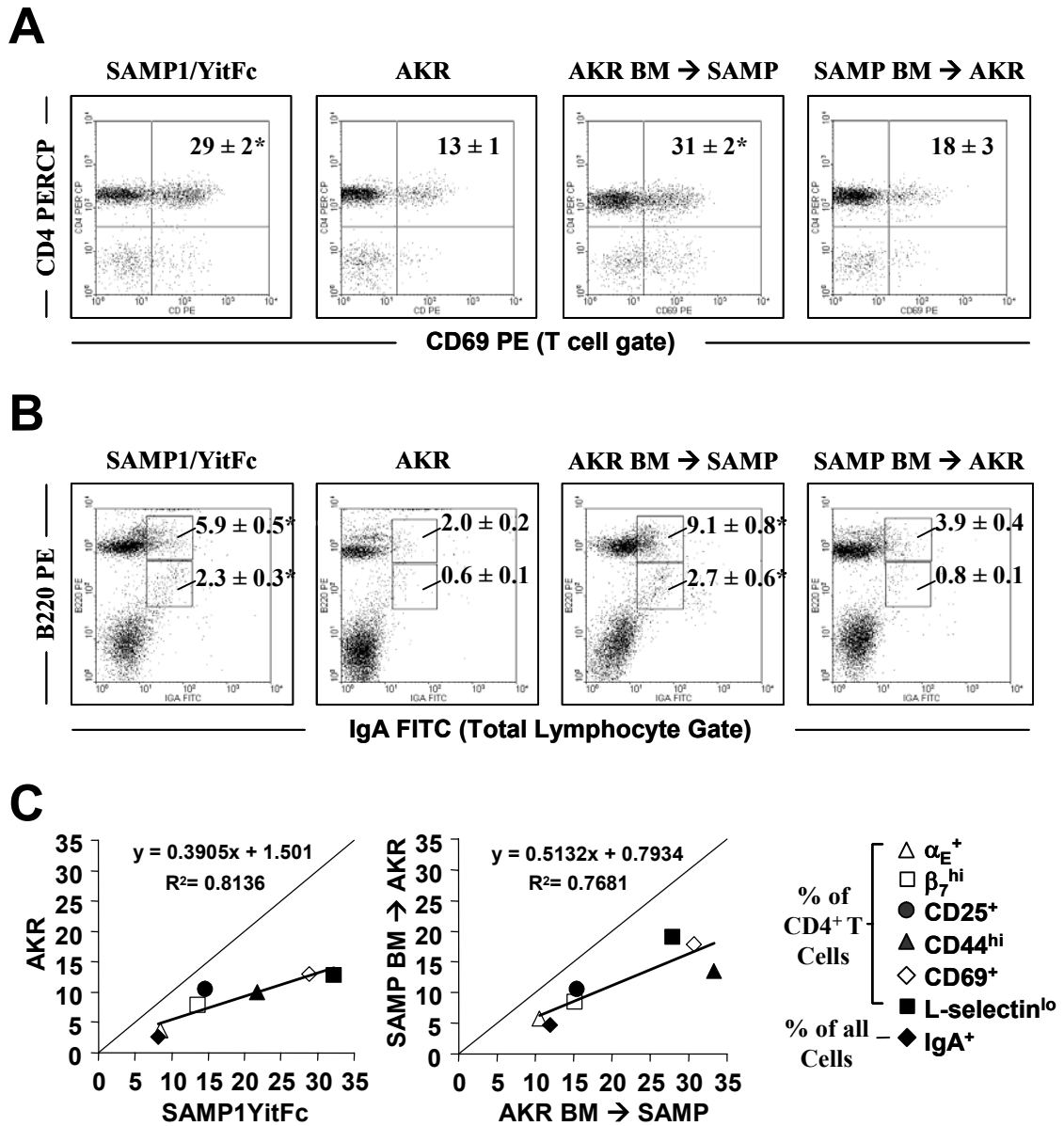


**Figure 5.7:** Flow cytometry of MLN lymphocyte populations in SAMP1/YitFc (n=3), AKR (n=3), AKR BM → SAMP (n=7) and SAMP BM → AKR (n=6) mice. Representative T cell-gated (CD4<sup>+</sup>CD8<sup>+</sup>) dotplots of CD4 (y) versus CD69 (x) expression, with average percentages of CD4<sup>+</sup> T cells that are CD69<sup>+</sup> (mean ± SEM) (A). Representative dotplots of B220 (x) versus IgA (y) expression, with averages of IgA<sup>+</sup>B220<sup>hi</sup> mature B cells and IgA<sup>+</sup>B220<sup>int</sup> plasmablasts as a percentage of all lymphocytes (mean ± SEM) (B). \*Significantly increased (P < 0.05) compared to AKR or SAMP BM → AKR mice. Plot showing the size of lymphocyte subsets that were significantly increased in SAMP1/YitFc (x) versus AKR (y) mice, including the percentage of IgA<sup>+</sup> cells and the percentage of CD4<sup>+</sup> T cells that were  $\alpha_E^+$ ,  $\beta_7^{hi}$ , CD25<sup>+</sup>, CD44<sup>hi</sup>, CD69<sup>+</sup>, and L-selectin<sup>lo</sup> (C, left). A second plot was made using the sizes of these subsets in SAMP BM → AKR (y) and AKR BM → SAMP (x) mice (C, right). The slopes of the best-fit lines through the points in the two plots, determined through linear regression, were not significantly different.

AKR mice are derived from SAMP1/YitFc bone marrow. Furthermore, most of the other lymphocyte populations that are increased in SAMP1/YitFc relative to AKR MLN were also increased in AKR BM  $\rightarrow$  SAMP MLN relative to SAMP BM  $\rightarrow$  AKR MLN, including the percentage of CD4<sup>+</sup> T cells that are  $\beta_7$  integrin<sup>hi</sup> ( $15 \pm 1\%$  versus  $8 \pm 2\%$ ),  $\alpha_E$  integrin<sup>+</sup> ( $11 \pm 1\%$  versus  $5.8 \pm 0.7\%$ ), CD25<sup>+</sup> ( $15 \pm 1\%$  versus  $11 \pm 2\%$ ), L-selectin<sup>lo</sup> ( $33 \pm 6\%$  versus  $14 \pm 2\%$ ), and CD44<sup>hi</sup> ( $28 \pm 2$  versus  $19 \pm 3\%$ )(Figure 5C). Plotting the size of each of these lymphocyte populations in SAMP1/YitFc on the y-axis relative to the size in AKR mice on the x-axis, the best-fit linear regression through these points has a similar slope that is not significantly different from the linear regression of sizes of the same populations in a plot of AKR BM  $\rightarrow$  SAMP on the x-axis versus SAMP BM  $\rightarrow$  AKR on the y-axis (Figure 5.7c). In contrast, the slope of the regression line through these points when SAMP BM  $\rightarrow$  AKR is plotted on the x-axis and AKR BM  $\rightarrow$  SAMP size is plotted on the y-axis is significantly different ( $p < 0.05$ ) compared to the slope of the regression line on the SAMP1/YitFc (x) versus AKR (y) plot. These data strongly suggest that the overall MLN composition of AKR BM  $\rightarrow$  SAMP mice closely resembles that seen in SAMP1/YitFc mice, despite the fact that most MLN cells in AKR BM  $\rightarrow$  SAMP are derived from AKR mice. Likewise, the MLN composition of SAMP BM  $\rightarrow$  AKR mice closely resembles that seen in AKR mice.

Previous studies have shown that SAMP1/YitFc MLN CD4<sup>+</sup> T cells express more IFN- $\gamma$  and TNF- $\alpha$  than do AKR MLN CD4<sup>+</sup> T cells (186) and adoptively transfer more severe ileitis to severe combined immunodeficient (SCID) mice as shown in chapter III. To test whether the above redistribution of MLN lymphocyte subset size according to recipient inflammatory status is accompanied by a change in the inflammatory potential

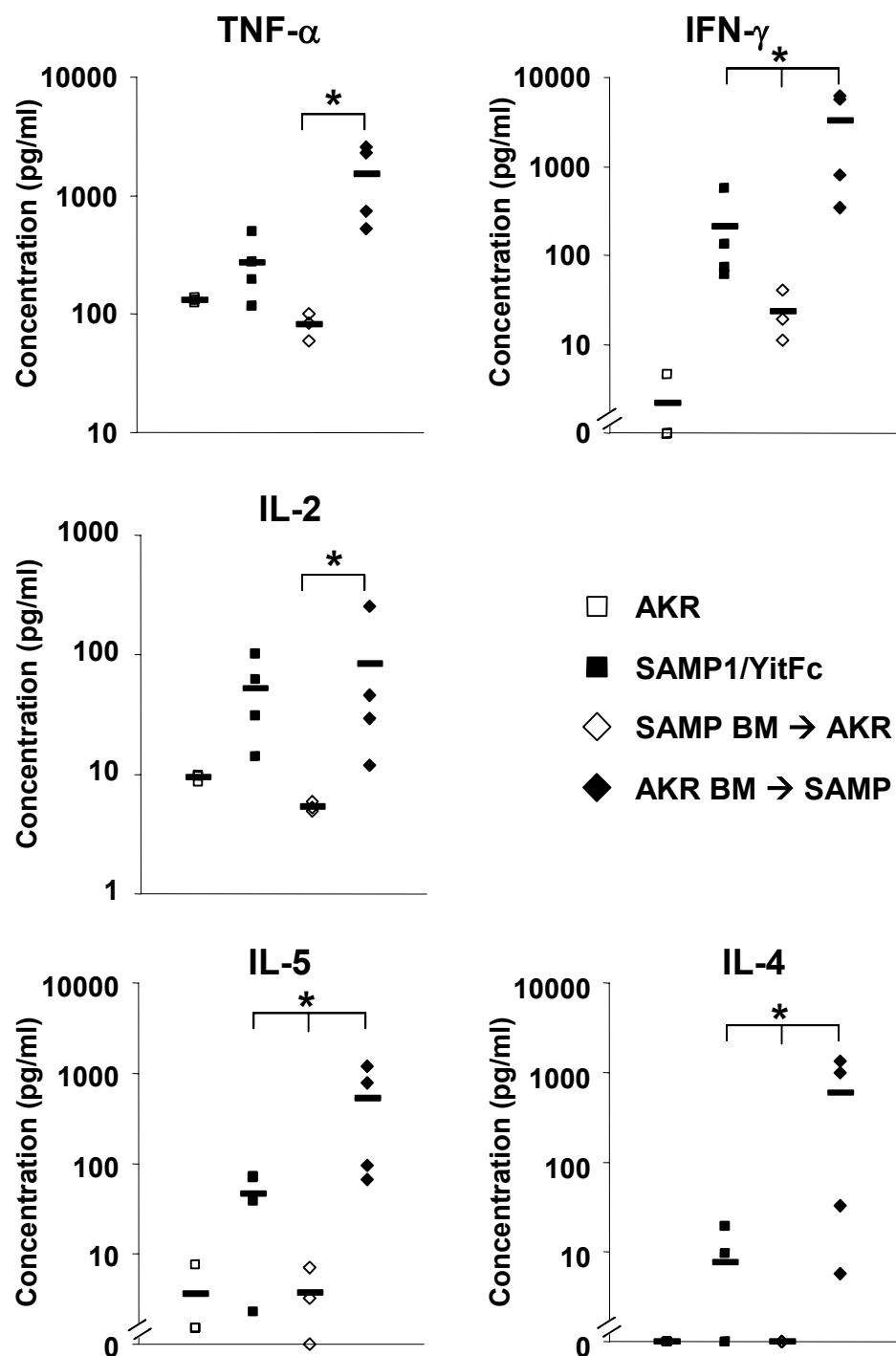


**Figure 5.8:** Levels of secreted TNF- $\alpha$ , IFN- $\gamma$ , IL-2, IL-4, and IL-5 measured in triplicate by cytometric bead array, from 48 hour cultures of AKR (open squares, n=3), SAMP1/YitFc (closed squares, n=4), SAMP BM  $\rightarrow$  AKR (open diamonds, n=3), and AKR BM  $\rightarrow$  SAMP (closed diamonds, n=4) MLN unfractionated CD4<sup>+</sup> T cells ( $10^5$ /well), stimulated with immobilized anti-CD3 antibody. Values for individual mice are shown along with the mean value (-) in each group. \*Significantly lower than levels produced by AKR BM  $\rightarrow$  SAMP cells ( $P < 0.05$ ).

of SAMP1YitFc- and AKR-derived CD4<sup>+</sup> T cells, cytokine expression by SAMP1/YitFc, AKR, and transplant recipient MLN CD4<sup>+</sup> T cells was measured by culturing these cells for 48 hours in the presence of anti-CD3 stimulation. Consistent with previous findings, SAMP1/YitFc T cells exhibit an overall pattern of significantly higher levels of cytokine production when compared to the cytokine profile of AKR cells by two-way ANOVA (Figure 5.8). Compared to SAMP BM → AKR cells, AKR BM → SAMP CD4<sup>+</sup> T cells produced significantly more TNF- $\alpha$  and IFN- $\gamma$ , with the average expression being greater than 18- and 130-fold higher, respectively, in AKR BM → SAMP mice. AKR BM → SAMP cells also produce 15-fold higher levels of IL-2 than that produced by SAMP BM → AKR cells, suggesting that AKR BM → SAMP CD4<sup>+</sup> T cells may proliferate at a higher rate than SAMP BM → AKR cells. Further, whereas SAMP BM → AKR produce little or no IL-4 and IL-5, AKR BM → SAMP T cells produce significantly greater amounts of both of these cytokines, suggesting that T cells derived from AKR bone marrow are capable of orchestrating both the Th1 and Th2 inflammatory responses that have been observed in SAMP1/YitFc ileitis (216;244). Interestingly, AKR BM → SAMP CD4<sup>+</sup> T cells produce even higher levels of cytokines than native SAMP1/YitFc T cells, which may account for the increased inflammatory scores in AKR BM → SAMP versus native SAMP1/YitFc mice. While SAMP BM → AKR cells produce significantly higher IFN- $\gamma$  compared to levels produced by native AKR cells, overall differences in cytokine expression pattern between these two groups measured by two-way ANOVA were not significant.

When transplanted into SAMP1/YitFc mice, certain subpopulations of AKR MLN lymphocytes expand to approximate the sizes of these populations in SAMP1/YitFc mice.

Many of these subsets, including  $\alpha_E^+$  CD4<sup>+</sup> T cells and CD25<sup>+</sup> CD4<sup>+</sup> T cells may represent regulatory T cell populations as discussed in Chapter III. Therefore, like SAMP1/YitFc regulatory cells, AKR-derived regulatory cells in AKR BM  $\rightarrow$  SAMP mice appear to expand as part of a futile compensatory effort to curb ileal inflammation in SAMP1/YitFc mice.

In addition to regulatory cell expansion, some AKR-derived CD4<sup>+</sup> T cells in AKR BM  $\rightarrow$  SAMP mice also acquire increased pathogenicity, since they not only participate in the severe inflammation seen in AKR BM  $\rightarrow$  SAMP mice, but they also exhibit elevated pro-inflammatory cytokine production. This increased expression includes not only the classic Th1 cytokines TNF- $\alpha$  and IFN- $\gamma$ , but also the proliferation-inducing IL-2 as well as the Th2 cytokines IL-4 and IL-5. This pattern of inflammation induced through both Th1 and Th2 pathways is seen in SAMP1/YitFc mice as described above, and thus AKR-derived T cells appear to fully recapitulate both pro-inflammatory pathways when transplanted into SAMP1/YitFc mice.



## VI. Conclusions and Future Directions

### Conclusions

In chapter III, I demonstrate that the expansion of CD4<sup>+</sup> T cell and B cell MLN populations in the context of SAMP1/YitFc ileitis is due to increases in actively proliferating cells within this compartment compared to MLN lymphocyte proliferation in normal mice. CD4<sup>+</sup> T cell expansion occurs primarily within two subsets that both express high levels of adhesion molecules but may have opposing functions. One of these subsets expresses high levels of both the  $\alpha_4\beta_7$  and  $\alpha_4\beta_1$  integrins. The finding in other studies that combinatorial blockade of both of these  $\alpha_4$  integrins is required to decrease severity of ileitis produced by SAMP1/YitFc T cells (Rivera-Nieves, Olson, et.al., *J. Immunol.* In Revision) suggests that this subset may be the primary disease-producing subset in this model.

The second subset specifically expresses the  $\alpha_E\beta_7$  integrin and expresses a pattern of surface markers (CD25<sup>+</sup> CD45RB<sup>lo</sup> L-selectin<sup>lo</sup>) consistent with a regulatory cell phenotype. This subset expresses high levels of IL-10 and only low levels of pro-inflammatory cytokines and inhibits the proliferation of effector T cells *in vitro*, demonstrating that SAMP1/YitFc MLN  $\alpha_E\beta_7^+$  CD4<sup>+</sup> T cells are Treg (208). However, while SAMP1/YitFc Treg are capable of preventing colitis induced by transferring effector T cells into SCID mice, these Treg cannot prevent the development of ileitis either in the adoptive transfer model or in the SAMP1/YitFc mouse itself.

Chemotactic responsiveness and chemokine receptor expression studies indicate that MLN CD4<sup>+</sup> T cells are mainly responsive to chemokines that mediate homing to

lymphoid organs. In contrast, the SAMP1/YitFc  $\alpha_E\beta_7^+$  subset expresses high level of chemokine receptors that mediate trafficking to other sites. CCR8, which I show in unstimulated populations to be exclusively expressed by  $\alpha_E\beta_7^+$  CD4<sup>+</sup> T cells, may promote the migration of SAMP1/YitFc  $\alpha_E\beta_7^+$  CD4<sup>+</sup> T cells towards leukocyte populations present in Th1 inflammation (263), where the high level of ICAM-1 and LFA-1 expression we have also observed on  $\alpha_E\beta_7^+$  CD4<sup>+</sup> T cells may mediate cell contact-dependent regulatory functions. This unique chemokine receptor profile may be responsible for the decreased homing to the MLN by  $\alpha_E\beta_7^+$  CD4<sup>+</sup> T cells relative to effector CD4<sup>+</sup> T cells observed in *in vivo* cell tracking assays. Based on the finding from these assays that effector CD4<sup>+</sup> T cells preferentially home to the MLN following adoptive transfer, the relative lack of homing of  $\alpha_E\beta_7^+$  CD4<sup>+</sup> T cells to this site may partially explain why SAMP1/YitFc Treg do not inhibit the ileitis-producing functions of these cells. Taken together, the results presented in chapter III demonstrate that SAMP1/YitFc ileitis develops and persists in spite of the increased production of functional Treg populations within the MLN of SAMP1/YitFc mice.

In chapter IV, I have demonstrated that the expanded population of SAMP1/YitFc MLN B cells exhibits increased production of IgA leading to specific elevations in local and systemic levels of this isotype. The majority of IgA is derived from B2 B cells, which represent the predominant population of B cells in both SAMP1/YitFc and wildtype MLN. I have also shown that B cell expansion in SAMP1/YitFc MLN correlates with expansion of the  $\alpha_E\beta_7^+$  CD4<sup>+</sup> T cell subset and that B cells preferentially interact with this subset in MLN cell suspensions. While culture of SAMP1/YitFc MLN

B cells with  $\alpha_E\beta_7^-$  CD4<sup>+</sup> T cells leads to high levels of IgG2a and IgM production, B cells cultured with  $\alpha_E\beta_7^+$  CD4<sup>+</sup> T cells produced mostly IgA, demonstrating that  $\alpha_E\beta_7^+$  CD4<sup>+</sup> T cells may be responsible for driving the unique IgA phenotype seen in SAMP1/YitFc mice.

The number of MLN B cells correlates with severity of inflammation in SAMP1/YitFc host ileitis. Further, SAMP1/YitFc MLN B cells cotransferred with CD4<sup>+</sup> T cells increase the severity of overall ileitis in SCID mice by increasing both neutrophil and CD3<sup>+</sup> T cell infiltration. The increased neutrophil infiltration may be explained by increased immune complex formation due to the high levels of IgA seen in SCID mice cotransferred with B cells and T cells. SAMP1/YitFc B cells express GITRL and abrogate  $\alpha_E^+$  CD4<sup>+</sup> T cell regulatory function in vitro, providing a mechanism that not only explains the increased T cell proliferation seen in SCID mice adoptively transferred with both B cells and T cells, but may also explain the lack of Treg efficacy in preventing adoptively transferred ileitis, assuming native SCID APC can also express GITRL. Taken together, the results presented in chapter IV demonstrate the importance of T cell/B cell interactions and B cell function in the pathogenesis of SAMP1/YitFc ileitis.

In chapter V, I have demonstrated that the primary susceptibility leading to the development of ileitis in SAMP1/YitFc mice is derived from a non-hematopoietic source, as SAMP1/YitFc bone marrow progenitor cells do not transmit this ileitis phenotype when transplanted into AKR mice. Further, we have shown that hematopoietic cells from normal mice transplanted into SAMP1/YitFc mice can fully orchestrate this ileal inflammatory response in the presence of this non-hematopoietic susceptibility. AKR-derived lymphocytes present in SAMP1/YitFc MLN acquire surface phenotypes and

cytokine production profiles similar to cells seen in native SAMP1/YitFc, but not native AKR, mice. Thus, these AKR-derived hematopoietic cells undergo maturation and reeducation within the SAMP1/YitFc mouse such that T cells derived from these AKR cells gain the capacity to produce ileitis.

Both native SAMP1/YitFc mice and SAMP1/YitFc mice reconstituted with AKR bone marrow display defects in both *in vivo* and *ex vivo* epithelial barrier function. In addition, we have demonstrated an epithelial cell-specific defect in Ppar $\gamma$  expression in SAMP1/YitFc versus wildtype mice, which may lead to unopposed activation of pro-inflammatory gene transcription pathways in SAMP1/YitFc epithelial cells. Taken together, the results in chapter V demonstrate that dysfunctional properties of epithelial cells, and not intrinsic immunological defects, likely represent the etiologic cause of Crohn's-like ileitis in SAMP1/YitFc mice.

### **Model Explaining Disease Development in SAMP1/YitFc Mice**

The findings presented in this dissertation suggest a multi-step paradigm that may explain the development of ileitis not only in the SAMP1/YitFc model but perhaps in subsets of Crohn's patients as well (Figure 6.1). While several of the steps described in this model have not been directly substantiated and the precise mechanisms of some of the proposed signals have yet to be elucidated, this model may serve as a useful basis for designing future studies aimed at assessing the validity of this proposed sequence of events. In this model, the precipitating factors leading to the development of disease are the genetic predisposition and potentially other unknown factors that lead to decreased expression of Ppar $\gamma$  in ileal epithelial cells. Decreased Ppar $\gamma$  expression results

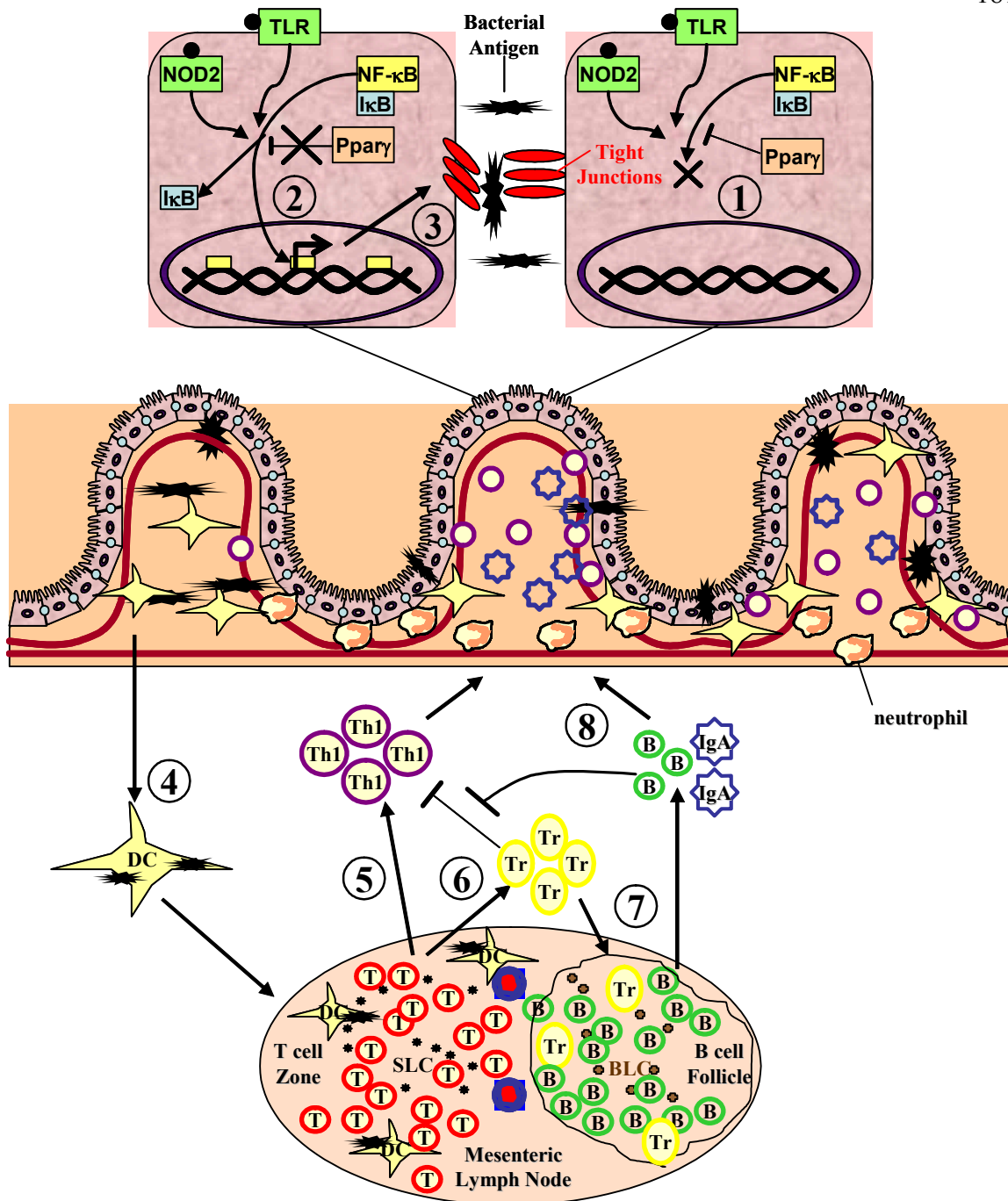


**Figure 6.1:** Model mechanism of SAMP1/YitFc ileitis development. In wildtype mice (1), epithelial NF-κB activation is prevented by Pparγ. In SAMP1/YitFc epithelium (2), decreased Pparγ expression leads to increased NF-κB-mediated transcription of many genes including those that increase epithelial permeability to bacterial antigen (3). This antigen is transported to the MLN (4) and likely presented to naïve T cells (T) by dendritic cells (DC). Induction of effector T cells (Th1) occurs, and these cells migrate to the intestine to promote chronic inflammation (5). Concomitantly, the MLN gives rise to increased regulatory T cells (Tr) (6), that inhibit Th1 cell functions and also migrate to B cell follicles to promote B cell (B) expansion and differentiation to IgA-producing cells (IgA) (7). These B cells inhibit regulatory T cell-mediated suppression of effector T cell function, and through immunoglobulin secretion lead to neutrophil accumulation and increases in active inflammation (8).

in decreased inhibition of NF- $\kappa$ B activation promoted by tonic signaling through Toll-like receptors and NOD2 (43). Increased gene transcription mediated by activated NF- $\kappa$ B results in increased expression of many proteins including those that can directly promote inflammation and leukocyte infiltration within the lamina propria (46) and those that disrupt cytoskeletal interactions with tight junction complexes resulting in decreased epithelial barrier function (135).

Increased epithelial permeability results in increased penetration of bacteria and/or bacterial antigens into sub-epithelial spaces where dendritic cells, present in large numbers specifically in the ileum (286), encounter this antigen and acquire a pro-inflammatory phenotype (287). These dendritic cells carry this antigen to the MLN, where interactions with MLN T cells result in the generation of the previously described pro-inflammatory Th1- and Th2-polarized T cells in SAMP1/YitFc MLN (186;244). These T cells, which may be identical to the  $\alpha_4\beta_1^{\text{hi}}$  and  $\alpha_4\beta_7^{\text{hi}}$  subset discussed above, use interactions between these integrins and their endothelial ligands, upregulated on SAMP1/YitFc ileal post-capillary venules, to migrate to the intestinal wall and initiate inflammatory lesion development (173).

The increased generation of polarized inflammatory cells is accompanied by increased generation of  $\alpha_E\beta_7^+$  CD4<sup>+</sup> regulatory T cells, which in turn drive the expansion of IgA-producing B cells. These regulatory cells are rendered incapable of preventing the further development of inflammation either through the inability to traffic to appropriate sites or through the inactivation of these regulatory functions by GITRL-expressing B cells or other APC such as DC's (210) that are programmed to perpetuate the inflammatory response. Increased B cells thus contribute to the development of

inflammation via this blockade of regulatory cells and possibly by immunoglobulin-mediated antigen opsonization or immune complex formation resulting in increased accumulation of myeloid cells in the inflammatory lesions. Because the increased NF- $\kappa$ B activation that serves as the precipitating cause of this disorder is likely enhanced (288), and not mitigated, by this inflammatory response, this cycle of events is continually repeated, resulting in chronic inflammation and not disease resolution.

### **Suggestions for Future Work**

Many future experiments will be required to assess the validity of the model presented above, beginning with experiments designed to establish a link between decreased epithelial Ppar $\gamma$  expression and increased epithelial permeability. We have shown that epithelial permeability in SAMP1/YitFc mice is increased in the small intestine, but not the colon, relative to normal AKR mice. Therefore, studies should investigate Ppar $\gamma$  expression in SAMP1/YitFc versus AKR colonic epithelial cells, with the hypothesis that Ppar $\gamma$  expression in the colon should be normal as well. Further, given the finding that epithelial barrier dysfunction is present prior to the development of inflammation (Scott, KGE, Reuter B, et.al., in preparation), Ppar $\gamma$  expression should be determined in 4 week SAMP1/YitFc versus AKR mice to determine whether decreased Ppar $\gamma$  expression causes or results from the inflammatory process in SAMP1/YitFc ileitis. Further Ppar $\gamma$  agonists, such as rosiglitazone (284), could be applied to *ex vivo* intestinal tissue in the TEER assay or orally administered to mice in which the *in vivo* permeability assay is performed in order to ascertain whether increasing Ppar $\gamma$  function can lead to a tightening of the epithelial barrier. In addition, transdominant mutant I $\kappa$ B molecules or

nitric oxide, which both serve as inhibitors of NF- $\kappa$ B function in experimental systems (46), could be used in these same assays to prove that the increase in SAMP1/YitFc ileal epithelial permeability is due to NF- $\kappa$ B-induced transcription pathways. Ultimately, the identification of the molecular mechanisms leading to increased SAMP1/YitFc epithelial permeability will likely require the establishment of immortalized cell lines from SAMP1/YitFc and AKR ileal epithelial cells. If these cell lines from SAMP1/YitFc mice still display barrier dysfunction in model epithelial systems, then these lines could be used to investigate the effects of specific molecular inhibitors, siRNA knock down of the specific protein expression, and/or transfection leading to overexpression of certain signaling molecules on the SAMP1/YitFc permeability phenotype.

Importantly, we have not definitively shown that the epithelial permeability defect is truly the source of the non-hematopoietic susceptibility that leads to SAMP1/YitFc ileitis. Endothelial cells also contain tight junctions and increased permeability of endothelial cells could also lead to increased inflammation. Examination of tight junction protein and Ppar $\gamma$  expression by SAMP1/YitFc endothelial cells obtained via laser-capture dissection could address this question. It is also conceivable that stromal cells or other populations that closely interact with leukocytes could be aberrant in SAMP1/YitFc mice thereby leading to immune activation. Ultimately the best way to prove that epithelial dysfunction and epithelial-specific decreases in Ppar $\gamma$  expression lead to SAMP1/YitFc ileitis would be the creation of a transgenic mouse in which Ppar $\gamma$  or tight junction protein genes are deleted specifically in epithelial cells using a cre/lox system under the control of an epithelial specific promoter. If such mice developed ileitis, the



contributions of these proteins to the SAMP1/YitFc phenotype would be confirmed.

Alternatively, generation of transgenic mice overexpressing Pparg in the epithelium and subsequent crossing of these mice onto the SAMP1/YitFc background could determine whether overexpression of Pparg protects SAMP1/YitFc mice from ileitis development.

Dendritic cell contributions to the SAMP1/YitFc ileitis phenotype have yet to be explored. Dendritic cells have been shown in other models to mediate the transmission of inflammatory signals from the epithelial surface to lymphoid organs where immune responses are initiated (287). Our unpublished observations suggest that dendritic cells represent less than 2% of SAMP1/YitFc MLN cells and difficulties in isolating lamina propria lymphocytes from SAMP1/YitFc mice have made recovery of sufficient numbers of dendritic cells from this compartment quite challenging. Since oral tolerance is broken in the context of Crohn's disease, utilizing techniques such as oral administration of fluorescently labeled bacterial antigen, might allow for the identification of dendritic cell populations that specifically transmit antigen from the intestinal interface to the MLN. Once phenotypically identified, these dendritic cells could be characterized according to localization within the intestinal wall, cytokine production, interactions with pro-inflammatory cells, the expression of GITRL, and the ability of these cells to block regulatory T cell function.

In experiments presented in chapter III, we were only able to narrow the size of the primary disease-producing SAMP1/YitFc MLN CD4<sup>+</sup> T cell subset to approximately 40% of the overall CD4<sup>+</sup> T cell population. Based on the increased size of the  $\alpha_4\beta_7^{\text{hi}}$   $\alpha_4\beta_1^{\text{hi}}$  CD4<sup>+</sup> T cell subset in SAMP1/YitFc versus AKR MLN and the previous finding that blockade of these integrins leads to disease amelioration, future experiments should

include identifying a FACS-based strategy to isolate this subset and testing the hypothesis that these cells (11% of CD4<sup>+</sup> T cells) may induce the highest levels of ileitis in the adoptive transfer model of any SAMP1/YitFc MLN subset. Identification of a precise pathogenic subset would allow cleaner comparisons with the  $\alpha_E\beta_7^+$  CD4<sup>+</sup> T cell subset. For instance, two color *in vivo* homing assays, using freshly isolated or *in vitro*-stimulated cells from these two subsets with and without antibody-based blockade of specific adhesion molecules or chemokine receptors, could result in the identification of many differential patterns and molecular requirements of regulatory versus effector T cell trafficking.

The data presented regarding chemokine receptor expression and chemotactic responsiveness by CD4<sup>+</sup> T cells and whole ileal tissue provide many preliminary findings that could be further explored. No differences existed in the chemotactic responsiveness of SAMP1/YitFc versus AKR unfractionated MLN CD4<sup>+</sup> T cells. However, since we show that SAMP1/YitFc cells activated in culture have a different chemokine receptor expression pattern than freshly isolated cells, it is possible that differences in MLN CD4<sup>+</sup> T cell chemotaxis between strains may only be found in cells that have been activated in culture. Differences in the chemotaxis of MLN  $\alpha_E\beta_7^+$  CD4<sup>+</sup> Treg versus effector CD4<sup>+</sup> T cells, particularly toward CCR8 ligands I-309 and TARC (263), should be explored given the exclusive expression of CCR8 on  $\alpha_E\beta_7^+$  T cells. Further, identification of the tissue-specific pattern of expression of these CCR8 ligands should be performed to determine the tissues to which  $\alpha_E\beta_7^+$  CD4<sup>+</sup> Treg likely can and cannot migrate.

The specific elevation of CCR1 levels in 4 week-old SAMP1/YitFc mice relative to age-matched AKR or older SAMP1/YitFc mice, indicates that this receptor, primarily

expressed by activated or memory T cells (256), and its ligands MIP-1 $\alpha$  and RANTES may play key roles in the migration of cells in the earliest phases of disease initiation. Immunostaining of CCR1 expression in the ileum and chemotaxis assays toward CCR1 ligands using cells from 4 week-old mice could lead to the identification of cell subsets involved in disease initiation. The elevated expression in other chemokine receptors at later stages of disease, including CXCR3, CCR6, CCR9, and CX<sub>3</sub>CR1 could form the basis of experiments in which the therapeutic efficacy of blocking one or more of these receptors is examined.

Further examination of SAMP1/YitFc B cell function should start with the identification of specific antigens recognized by the increased IgA present in SAMP1/YitFc mice. This type of biochemical analysis has been performed in studies in other animal models by identifying reactivity of immunoglobulin isotypes isolated from serum or cell cultures against protein extracts from specific bacterial species found in the intestinal flora (74;229). If a few antigens are identified that demonstrate high seroreactivity, these antigens could be used in immunohistochemical studies attempting to identify immune complex formation in the submucosal regions in which we identified substantial neutrophil accumulation. If these immune complexes could be formed by *in vitro* methods, the role these complexes play in neutrophil recruitment could be assessed directly by analysis of neutrophil spreading on surfaces coated with these complexes (276) or in flow-based assays.

While we have demonstrated that SAMP1/YitFc B cells are pro-inflammatory in the SCID adoptive transfer model, we have not definitively shown that the increased IgA-expressing cells in SAMP1/YitFc mice are responsible for these pro-inflammatory

properties. Despite the difficulties of backcrossing gene knock-out mice to the mixed background of the SAMP1/YitFc strain, crossing IgA  $-/-$  mice onto the SAMP1/YitFc background would provide the only method that could address the specific function of IgA $^{+}$  cells in the context of SAMP1/YitFc ileitis. Rituximab is a humanized anti-CD20 antibody that has been shown to be effective in treating autoimmune diseases such as rheumatoid arthritis through a mechanism involving B cell depletion (289). Given the pro-inflammatory properties of B cells in the adoptive transfer, the therapeutic efficacy of anti-mouse CD20 antibodies should be assessed in the SAMP1/YitFc model. If this therapy proves to ameliorate disease, clinical trials analyzing the therapeutic benefit of depleting B cells with rituximab in Crohn's patients could be warranted.

## Reference List

1. Loftus,E.V., Jr. 2004. Clinical epidemiology of inflammatory bowel disease: Incidence, prevalence, and environmental influences. *Gastroenterology* 126:1504-1517.
2. Lapidus,A., Bernell,O., Hellers,G., Persson,P.G., and Lofberg,R. 1997. Incidence of Crohn's disease in Stockholm County 1955-1989. *Gut* 41:480-486.
3. Loftus,E.V., Jr., Silverstein,M.D., Sandborn,W.J., Tremaine,W.J., Harmsen,W.S., and Zinsmeister,A.R. 1998. Crohn's disease in Olmsted County, Minnesota, 1940-1993: incidence, prevalence, and survival. *Gastroenterology* 114:1161-1168.
4. Yao,T., Matsui,T., and Hiwatashi,N. 2000. Crohn's disease in Japan: diagnostic criteria and epidemiology. *Dis.Colon Rectum* 43:S85-S93.
5. Trallori,G., Palli,D., Saieva,C., Bardazzi,G., Bonanomi,A.G., d'Albasio,G., Galli,M., Vannozzi,G., Milla,M., Tarantino,O. *et al.* 1996. A population-based study of inflammatory bowel disease in Florence over 15 years (1978-92). *Scand.J.Gastroenterol.* 31:892-899.
6. Appleyard,C.B., Hernandez,G., and Rios-Bedoya,C.F. 2004. Basic epidemiology of inflammatory bowel disease in Puerto Rico. *Inflamm.Bowel.Dis.* 10:106-111.
7. Loftus,E.V., Jr., Schoenfeld,P., and Sandborn,W.J. 2002. The epidemiology and natural history of Crohn's disease in population-based patient cohorts from North America: a systematic review. *Aliment.Pharmacol.Ther.* 16:51-60.
8. Friedman,S. and Blumberg,R.S. 2001. Inflammatory Bowel Disease. In Harrison's Principles of Internal Medicine. Braunwald E., Fauci A.S., Kasper D.L., Hauser S.L., Longo D.L., and Jameson J.L., editors. McGraw-Hill, New York. 1679-1692.
9. Crohn,B.B., Ginzburg,L., and Oppenheimer,G.D. 1932. Regional ileitis: a pathologic and clinical entity. 1932. *Mt.Sinai.J.Med.* 99:1323-1329.
10. Hendrickson,B.A., Gokhale,R., and Cho,J.H. 2002. Clinical aspects and pathophysiology of inflammatory bowel disease. *Clin.Microbiol.Rev.* 15:79-94.
11. Cherwinski,H.M., Schumacher,J.H., Brown,K.D., and Mosmann,T.R. 1987. Two types of mouse helper T cell clone. III. Further differences in lymphokine synthesis between Th1 and Th2 clones revealed by RNA hybridization, functionally monospecific bioassays, and monoclonal antibodies. *J.Exp.Med.* 166:1229-1244.

12. Cher,D.J. and Mosmann,T.R. 1987. Two types of murine helper T cell clone. II. Delayed-type hypersensitivity is mediated by TH1 clones. *J.Immunol.* 138:3688-3694.
13. Mosmann,T.R., Cherwinski,H., Bond,M.W., Giedlin,M.A., and Coffman,R.L. 1986. Two types of murine helper T cell clone. I. Definition according to profiles of lymphokine activities and secreted proteins. *J.Immunol.* 136:2348-2357.
14. Romagnani,S. 1997. The Th1/Th2 paradigm. *Immunol.Today* 18:263-266.
15. Parronchi,P., Romagnani,P., Annunziato,F., Sampognaro,S., Becchio,A., Giannarini,L., Maggi,E., Pupilli,C., Tonelli,F., and Romagnani,S. 1997. Type 1 T-helper cell predominance and interleukin-12 expression in the gut of patients with Crohn's disease. *Am.J.Pathol.* 150:823-832.
16. MacDonald,T.T., Hutchings,P., Choy,M.Y., Murch,S., and Cooke,A. 1990. Tumour necrosis factor-alpha and interferon-gamma production measured at the single cell level in normal and inflamed human intestine. *Clin.Exp.Immunol.* 81:301-305.
17. Fuss,I.J., Neurath,M., Boirivant,M., Klein,J.S., de la,M.C., Strong,S.A., Fiocchi,C., and Strober,W. 1996. Disparate CD4+ lamina propria (LP) lymphokine secretion profiles in inflammatory bowel disease. Crohn's disease LP cells manifest increased secretion of IFN-gamma, whereas ulcerative colitis LP cells manifest increased secretion of IL-5. *J.Immunol.* 157:1261-1270.
18. Monteleone,G., Biancone,L., Marasco,R., Morrone,G., Marasco,O., Luzzza,F., and Pallone,F. 1997. Interleukin 12 is expressed and actively released by Crohn's disease intestinal lamina propria mononuclear cells. *Gastroenterology* 112:1169-1178.
19. Egan,L.J. and Sandborn,W.J. 2004. Advances in the treatment of Crohn's disease. *Gastroenterology* 126:1574-1581.
20. Luger,A., Schmidt,M., Luger,N., Pauels,H.G., Domschke,W., and Kucharzik,T. 2001. Infliximab induces apoptosis in monocytes from patients with chronic active Crohn's disease by using a caspase-dependent pathway. *Gastroenterology* 121:1145-1157.
21. ten Hove,T., van Montfrans,C., Peppelenbosch,M.P., and van Deventer,S.J. 2002. Infliximab treatment induces apoptosis of lamina propria T lymphocytes in Crohn's disease. *Gut* 50:206-211.
22. Hanauer,S.B., Feagan,B.G., Lichtenstein,G.R., Mayer,L.F., Schreiber,S., Colombel,J.F., Rachmilewitz,D., Wolf,D.C., Olson,A., Bao,W. *et al.* 2002. Maintenance infliximab for Crohn's disease: the ACCENT I randomised trial. *Lancet* 359:1541-1549.

23. Targan,S.R., Hanauer,S.B., van Deventer,S.J., Mayer,L., Present,D.H., Braakman,T., DeWoody,K.L., Schaible,T.F., and Rutgeerts,P.J. 1997. A short-term study of chimeric monoclonal antibody cA2 to tumor necrosis factor alpha for Crohn's disease. Crohn's Disease cA2 Study Group. *N.Engl.J.Med.* 337:1029-1035.
24. Jonkers,D. and Stockbrugger,R. 2003. Probiotics and inflammatory bowel disease. *J.R.Soc.Med.* 96:167-171.
25. Hulten,K., Almashhrawi,A., El-Zaatari,F.A., and Graham,D.Y. 2000. Antibacterial therapy for Crohn's disease: a review emphasizing therapy directed against mycobacteria. *Dig.Dis.Sci.* 45:445-456.
26. Ghosh,S., Goldin,E., Gordon,F.H., Malchow,H.A., Rask-Madsen,J., Rutgeerts,P., Vyhnaek,P., Zadorova,Z., Palmer,T., and Donoghue,S. 2003. Natalizumab for active Crohn's disease. *N.Engl.J.Med.* 348:24-32.
27. Halfvarson,J., Bodin,L., Tysk,C., Lindberg,E., and Jarnerot,G. 2003. Inflammatory bowel disease in a Swedish twin cohort: a long-term follow-up of concordance and clinical characteristics. *Gastroenterology* 124:1767-1773.
28. Shivananda,S., Lennard-Jones,J., Logan,R., Fear,N., Price,A., Carpenter,L., and van Blankenstein,M. 1996. Incidence of inflammatory bowel disease across Europe: is there a difference between north and south? Results of the European Collaborative Study on Inflammatory Bowel Disease (EC-IBD). *Gut* 39:690-697.
29. Sonnenberg,A. and Wasserman,I.H. 1991. Epidemiology of inflammatory bowel disease among U.S. military veterans. *Gastroenterology* 101:122-130.
30. Ogunbi,S.O., Ransom,J.A., Sullivan,K., Schoen,B.T., and Gold,B.D. 1998. Inflammatory bowel disease in African-American children living in Georgia. *J.Pediatr.* 133:103-107.
31. Hugot,J.P., Alberti,C., Berrebi,D., Bingen,E., and Cezard,J.P. 2003. Crohn's disease: the cold chain hypothesis. *Lancet* 362:2012-2015.
32. Ma,T.Y. 1997. Intestinal epithelial barrier dysfunction in Crohn's disease. *Proc.Soc.Exp.Biol.Med.* 214:318-327.
33. Cosnes,J., Carbonnel,F., Beaugerie,L., Le Quintrec,Y., and Gendre,J.P. 1996. Effects of cigarette smoking on the long-term course of Crohn's disease. *Gastroenterology* 110:424-431.
34. Persson,P.G., Ahlbom,A., and Hellers,G. 1990. Inflammatory bowel disease and tobacco smoke--a case-control study. *Gut* 31:1377-1381.

35. Sonnenberg,A., McCarty,D.J., and Jacobsen,S.J. 1991. Geographic variation of inflammatory bowel disease within the United States. *Gastroenterology* 100:143-149.
36. ACHESON,E.D. 1960. The distribution of ulcerative colitis and regional enteritis in United States veterans with particular reference to the Jewish religion. *Gut* 1:291-293.
37. Ahmad,T., Tamboli,C.P., Jewell,D., and Colombel,J.F. 2004. Clinical relevance of advances in genetics and pharmacogenetics of IBD. *Gastroenterology* 126:1533-1549.
38. Bonen,D.K. and Cho,J.H. 2003. The genetics of inflammatory bowel disease. *Gastroenterology* 124:521-536.
39. Hugot,J.P., Laurent-Puig,P., Gower-Rousseau,C., Olson,J.M., Lee,J.C., Beaugerie,L., Naom,I., Dupas,J.L., Van Gossum,A., Orholm,M. *et al.* 1996. Mapping of a susceptibility locus for Crohn's disease on chromosome 16. *Nature* 379:821-823.
40. Hugot,J.P., Chamaillard,M., Zouali,H., Lesage,S., Cezard,J.P., Belaiche,J., Almer,S., Tysk,C., O'Morain,C.A., Gassull,M. *et al.* 2001. Association of NOD2 leucine-rich repeat variants with susceptibility to Crohn's disease. *Nature* 411:599-603.
41. Ogura,Y., Bonen,D.K., Inohara,N., Nicolae,D.L., Chen,F.F., Ramos,R., Britton,H., Moran,T., Karaliuskas,R., Duerr,R.H. *et al.* 2001. A frameshift mutation in NOD2 associated with susceptibility to Crohn's disease. *Nature* 411:603-606.
42. Lesage,S., Zouali,H., Cezard,J.P., Colombel,J.F., Belaiche,J., Almer,S., Tysk,C., O'Morain,C., Gassull,M., Binder,V. *et al.* 2002. CARD15/NOD2 mutational analysis and genotype-phenotype correlation in 612 patients with inflammatory bowel disease. *Am.J.Hum.Genet.* 70:845-857.
43. Girardin,S.E., Hugot,J.P., and Sansonetti,P.J. 2003. Lessons from Nod2 studies: towards a link between Crohn's disease and bacterial sensing. *Trends Immunol.* 24:652-658.
44. Boone,D.L. and Ma,A. 2003. Connecting the dots from Toll-like receptors to innate immune cells and inflammatory bowel disease. *J.Clin.Invest.* 111:1284-1286.
45. Ogura,Y., Inohara,N., Benito,A., Chen,F.F., Yamaoka,S., and Nunez,G. 2001. Nod2, a Nod1/Apaf-1 family member that is restricted to monocytes and activates NF-kappaB. *J.Biol.Chem.* 276:4812-4818.



46. Chen,F., Castranova,V., Shi,X., and Demers,L.M. 1999. New insights into the role of nuclear factor-kappaB, a ubiquitous transcription factor in the initiation of diseases. *Clin.Chem.* 45:7-17.
47. Chamaillard,M., Philpott,D., Girardin,S.E., Zouali,H., Lesage,S., Chareyre,F., Bui,T.H., Giovannini,M., Zaehring,U., Penard-Lacronique,V. *et al.* 2003. Gene-environment interaction modulated by allelic heterogeneity in inflammatory diseases. *Proc.Natl.Acad.Sci.U.S.A* 100:3455-3460.
48. Ellis,R.D., Goodlad,J.R., Limb,G.A., Powell,J.J., Thompson,R.P., and PUNCHARD,N.A. 1998. Activation of nuclear factor kappa B in Crohn's disease. *Inflamm.Res.* 47:440-445.
49. Simmons,J.D., Mullighan,C., Welsh,K.I., and Jewell,D.P. 2000. Vitamin D receptor gene polymorphism: association with Crohn's disease susceptibility. *Gut* 47:211-214.
50. Satsangi,J., Parkes,M., Louis,E., Hashimoto,L., Kato,N., Welsh,K., Terwilliger,J.D., Lathrop,G.M., Bell,J.I., and Jewell,D.P. 1996. Two stage genome-wide search in inflammatory bowel disease provides evidence for susceptibility loci on chromosomes 3, 7 and 12. *Nat.Genet.* 14:199-202.
51. Hampe,J., Schreiber,S., Shaw,S.H., Lau,K.F., Bridger,S., Macpherson,A.J., Cardon,L.R., Sakul,H., Harris,T.J., Buckler,A. *et al.* 1999. A genomewide analysis provides evidence for novel linkages in inflammatory bowel disease in a large European cohort. *Am.J.Hum.Genet.* 64:808-816.
52. Yang,H., Plevy,S.E., Taylor,K., Tyan,D., Fischel-Ghodsian,N., McElree,C., Targan,S.R., and Rotter,J.I. 1999. Linkage of Crohn's disease to the major histocompatibility complex region is detected by multiple non-parametric analyses. *Gut* 44:519-526.
53. Allen,R.L., Bowness,P., and McMichael,A. 1999. The role of HLA-B27 in spondyloarthritis. *Immunogenetics* 50:220-227.
54. Louis,E., Peeters,M., Franchimont,D., Seidel,L., Fontaine,F., Demolin,G., Croes,F., Dupont,P., Davin,L., Omri,S. *et al.* 2000. Tumour necrosis factor (TNF) gene polymorphism in Crohn's disease (CD): influence on disease behaviour? *Clin.Exp.Immunol.* 119:64-68.
55. Peltekova,V.D., Wintle,R.F., Rubin,L.A., Amos,C.I., Huang,Q., Gu,X., Newman,B., Van Oene,M., Cescon,D., Greenberg,G. *et al.* 2004. Functional variants of OCTN cation transporter genes are associated with Crohn disease. *Nat.Genet.* 36:471-475.
56. Rioux,J.D., Daly,M.J., Silverberg,M.S., Lindblad,K., Steinhart,H., Cohen,Z., Delmonte,T., Kocher,K., Miller,K., Guschwan,S. *et al.* 2001. Genetic variation in

the 5q31 cytokine gene cluster confers susceptibility to Crohn disease.  
*Nat. Genet.* 29:223-228.

57. Matsuzawa,J., Sugimura,K., Matsuda,Y., Takazoe,M., Ishizuka,K., Mochizuki,T., Seki,S.S., Yoneyama,O., Bannnai,H., Suzuki,K. *et al.* 2003. Association between K469E allele of intercellular adhesion molecule 1 gene and inflammatory bowel disease in a Japanese population. *Gut* 52:75-78.
58. Elmgreen,J., Sorensen,H., and Berkowicz,A. 1984. Polymorphism of complement C3 in chronic inflammatory bowel disease. Predominance of the C3F gene in Crohn's disease. *Acta Med.Scand.* 215:375-378.
59. Rioux,J.D., Silverberg,M.S., Daly,M.J., Steinhart,A.H., McLeod,R.S., Griffiths,A.M., Green,T., Brettin,T.S., Stone,V., Bull,S.B. *et al.* 2000. Genomewide search in Canadian families with inflammatory bowel disease reveals two novel susceptibility loci. *Am.J.Hum.Genet.* 66:1863-1870.
60. Kyo,K., Muto,T., Nagawa,H., Lathrop,G.M., and Nakamura,Y. 2001. Associations of distinct variants of the intestinal mucin gene MUC3A with ulcerative colitis and Crohn's disease. *J.Hum.Genet.* 46:5-20.
61. Cho,J.H., Nicolae,D.L., Gold,L.H., Fields,C.T., LaBuda,M.C., Rohal,P.M., Pickles,M.R., Qin,L., Fu,Y., Mann,J.S. *et al.* 1998. Identification of novel susceptibility loci for inflammatory bowel disease on chromosomes 1p, 3q, and 4q: evidence for epistasis between 1p and IBD1. *Proc.Natl.Acad.Sci.U.S.A* 95:7502-7507.
62. Duerr,R.H., Barmada,M.M., Zhang,L., Achkar,J.P., Cho,J.H., Hanauer,S.B., Brant,S.R., Bayless,T.M., Baldassano,R.N., and Weeks,D.E. 2002. Evidence for an inflammatory bowel disease locus on chromosome 3p26: linkage, transmission/disequilibrium and partitioning of linkage. *Hum.Mol.Genet.* 11:2599-2606.
63. Duerr,R.H., Barmada,M.M., Zhang,L., Pfutzer,R., and Weeks,D.E. 2000. High-density genome scan in Crohn disease shows confirmed linkage to chromosome 14q11-12. *Am.J.Hum.Genet.* 66:1857-1862.
64. de Jong,D.J., Franke,B., Naber,A.H., Willemen,J.J., Heister,A.J., Brunner,H.G., de Kovel,C.G., and Hol,F.A. 2003. No evidence for involvement of IL-4R and CD11B from the IBD1 region and STAT6 in the IBD2 region in Crohn's disease. *Eur.J.Hum.Genet.* 11:884-887.
65. Hampe,J., Hermann,B., Bridger,S., Macpherson,A.J., Mathew,C.G., and Schreiber,S. 1998. The interferon-gamma gene as a positional and functional candidate gene for inflammatory bowel disease. *Int.J.Colorectal Dis.* 13:260-263.

66. Buning,C., Genschel,J., Weltrich,R., Lochs,H., and Schmidt,H. 2003. The interleukin-25 gene located in the inflammatory bowel disease (IBD) 4 region: no association with inflammatory bowel disease. *Eur.J.Immunogenet.* 30:329-333.
67. Parkes,M., Satsangi,J., and Jewell,D. 1998. Contribution of the IL-2 and IL-10 genes to inflammatory bowel disease (IBD) susceptibility. *Clin.Exp.Immunol.* 113:28-32.
68. Wirtz,S. and Neurath,M.F. 2000. Animal models of intestinal inflammation: new insights into the molecular pathogenesis and immunotherapy of inflammatory bowel disease. *Int.J.Colorectal.Dis.* 15:144-160.
69. Hibi,T., Ogata,H., and Sakuraba,A. 2002. Animal models of inflammatory bowel disease. *J.Gastroenterol.* 37:409-417.
70. Pizarro,T.T., Arseneau,K.O., Bamias,G., and Cominelli,F. 2003. Mouse models for the study of Crohn's disease. *Trends.Mol.Med.* 9:218-222.
71. Strober,W., Fuss,I.J., and Blumberg,R.S. 2002. The immunology of mucosal models of inflammation. *Annu.Rev.Immunol* 20:495-549.
72. Elson,C.O., Cong,Y., and Sundberg,J. 2000. The C3H/HeJBir mouse model: a high susceptibility phenotype for colitis. *Int.Rev.Immunol.* 19:63-75.
73. Sundberg,J.P., Elson,C.O., Bedigian,H., and Birkenmeier,E.H. 1994. Spontaneous, heritable colitis in a new substrain of C3H/HeJ mice. *Gastroenterology* 107:1726-1735.
74. Brandwein,S.L., McCabe,R.P., Cong,Y., Waites,K.B., Ridwan,B.U., Dean,P.A., Ohkusa,T., Birkenmeier,E.H., Sundberg,J.P., and Elson,C.O. 1997. Spontaneously colitic C3H/HeJBir mice demonstrate selective antibody reactivity to antigens of the enteric bacterial flora. *J.Immunol* 159:44-52.
75. Cong,Y., Brandwein,S.L., McCabe,R.P., Lazenby,A., Birkenmeier,E.H., Sundberg,J.P., and Elson,C.O. 1998. CD4+ T cells reactive to enteric bacterial antigens in spontaneously colitic C3H/HeJBir mice: increased T helper cell type 1 response and ability to transfer disease. *J.Exp.Med.* 187:855-864.
76. Cong,Y., Weaver,C.T., Lazenby,A., and Elson,C.O. 2000. Colitis induced by enteric bacterial antigen-specific CD4+ T cells requires CD40-CD40 ligand interactions for a sustained increase in mucosal IL-12. *J.Immunol.* 165:2173-2182.
77. Cong,Y., Weaver,C.T., Lazenby,A., and Elson,C.O. 2002. Bacterial-reactive T regulatory cells inhibit pathogenic immune responses to the enteric flora. *J.Immunol.* 169:6112-6119.

78. Singh,B., Read,S., Asseman,C., Malmstrom,V., Mottet,C., Stephens,L.A., Stepankova,R., Tlaskalova,H., and Powrie,F. 2001. Control of intestinal inflammation by regulatory T cells. *Immunol Rev.* 182:190-200.
79. Powrie,F., Leach,M.W., Mauze,S., Caddle,L.B., and Coffman,R.L. 1993. Phenotypically distinct subsets of CD4+ T cells induce or protect from chronic intestinal inflammation in C. B-17 scid mice. *Int.Immunol* 5:1461-1471.
80. Mudter,J., Wirtz,S., Galle,P.R., and Neurath,M.F. 2002. A new model of chronic colitis in SCID mice induced by adoptive transfer of CD62L+ CD4+ T cells: insights into the regulatory role of interleukin-6 on apoptosis. *Pathobiology* 70:170-176.
81. Birkeland,M.L., Johnson,P., Trowbridge,I.S., and Pure,E. 1989. Changes in CD45 isoform expression accompany antigen-induced murine T-cell activation. *Proc.Natl.Acad.Sci.U.S.A.* 86:6734-6738.
82. Powrie,F., Leach,M.W., Mauze,S., Menon,S., Caddle,L.B., and Coffman,R.L. 1994. Inhibition of Th1 responses prevents inflammatory bowel disease in scid mice reconstituted with CD45RBhi CD4+ T cells. *Immunity.* 1:553-562.
83. Murata,K., Nose,M., Ndhlovu,L.C., Sato,T., Sugamura,K., and Ishii,N. 2002. Constitutive OX40/OX40 ligand interaction induces autoimmune-like diseases. *J.Immunol* 169:4628-4636.
84. Mottet,C., Uhlig,H.H., and Powrie,F. 2003. Cutting Edge: Cure of Colitis by CD4(+)/CD25(+) Regulatory T Cells. *J.Immunol* 170:3939-3943.
85. Lehmann,J., Huehn,J., de la Rosa,M., Maszyrna,F., Kretschmer,U., Krenn,V., Brunner,M., Scheffold,A., and Hamann,A. 2002. Expression of the integrin alpha Ebeta 7 identifies unique subsets of CD25+ as well as CD25- regulatory T cells. *Proc.Natl.Acad.Sci.U.S.A.* 99:13031-13036.
86. Uraushihara,K., Kanai,T., Ko,K., Totsuka,T., Makita,S., Iiyama,R., Nakamura,T., and Watanabe,M. 2003. Regulation of murine inflammatory bowel disease by CD25+ and. *J.Immunol.* 171:708-716.
87. Powrie,F., Carlino,J., Leach,M.W., Mauze,S., and Coffman,R.L. 1996. A critical role for transforming growth factor-beta but not interleukin 4 in the suppression of T helper type 1-mediated colitis by CD45RB(low) CD4+ T cells. *J.Exp.Med.* 183:2669-2674.
88. Asseman,C., Mauze,S., Leach,M.W., Coffman,R.L., and Powrie,F. 1999. An essential role for interleukin 10 in the function of regulatory T cells that inhibit intestinal inflammation. *J.Exp.Med.* 190:995-1004.

89. Read,S., Malmstrom,V., and Powrie,F. 2000. Cytotoxic T lymphocyte-associated antigen 4 plays an essential role in the function of CD25(+)CD4(+) regulatory cells that control intestinal inflammation. *J.Exp.Med.* 192:295-302.
90. Kuhn,R., Lohler,J., Rennick,D., Rajewsky,K., and Muller,W. 1993. Interleukin-10-deficient mice develop chronic enterocolitis. *Cell* 75:263-274.
91. Davidson,N.J., Hudak,S.A., Lesley,R.E., Menon,S., Leach,M.W., and Rennick,D.M. 1998. IL-12, but not IFN-gamma, plays a major role in sustaining the chronic phase of colitis in IL-10-deficient mice. *J.Immunol.* 161:3143-3149.
92. Sellon,R.K., Tonkonogy,S., Schultz,M., Dieleman,L.A., Grenther,W., Balish,E., Rennick,D.M., and Sartor,R.B. 1998. Resident enteric bacteria are necessary for development of spontaneous colitis and immune system activation in interleukin-10-deficient mice. *Infect.Immun.* 66:5224-5231.
93. Kullberg,M.C., Ward,J.M., Gorelick,P.L., Caspar,P., Hieny,S., Cheever,A., Jankovic,D., and Sher,A. 1998. Helicobacter hepaticus triggers colitis in specific-pathogen-free interleukin-10 (IL-10)-deficient mice through an IL-12- and gamma interferon-dependent mechanism. *Infect.Immun.* 66:5157-5166.
94. Bristol,I.J., Farmer,M.A., Cong,Y., Zheng,X.X., Strom,T.B., Elson,C.O., Sundberg,J.P., and Leiter,E.H. 2000. Heritable susceptibility for colitis in mice induced by IL-10 deficiency. *Inflamm.Bowel.Dis.* 6:290-302.
95. Farmer,M.A., Sundberg,J.P., Bristol,I.J., Churchill,G.A., Li,R., Elson,C.O., and Leiter,E.H. 2001. A major quantitative trait locus on chromosome 3 controls colitis severity in IL-10-deficient mice. *Proc.Natl.Acad.Sci.U.S.A* 98:13820-13825.
96. Willerford,D.M., Chen,J., Ferry,J.A., Davidson,L., Ma,A., and Alt,F.W. 1995. Interleukin-2 receptor alpha chain regulates the size and content of the peripheral lymphoid compartment. *Immunity.* 3:521-530.
97. Sadlack,B., Merz,H., Schorle,H., Schimpl,A., Feller,A.C., and Horak,I. 1993. Ulcerative colitis-like disease in mice with a disrupted interleukin-2 gene. *Cell* 75:253-261.
98. Suzuki,H., Kundig,T.M., Furlonger,C., Wakeham,A., Timms,E., Matsuyama,T., Schmits,R., Simard,J.J., Ohashi,P.S., Griesser,H. *et al.* 1995. Dereglated T cell activation and autoimmunity in mice lacking interleukin-2 receptor beta. *Science* 268:1472-1476.
99. Ehrhardt,R.O., Ludviksson,B.R., Gray,B., Neurath,M., and Strober,W. 1997. Induction and prevention of colonic inflammation in IL-2-deficient mice. *J.Immunol.* 158:566-573.

100. Schultz,M., Tonkonogy,S.L., Sellon,R.K., Veltkamp,C., Godfrey,V.L., Kwon,J., Grenther,W.B., Balish,E., Horak,I., and Sartor,R.B. 1999. IL-2-deficient mice raised under germfree conditions develop delayed mild focal intestinal inflammation. *Am.J.Physiol* 276:G1461-G1472.
101. Kneitz,B., Herrmann,T., Yonehara,S., and Schimpl,A. 1995. Normal clonal expansion but impaired Fas-mediated cell death and anergy induction in interleukin-2-deficient mice. *Eur.J.Immunol.* 25:2572-2577.
102. Wirtz,S., Finotto,S., Kanzler,S., Lohse,A.W., Blessing,M., Lehr,H.A., Galle,P.R., and Neurath,M.F. 1999. Cutting edge: chronic intestinal inflammation in STAT-4 transgenic mice: characterization of disease and adoptive transfer by TNF- plus IFN-gamma-producing CD4+ T cells that respond to bacterial antigens. *J.Immunol.* 162:1884-1888.
103. Kontoyiannis,D., Pasparakis,M., Pizarro,T.T., Cominelli,F., and Kollias,G. 1999. Impaired on/off regulation of TNF biosynthesis in mice lacking TNF AU-rich elements: implications for joint and gut-associated immunopathologies. *Immunity* 10:387-398.
104. Kontoyiannis,D., Boulougouris,G., Manoloukos,M., Armaka,M., Apostolaki,M., Pizarro,T., Kotlyarov,A., Forster,I., Flavell,R., Gaestel,M. *et al.* 2002. Genetic dissection of the cellular pathways and signaling mechanisms in modeled tumor necrosis factor-induced Crohn's-like inflammatory bowel disease. *J.Exp.Med.* 196:1563-1574.
105. Takeda,K., Clausen,B.E., Kaisho,T., Tsujimura,T., Terada,N., Forster,I., and Akira,S. 1999. Enhanced Th1 activity and development of chronic enterocolitis in mice devoid of Stat3 in macrophages and neutrophils. *Immunity* 10:39-49.
106. Welte,T., Zhang,S.S., Wang,T., Zhang,Z., Hesslein,D.G., Yin,Z., Kano,A., Iwamoto,Y., Li,E., Craft,J.E. *et al.* 2003. STAT3 deletion during hematopoiesis causes Crohn's disease-like pathogenesis and lethality: a critical role of STAT3 in innate immunity. *Proc.Natl.Acad.Sci.U.S.A.* 100:1879-1884.
107. Rudolph,U., Finegold,M.J., Rich,S.S., Harriman,G.R., Srinivasan,Y., Brabet,P., Boulay,G., Bradley,A., and Birnbaumer,L. 1995. Ulcerative colitis and adenocarcinoma of the colon in G alpha i2-deficient mice. *Nat.Genet.* 10:143-150.
108. Dalwadi,H., Wei,B., Schrage,M., Su,T.T., Rawlings,D.J., and Braun,J. 2003. B cell developmental requirement for the G alpha i2 gene. *J.Immunol* 170:1707-1715.
109. Mombaerts,P., Mizoguchi,E., Grusby,M.J., Glimcher,L.H., Bhan,A.K., and Tonegawa,S. 1993. Spontaneous development of inflammatory bowel disease in T cell receptor mutant mice. *Cell* 75:274-282.

110. Mizoguchi,A., Mizoguchi,E., Smith,R.N., Preffer,F.I., and Bhan,A.K. 1997. Suppressive role of B cells in chronic colitis of T cell receptor alpha mutant mice. *J.Exp.Med.* 186:1749-1756.
111. Mizoguchi,A., Mizoguchi,E., Takedatsu,H., Blumberg,R.S., and Bhan,A.K. 2002. Chronic intestinal inflammatory condition generates IL-10-producing regulatory B cell subset characterized by CD1d upregulation. *Immunity* 16:219-230.
112. Dohi,T., Fujihashi,K., Koga,T., Shirai,Y., Kawamura,Y.I., Ejima,C., Kato,R., Saitoh,K., and McGhee,J.R. 2003. T helper type-2 cells induce ileal villus atrophy, goblet cell metaplasia, and wasting disease in T cell-deficient mice. *Gastroenterology* 124:672-682.
113. Okayasu,I., Hatakeyama,S., Yamada,M., Ohkusa,T., Inagaki,Y., and Nakaya,R. 1990. A novel method in the induction of reliable experimental acute and chronic ulcerative colitis in mice. *Gastroenterology* 98:694-702.
114. Mahler,M., Bristol,I.J., Leiter,E.H., Workman,A.E., Birkenmeier,E.H., Elson,C.O., and Sundberg,J.P. 1998. Differential susceptibility of inbred mouse strains to dextran sulfate sodium-induced colitis. *Am.J.Physiol* 274:G544-G551.
115. Kitajima,S., Takuma,S., and Morimoto,M. 1999. Changes in colonic mucosal permeability in mouse colitis induced with dextran sulfate sodium. *Exp.Anim* 48:137-143.
116. Dieleman,L.A., Ridwan,B.U., Tennyson,G.S., Beagley,K.W., Bucy,R.P., and Elson,C.O. 1994. Dextran sulfate sodium-induced colitis occurs in severe combined immunodeficient mice. *Gastroenterology* 107:1643-1652.
117. Ohtsuka,Y. and Sanderson,I.R. 2003. Dextran sulfate sodium-induced inflammation is enhanced by intestinal epithelial cell chemokine expression in mice. *Pediatr.Res.* 53:143-147.
118. Ohkawara,T., Nishihira,J., Takeda,H., Hige,S., Kato,M., Sugiyama,T., Iwanaga,T., Nakamura,H., Mizue,Y., and Asaka,M. 2002. Amelioration of dextran sulfate sodium-induced colitis by anti-macrophage migration inhibitory factor antibody in mice. *Gastroenterology* 123:256-270.
119. Andres,P.G., Beck,P.L., Mizoguchi,E., Mizoguchi,A., Bhan,A.K., Dawson,T., Kuziel,W.A., Maeda,N., MacDermott,R.P., Podolsky,D.K. *et al.* 2000. Mice with a selective deletion of the CC chemokine receptors 5 or 2 are protected from dextran sodium sulfate-mediated colitis: lack of CC chemokine receptor 5 expression results in a NK1.1+ lymphocyte-associated Th2-type immune response in the intestine. *J.Immunol.* 164:6303-6312.
120. Rijcken,E.M., Laukoetter,M.G., Anthoni,C., Meier,S., Mennigen,R., Spiegel,H.U., Bruewer,M., Senninger,N., Vestweber,D., and Kriegelstein,C.F.

2004. Immunoblockade of PSGL-1 attenuates established experimental murine colitis by reduction of leukocyte rolling. *Am.J.Physiol Gastrointest.Liver Physiol* 287:G115-G124.
121. Hamamoto,N., Maemura,K., Hirata,I., Murano,M., Sasaki,S., and Katsu,K. 1999. Inhibition of dextran sulphate sodium (DSS)-induced colitis in mice by intracolonicly administered antibodies against adhesion molecules (endothelial leucocyte adhesion molecule-1 (ELAM-1) or intercellular adhesion molecule-1 (ICAM-1)). *Clin.Exp.Immunol.* 117:462-468.
  122. Soriano,A., Salas,A., Salas,A., Sans,M., Gironella,M., Elena,M., Anderson,D.C., Pique,J.M., and Panes,J. 2000. VCAM-1, but not ICAM-1 or MAdCAM-1, immunoblockade ameliorates DSS-induced colitis in mice. *Lab Invest* 80:1541-1551.
  123. Kato,S., Hokari,R., Matsuzaki,K., Iwai,A., Kawaguchi,A., Nagao,S., Miyahara,T., Itoh,K., Ishii,H., and Miura,S. 2000. Amelioration of murine experimental colitis by inhibition of mucosal addressin cell adhesion molecule-1. *J.Pharmacol.Exp.Ther.* 295:183-189.
  124. Neurath,M.F., Fuss,I., Kelsall,B.L., Stuber,E., and Strober,W. 1995. Antibodies to interleukin 12 abrogate established experimental colitis in mice. *J.Exp.Med.* 182:1281-1290.
  125. Boirivant,M., Fuss,I.J., Chu,A., and Strober,W. 1998. Oxazolone colitis: A murine model of T helper cell type 2 colitis treatable with antibodies to interleukin 4. *J.Exp.Med.* 188:1929-1939.
  126. Neurath,M.F., Fuss,I., Kelsall,B.L., Presky,D.H., Waegell,W., and Strober,W. 1996. Experimental granulomatous colitis in mice is abrogated by induction of TGF-beta-mediated oral tolerance. *J.Exp.Med.* 183:2605-2616.
  127. Panwala,C.M., Jones,J.C., and Viney,J.L. 1998. A novel model of inflammatory bowel disease: mice deficient for the multiple drug resistance gene, *mdr1a*, spontaneously develop colitis. *J.Immunol.* 161:5733-5744.
  128. Macpherson,A.J., Martinic,M.M., and Harris,N. 2002. The functions of mucosal T cells in containing the indigenous commensal flora of the intestine. *Cell Mol.Life Sci.* 59:2088-2096.
  129. Schneeberger,E.E. and Lynch,R.D. 2004. The tight junction: a multifunctional complex. *Am.J.Physiol Cell Physiol* 286:C1213-C1228.
  130. Gewirtz,A.T., Liu,Y., Sitaraman,S.V., and Madara,J.L. 2002. Intestinal epithelial pathobiology: past, present and future. *Best.Pract.Res.Clin.Gastroenterol.* 16:851-867.



131. Clayburgh,D.R., Shen,L., and Turner,J.R. 2004. A porous defense: the leaky epithelial barrier in intestinal disease. *Lab Invest* 84:282-291.
132. Furuse,M., Furuse,K., Sasaki,H., and Tsukita,S. 2001. Conversion of zonulae occludentes from tight to leaky strand type by introducing claudin-2 into Madin-Darby canine kidney I cells. *J.Cell Biol.* 153:263-272.
133. Turksen,K. and Troy,T.C. 2004. Barriers built on claudins. *J.Cell Sci.* 117:2435-2447.
134. Simonovic,I., Rosenberg,J., Koutsouris,A., and Hecht,G. 2000. Enteropathogenic Escherichia coli dephosphorylates and dissociates occludin from intestinal epithelial tight junctions. *Cell Microbiol.* 2:305-315.
135. Ma,T.Y., Iwamoto,G.K., Hoa,N.T., Akotia,V., Pedram,A., Boivin,M.A., and Said,H.M. 2004. TNF-alpha-induced increase in intestinal epithelial tight junction permeability requires NF-kappa B activation. *Am.J.Physiol.Gastrointest.Liver Physiol.* 286:G367-G376.
136. Berkes,J., Viswanathan,V.K., Savkovic,S.D., and Hecht,G. 2003. Intestinal epithelial responses to enteric pathogens: effects on the tight junction barrier, ion transport, and inflammation. *Gut* 52:439-451.
137. Scott,K.G., Meddings,J.B., Kirk,D.R., Lees-Miller,S.P., and Buret,A.G. 2002. Intestinal infection with Giardia spp. reduces epithelial barrier function in a myosin light chain kinase-dependent fashion. *Gastroenterology* 123:1179-1190.
138. El Asmar,R., Panigrahi,P., Bamford,P., Berti,I., Not,T., Coppa,G.V., Catassi,C., Fasano,A., and El Asmar,R. 2002. Host-dependent zonulin secretion causes the impairment of the small intestine barrier function after bacterial exposure. *Gastroenterology* 123:1607-1615.
139. Bruewer,M., Luegering,A., Kucharzik,T., Parkos,C.A., Madara,J.L., Hopkins,A.M., and Nusrat,A. 2003. Proinflammatory cytokines disrupt epithelial barrier function by apoptosis-independent mechanisms. *J.Immunol* 171:6164-6172.
140. Macpherson,A.J., Hunziker,L., McCoy,K., and Lamarre,A. 2001. IgA responses in the intestinal mucosa against pathogenic and non-pathogenic microorganisms. *Microbes.Infect.* 3:1021-1035.
141. Yoshida,M., Claypool,S.M., Wagner,J.S., Mizoguchi,E., Mizoguchi,A., Roopenian,D.C., Lencer,W.I., and Blumberg,R.S. 2004. Human neonatal Fc receptor mediates transport of IgG into luminal secretions for delivery of antigens to mucosal dendritic cells. *Immunity.* 20:769-783.

142. Ayabe,T., Ashida,T., Kohgo,Y., and Kono,T. 2004. The role of Paneth cells and their antimicrobial peptides in innate host defense. *Trends Microbiol.* 12:394-398.
143. Cario,E. and Podolsky,D.K. 2000. Differential alteration in intestinal epithelial cell expression of toll-like receptor 3 (TLR3) and TLR4 in inflammatory bowel disease. *Infect.Immun.* 68:7010-7017.
144. Akira,S. and Takeda,K. 2004. Toll-like receptor signalling. *Nat.Rev.Immunol.* 4:499-511.
145. Pizarro,T.T., Michie,M.H., Bentz,M., Woraratanadharm,J., Smith,M.F., Jr., Foley,E., Moskaluk,C.A., Bickston,S.J., and Cominelli,F. 1999. IL-18, a novel immunoregulatory cytokine, is up-regulated in Crohn's disease: expression and localization in intestinal mucosal cells. *J.Immunol.* 162:6829-6835.
146. Dwinell,M.B., Johanesen,P.A., and Smith,J.M. 2003. Immunobiology of epithelial chemokines in the intestinal mucosa. *Surgery* 133:601-607.
147. Debard,N., Sierro,F., and Kraehenbuhl,J.P. 1999. Development of Peyer's patches, follicle-associated epithelium and M cell: lessons from immunodeficient and knockout mice. *Semin.Immunol.* 11:183-191.
148. Wagner,N., Löhler,J., Kunkel,E.J., Ley,K., Leung,E., Krissansen,G., Rajewsky,K., and Müller,W. 1996. Critical role for  $\beta$ 7-integrins in formation of the gut-associated lymphoid tissue. *Nature* 382:366-370.
149. Andrew,D.P., Rott,L.S., Kilshaw,P.J., and Butcher,E.C. 1996. Distribution of alpha 4 beta 7 and alpha E beta 7 integrins on thymocytes, intestinal epithelial lymphocytes and peripheral lymphocytes. *Eur.J.Immunol.* 26:897-905.
150. Rott,L.S., Briskin,M.J., and Butcher,E.C. 2000. Expression of alpha4beta7 and E-selectin ligand by circulating memory B cells: implications for targeted trafficking to mucosal and systemic sites. *J.Leukoc.Biol.* 68:807-814.
151. Hamann,A., Andrew,D.P., Jablonski-Westrich,D., Holzmann,B., and Butcher,E.C. 1994. Role of alpha 4-integrins in lymphocyte homing to mucosal tissues in vivo. *J.Immunol* 152:3282-3293.
152. Berlin,C., Berg,E.L., Briskin,M.J., Andrew,D.P., Kilshaw,P.J., Holzmann,B., Weissman,I.L., Hamann,A., and Butcher,E.C. 1993. Alpha 4 beta 7 integrin mediates lymphocyte binding to the mucosal vascular addressin MAdCAM-1. *Cell* 74:185.
153. Streeter,P.R., Berg,E.L., Rouse,B.T., Bargatze,R.F., and Butcher,E.C. 1988. A tissue-specific endothelial cell molecule involved in lymphocyte homing. *Nature* 331:41-46.

154. Butcher,E.C., Williams,M., Youngman,K., Rott,L., and Briskin,M. 1999. Lymphocyte trafficking and regional immunity. *Adv.Immunol* 72:209-53.:209-253.
155. Neutra,M.R., Mantis,N.J., and Kraehenbuhl,J.P. 2001. Collaboration of epithelial cells with organized mucosal lymphoid tissues. *Nat.Immunol.* 2:1004-1009.
156. Kunkel,E.J., Ramos,C.L., Steeber,D.A., Müller,W., Wagner,N., Tedder,T.F., and Ley,K. 1998. The roles of L-selectin,  $\beta_7$  integrins and P-selectin in leukocyte rolling and adhesion in high endothelial venules of Peyer's patches. *J.Immunol.* 161:2449-2456.
157. Bargatze,R.F., Jutila,M.A., and Butcher,E.C. 1995. Distinct roles of L-selectin and integrins alpha 4 beta 7 and LFA-1 in lymphocyte homing to Peyer's patch-HEV in situ: the multistep model confirmed and refined. *Immunity* 3:99-108.
158. Sperandio,M., Forlow,S.B., Thatte,J., Ellies,L.G., Marth,J.D., and Ley,K. 2001. Differential requirements for core2 glucosaminyltransferase for endothelial L-selectin ligand function in vivo. *J.Immunol.* 167:2268-2274.
159. Berg,E.L., McEvoy,L.M., Berlin,C., Bargatze,R.F., and Butcher,E.C. 1993. L-selectin-mediated lymphocyte rolling on MAdCAM-1. *Nature* 366:695-698.
160. Olson,T.S. and Ley,K. 2002. Chemokines and chemokine receptors in leukocyte trafficking. *Am.J.Physiol.Regul.Integr.Comp.Physiol.* 283:R7-28.
161. Ebisuno,Y., Tanaka,T., Kanemitsu,N., Kanda,H., Yamaguchi,K., Kaisho,T., Akira,S., and Miyasaka,M. 2003. Cutting edge: the B cell chemokine CXC chemokine ligand 13/B lymphocyte chemoattractant is expressed in the high endothelial venules of lymph nodes and Peyer's patches and affects B cell trafficking across high endothelial venules. *J.Immunol.* 171:1642-1646.
162. Mowat,A.M. 2003. Anatomical basis of tolerance and immunity to intestinal antigens. *Nat.Rev.Immunol* 3:331-341.
163. Monack,D.M., Bouley,D.M., and Falkow,S. 2004. Salmonella typhimurium Persists within Macrophages in the Mesenteric Lymph Nodes of Chronically Infected Nramp1<sup>+/+</sup> Mice and Can Be Reactivated by IFN{gamma} Neutralization. *J.Exp.Med.* 199:231-241.
164. Yrlid,U. and Wick,M.J. 2002. Antigen presentation capacity and cytokine production by murine splenic dendritic cell subsets upon Salmonella encounter. *J.Immunol.* 169:108-116.
165. Wagner,N., Lohler,J., Tedder,T.F., Rajewsky,K., Muller,W., and Steeber,D.A. 1998. L-selectin and beta7 integrin synergistically mediate lymphocyte migration to mesenteric lymph nodes. *Eur.J.Immunol* 28:3832-3839.

166. Streeter,P.R., Rouse,B.T., and Butcher,E.C. 1988. Immunohistologic and functional characterization of a vascular addressin involved in lymphocyte homing into peripheral lymph nodes. *J.Cell Biol.* 107:1853-1862.
167. Farstad,I.N., Halstensen,T.S., Lien,B., Kilshaw,P.J., Lazarovits,A.I., Brandtzaeg,P., and Lazarovitz,A.I. 1996. Distribution of beta 7 integrins in human intestinal mucosa and organized gut-associated lymphoid tissue. *Immunology* 89:227-237.
168. Henninger,D.D., Panes,J., Eppihimer,M., Russell,J., Gerritsen,M., Anderson,D.C., and Granger,D.N. 1997. Cytokine-induced VCAM-1 and ICAM-1 expression in different organs of the mouse. *J.Immunol.* 158:1825-1832.
169. Sans,M., Panes,J., Ardite,E., Elizalde,J.I., Arce,Y., Elena,M., Palacin,A., Fernandez-Checa,J.C., Anderson,D.C., Lobb,R. *et al.* 1999. VCAM-1 and ICAM-1 mediate leukocyte-endothelial cell adhesion in rat experimental colitis. *Gastroenterology* 116:874-883.
170. Meenan,J., Spaans,J., Grool,T.A., Pals,S.T., Tytgat,G.N., and van Deventer,S.J. 1997. Altered expression of alpha 4 beta 7, a gut homing integrin, by circulating and mucosal T cells in colonic mucosal inflammation. *Gut* 40:241-246.
171. Sans,M., Salas,A., Soriano,A., Prats,N., Gironella,M., Pizcueta,P., Elena,M., Anderson,D.C., Pique,J.M., and Panes,J. 2001. Differential role of selectins in experimental colitis. *Gastroenterology* 120:1162-1172.
172. Laroux,F.S. and Grisham,M.B. 2001. Immunological Basis of Inflammatory Bowel Disease: Role of the Microcirculation. *Microcirculation* 8:283-301.
173. Burns,R.C., Rivera-Nieves,J., Moskaluk,C.A., Matsumoto,S., Cominelli,F., and Ley,K. 2001. Antibody blockade of ICAM-1 and VCAM-1 ameliorates inflammation in the SAMP-1/Yit adoptive transfer model of Crohn's disease in mice. *Gastroenterology* 121:1428-1436.
174. Campbell,D.J., Kim,C.H., and Butcher,E.C. 2003. Chemokines in the systemic organization of immunity. *Immunol Rev.* 195:58-71.
175. Kunkel,E.J., Campbell,J.J., Haraldsen,G., Pan,J., Boisvert,J., Roberts,A.I., Ebert,E.C., Vierra,M.A., Goodman,S.B., Genovese,M.C. *et al.* 2000. Lymphocyte CC chemokine receptor 9 and epithelial thymus-expressed chemokine (TECK) expression distinguish the small intestinal immune compartment: Epithelial expression of tissue-specific chemokines as an organizing principle in regional immunity. *J.Exp.Med.* 192:761-768.
176. Campbell,D.J. and Butcher,E.C. 2002. Rapid acquisition of tissue-specific homing phenotypes by CD4(+) T cells activated in cutaneous or mucosal lymphoid tissues. *J.Exp.Med.* 195:135-141.

177. Svensson,M., Marsal,J., Ericsson,A., Carramolino,L., Broden,T., Marquez,G., and Agace,W.W. 2002. CCL25 mediates the localization of recently activated CD8alphabeta(+) lymphocytes to the small-intestinal mucosa. *J.Clin.Invest.* 110:1113-1121.
178. Pabst,O., Ohl,L., Wendland,M., Wurbel,M.A., Kremmer,E., Malissen,B., and Forster,R. 2004. Chemokine Receptor CCR9 Contributes to the Localization of Plasma Cells to the Small Intestine. *J.Exp.Med.* 199:411-416.
179. Kunkel,E.J. and Butcher,E.C. 2002. Chemokines and the tissue-specific migration of lymphocytes. *Immunity* 16:1-4.
180. Tanaka,Y., Imai,T., Baba,M., Ishikawa,I., Uehira,M., Nomiyama,H., and Yoshie,O. 1999. Selective expression of liver and activation-regulated chemokine (LARC) in intestinal epithelium in mice and humans. *Eur.J.Immunol* 29:633-642.
181. Shibahara,T., Wilcox,J.N., Couse,T., and Madara,J.L. 2001. Characterization of epithelial chemoattractants for human intestinal intraepithelial lymphocytes. *Gastroenterology* 120:60-70.
182. Dwinell,M.B., Lugerling,N., Eckmann,L., and Kagnoff,M.F. 2001. Regulated production of interferon-inducible T-cell chemoattractants by human intestinal epithelial cells. *Gastroenterology* 120:49-59.
183. Cheroutre,H. 2004. Starting at the beginning: new perspectives on the biology of mucosal T cells. *Annu.Rev.Immunol.* 22:217-246.
184. Das,G., Augustine,M.M., Das,J., Bottomly,K., Ray,P., and Ray,A. 2003. An important regulatory role for CD4+CD8{alpha}{alpha} T cells in the intestinal epithelial layer in the prevention of inflammatory bowel disease. *Proc.Natl.Acad.Sci.U.S.A.* ..
185. Chen,Y., Chou,K., Fuchs,E., Havran,W.L., and Boismenu,R. 2002. Protection of the intestinal mucosa by intraepithelial gamma delta T cells. *Proc.Natl.Acad.Sci.U.S.A.* 99:14338-14343.
186. Kosiewicz,M.M., Nast,C.C., Krishnan,A., Rivera-Nieves,J., Moskaluk,C.A., Matsumoto,S., Kozaiwa,K., and Cominelli,F. 2001. Th1-type responses mediate spontaneous ileitis in a novel murine model of Crohn's disease. *J.Clin.Invest.* 107:695-702.
187. Cepek,K.L., Shaw,S.K., Parker,C.M., Russell,G.J., Morrow,J.S., Rimm,D.L., and Brenner,M.B. 1994. Adhesion between epithelial cells and T lymphocytes mediated by E-cadherin and the alpha E beta 7 integrin. *Nature* 372:190-193.
188. Schon,M.P., Arya,A., Murphy,E.A., Adams,C.M., Strauch,U.G., Agace,W.W., Marsal,J., Donohue,J.P., Her,H., Beier,D.R. *et al.* 1999. Mucosal T lymphocyte

- numbers are selectively reduced in integrin alpha E (CD103)-deficient mice. *J.Immunol* 162:6641-6649.
189. Strauch,U.G., Mueller,R.C., Li,X.Y., Cernadas,M., Higgins,J.M., Binion,D.G., and Parker,C.M. 2001. Integrin alpha E(CD103)beta 7 mediates adhesion to intestinal microvascular endothelial cell lines via an E-cadherin-independent interaction. *J.Immunol* 166:3506-3514.
  190. Berland,R. and Wortis,H.H. 2002. Origins and functions of B-1 cells with notes on the role of CD5. *Annu.Rev.Immunol* 20:253-300.
  191. Kroese,F.G., de Waard,R., and Bos,N.A. 1996. B-1 cells and their reactivity with the murine intestinal microflora. *Semin.Immunol* 8:11-18.
  192. Kroese,F.G., Butcher,E.C., Stall,A.M., Lalor,P.A., Adams,S., and Herzenberg,L.A. 1989. Many of the IgA producing plasma cells in murine gut are derived from self-replenishing precursors in the peritoneal cavity. *Int.Immunol* 1:75-84.
  193. Bos,N.A., Cebra,J.J., and Kroese,F.G. 2000. B-1 cells and the intestinal microflora. *Curr.Top.Microbiol.Immunol* 252:211-20.:211-220.
  194. Kroese,F.G. and Bos,N.A. 1999. Peritoneal B-1 cells switch in vivo to IgA and these IgA antibodies can bind to bacteria of the normal intestinal microflora. *Curr.Top.Microbiol.Immunol* 246:343-9; discussion 350.:343-349.
  195. Ansel,K.M., Harris,R.B., and Cyster,J.G. 2002. CXCL13 is required for B1 cell homing, natural antibody production, and body cavity immunity. *Immunity*. 16:67-76.
  196. Friedman,A. and Weiner,H.L. 1994. Induction of anergy or active suppression following oral tolerance is determined by antigen dosage. *Proc.Natl.Acad.Sci.U.S.A* 91:6688-6692.
  197. Duchmann,R., Schmitt,E., Knolle,P., Meyer zum Buschenfelde,K.H., and Neurath,M. 1996. Tolerance towards resident intestinal flora in mice is abrogated in experimental colitis and restored by treatment with interleukin-10 or antibodies to interleukin-12. *Eur.J.Immunol.* 26:934-938.
  198. Spahn,T.W., Weiner,H.L., Rennert,P.D., Lugering,N., Fontana,A., Domschke,W., and Kucharzik,T. 2002. Mesenteric lymph nodes are critical for the induction of high-dose oral tolerance in the absence of Peyer's patches. *Eur.J.Immunol.* 32:1109-1113.
  199. Annacker,O. and Powrie,F. 2002. Homeostasis of intestinal immune regulation. *Microbes.Infect.* 4:567-574.

200. Bouma, G. and Strober, W. 2003. The immunological and genetic basis of inflammatory bowel disease. *Nat.Rev.Immunol* 3:521-533.
201. Groux, H., O'Garra, A., Bigler, M., Rouleau, M., Antonenko, S., de Vries, J.E., and Roncarolo, M.G. 1997. A CD4<sup>+</sup> T-cell subset inhibits antigen-specific T-cell responses and prevents colitis. *Nature* 389:737-742.
202. Nakamura, K., Kitani, A., and Strober, W. 2001. Cell contact-dependent immunosuppression by CD4(+)CD25(+) regulatory T cells is mediated by cell surface-bound transforming growth factor beta. *J.Exp.Med.* 194:629-644.
203. Dieckmann, D., Bruett, C.H., Ploettner, H., Lutz, M.B., and Schuler, G. 2002. Human CD4(+)CD25(+) regulatory, contact-dependent T cells induce interleukin 10-producing, contact-independent type 1-like regulatory T cells [corrected]. *J.Exp.Med.* 196:247-253.
204. Kitani, A., Fuss, I., Nakamura, K., Kumaki, F., Usui, T., and Strober, W. 2003. Transforming Growth Factor (TGF)- $\beta$ 1-producing Regulatory T Cells Induce Smad-mediated Interleukin 10 Secretion That Facilitates Coordinated Immunoregulatory Activity and Amelioration of TGF- $\beta$ 1-mediated Fibrosis. *J.Exp.Med.* ..
205. Schubert, L.A., Jeffery, E., Zhang, Y., Ramsdell, F., and Ziegler, S.F. 2001. Scurfin (FOXP3) acts as a repressor of transcription and regulates T cell activation. *J.Biol.Chem.* 276:37672-37679.
206. Fontenot, J.D., Gavin, M.A., and Rudensky, A.Y. 2003. Foxp3 programs the development and function of CD4<sup>+</sup>CD25<sup>+</sup> regulatory T cells. *Nat.Immunol.* 4:330-336.
207. Chen, W., Jin, W., Hardegen, N., Lei, K.J., Li, L., Marinos, N., McGrady, G., and Wahl, S.M. 2003. Conversion of peripheral CD4<sup>+</sup>. *J.Exp.Med.* 198:1875-1886.
208. Vieira, P.L., Christensen, J.R., Minaee, S., O'Neill, E.J., Barrat, F.J., Boonstra, A., Barthlott, T., Stockinger, B., Wraith, D.C., and O'Garra, A. 2004. IL-10-secreting regulatory T cells do not express Foxp3 but have comparable regulatory function to naturally occurring CD4<sup>+</sup>CD25<sup>+</sup> regulatory T cells. *J.Immunol.* 172:5986-5993.
209. Huehn, J., Siegmund, K., Lehmann, J.C., Siewert, C., Haubold, U., Feuerer, M., Debes, G.F., Lauber, J., Frey, O., Przybylski, G.K. *et al.* 2004. Developmental stage, phenotype, and migration distinguish naive- and effector/memory-like CD4<sup>+</sup> regulatory T cells. *J.Exp.Med.* 199:303-313.
210. Kim, J.D., Choi, B.K., Bae, J.S., Lee, U.H., Han, I.S., Lee, H.W., Youn, B.S., Vinay, D.S., and Kwon, B.S. 2003. Cloning and characterization of GITR ligand. *Genes Immun.* 4:564-569.

211. Tone,M., Tone,Y., Adams,E., Yates,S.F., Frewin,M.R., Cobbold,S.P., and Waldmann,H. 2003. Mouse glucocorticoid-induced tumor necrosis factor receptor ligand is costimulatory for T cells. *Proc.Natl.Acad.Sci.U.S.A.* 100:15059-15064.
212. McHugh,R.S., Whitters,M.J., Piccirillo,C.A., Young,D.A., Shevach,E.M., Collins,M., and Byrne,M.C. 2002. CD4(+)CD25(+) immunoregulatory T cells: gene expression analysis reveals a functional role for the glucocorticoid-induced TNF receptor. *Immunity* 16:311-323.
213. Shimizu,J., Yamazaki,S., Takahashi,T., Ishida,Y., and Sakaguchi,S. 2002. Stimulation of CD25(+)CD4(+) regulatory T cells through GITR breaks immunological self-tolerance. *Nat.Immunol* 3:135-142.
214. Greenstein,R.J. 2003. Is Crohn's disease caused by a mycobacterium? Comparisons with leprosy, tuberculosis, and Johne's disease. *Lancet Infect.Dis.* 3:507-514.
215. Mishina,D., Katsel,P., Brown,S.T., Gilberts,E.C., and Greenstein,R.J. 1996. On the etiology of Crohn disease. *Proc.Natl.Acad.Sci.U.S.A* 93:9816-9820.
216. Bamias,G., Marini,M., Moskaluk,C.A., Odashima,M., Ross,W.G., Rivera-Nieves,J., and Cominelli,F. 2002. Down-regulation of intestinal lymphocyte activation and Th1 cytokine production by antibiotic therapy in a murine model of Crohn's disease. *J.Immunol* 169:5308-5314.
217. Reinecker,H.C., Steffen,M., Witthoeft,T., Pflueger,I., Schreiber,S., MacDermott,R.P., and Raedler,A. 1993. Enhanced secretion of tumour necrosis factor-alpha, IL-6, and IL-1 beta by isolated lamina propria mononuclear cells from patients with ulcerative colitis and Crohn's disease. *Clin.Exp.Immunol.* 94:174-181.
218. van Deventer,S.J. 1997. Tumour necrosis factor and Crohn's disease. *Gut* 40:443-448.
219. Lala,S., Ogura,Y., Osborne,C., Hor,S.Y., Bromfield,A., Davies,S., Ogunbiyi,O., Nunez,G., and Keshav,S. 2003. Crohn's disease and the NOD2 gene: a role for paneth cells. *Gastroenterology* 125:47-57.
220. Lopez-Cubero,S.O., Sullivan,K.M., and McDonald,G.B. 1998. Course of Crohn's disease after allogeneic marrow transplantation. *Gastroenterology* 114:433-440.
221. Knoflach,P., Park,B.H., Cunningham,R., Weiser,M.M., and Albini,B. 1987. Serum antibodies to cow's milk proteins in ulcerative colitis and Crohn's disease. *Gastroenterology* 92:479-485.
222. Duchmann,R., Kaiser,I., Hermann,E., Mayet,W., Ewe,K., and Meyer zum Buschenfelde,K.H. 1995. Tolerance exists towards resident intestinal flora but is



- broken in active inflammatory bowel disease (IBD). *Clin.Exp.Immunol.* 102:448-455.
223. Kraus,T.A., Toy,L., Chan,L., Childs,J., and Mayer,L. 2004. Failure to induce oral tolerance to a soluble protein in patients with inflammatory bowel disease. *Gastroenterology* 126:1771-1778.
  224. Meddings,J. 2000. Barrier dysfunction and Crohn's disease. *Ann.N.Y.Acad.Sci.* 915:333-8.:333-338.
  225. Chatila,T.A., Blaeser,F., Ho,N., Lederman,H.M., Voulgaropoulos,C., Helms,C., and Bowcock,A.M. 2000. JM2, encoding a fork head-related protein, is mutated in X-linked autoimmunity-allergic dysregulation syndrome. *J.Clin.Invest* 106:R75-R81.
  226. Macpherson,A., Khoo,U.Y., Forgacs,I., Philpott-Howard,J., and Bjarnason,I. 1996. Mucosal antibodies in inflammatory bowel disease are directed against intestinal bacteria. *Gut* 38:365-375.
  227. Koninckx,C.R., Giliams,J.P., Polanco,I., and Pena,A.S. 1984. IgA antigliadin antibodies in celiac and inflammatory bowel disease. *J.Pediatr.Gastroenterol.Nutr.* 3:676-682.
  228. D'Alessandro,M., Mariani,P., Lomanto,D., Bachetoni,A., and Speranza,V. 2002. Alterations in serum anti-alpha-galactosyl antibodies in patients with Crohn's disease and ulcerative colitis. *Clin.Immunol.* 103:63-68.
  229. Lodes,M.J., Cong,Y., Elson,C.O., Mohamath,R., Landers,C.J., Targan,S.R., Fort,M., and Hershsberg,R.M. 2004. Bacterial flagellin is a dominant antigen in Crohn disease. *J.Clin.Invest* 113:1296-1306.
  230. Sutton,C.L., Kim,J., Yamane,A., Dalwadi,H., Wei,B., Landers,C., Targan,S.R., and Braun,J. 2000. Identification of a novel bacterial sequence associated with Crohn's disease. *Gastroenterology* 119:23-31.
  231. Cohavy,O., Harth,G., Horwitz,M., Eggena,M., Landers,C., Sutton,C., Targan,S.R., and Braun,J. 1999. Identification of a novel mycobacterial histone H1 homologue (HupB) as an antigenic target of pANCA monoclonal antibody and serum immunoglobulin A from patients with Crohn's disease. *Infect.Immun.* 67:6510-6517.
  232. Landers,C.J., Cohavy,O., Misra,R., Yang,H., Lin,Y.C., Braun,J., and Targan,S.R. 2002. Selected loss of tolerance evidenced by Crohn's disease-associated immune responses to auto- and microbial antigens. *Gastroenterology* 123:689-699.
  233. Mow,W.S., Vasiliasukas,E.A., Lin,Y.C., Fleshner,P.R., Papadakis,K.A., Taylor,K.D., Landers,C.J., Abreu-Martin,M.T., Rotter,J.I., Yang,H. *et al.* 2004.

- Association of antibody responses to microbial antigens and complications of small bowel Crohn's disease. *Gastroenterology* 126:414-424.
234. Hollander,D., Vadheim,C.M., Brettholz,E., Petersen,G.M., Delahunty,T., and Rotter,J.I. 1986. Increased intestinal permeability in patients with Crohn's disease and their relatives. A possible etiologic factor. *Ann.Intern.Med.* 105:883-885.
  235. May,G.R., Sutherland,L.R., and Meddings,J.B. 1993. Is small intestinal permeability really increased in relatives of patients with Crohn's disease? *Gastroenterology* 104:1627-1632.
  236. Yacyshyn,B.R. and Meddings,J.B. 1995. CD45RO expression on circulating CD19+ B cells in Crohn's disease correlates with intestinal permeability. *Gastroenterology* 108:132-137.
  237. Dubuquoy,L., Jansson,E.A., Deeb,S., Rakotobe,S., Karoui,M., Colombel,J.F., Auwerx,J., Pettersson,S., and Desreumaux,P. 2003. Impaired expression of peroxisome proliferator-activated receptor gamma in ulcerative colitis. *Gastroenterology* 124:1265-1276.
  238. Daynes,R.A. and Jones,D.C. 2002. Emerging roles of PPARs in inflammation and immunity. *Nat.Rev.Immunol* 2:748-759.
  239. Katayama,K., Wada,K., Nakajima,A., Mizuguchi,H., Hayakawa,T., Nakagawa,S., Kadowaki,T., Nagai,R., Kamisaki,Y., Blumberg,R.S. *et al.* 2003. A novel PPAR gamma gene therapy to control inflammation associated with inflammatory bowel disease in a murine model. *Gastroenterology* 124:1315-1324.
  240. Dieckgraefe,B.K. and Korzenik,J.R. 2002. Treatment of active Crohn's disease with recombinant human granulocyte-macrophage colony-stimulating factor. *Lancet* 360:1478-1480.
  241. Matsumoto,S., Okabe,Y., Setoyama,H., Takayama,K., Ohtsuka,J., Funahashi,H., Imaoka,A., Okada,Y., and Umesaki,Y. 1998. Inflammatory bowel disease-like enteritis and caecitis in a senescence accelerated mouse P1/Yit strain. *Gut* 43:71-78.
  242. Rivera-Nieves,J., Bamias,G., Vidrich,A., Marini,M., Pizarro,T.T., McDuffie,M.J., Moskaluk,C.A., Cohn,S.M., and Cominelli,F. 2003. Emergence of perianal fistulizing disease in the SAMP1/YitFc mouse, a spontaneous model of chronic ileitis. *Gastroenterology* 124:972-982.
  243. Marini,M., Bamias,G., Rivera-Nieves,J., Moskaluk,C.A., Hoang,S.B., Ross,W.G., Pizarro,T.T., and Cominelli,F. 2003. TNF-alpha neutralization ameliorates the severity of murine Crohn's-like ileitis by abrogation of intestinal epithelial cell apoptosis. *Proc.Natl.Acad.Sci.U.S.A.* 100:8366-8371.

244. Takedatsu,H., Mitsuyama,K., Matsumoto,S., Handa,K., Suzuki,A., Takedatsu,H., Funabashi,H., Okabe,Y., Hara,T., Toyonaga,A. *et al.* 2004. Interleukin-5 participates in the pathogenesis of ileitis in SAMP1/Yit mice. *Eur.J.Immunol.* 34:1561-1569.
245. Kozaiwa,K., Sugawara,K., Smith,M.F., Jr., Carl,V., Yamschikov,V., Belyea,B., McEwen,S.B., Moskaluk,C.A., Pizarro,T.T., Cominelli,F. *et al.* 2003. Identification of a quantitative trait locus for ileitis in a spontaneous mouse model of Crohn's disease: SAMP1/YitFc. *Gastroenterology* 125:477-490.
246. Ziegler,S.F., Levin,S.D., Johnson,L., Copeland,N.G., Gilbert,D.J., Jenkins,N.A., Baker,E., Sutherland,G.R., Feldhaus,A.L., and Ramsdell,F. 1994. The mouse CD69 gene. Structure, expression, and mapping to the NK gene complex. *J.Immunol* 152:1228-1236.
247. Ohgama,J., Katoh,M., Hirano,M., Arase,H., Arase-Fukushi,N., Mishima,M., Iwabuchi,K., Ogasawara,K., and Onoe,K. 1994. Functional studies on MEL-14+ and MEL-14- T cells in peripheral lymphoid tissues. *Immunobiology* 190:225-242.
248. Lowenthal,J.W., Zubler,R.H., Nabholz,M., and MacDonald,H.R. 1985. Similarities between interleukin-2 receptor number and affinity on activated B and T lymphocytes. *Nature* 315:669-672.
249. Lazarus,N.H., Kunkel,E.J., Johnston,B., Wilson,E., Youngman,K.R., and Butcher,E.C. 2003. A common mucosal chemokine (mucosae-associated epithelial chemokine/CCL28) selectively attracts IgA plasmablasts. *J.Immunol* 170:3799-3805.
250. Kwon,B., Kim,B.S., Cho,H.R., Park,J.E., and Kwon,B.S. 2003. Involvement of tumor necrosis factor receptor superfamily(TNFRSF) members in the pathogenesis of inflammatory diseases. *Exp.Mol.Med.* 35:8-16.
251. Ley,K. 2001. Pathways and bottlenecks in the web of inflammatory adhesion molecules and chemoattractants. *Immunol Res.* 24:87-95.
252. Sims,T.N. and Dustin,M.L. 2002. The immunological synapse: integrins take the stage. *Immunol.Rev.* 186:100-117.
253. Nagasawa,T., Hirota,S., Tachibana,K., Takakura,N., Nishikawa,S., Kitamura,Y., Yoshida,N., Kikutani,H., and Kishimoto,T. 1996. Defects of B-cell lymphopoiesis and bone-marrow myelopoiesis in mice lacking the CXC chemokine PBSF/SDF-1. *Nature* 382:635-638.
254. Forster,R., Schubel,A., Breitfeld,D., Kremmer,E., Renner-Muller,I., Wolf,E., and Lipp,M. 1999. CCR7 coordinates the primary immune response by establishing functional microenvironments in secondary lymphoid organs. *Cell* 99:23-33.

255. Bonecchi,R., Bianchi,G., Bordignon,P.P., D'Ambrosio,D., Lang,R., Borsatti,A., Sozzani,S., Allavena,P., Gray,P.A., Mantovani,A. *et al.* 1998. Differential expression of chemokine receptors and chemotactic responsiveness of type 1 T helper cells (Th1s) and Th2s. *J.Exp.Med.* 187:129-134.
256. Loetscher,P., Seitz,M., Baggiolini,M., and Moser,B. 1996. Interleukin-2 regulates CC chemokine receptor expression and chemotactic responsiveness in T lymphocytes. *J.Exp.Med.* 184:569-577.
257. Varona,R., Zaballos,A., Gutierrez,J., Martin,P., Roncal,F., Albar,J.P., Ardavin,C., and Marquez,G. 1998. Molecular cloning, functional characterization and mRNA expression analysis of the murine chemokine receptor CCR6 and its specific ligand MIP-3alpha. *FEBS Lett.* 440:188-194.
258. Schmittgen,T.D. and Zakrajsek,B.A. 2000. Effect of experimental treatment on housekeeping gene expression: validation by real-time, quantitative RT-PCR. *J.Biochem.Biophys.Methods* 46:69-81.
259. Sallusto,F., Palermo,B., Lenig,D., Miettinen,M., Matikainen,S., Julkunen,I., Forster,R., Burgstahler,R., Lipp,M., and Lanzavecchia,A. 1999. Distinct patterns and kinetics of chemokine production regulate dendritic cell function. *Eur.J.Immunol* 29:1617-1625.
260. Selvan,R.S., Zhou,L.J., and Krangel,M.S. 1997. Regulation of I-309 gene expression in human monocytes by endogenous interleukin-1. *Eur.J.Immunol.* 27:687-694.
261. Iellem,A., Colantonio,L., Bhakta,S., Sozzani,S., Mantovani,A., Sinigaglia,F., and D'Ambrosio,D. 2000. Inhibition by IL-12 and IFN-alpha of I-309 and macrophage-derived chemokine production upon TCR triggering of human Th1 cells. *Eur.J.Immunol.* 30:1030-1039.
262. Kosiewicz,M.M., Alard,P., and Streilein,J.W. 1998. Alterations in cytokine production following intraocular injection of soluble protein antigen: impairment in IFN-gamma and induction of TGF-beta and IL-4 production. *J.Immunol.* 161:5382-5390.
263. Iellem,A., Mariani,M., Lang,R., Recalde,H., Panina-Bordignon,P., Sinigaglia,F., and D'Ambrosio,D. 2001. Unique chemotactic response profile and specific expression of chemokine receptors CCR4 and CCR8 by CD4(+)CD25(+) regulatory T cells. *J.Exp.Med.* 194:847-853.
264. Vermeire,S. and Rutgeerts,P. 2004. Antibody responses in Crohn's disease. *Gastroenterology* 126:601-604.

265. McAdam,A.J., Greenwald,R.J., Levin,M.A., Chernova,T., Malenkovich,N., Ling,V., Freeman,G.J., and Sharpe,A.H. 2001. ICOS is critical for CD40-mediated antibody class switching. *Nature* 409:102-105.
266. Coffman,R.L., Lebman,D.A., and Shrader,B. 1989. Transforming growth factor beta specifically enhances IgA production by lipopolysaccharide-stimulated murine B lymphocytes. *J.Exp.Med.* 170:1039-1044.
267. Cazac,B.B. and Roes,J. 2000. TGF-beta receptor controls B cell responsiveness and induction of IgA in vivo. *Immunity* 13:443-451.
268. Breitfeld,D., Ohl,L., Kremmer,E., Ellwart,J., Sallusto,F., Lipp,M., and Forster,R. 2000. Follicular B helper T cells express CXC chemokine receptor 5, localize to B cell follicles, and support immunoglobulin production. *J.Exp.Med.* 192:1545-1552.
269. Mizoguchi,E., Mizoguchi,A., Preffer,F.I., and Bhan,A.K. 2000. Regulatory role of mature B cells in a murine model of inflammatory bowel disease. *Int.Immunol* 12:597-605.
270. Bishop,G.G., McPherson,J.A., Sanders,J.M., Hesselbacher,S.E., Feldman,M.J., McNamara,C.A., Gimple,L.W., Powers,E.R., Mousa,S.A., and Sarembock,I.J. 2001. Selective  $\alpha_v\beta_3$ -receptor blockade reduces macrophage infiltration and restenosis after balloon angioplasty in the atherosclerotic rabbit. *Circulation* 103:1906-1911.
271. Kazemi-Shirazi,L., Gasche,C.H., Natter,S., Gangl,A., Smolen,J., Spitzauer,S., Valent,P., Kraft,D., and Valenta,R. 2002. IgA autoreactivity: a feature common to inflammatory bowel and connective tissue diseases. *Clin.Exp.Immunol* 128:102-109.
272. Tafuri,A., Shahinian,A., Bladt,F., Yoshinaga,S.K., Jordana,M., Wakeham,A., Boucher,L.M., Bouchard,D., Chan,V.S., Duncan,G. *et al.* 2001. ICOS is essential for effective T-helper-cell responses. *Nature* 409:105-109.
273. Grewal,I.S. and Flavell,R.A. 1998. CD40 and CD154 in cell-mediated immunity. *Annu.Rev.Immunol* 16:111-35.:111-135.
274. Schaerli,P., Willimann,K., Lang,A.B., Lipp,M., Loetscher,P., and Moser,B. 2000. CXC chemokine receptor 5 expression defines follicular homing T cells with B cell helper function. *J.Exp.Med.* 192:1553-1562.
275. Shanahan,F. 2002. Crohn's disease. *Lancet* 359:62-69.
276. Tang,T., Rosenkranz,A., Assmann,K.J., Goodman,M.J., Gutierrez-Ramos,J.C., Carroll,M.C., Cotran,R.S., and Mayadas,T.N. 1997. A role for Mac-1 (CD11b/CD18) in immune complex-stimulated neutrophil function in vivo: Mac-1

- deficiency abrogates sustained Fcgamma receptor-dependent neutrophil adhesion and complement-dependent proteinuria in acute glomerulonephritis. *J.Exp.Med.* 186:1853-1863.
277. Walker,L.S., Gulbranson-Judge,A., Flynn,S., Brocker,T., and Lane,P.J. 2000. Co-stimulation and selection for T-cell help for germinal centres: the role of CD28 and OX40. *Immunol Today* 21:333-337.
  278. Amano,M., Baumgarth,N., Dick,M.D., Brossay,L., Kronenberg,M., Herzenberg,L.A., and Strober,S. 1998. CD1 expression defines subsets of follicular and marginal zone B cells in the spleen: beta 2-microglobulin-dependent and independent forms. *J.Immunol* 161:1710-1717.
  279. Hisamatsu,T., Suzuki,M., Reinecker,H.C., Nadeau,W.J., McCormick,B.A., and Podolsky,D.K. 2003. CARD15/NOD2 functions as an antibacterial factor in human intestinal epithelial cells. *Gastroenterology* 124:993-1000.
  280. Wyatt,J., Vogelsang,H., Hubl,W., Waldhoer,T., and Lochs,H. 1993. Intestinal permeability and the prediction of relapse in Crohn's disease. *Lancet* 341:1437-1439.
  281. Meddings,J.B. and Gibbons,I. 1998. Discrimination of site-specific alterations in gastrointestinal permeability in the rat. *Gastroenterology* 114:83-92.
  282. Mardiney,M., III and Malech,H.L. 1996. Enhanced engraftment of hematopoietic progenitor cells in mice treated with granulocyte colony-stimulating factor before low-dose irradiation: implications for gene therapy. *Blood* 87:4049-4056.
  283. Dvorak,A.M. and Dickersin,G.R. 1980. Crohn's disease: transmission electron microscopic studies. I. Barrier function. Possible changes related to alterations of cell coat, mucous coat, epithelial cells, and Paneth cells. *Hum.Pathol.* 11:561-571.
  284. Ricote,M., Huang,J.T., Welch,J.S., and Glass,C.K. 1999. The peroxisome proliferator-activated receptor(PPARgamma) as a regulator of monocyte/macrophage function. *J.Leukoc.Biol.* 66:733-739.
  285. Mansen,A., Guardiola-Diaz,H., Rafter,J., Branting,C., and Gustafsson,J.A. 1996. Expression of the peroxisome proliferator-activated receptor (PPAR) in the mouse colonic mucosa. *Biochem.Biophys.Res.Comm.* 222:844-851.
  286. Becker,C., Wirtz,S., Blessing,M., Pirhonen,J., Strand,D., Bechthold,O., Frick,J., Galle,P.R., Autenrieth,I., and Neurath,M.F. 2003. Constitutive p40 promoter activation and IL-23 production in the terminal ileum mediated by dendritic cells. *J.Clin.Invest* 112:693-706.
  287. Rescigno,M. and Borrow,P. 2001. The host-pathogen interaction: new themes from dendritic cell biology. *Cell* 106:267-270.

288. Monteleone,G., Mann,J., Monteleone,I., Vavassori,P., Bremner,R., Fantini,M., Del Vecchio,B., Tersigni,R., Alessandroni,L., Mann,D. *et al.* 2003. A failure of TGFbeta 1 negative regulation maintains sustained NF-KB activation in gut inflammation. *J.Biol.Chem.* ..
289. Kazkaz,H. and Isenberg,D. 2004. Anti B cell therapy (rituximab) in the treatment of autoimmune diseases. *Curr.Opin.Pharmacol.* 4:398-402.